frontiers | Research Topics

Molecular mechanisms of bacterial disease in cultured fishes

Edited by
Lixing Huang, Huanying Pang, Ha Thanh Dong and Najiah Musa

Published in
Frontiers in Veterinary Science

ISSN 1664-8714
ISBN 978-2-83250-909-8
DOI 10.3389/978-2-83250-909-8

About Frontiers

Frontiers is more than just an open access publisher of scholarly articles: it is a pioneering approach to the world of academia, radically improving the way scholarly research is managed. The grand vision of Frontiers is a world where all people have an equal opportunity to seek, share and generate knowledge. Frontiers provides immediate and permanent online open access to all its publications, but this alone is not enough to realize our grand goals.

Frontiers journal series

The Frontiers journal series is a multi-tier and interdisciplinary set of open-access, online journals, promising a paradigm shift from the current review, selection and dissemination processes in academic publishing. All Frontiers journals are driven by researchers for researchers; therefore, they constitute a service to the scholarly community. At the same time, the *Frontiers journal series* operates on a revolutionary invention, the tiered publishing system, initially addressing specific communities of scholars, and gradually climbing up to broader public understanding, thus serving the interests of the lay society, too.

Dedication to quality

Each Frontiers article is a landmark of the highest quality, thanks to genuinely collaborative interactions between authors and review editors, who include some of the world's best academicians. Research must be certified by peers before entering a stream of knowledge that may eventually reach the public - and shape society; therefore, Frontiers only applies the most rigorous and unbiased reviews. Frontiers revolutionizes research publishing by freely delivering the most outstanding research, evaluated with no bias from both the academic and social point of view. By applying the most advanced information technologies, Frontiers is catapulting scholarly publishing into a new generation.

What are Frontiers Research Topics?

Frontiers Research Topics are very popular trademarks of the *Frontiers journals series*: they are collections of at least ten articles, all centered on a particular subject. With their unique mix of varied contributions from Original Research to Review Articles, Frontiers Research Topics unify the most influential researchers, the latest key findings and historical advances in a hot research area.

Find out more on how to host your own Frontiers Research Topic or contribute to one as an author by contacting the Frontiers editorial office: frontiersin.org/about/contact

Molecular mechanisms of bacterial disease in cultured fishes

Topic editors

Lixing Huang — Jimei University, China
Huanying Pang — Guangdong Ocean University, China
Ha Thanh Dong — Asian Institute of Technology, Thailand
Najiah Musa — University of Malaysia Terengganu, Malaysia

Citation

Huang, L., Pang, H., Dong, H. T., Musa, N., eds. (2022). *Molecular mechanisms of bacterial disease in cultured fishes*. Lausanne: Frontiers Media SA.
doi: 10.3389/978-2-83250-909-8

Table of contents

04 Editorial: Molecular mechanisms of bacterial disease in cultured fishes
Musa Najiah, Lixing Huang, Huanying Pang and Valentina Virginia Ebani

07 VasH Contributes to Virulence of *Aeromonas hydrophila* and Is Necessary to the T6SS-mediated Bactericidal Effect
Jihong Li, Zhihao Wu, Changsong Wu, Dan-Dan Chen, Yang Zhou and Yong-An Zhang

22 Antimicrobial Resistance of *Escherichia coli* From Aquaculture Farms and Their Environment in Zhanjiang, China
Cui-Yi Liao, Balamuralikrishnan Balasubramanian, Jin-Ju Peng, Song-Ruo Tao, Wen-Chao Liu and Yi Ma

34 Function and Characterization of an Alanine Dehydrogenase Homolog From *Nocardia seriolae*
Guoquan Chen, Ziyang Tan, Yansheng Liu, Tingting Weng, Liqun Xia and Yishan Lu

45 CRISPR/Cas12a Based Rapid Molecular Detection of Acute Hepatopancreatic Necrosis Disease in Shrimp
Chenglong Li, Nan Lin, Zhihua Feng, Minhua Lin, Biyun Guan, Kunsen Chen, Wangwang Liang, Qiaohuang Wang, Miaomiao Li, Yu You and Qi Chen

55 Selection of the Amino Acid and Saccharide That Increase the Tetracycline Susceptibility of *Vibrio splendidus*
Guohua Jiang, Yanan Li, Ya Li, Weiwei Zhang and Chenghua Li

66 RNA-Sequencing Analysis of the Spleen and Gill of *Takifugu rubripes* in Response to *Vibrio harveyi* Infection
Dongxu Gao, Wei Lei, Chenshi Wang, Ping Ni, Xiaoyu Cui, Xindi Huang and Shigen Ye

76 Quorum Sensing Controls the CRISPR and Type VI Secretion Systems in *Aliivibrio wodanis* 06/09/139
Amudha Deepalakshmi Maharajan, Erik Hjerde, Hilde Hansen and Nils Peder Willassen

93 Co-infection of *Candidatus* Piscichlamydia Trichopodus (Order *Chlamydiales*) and *Henneguya* sp. (Myxosporea, Myxobolidae) in Snakeskin Gourami *Trichopodus pectoralis* (Regan 1910)
Nguyen Dinh-Hung, Ha Thanh Dong, Chayanit Soontara, Channarong Rodkhum, Sukkrit Nimitkul, Prapansak Srisapoome, Pattanapon Kayansamruaj and Satid Chatchaiphan

102 Detection of Virulence-Associated Genes and *in vitro* Gene Transfer From *Aeromonas* sp. Isolated From Aquatic Environments of Sub-himalayan West Bengal
Preeti Mangar, Partha Barman, Anoop Kumar, Aniruddha Saha and Dipanwita Saha

frontiers | Frontiers in Veterinary Science

TYPE Editorial
PUBLISHED 17 November 2022
DOI 10.3389/fvets.2022.1073631

OPEN ACCESS

EDITED AND REVIEWED BY
Michael Kogut,
United States Department of Agriculture (USDA), United States

*CORRESPONDENCE
Musa Najiah
najiah@umt.edu.my

SPECIALTY SECTION
This article was submitted to Veterinary Infectious Diseases, a section of the journal Frontiers in Veterinary Science

RECEIVED 18 October 2022
ACCEPTED 24 October 2022
PUBLISHED 17 November 2022

CITATION
Najiah M, Huang L, Pang H and Ebani VV (2022) Editorial: Molecular mechanisms of bacterial disease in cultured fishes.
Front. Vet. Sci. 9:1073631.
doi: 10.3389/fvets.2022.1073631

Editorial: Molecular mechanisms of bacterial disease in cultured fishes

Musa Najiah[1]*, Lixing Huang[2], Huanying Pang[3] and Valentina Virginia Ebani[4]

[1]Faculty of Fisheries and Food Science, Universiti Malaysia Terengganu, Kuala Nerus, Malaysia, [2]Fisheries College, Fujian Engineering Research Center of Aquatic Breeding and Healthy Aquaculture, Jimei University, Xiamen, China, [3]Fisheries College, Guangdong Ocean University, Zhanjiang, China, [4]Department of Veterinary Sciences, University of Pisa, Pisa, Italy

KEYWORDS

bacterial infection, bacterial communication, bacteria-host interaction, virulence regulation, virulence factors interaction

Editorial on the Research Topic
Molecular mechanisms of bacterial disease in cultured fishes

Aquaculture is the fastest growing food production industry in the world, contributing nearly half of the global fish consumption. The world aquaculture recorded a total production (land and marine) of 87.5 million tons in 2020, which is a huge leap forward from 21.8 million tons in the 1990s (1). Aquaculture is facing diseases of various etiologies including bacteria. Although antimicrobial treatment is permitted under strict regulation, antimicrobial use should be refrained from in light of the risk of inducing antimicrobial resistance. It is crucial to seek novel effective solutions toward a healthier aquaculture practice, which requires us to have a clearer and deeper understanding of the disease mechanisms, including the host responses. Bacterial disease mechanisms are complicated, and vary considerably between bacteria. This Research Topic presents the current state of knowledge in molecular mechanisms of bacterial diseases in cultured fishes.

Bacterial communication and regulatory mechanism

Bacteria use quorum sensing (QS) to communicate with one another via signal molecules called autoinducers (AIs), and coordinate their behaviors for survival according to cell density. This subsequently activates QS transcriptional regulator to control functions such as biofilm formation, motility, bioluminescence, secretion, and virulence. These dynamically interconnected communication and regulatory mechanisms remain to be fully elucidated. Bacteria use different QS-dependent strategies to compete for space, including clustered regularly interspaced short palindromic repeats

(CRISPR) and type VI secretion systems (T6SSs). While T6SSs function primarily in competition against rival bacteria in polymicrobial environments, they also involve in pathogenesis of some diseases. In the study of QS and survival strategies of *Aliivibrio wodanis* that co-exists with *Moritella viscosa* in winter ulcer disease in Atlantic salmon, Maharajan et al. demonstrate that cell density and temperature influence QS-related genes, where low temperature (at which winter ulcer occurs) activates AHL-mediated AinS/AinR system that regulates CRISPR-Cas and T6SSs via LitR master QS regulator. The interactions between *A. wodanis* and *M. viscosa*, and with the host is, however, yet to be investigated.

Bacteria-parasite interaction

While bacterial co-occurrence in disease such as that of winter ulcer disease needs explanation, bacteria-parasite interaction in the form of co-infection is also a concern in aquaculture. Dinh-Hung et al. describe co-infection of myxozoan gill parasite, *Henneguya* sp. with a novel intracellular Chlamydia-like organism, *Candidatus Piscichlamydia trichopodus* in snakeskin gourami *Trichopodus pectoralis*. Further studies on how parasites and bacteria co-interact with host may provide insight into the molecular mechanisms of disease. Could there be similarity with the probable remote "talk" between gill monogenean, *Dactylogyrus lamellatus* and host intestinal microbiota (2)?

Bacterial persistence

Bacterial persistence is a phenomenon where very small subpopulations of isogenic bacterial cells (persister cells) undergo dormant cell cycle to survive sudden environmental insults such as antibiotic treatments. The dormancy state confers high tolerance to multiple antibiotics, but the mechanisms involved are still not identified. Here Jiang et al. report the use of selected amino acids and saccharides to revert *Vibrio splendidus* persister cells to allow complete elimination by tetracycline treatment.

Host immune response to bacterial infection

The immune response mechanisms against bacterial infection are behind the host tolerance and resistance to bacterial diseases. In the transcriptomic analysis of *Vibrio harveyi* infection in *Takifugu rubripes*, Gao et al. show that nucleotide-binding and oligomerization domain (NOD)-like receptor signaling pathway and cytokine-cytokine interaction are most enriched in spleen and gill, respectively. This study provides an understanding into immune response mechanisms and development of disease resistance markers against *V. harveyi*.

Mobile genetic elements

Virulence associated mobile genetic elements are widespread in the aquatic environment among various genera of bacteria e.g., *Vibrio*, *Photobacterium damselae* and *Staphylococcus aureus*. There are also evidences that *Aeromonas* can actively involve in transferring genetic material with phylogenetically distant bacteria. *Aeromonas* pathogenicity has been attributed to multiple virulence factors contributing to different mechanisms of infection, including haemolysins, proteases, elastases, lipases, enterotoxins, phospholipases, chitinases, and deoxyribonucleases. Of these, pore-forming toxins (encoded by *aer*A gene) and cytotoxic enterotoxins (by *act*, *alt*, and *ast* genes) are the primary elements of virulence in *Aeromonas*. In this Research Topic, Mangar et al. examine the virulence factors of *A. veronii*, as well as severity of lesions and mortality induced in *Anabas testudineus* in association with *aer/haem*, *ascV*, *fla*, and *aspA*.

T6SS transcriptional activator

In a study of virulent *A. hydrophila* from grass carp *Ctenopharyngodon idella*, Li et al. reveal that σ54-transcriptional activator, VasH is strictly required for T6SS functionality. This supports that VasH protein not only contributes to bacterial cytotoxicity, anti-host killing (resistance against host immune cleaning), but is also needed for systemic dissemination of *A. hydrophila*.

Induction of host cell apoptosis

Many bacteria are able to induce apoptosis in infected host cells to gain access to tissues. Alanine dehydrogenase (ALD) is a microbial enzyme catalyzing interconversion between alanine and pyruvate in microbial metabolism. Chen et al. describe an ALD homolog (NsALD) from *Nocardia seriolae* that causes chronic, systemic, granulomatous disease in aquaculture. They show that NsALD activates caspase-3 and triggers apoptosis in host cells.

Besides the molecular aspects highlighted in the seven articles above, this Research Topic also incorporates one article each on antimicrobial resistance (AMR), and advancement in

disease detection. AMR is a global threat to animal and human health. Antimicrobial residues resulting from aquaculture use not only pose a food safety concern, but also trigger emergence of multi-antimicrobial resistance in bacteria including those in the wild species (3). Liao et al. investigate the AMR profile and associated genes in *Escherichia coli* from aquaculture farms (water, soil, sediment). They reveal the resistance rates to 23 antimicrobials, and the detection rates of AMR genes. Acute hepatopancreatic necrosis disease (AHPND) is a disease that can cause high mortality in cultured penaeid shrimp. AHPND is mainly caused by *Vibrio* species bearing pVA1 plasmid that encodes pirA$_{VP}$ and pirB$_{VP}$ toxins. Li et al. describe the development of recombinase polymerase amplification (RPA)-CRISPR/Cas12a assay for detection of *pirA$_{VP}$* and *pirB$_{VP}$* genes, and coupled with lateral flow strip readout.

Concluding remarks

The molecular mechanisms of bacterial diseases in cultured fishes are yet to be fully understood. The bacteria-host and virulence factors interaction much remain to be elucidated. This Research Topic lays a foundation for further investigation into the mechanisms involved, and provides new insights into molecular basis of pathogenicity. A better understanding at molecular level will allow for effective risk monitoring for bacterial diseases.

Author contributions

All authors listed have made a substantial, direct, and intellectual contribution to the work and approved it for publication.

Acknowledgments

The authors acknowledge the support of their respective affiliated institutions: Universiti Malaysia Terengganu, Jimei University, Guangdong Ocean University, and University of Pisa.

Conflict of interest

The authors declare that the research was conducted in the absence of any commercial or financial relationships that could be construed as a potential conflict of interest.

Publisher's note

References

1. FAO. *The State of World Fisheries and Aquaculture 2022*. Towards Blue Transformation. Rome: FAO (2022). p. 3. doi: 10.4060/cc0461en

2. Wang L, Zhang D, Xie J, Chang O, Wang Q, Shi C, et al. Do ectoparasites on fish gills "talk" with gut microbiota far away? *Aquaculture*. (2023) 562:738880. doi: 10.1016/j.aquaculture.2022.738880

3. Najiah M, Nadirah M, Sakri I, Shaharom-Harrison F. Bacteria associated with wild mud crab (*Scylla serrata*) from Setiu Wetland, Malaysia with emphasis on antibiotic resistances. *Pak J Biol Sci.* (2010) 13:293–7. doi: 10.3923/pjbs.2010.293.297

frontiers in Veterinary Science

ORIGINAL RESEARCH
published: 13 December 2021
doi: 10.3389/fvets.2021.793458

VasH Contributes to Virulence of *Aeromonas hydrophila* and Is Necessary to the T6SS-mediated Bactericidal Effect

Jihong Li[1,2], *Zhihao Wu*[3], *Changsong Wu*[3], *Dan-Dan Chen*[1], *Yang Zhou*[3,4,5]* and *Yong-An Zhang*[1,3,4,5]*

[1] Institute of Hydrobiology, Chinese Academy of Sciences (CAS), Wuhan, China, [2] University of Chinese Academy of Sciences, Beijing, China, [3] State Key Laboratory of Agricultural Microbiology, College of Fisheries, Huazhong Agricultural University, Wuhan, China, [4] Engineering Research Center of Green Development for Conventional Aquatic Biological Industry in the Yangtze River Economic Belt, Ministry of Education, Wuhan, China, [5] Guangdong Laboratory for Lingnan Modern Agriculture, Guangzhou, China

Aeromonas hydrophila is a Gram-negative bacterium that is commonly distributed in aquatic surroundings and has been considered as a pathogen of fish, amphibians, reptiles, and mammals. In this study, a virulent strain *A. hydrophila* GD18, isolated from grass carp (*Ctenopharyngodon idella*), was characterized to belong to a new sequence type ST656. Whole-genome sequencing and phylogenetic analysis showed that GD18 was closer to environmental isolates, however distantly away from the epidemic ST251 clonal group. The type VI secretion system (T6SS) was known to target both eukaryotic and prokaryotic cells by delivering various effector proteins in diverse niches by Gram-negative bacteria. Genome-wide searching and hemolysin co-regulated protein (Hcp) expression test showed that GD18 possessed a functional T6SS and is conditionally regulated. Further analysis revealed that VasH, a σ54-transcriptional activator, was strictly required for the functionality of T6SS in *A. hydrophila* GD18. Mutation of *vas*H gene by homologous recombination significantly abolished the bactericidal property. Then the virulence contribution of VasH was characterized in both *in vitro* and *in vivo* models. The results supported that VasH not only contributed to the bacterial cytotoxicity and resistance against host immune cleaning, but also was required for virulence and systemic dissemination of *A. hydrophila* GD18. Taken together, these findings provide a perspective for understanding the VasH-mediated regulation mechanism and T6SS-mediated virulence and bactericidal effect of *A. hydrophila*.

Keywords: ***Aeromonas hydrophila*, whole-genome sequencing, T6SS, VasH, virulence**

OPEN ACCESS

Edited by:
Lixing Huang,
Jimei University, China

Reviewed by:
Xiaojun Zhang,
Yangzhou University, China
Dahai Yang,
East China University of Science and Technology, China

***Correspondence:**
Yang Zhou
zhouyang@mail.hzau.edu.cn
Yong-An Zhang
yonganzhang@mail.hzau.edu.cn

Specialty section:
This article was submitted to Veterinary Infectious Diseases, a section of the journal Frontiers in Veterinary Science

Received: *26 October 2021*
Accepted: *09 November 2021*
Published: *13 December 2021*

Citation:
Li J, Wu Z, Wu C, Chen D-D, Zhou Y and Zhang Y-A (2021) VasH Contributes to Virulence of Aeromonas hydrophila and Is Necessary to the T6SS-mediated Bactericidal Effect. Front. Vet. Sci. 8:793458. doi: 10.3389/fvets.2021.793458

INTRODUCTION

Aeromonas hydrophila is an opportunistic pathogen widespread in aquatic environments. This bacterium could cause multiple diseases in different animal species, such as fish, amphibians, reptiles, and humans (1). In fish, *A. hydrophila* can cause outbreaks of motile *Aeromonas* septicemia (MAS) with symptoms including reddened fins, inflammation of the anus, diffuse hemorrhages on the skin, exophthalmia, and abdominal swelling (2). This pathogen has frequently caused a high

mortality rate in commercial aquaculture throughout China since 1989 (3). In recent years, MAS caused by *A. hydrophila* has hindered the rapid development of carp industry in China and catfish industry in the United States (4, 5). Grass carp (*Ctenopharyngodon idellus*) is the fish species with the most significant reported production in aquaculture globally, with a proportion of up to 5.5 million tons per year (6). Increased incidence of infection and the broad spectrum of antibiotic resistance has made *A. hydrophila* a severe threat to the aquaculture industry.

The dynamic characteristics and overlapping classification have made the turbulent nature of classification within *Aeromonas* spp. (7). Multilocus sequence typing (MLST) permitted accurate strain genotyping and the phylogenetic evaluation of concatenated core genome gene sequences, offering a valuable tool for epidemiological outbreak tracing, host range evolution, and ecological research (8). The derived sequence types (STs) shed light on the relationship among the taxa belonging to the genus *Aeromonas*. ST251 is regarded as the virulent strain clonal group of *A. hydrophila*, accountable for the recent years' MAS (9). However, MLST, defined through housekeeping genes as sequence types (STs) and clone groups, has limited ability to further identify genetically related strains in STs. Latest, whole-genome sequencing (WGS) of pathogens has become more accessible and affordable as a tool for regular monitoring and detection of a potential outbreak. It offers information on the bacterial genome at a much more satisfactory resolution than MLST (10). Application of WGS made accurate diagnoses possible and has facilitated the investigations of disease outbreaks (11). Although there have been increasing *A. hydrophila* genome sequences available in the database, complete whole genome sequence and detailed genomic analysis of grass carp isolated strains are still very limited.

The Type VI Secretion System (T6SS) is a versatile weapon employed by bacteria to protect themselves against predators, disrupt eukaryotic cells, and fight against different microorganisms (12). As identified in more than 25% of sequenced Gram-negative bacteria, T6SS is a contact-dependent toxin delivery machine that can directly kill competitors or hosts through protein toxin translocation (13–16). The component of T6SS has 13 core genes, while additional elements likely to participate in the delivery of the effector (17). The tail tube of T6SS is made of hemolysin co-regulated protein (Hcp), capped by a puncturing device containing proteins (12). Hcp is essential for the structural integrity of T6SS apparatus and Hcp could be secreted with different effectors (18, 19). The secretion of Hcp is a dependable marker of workable T6SS (20). T6SSs are strictly regulated and the transcription was directly or indirectly modified by regulators, including the QS system, sigma 54 factors, H-NS, and Fur (17, 21–23). In *Vibrio cholerae* and *V. fischeri*, VasH is a transcriptional regulator of T6SS and contains a DNA-binding sigma54 motif, which is critical for the ability to activate transcription of T6SS genes (24–26). Earlier studies showed that the deletion of *vas*H inhibited the expression and secretion of Hcp in *A. dhakensis* SSU, previously considered as an *A. hydrophila* strain (7, 23). In *A. hydrophila*, many of the T6SS components still await demonstration of function, including whether VasH is deployed and the role it plays in *A. hydrophila* survival and infection.

In the present study, an *A. hydrophila* strain GD18 was isolated from diseased grass carp. MLST analysis showed that GD18 belongs to a new sequence type ST656. To further discriminate GD18 genetically, WGS was applied and the evolution relationship between GD18 and other *A. hydrophila* isolates was clarified. Further analysis found that *A. hydrophila* GD18 possesses a complete and functional T6SS. Then the role of VasH in T6SS-mediated virulence and the bactericidal effect was preliminarily deciphered.

MATERIALS AND METHODS

Plasmids, Bacterial Strains, Cell Line, and Experimental Fish

For the bacterial strains, plasmids, and primers used in this study, see **Table 1** and **Supplementary Table 1**. *A. hydrophila* strain GD18 was isolated from diseased grass carp (*C. idella*). The morphology of bacterial cells was determined by transmission electron microscopy (TEM; Hitachi H-7650, Japan). The β-hemolytic phenotype was observed on sheep's blood agar. Luria Agar (LA) (Hopebio, China) plates with 0.3% (*w*/*v*) agar was used to analyze the swimming motility of different strains. Wild-type strain and its mutant were grown in Luria Broth (LB) broth (Hopebio, China) at 28°C. *E. coli* χ7213 was grown in LB medium supplemented with 50 μg/mL diaminopimelic acid (SCRC, China) at 37°C. CIK cells were cultured at 28°C, 5% CO_2 in M199 medium (Invitrogen, USA). All mediums contained 10% fetal bovine serum (FBS, Invitrogen, USA) supplemented with 1% penicillin-streptomycin (Invitrogen, USA). Rabbit polyclonal antibody targeting Hcp was produced in our laboratory. Anti-GAPDH polyclonal antibody (Cat # A19056) and HRP goat anti-rabbit IgG (Cat # AS014) were purchased from Abclonal.

Healthy grass carp (weighing 200 ± 20 g) were from Xiantao Hatchery (Hubei, China). AB line wild-type zebrafish used in this work were from the Institute of Hydrobiology, Chinese Academy of Sciences (Wuhan, China). Zebrafish were maintained at a density of 10 fish/tank in 8 L tanks. Before infection, fish were acclimatized to the environment for 2 weeks. The animal experiments were performed following animal welfare standards and were approved by the Ethical Committee of Institute of hydrobiology, Chinese Academy of Sciences.

Genome Sequencing and Assembly

Genomic DNA was extracted from *A. hydrophila* strains GD18 using a TIANamp Bacteria DNA kit (Tiangen, China) according to the manufacturer's instructions. Paired-end (PE) libraries had insert size of 500 bp and 2,000 bp. The sequence of cDNA was generated with an Illumina GA IIx sequencer (Illumina Inc., USA). Sequencing was performed at the Beijing Novogene Technology Co., Ltd. One shotgun run and one 8 kb-library span paired-end run were carried out. De Novo assembly of the raw reads was done by Assembler Software Newbler (version 2.7; Roche/454 Life Science) using default parameters. To obtain clean data, raw reads were processed by removing reads with 5 bp of ambiguous bases, 20 bp of low quality (≤Q20) bases, adapter

TABLE 1 | Strains and plasmids used in this study.

Strains and plasmids	Description	Source
Strains		
Aeromonas hydrophila		
GD18	Wild type	Lab collection
J-1	Wild type	(27)
Δ*vas*H	*vas*H deletion mutant	This work
Δ*hcp*1/2	*hcp*1 and *hcp*2 double-deletion mutant	This work
Escherichia coli		
χ7213	*thr*-1 *leu*B6 *fhu*A21 *lac*Y1 *gln*V44 *rec*A1 Δ*asd*A4 Δ(*zhf*-2::Tn10) *thi*-1	(28)
Plasmids		
pRE112	Suicide vector, *sac*B, mob$^-$(RP4)R6K ori, Cm^r	(29)
pRE112-*vas*H	pRE112 derivative, designed for knockout of *vas*H, Cm^r	This work
pRE112-*hcp*1	pRE112 derivative, designed for knockout of *hcp*1, Cm^r	This work
pRE112-*hcp*2	pRE112 derivative, designed for knockout of *hcp2*, Cm^r	This work

contamination, and duplicated reads. The final 100× libraries were generated with clean-read data. The reads were assembled with SOAPdenovo v1.05.

Gene Prediction and Annotation

Putative coding sequences (CDSs) were predicted by Glimmer version 3.0. Transfer RNA (tRNA) genes were explored by the tRNA scan-SE. The rRNAmmer was used to analyze Ribosome RNA (rRNA) genes, while the Rfam database was used to predict small nuclear RNAs (snRNA). Based on the homologous blast method, the transposons were identified using transposon PSI. We used web server PHAST (http://phast.wishartlab.com/) to find prophage sequences and CRISPR Finder.2.3.3 to search for the CRISPR arrays. Functional annotation of CDSs was performed by searching the non-redundant protein database from the NCBI. COGs (clusters of orthologous groups) were obtained from the eggNOG (version 3) database. Proteins with 30% similarity were judged as orthologs and paralogs (30). Metabolic pathways were estimated using Kyoto Encyclopedia of Genes and Genomes (KEGG) database (30). The statistical enrichment of differentially expressed genes in the KEGG pathway was investigated using **KOBAS** software. Genomic islands (GIs) were analyzed by IslandViewer tool. The genome map was drawn by CGView.

MLST and Phylogenetic Analysis

MLST was performed by amplifying six housekeeping genes (*gyr*B, *gro*L, *glt*A, *met*G, *pps*A and *rec*A) with primers (**Supplementary Table 1**) as previously described (8). Six housekeeping genes were amplified with primers (**Supplementary Table 1**). The sequences of distinct alleles were deposited in the *Aeromonas* spp. MLST database (http://pubmlst.org/aeromonas). The STs were determined by the combination of assigned alleles.

The sets of 1,246 concatenated genes used as input for constructing whole cohort phylogenetic trees were generated using OrthoMCL (31). The BLASTp results were transformed into a normalized similarity matrix through OrthoMCL. Markov Cluster algorithm (MCL) was used to cluster orthologous sequences. All of the single-copy homologous proteins and their sequences were extracted from the OrthoMCL clustering results. Multi-sequence alignment of single-copy homologous protein was then sequenced using MAFFT (32). Use Gblocks (Version 0.91b) was used to extract conservative sites of multiple sequence alignment results (33). Maximum likelihood trees were generated with RAxML version 8.0.26 with GTR-GAAMA (34). *Bootstrap* analysis *used* 1,000 *pseudo-replicates*. A phylogenetic tree was further visualized using the iTOL tree website (http://itol.embl.de/).

Construction of *A. hydrophila* Mutants

The mutation of *A. hydrophila* genes was exercised as described previously (35). Primers and plasmids used in this experiment are listed in **Table 1** and **Supplementary Table 1**. The primers were designed based on the whole genome of *A. hydrophila* GD18. The upstream and downstream flanking fragments of *vas*H were amplified with primers P1/2 or P3/4 and were cloned into *Kpn*I sites of pRE112 vector to construct pRE112-Δ*vas*H. We used the donor *E. coli* χ7213 to transfer the suicide plasmids. The mutation was verified by PCR via primers P1/P4. The double-mutant strain Δ*hcp*1/2 was constructed using the same method.

Hcp Protein Secretion Assay

Western blot analysis was conducted to explore the secretion of Hcp in *A. hydrophila* GD18 and mutant strains as described previously (36). Bacteria were grown in 10 mL LB medium at different temperature conditions, and then centrifuged at 10 000×*g* for 10 min. The cell pellets were resuspended with PBS and supernatants were collected and filtered using a 0.22-μm filter. The samples were separated by 12% SDS-PAGE and transblotted onto *PVDF membrane* (Millipore, USA). The membrane was blocked by 5% non-fat dry milk, then indicated primary antibodies (anti-Hcp at 1:1,000) were used, following secondary antibodies (HRP-conjugated anti-rabbit IgG, 1:5,000).

Then, blot bands were visualized with an Image Quant LAS 4,000 system (GE Healthcare, USA).

The Growth Curve and Virulence Determination

Growth of the Δ*vas*H strain was compared with growth of the wild-type strain GD18 (37). The bacteria were grown in LB medium at 28°C for 8 h with shaking. Then cultures were then inoculated (1:500, v/v) into fresh LB medium. OD_{600} nm reads were taken hourly for 24 h.

The bacterial median lethal doses (LD_{50}) were determined in a zebrafish animal infection model as previously described (38, 39). Prior to infection, bacteria were washed in triplicates with sterile PBS and serially diluted. Dilutions were intraperitoneally injected into six groups of zebrafish, 10 fish per group. Negative control zebrafish were injected only with PBS. The fish were observed for 2 weeks and surviving fish were sacrificed on day 14 post-infection. LD_{50} values were determined based on *Karber's* methods (40).

The systemic dissemination capacity of *A. hydrophila* strains were further investigated using grass carp as an infection model. Briefly, grass carp i.p. infected with 10 LD^{50} (2.73×10^3 CFU/fish) by *A. hydrophila* were euthanized and dissected 24 h post-infection. The target organs spleen, kidney, and liver were collected, weighed, and homogenized with PBS. Homogenized samples were plated on LB plates for bacterial count with a ten-fold dilution method.

Whole Blood Killing and LDH Cytotoxicity Assay

Whole blood killing assay was performed as described by Xie et al. (37). Blood exsanguinated from adult grass carp caudal vein using a sterile syringe with pre-added anticoagulant heparinized following anesthetized with MS-222. 900 μL heparinized blood was mixed with 100 μL bacteria cultures at a concentration of 1×10^5 CFU/mL. The mixtures were then placed at 28°C. 100 μL mixtures were taken at 2 h, serially diluted, spread on LA agar, and incubated at 28°C overnight.

LDH release was assayed using the LDH Cytotoxicity Assay Kit (Promega, USA). CIK cell monolayers were incubated with the GD18 and mutants at a multiplicity of infection (MOI) of 5 for 2 h. The supernatants were collected for measuring the LDH release. The percentage of cytotoxicity was calculated according to the manufacturer's instructions: [(OD_{490nm} sample - OD_{490nm} spontaneous)/ (OD_{490nm} maximum release - OD_{490nm} spontaneous)] ×100. OD_{490nm} spontaneous represented LDH release from uninfected cells into the culture supernatant and OD_{490nm} maximum release indicated LDH release acquired by lysis of the uninfected cells. At least three independent experiments were executed in triplicate wells.

Bacterial Competition Assays

The bacterial competition assay was carried out as previously described with minor modifications (41). *E. coli* DH5α was transformed with pET-28a to confer kanamycin resistance. All bacteria strains were grown to the logarithmic phase (OD_{600nm} of 0.5). The attacker *A. hydrophila* (ampicillin-resistant) and the prey *E. coli* DH5α (kanamycin-resistant) were mixed at a ratio of 1:5. The mixture was incubated on LA plates with a nitrocellulose membrane at 28°C for 3 h. Surviving *E. coli* were collected and serially diluted onto kanamycin LB plates, then incubated for 24 h. Each assay was performed three independent times in triplicate.

Analysis of T6SS Core Genes Expression Levels by qRT-PCR

Gene expression of T6SS core genes was measured by qRT-PCR (42). *A. hydrophila* strains were incubated in LB medium or LB medium with 50% grass carp serum until mid-log phase ($OD_{600\ nm}$ of 0.6) and used for RNA-extraction. Total RNA was isolated using Trizol reagent (Invitrogen, USA). Reverse transcription was carried out using M-MLV reverse system (Promega, USA) and the random primers following the manufacturer's instructions. Quantitative real-time PCR (qPCR) using Fast SYBR Green PCR Master Mix (Bio-Rad, USA) was run on the CFX96 Real-Time System (Bio-Rad, USA). All primers used for qPCR are shown in **Supplementary Table 1**. Gene expression was calculated according to the $2^{-\Delta\Delta CT}$ method. The 16sRNA gene was used as a reference gene for normalization. The relative expression level was obtained as the ratio compared to that of the wild-type strain GD18. All *experiments were* independently conducted three times.

Statistical Analysis

Prism GraphPad 8 (GraphPad Software) was employed for statistical analysis. Unpaired *t*-tests and two-way ANOVA followed by multiple comparisons were used for statistical analysis. A *p*-value of < 0.05 was significant statistically ($^*p < 0.05$, $^{**}p < 0.01$, $^{***}p < 0.001$, $^{****}p < 0.0001$). *All* the *experiments were repeated* thrice independently before analyzing data.

RESULTS

Biological Characteristics and Multilocus Sequence Type Analysis of Virulent *A. hydrophila* GD18

A. hydrophila GD18 was isolated from sick grass carp (*C. idella*) in Guangdong province, China, in 2017. Observed by transmission electron microscopy, *A. hydrophila* GD18 is rod-shaped and possesses one polar flagellum (**Figure 1A**). Consistently, it could spread on a swimming agar plate (**Figure 1B**). Typical β-hemolysis was also detected, indicating *A. hydrophila* GD18 could produce and secrete β-hemolysins (**Figure 1C**). The grass carp intraperitoneally (*i.p.*) infected by *A. hydrophila* GD18 showed the same symptoms as the naturally infected fish, such as diffuse hemorrhages on the skin and abdominal swelling. After dissection, massive ascites flowed out, and internal organs exhibited hyperemia (**Figure 1D**). Zebrafish is a model animal for measuring the virulence of *A. hydrophila* (43). The LD_{50} of GD18 in zebrafish was 2.73×10^2 CFU/fish, which was indicative of its high pathogenicity to fish.

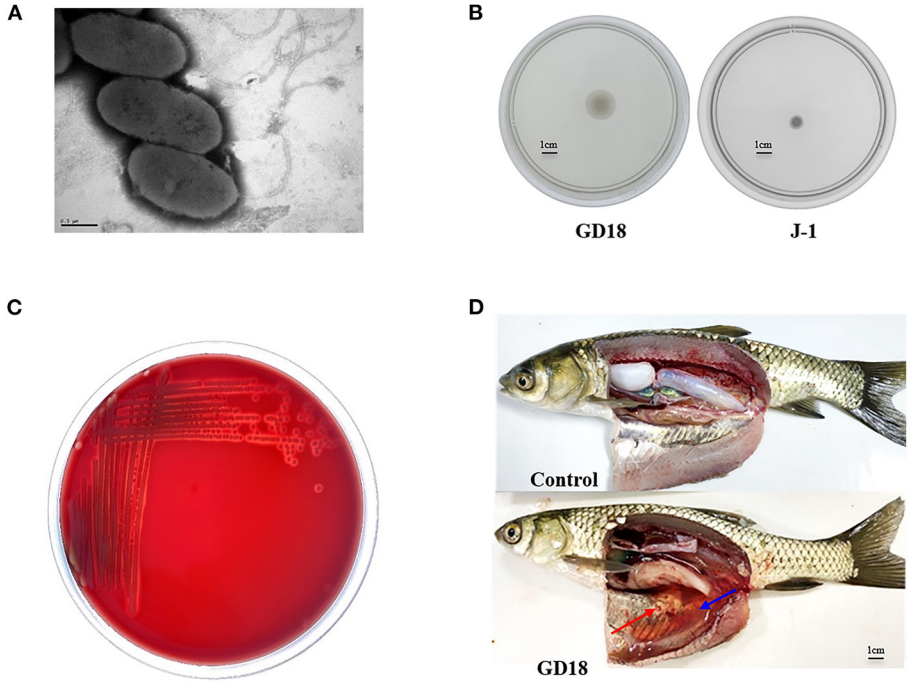

FIGURE 1 | Biological characteristics of *A. hydrophila* GD18. **(A)** Morphological characteristics of *A. hydrophila* GD18 observed under a transmission electron microscopy. **(B)** Swimming motility of *A. hydrophila* GD18. **(C)** The hemolytic activity of *A. hydrophila* GD18 was confirmed by plating on a blood agar plate. **(D)** Grass carp i.p. infected with 2.73×10^3 CFU/fish by *A. hydrophila* GD18 displayed typical symptoms of motile *Aeromonas* septicemia after 24 h. The blue arrow indicates massive ascites and the red arrow indicates the peritoneal mucosa bleeding spots.

TABLE 2 | The multilocus sequence typing (MLST) of *A. hydrophila*.

Strains	Host	Country	Year	ST	Allele					
					*gyr*B	*gro*L	*glt*A	*met*G	*pps*A	*rec*A
GD18	Grass carp	Guangdong, China	2017	**656**	415	164	160	267	457	160
J-1	Crucian carp	Jiangsu, China	1989	**251**	210	214	122	211	221	217

To emphasize that this is the result of the ST sequence type.

To determine the epidemiological relation of *A. hydrophila* GD18 with other isolates, MLST was performed. The concatenated sequences of the six alleles (*gyr*B, *gro*L, *glt*A, *met*G, *pps*A, and *rec*A) of GD18 were different from the ST251 group, which is considered to be accountable for the ongoing MAS outbreaks in China and the Southeastern United States. GD18 was found to belong to a new ST656, which hasn't been reported so far (see **Table 2**).

Genome Sequencing and Phylogenetic Analysis

Considering the new ST of *A. hydrophila* GD18, whole-genome sequencing was applied. The genome size is 4,946,275 bp with 61.03% GC content (**Figure 2**). A total of 126 non-coding RNAs were also predicted in the GD18 genome. The analysis showed that there were no plasmids. CRISPR is a specific family of DNA direct repeat sequences that is broadly distributed in prokaryotic genomes. One CRISPR array was predicted in the GD18 genome.

A total of 4,571 open reading frames (ORFs) were found with an average length of 904 bp, constituting 83.57% of the genome. 4,051 out of the 4,571 ORFs were annotated into 24 categories in the COG database (**Figure 3A**). The six most abundant categories were amino acid transport and metabolism (367), signal transduction mechanisms (343), transcription (302), translation, ribosomal structure and biogenesis (262), energy production and conversion (257), and cell wall/membrane/envelope biogenesis (236). The numbers of genes annotated in the RNA processing and modification (1), and chromatin structure and dynamics (1) categories are the least.

KEGG database is a collection of the molecular interaction and reaction networks in cells and organisms. 1,863 out of the 4,571 ORFs were annotated into 36 biological pathways of six superfamilies in the KEGG database (**Figure 3B**). Consistent with those derived from the COG database, the metabolism

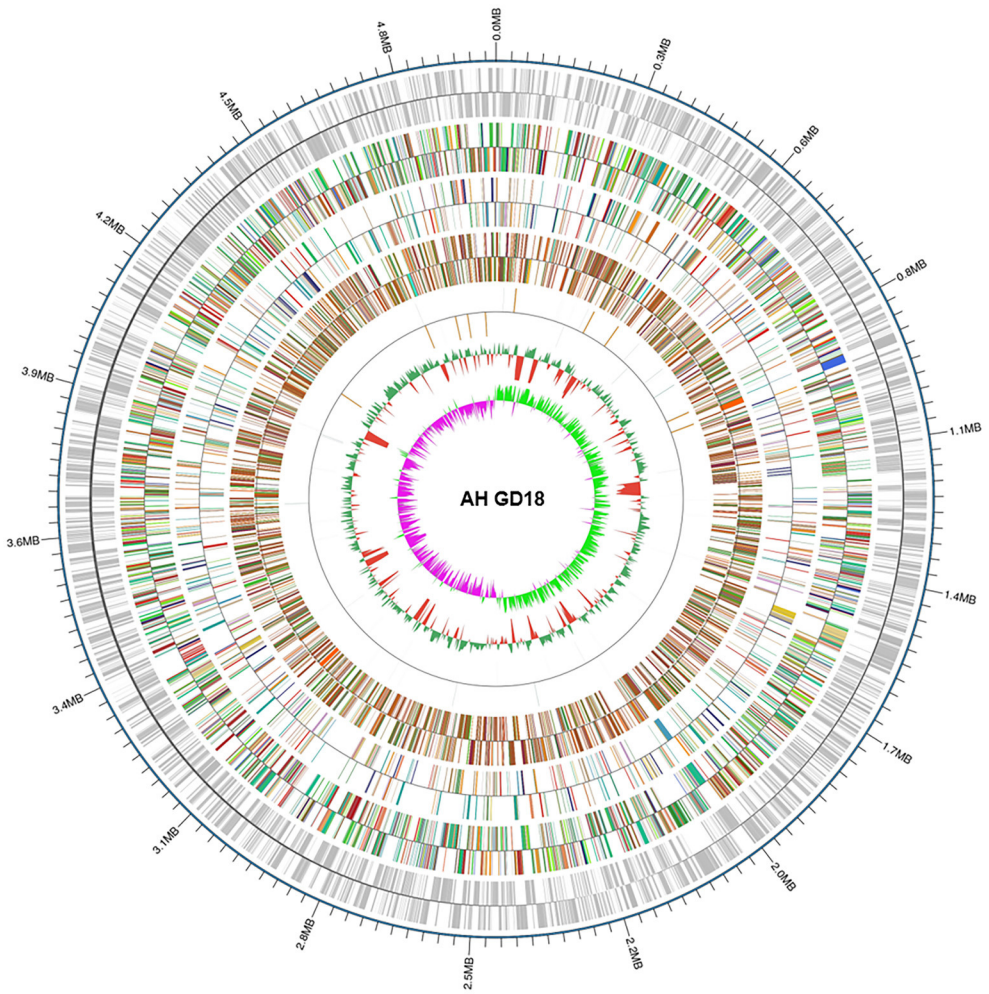

FIGURE 2 | Genome map of *A. hydrophila* GD18. Circular map for the whole genome of *A. hydrophila* GD18. From the outside to the center: genome sequence coordinates, gene annotation (COG, eggNOG, KEGG, and GO categories), ncRNA, GC content, and GC skew (G – C/G + C).

superfamily was the most abundant with total of 894 genes. Notably, the second most abundant was the environmental information processing superfamily, with 160 genes in the signal transduction pathway and 205 genes in the membrane transport pathway, coincident with its ecological adaption. Furthermore, 27 and 62 genes were annotated to have the functions of infectious diseases and drug resistance, respectively.

We then performed phylogenetic analysis to investigate the evolutionary relationship of GD18 with other *A. hydrophila* isolates. The phylogeny tree was built with 78 fish and environmental *A. hydrophila* strains based on the 1,246 core genes (**Figure 4**). Strain L14f, isolated from a lake water sample in Malaysia, was found in close proximity to GD18. Most of the strains in the clade to which the GD18 strain belongs are environmental isolates. The epidemic strains including Chinese isolates NJ-35, J-1, and American isolates ML09-119, AL09-71 and pc104A formed separate linages, and fell into nearby clades. The ST251 strains also clustered closely but distantly related to ST656 strain GD18. Based on this phylogenetic analysis, GD18 was closer to environmental isolates, including the *A. hydrophila* reference strain ATCC 7966^{T} than to epidemic strains. Hence, the mechanism of how *A. hydrophila* GD18 balances the environmental adaptability with virulence is worth further study.

T6SS in *A. hydrophila* GD18 and the Regulation Condition

Bacterial cells communicate with their surroundings via the secretory system. As one of the most recently identified secretion systems, T6SS can convey toxins into eukaryotic cells as well as other bacteria, highlighting the importance of the T6SS not only in the context of infection and disease but for efficient competition with indigenous microbiota for limited resources (17). The T6SS gene cluster of GD18 was found to cover 21 kb with 25 conserved T6SS core genes from AHG_GM1911 to _GM1935 (**Figure 5A**). AHG_GM1911, named *hcp*2, encoded the ortholog of the Hcp superfamily. There were two VgrG superfamily genes in the T6SS gene cluster. AHG_GM1912 was named *vgr*G2 and AHG_GM1935

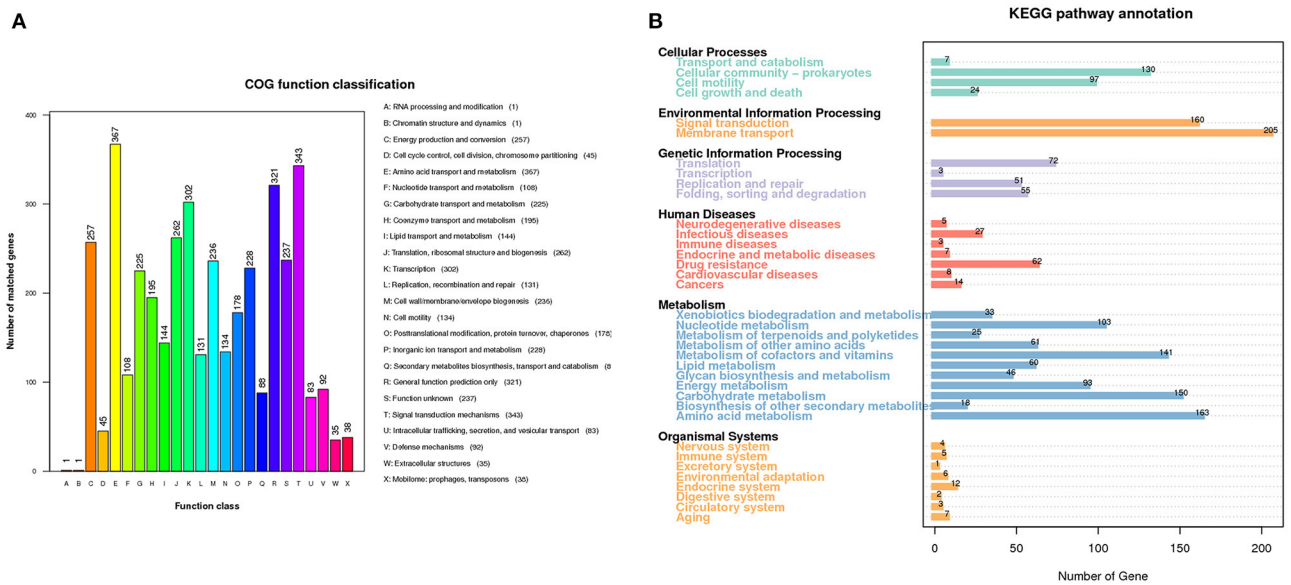

FIGURE 3 | Gene functional analysis of *A. hydrophila* GD18. **(A)** Gene functional classifications of *A. hydrophila* GD18 based on the Clusters of Orthologous Groups (COG) proteins database. **(B)** Metabolic pathways categories of *A. hydrophila* GD18 genes based on the KEGG database.

was named *vgr*G3. AHG_GM1934 encoded a PAAR-repeat protein which assembles a sharp appendix on the VgrG tip. AHG_GM1918 named *vip*A, and AHG _GM1919 named *vip*B, formed a polymerization sheath structure surrounding the tube rings. AHG_GM1928 belonged to the ClpV1 superfamily and was named *clp*V, dissociating the VipA/VipB complex to power the T6SS. The gene encoding the other Hcp (named *hcp*1) and the two genes encoding VgrG (named *vgr*G1 and *vgr*G4) were also found outside the T6SS cluster. The secretion of Hcp is thought to be a reliable marker of functional T6SS (44). When GD18 grew to 6 h, Hcp was detectable in both whole-cell and supernatant samples, suggesting that T6SS of GD18 is functional (**Supplementary Figure 1**).

Conditional expression of T6SS is thought to be favorable for the survival of bacteria in the natural habitat and interaction with their hosts. The regulation condition of T6SS in GD18 was investigated. We first compared the transcriptional levels of the T6SS genes at 28°C with that at 16°C. The transcriptional levels of *tle*1 (45), *hcp* and *vas*H exhibited 1.9-fold ($p < 0.05$), 4.7-fold ($p < 0.0001$) and 2.7-fold ($p < 0.0001$) increase, respectively, at 16°C compared to the 28°C culture conditions (**Figure 5B**). In consistence, the expression of the Hcp protein increased with temperature decreasing in both whole-cell and culture supernatant samples (**Figure 5C**). The Hcp could not be detected in the supernatant when the temperature was raised to 37°C, indicating the inactivation of T6SS at this temperature.

It has been proved that the T6SS expression of *Pseudomonas aeruginosa*, *Salmonella* Typhimurium, and avian pathogenic *Escherichia coli* was increased during infection (42, 44–46). Considering the bactericidal property, fish serum was used to simulate *in vivo* conditions. It was revealed that the transcripts of all the T6SS core genes, including *hcp*, *vas*H, *clp*V, and *dot*U, increased under grass carp serum conditions relative to LB conditions. In particular, the highest up-regulated gene was *vas*H (3.7-fold) ($p < 0.0001$) (**Figure 5D**). In summary, T6SS is conditionally regulated in GD18.

VasH Contributes to the T6SS-mediated Bactericidal Activity of *A. hydrophila* GD18

Transcription of *hcp* is regulated by a multiple bacterial enhancer binding protein (bEBP) VasH in *V. cholera* (47). In *A. hydrophila* GD18, the large T6SS gene cluster contains gene *vas*H. To explore the function of VasH in GD18, a *vas*H deletion mutant (Δ*vas*H) was constructed by homologous recombination (**Figure 6A**). Δ*vas*H mutant has a similar growth rate with **wild-type** strain in culture condition (**Figure 6B**).

Deletion of the *vas*H gene totally abolished the transcription of *hcp* and the expression of Hcp, indicating the inactivation of T6SS (**Figures 6C,D**). In addition, the transcription of T6SS core genes, including *vgr*G, AHG_GM1916 (hypothetical protein-coding gene), antibacterial effector *tle*1 significantly decreased in Δ*vas*H than in the wild-type strain (**Figure 6C**). On the contrary, the impact of *vas*H mutation on *vip*A and *vip*B transcripts was relatively limited.

To determine whether VasH contributed to the bactericidal activity of *A. hydrophila* GD18, growth competition experiments were conducted (**Figure 7**). When co-cultured with *A. hydrophila* GD18, the survived *E. coli* reduced six $\log_{10}$ in number compared to *E. coli* cultured alone. Compared with the wild-type strain group, the inhibition of *E. coli* growth by Δ*vas*H was markedly reduced. Δ*hcp*1/2 was set as a positive control. These results suggested that the T6SS is vital to the antibacterial activity of *A. hydrophila* GD18 and that VasH takes part in T6SS regulation and mediating the bactericidal activity.

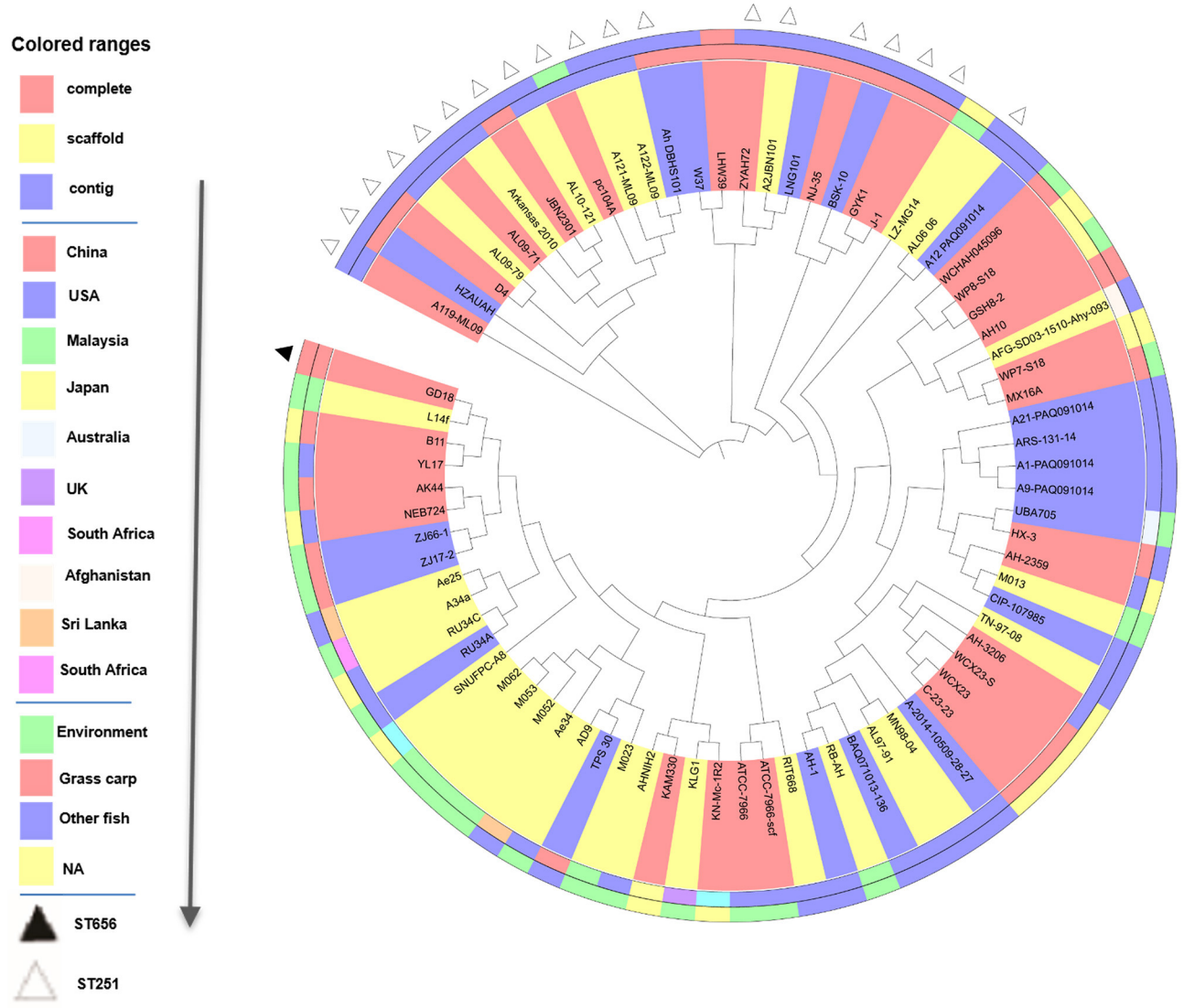

FIGURE 4 | Phylogenetic tree analysis of 78 *A. hydrophila* strains. Phylogenetic tree based on the 1246 core genes of the 78 *A. hydrophila* isolates. Sequencing type, isolation country, and source of *A. hydrophila* strains are color-coded in the following rings. On the outermost ring, STs are distinguished by triangles.

VasH Contributes to Cytotoxicity and Resistance Against Fish Blood Killing

The cytotoxic effect of *A. hydrophila* strains was tested by determining the activity of the LDH enzyme of CIK cells. Compared to the wild-type strain, Δ*vas*H infection caused a significant decreased (53%) ($p < 0.001$) of LDH release by CIK cells after 2 h of infection at a MOI of 5 (**Figure 8A**).

Furthermore, we explored the resistance against host killing of *A. hydrophila* strains in grass carp blood. Both of the Δ*vas*H and wild-type strains proliferate after incubation with heparinized fish blood, suggesting whole blood cannot effectively kill both Δ*vas*H and wild-type strains. However, after 2 h of incubation, the bacteria number of Δ*vas*H was 4.29×10^4 CFU/mL and that of wild-type strain was 9.46×10^4 CFU/mL, demonstrating Δ*vas*H was less resistant to the bactericidal effect of grass carp blood ($p < 0.0001$) (**Figure 8B**).

VasH Is Required for Virulence and Systemic Dissemination of *A. hydrophila* GD18

To determine whether the mutation of *vas*H affects virulence, we further calculated the LD_{50} values of different strains using a zebrafish intraperitoneally infection model. The LD_{50} value of *A.hydrophila* GD18 was 2.73×10^2 CFU (see **Table 3**), while Δ*vas*H had a nearly 4.4-fold higher LD_{50} value. The results indicated that VasH contributes to the virulence of *A. hydrophila* GD18. Moreover, the deletion of the *vas*H decreased capacity of systemic dissemination. The bacterial loads of the Δ*vas*H in

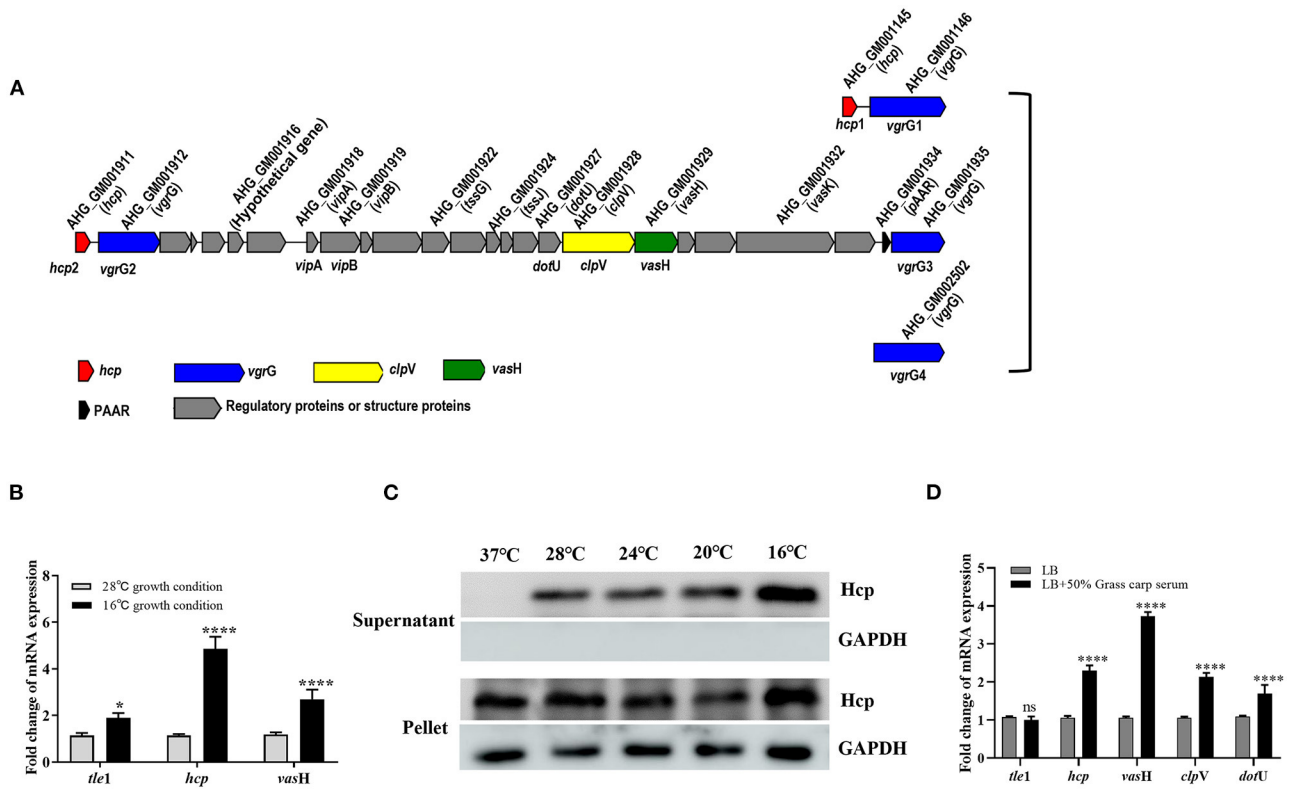

FIGURE 5 | T6SS is conditionally regulated in *A. hydrophila* GD18. **(A)** Genetic organization of the T6SS major structural gene cluster in *A. hydrophila* GD18. **(B)** Transcripts of the T6SS genes are elevated at 16°C comparing to that at 28°C. **(C)** Expression and secretion of Hcp protein at different temperatures. Anti-GAPDH antibody served as an internal reference. **(D)** Grass carp serum significantly upregulated transcripts of T6SS core genes at 28°C. The transcripts in the indicated conditions were analyzed by qRT-PCR. In B and D, *A. hydrophila* cultures were grown until mid-log phase ($OD600_{nm}$ of 0.6) and used for RNA-extraction. The data was presented as the mean ± SD of three independent experiments. In C, the data was from one representative experiment with at least three independent biological replicates. Statistical significance was calculated by 2-way ANOVA followed by Sidak's multiple comparisons test. ns, not significant; $^{*}p < 0.05$; $^{****}p < 0.0001$.

the organs, including spleen, kidney, and liver were reduced by 42, 93, and 80%, respectively, comparing to those of wild-type (**Figure 9**).

DISCUSSION

Aeromonas hydrophila is ubiquitous in various aquatic environments and causes disease in fish, reptiles, amphibians, and humans (48). This organism has evolved a variety of successful apparatus under competitive forces to adapt to various habitats both *in vitro* and *in vivo*. In this study, *A. hydrophila* GD18 was isolated from sick grass carp. Because of the high yield and desirable flavor, grass carp is one of the most dominant freshwater fish species in China. Nevertheless, the decline of the aquaculture environment and germplasm degradation of grass carp species lead to increasing *A. hydrophila* infection, resulted in heightened economic losses, which raised more and more attention (49).

Observation with the transmission electron microscope clearly showed that *A. hydrophila* GD18 possesses polar flagellum. And the swimming motility halo of GD18 tested by the swimming plate showed a distinct motile phenotype with a large diffuse spreading diameter. It is known that polar flagella are usually important locomotive organelles and virulence factors for bacterial motility and colonization (50). Motile aeromonad is the causative agent of MAS in fish (51). Motility takes a leading role in the initial phases of the infection in bacterial pathogens (50). The above phenotype and the presence of β-hemolysins alluded to the pathogenic capabilities of GD18. The grass carp intraperitoneally infected by GD18 also exhibited clinical signs typical of hemorrhagic septicemia. Furthermore, the LD_{50} of GD18 in zebrafish (2.73×10^2 CFU/fish) was much less than the "virulence" criteria ($<1.0 \times 10^6$ CFU/fish) used by Pang et al. (9), indicating that GD18 could be classified as a high virulent strain.

Accompanied with confusion and argument, the taxonomy of the genus *Aeromonas* is complicated (48). MLST is an explicit method to identify the bacterial isolates based on the allelic profiles of house-keeping genes (48). The previous study concluded that ST251 is a risky group and would be responsible for the MAS outbreaks in recent years, as 17 virulent strains including the five epidemic strains all belonged to ST251 (9). Moreover, there was a high relevance between the genetic phylogeny and pathogenicity. The strains

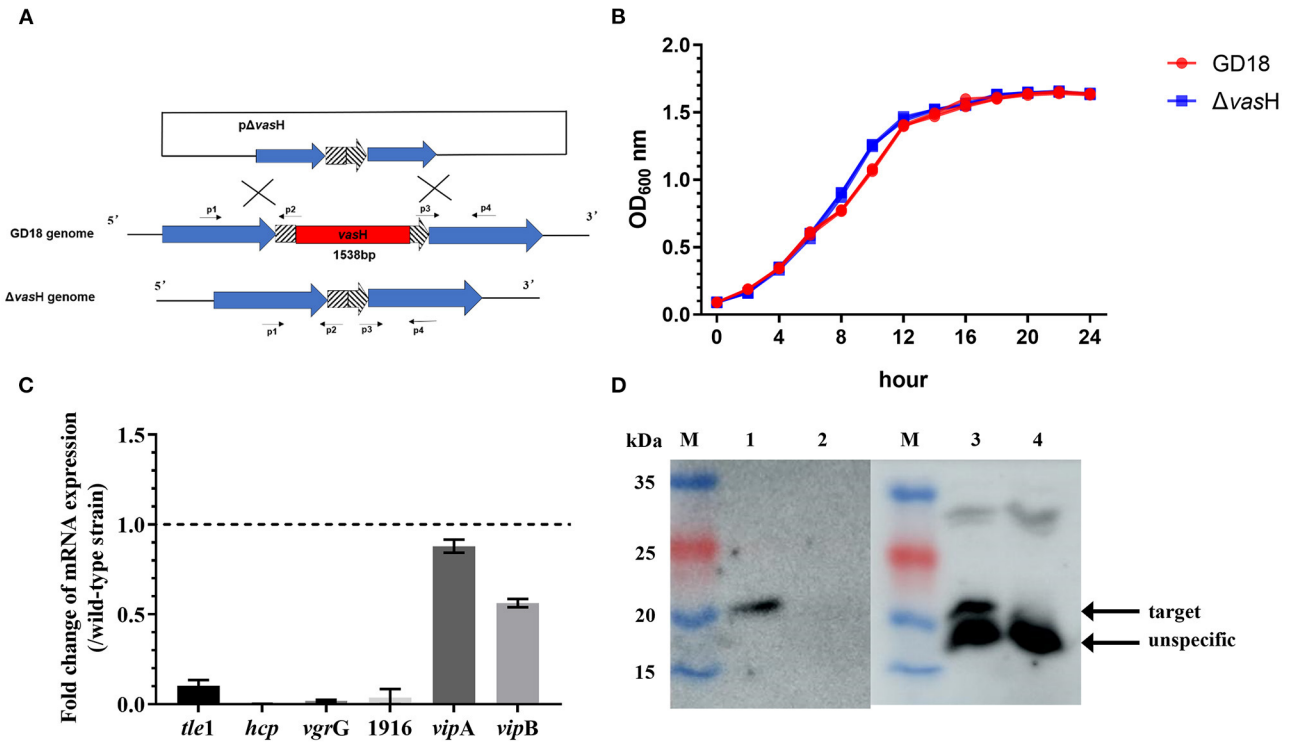

FIGURE 6 | Construction and phenotypic characterization of Δ*vas*H strain. **(A)** Construction strategy of Δ*vas*H by homologous recombination. **(B)** Growth curves in LB medium over a 24 h period at 28°C. **(C)** Fold change of transcriptional levels of the T6SS genes in Δ *vas*H comparing to that in the wild-type strain at 28°C. The mRNA level of each gene was normalized to that of 16S rRNA. The data was presented as the mean ± SD of three independent experiments. **(D)** Hcp expression and secretion in whole-cell and supernatants of wild-type and mutant strains. Lane M, PageRuler prestained protein ladder; lane 1, GD18 supernatant; lane 2, Δ*vas*H supernatant; lane 3, GD18 whole-cell; lane 4, Δ*vas*H whole-cell. The data was from one representative experiment with at least three independent biological replicates.

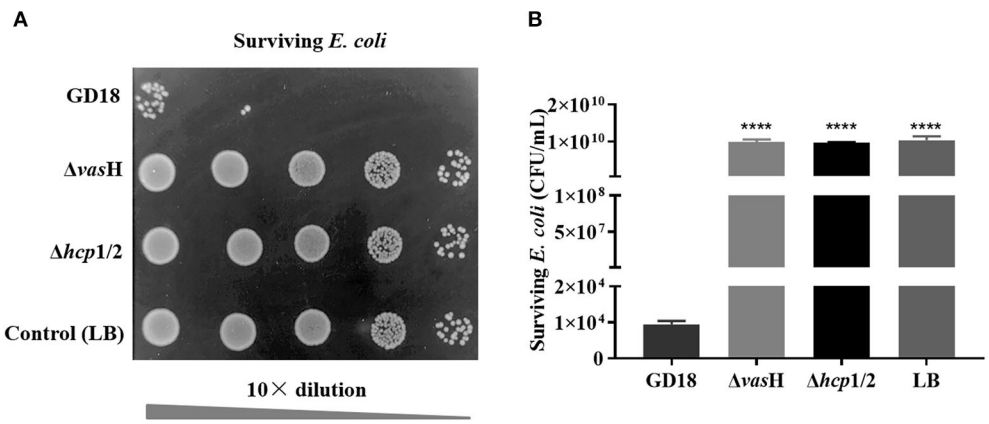

FIGURE 7 | VasH contributes to the bactericidal effect of *A. hydrophila.* The survival of *Escherichia coli* was determined post-incubation with different *A. hydrophila* strains as indicated. **(A)** The surviving *E. coli* cells were serially diluted and determined on the LA plates supplemented with kanamycin. Control indicates incubation of *E. coli* with sterile LB medium alone. Δ*hcp*1/2 mutant group was set as the T6SS defective control group. **(B)** The data was presented as the mean ± SD of three independent experiments. Statistical significance was calculated by unpaired *t*- test. ****$p < 0.0001$.

that belonged to ST251 clonal group all exhibited virulence while the other ST strains were avirulent in zebrafish (9). *A. hydrophila* GD18 was determined to belong to a novel serotype of ST656, which hasn't been described in any published literature. Considering its pathogenic potential verified in this study, complete genome sequencing was carried out to provide a comprehensive understanding of this strain.

According to COG and KEGG-based functionally annotation, the core genome was enriched in metabolism-related genes, followed by environmental information processing superfamily

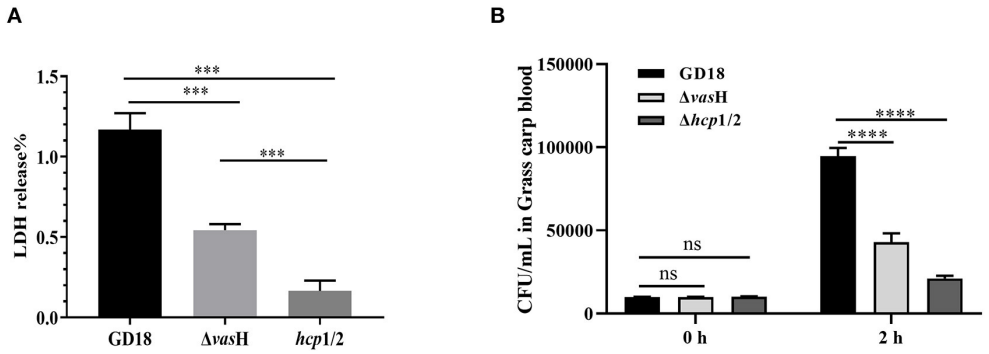

FIGURE 8 | VasH contributes to cytotoxicity and resistance against fish blood killing. **(A)** Cytotoxicity results after 2 h of incubation. **(B)** Bacteira number following 2 h of incubation with whole blood of grass carp. The data was presented as the mean ± SD of three independent experiments. In A, statistical significance was calculated by unpaired t- test. In B, statistical significance was calculated by 2-way ANOVA followed by Sidak's multiple comparisons test. ns, not significant; ***$p < 0.001$, ****$p < 0.0001$.

TABLE 3 | Calculations of LD_{50}s of the *A. hydrophila* GD18 and mutant strains in zebrafish.

Dose of challenge CFU	Number of death/Total			Survival rate (%)		
	GD18	Δ*vas*H	Δ*hcp*1/2	GD18	Δ*vas*H	Δ*hcp*1/2
10^5	10/10	10/10	10/10	0	0	0
10^4	10/10	8/10	5/10	0	20	50
10^3	9/10	5/10	2/10	10	50	80
10^2	0/10	0/10	0/10	100	100	100
LD^*_{50}	2.73×10^2	1.19×10^3	5.62×10^3			

**The LD_{50} was calculated according to Karber's method.*

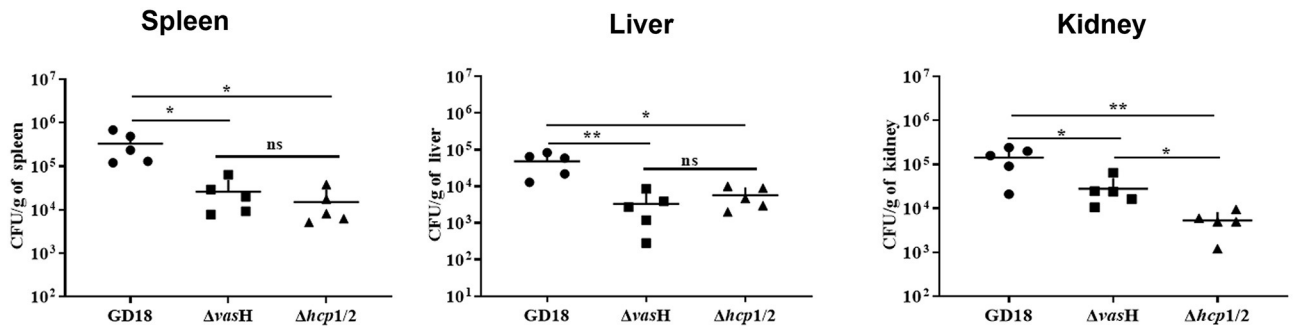

FIGURE 9 | VasH is required for systemic dissemination of *A. hydrophila* GD18. Grass carp i.p. infected with 2.73×10^3 CFU/fish by *A. hydrophila* were euthanized and dissected 24 h post-infection. The data was presented as mean ± SD of five biological replicates from one representative experiment of three independent experiments. Statistical significance was calculated by unpaired *t*- test. ns, not significant; *$p < 0.05$; **$p < 0.01$.

like signal transduction pathway. To note, both COG and KEGG databases produced consistent results, explaining the relationship between the gene function and environmental adaption mechanism of *A. hydrophila* GD18. Previously, the comparative genome analysis of 49 *A. hydrophila* genomes revealed that core genes were higher among the classes of substance dependence, amino acid metabolism, cell cycle and endocrine system, yet not mentioned genes related to environmental information processing and environmental adaptation (52). These genomic features reflect the evolutionary adaptation of *A. hydrophila* strains to different environments and infection strategies.

To determine the evolutionary relationships of GD18 with other *A. hydrophila* strains, 78 *A. hydrophila* genome sequences (31 complete, 28 scaffold, and 19 contig genomes) were obtained from the NCBI database. Phylogenic analysis based on core-genome demonstrated that GD18 clustered in one branch with strain L14f, B11, YL17, AK44, NEB724, ZJ66-1, and ZJ17-2. Five of these strains were environmental isolates. The branch was distantly away from the ST251 clone. According to available

literature, L14f was isolated from lake water, B11 was isolated from diseased *Anguilla japonica* (53), and YL17 was isolated from a compost pile (53). Among them, B11 was the only know virulence strain, with a LD_{50} of 2.98×10^4 CFU/ml (1.49×10^3 CFU/fish) in zebrafish (53). The pathogenicity of the other isolates has not been reported so far. In the previous studies of *V. cholera*, environmental strains were considered a repository of virulence genes (54–56). The possibility for "mixing and matching" of genes in the environment pool resulting in new pathogenic variants should be taken more seriously. Similarly, *A. hydrophila* exists in aquatic ecosystems as an inherent resident globally. Further studies on the ecology and evolution of *A. hydrophila* will undoubtedly provide valuable perceptions into the epidemiology of MAS. For strain GD18, the close evolutionary relationship with environmental strains and pathogenic characteristics make it particularly important to uncover the mechanism of balancing the relationship between the two aspects.

T6SS is vital in interbacterial competition and is a major virulence determinant for numerous Gram-negative bacteria. T6SS translocates effectors into the extracellular surroundings, and frequently into neighboring prokaryotic or eukaryotic cells (17). Our study discovered that *A. hydrophila* GD18 gemome has a complete T6SS cluster. Further detection of Hcp in the culture supernatants confirmed the T6SS was functional. For allowing the bacteria to thrive in a competitive environment and to occupy the niche successfully, the expression of T6SS is tightly regulated. In *Yersinia pestis* and *V. cholerae* O1 strains, the T6SS gene cluster has been shown to be induced at low temperature rather than host body temperature. Along these lines, the activation of T6SS was regarded to assist the environmental survival and infection (56). In *A. hydrophila* GD18, Hcp and VasH expression was strongly induced by low temperature (16°C), suggesting that the activation of T6SS promotes the *A. hydrophila* environmental survival. To note, the secretion of Hcp was totally abrogated at 37°C. As *A. hydrophila* GD18 was fish-isolated, the pathogenicity to warm-blooded animals was still unknown. Fernández-Bravo et al. presented a human case of necrotizing fasciitis due to co-infection with 4 *A. hydrophila* strains (NF1–NF4). NF1 strain was determined to be phylogenetically distinct and exhibited contact-dependent killing of NF2 mediated by T6SS at 37°C (57). Therefore, different *A. hydrophila* isolates may employ particular temperature-regulation mechanisms of T6SS to adapt to different environments and hosts.

The importance of T6SS in pathogenesis is becoming increasingly evident. The known genes related to T6SS integration have also been shown to contribute to the virulence of *Aeromonas* (58, 59), *Salmonella* (60), *Fracisella* (61), and *Edwardsiella* (62). Consistent enhancement of transcripts of T6SS genes under grass carp serum conditions suggests an essential role for the T6SS in *A. hydrophila* infection. Among them, *vas*H, a σ^{54}-transcriptional activator coding-gene, with the highest upregulation attracted our attention. To assess the function of VasH in *A. hydrophila*, a *vas*H mutant was constructed. It showed that the secretion and expression of Hcp were abolished in Δ*vas*H. In addition, the transcription of T6SS core genes *vgr*G, AHG_GM1916, and *tle*1 all decreased in Δ*vas*H than in the wild-type strain. In *V. cholera* O1, VasH is necessary for the functional T6SS as it regulated Hcp production (63). Suarez et al. provided evidence that *vas*H was necessary for the expression of Hcp in clinical *A. hydrophila* isolate SSU, which was later reclassified as *A. dhakensis* (7, 23). In *V. fischeri*, it was shown that σ54 interacts with RNA polymerase at the promoter region of *hcp*. Meanwhile it was proposed that hexameric VasH binds to the upstream of promoter (26). Results in this study indicated that VasH in *A. hydrophila* GD18 involved in the transcription regulation of not only T6SS apparatus protein but also anti-bacterial effector protein such as Tle1 (45). Future investigations are required to determine the regulation mechanism.

Pathogens using T6SS as an anti-microbial weapon can effectively compete with the natural microflora for limited resources (46). Therefore, we sought to determine whether VasH-mediated T6SS regulation provides competition and pathogenesis fitness to *A. hydrophila* GD18. The mutation of *vas*H significantly reduced the antibacterial activity, similar with the T6SS defective mutant Δ*hcp*1/2. The affected bactericidal capacity in Δ*vas*H could attribute to the failure of producing and assembling a functionally T6SS structure or decreased transcription of the antibacterial effectors. Wang et al. illustrated that T6SS of *A. hydrophila* contributes to the survival and infection (35). Our results supported that the disruption of the *A. hydrophila* T6SS and VasH resulted in defective anti-host killing, cytotoxicity, diminished systemic dissemination ability, and attenuated virulence in grass carp.

A. hydrophila is a ubiquitous organism in aquatic environments and also an important opportunistic pathogen. The mechanism of this waterborne pathogen to balance the environmental persistence and outbreak potential is intriguing. In this study, we reported the complete genome of a fish-pathogenic *A. hydrophila* strain GD18, which belongs to a new sequence type ST656. GD18 was found to be closely related to environmental isolates but showed high pathogenicity to fish hosts. The further analysis supported that T6SS greatly contributed to the bactericidal activity and pathogenicity and was regulated by the bacterial enhancer-binding protein VasH. The high-quality whole-genome sequences generated in this study laid an essential foundation for future studies. Moreover, investigation of the VasH would provide valuable perception into the regulation of T6SS and exciting candidates for an attractive target of therapeutics, vaccine, and antimicrobial drug development against *A. hydrophila*.

DATA AVAILABILITY STATEMENT

The data presented in the study are deposited in the Dryad Digital repository. Please refer to the

following link: https://datadryad.org/stash/share/YHITTMMGU86518rOZ1KxNEVtE04nDhDUfUztyW2owZo.

ETHICS STATEMENT

The animal study was reviewed and approved by the Ethical Committee of Institute of hydrobiology, Chinese Academy of Sciences.

AUTHOR CONTRIBUTIONS

Y-AZ and YZ: conceived and designed the experiments and writing—review and editing. JL and ZW: performed the experiments. JL, ZW, CW, and D-DC: data curation. JL: writing—original draft. All authors have read and agreed to the published version of the manuscript.

FUNDING

The study was supported by the National Natural Science Foundation of China (31772889, 32073022, and 32002431) and China Agriculture Research System (CARS-46).

SUPPLEMENTARY MATERIAL

The Supplementary Material for this article can be found online at: https://www.frontiersin.org/articles/10.3389/fvets.2021.793458/full#supplementary-material

REFERENCES

1. Ji Y, Li J, Qin Z, Li A, Gu Z, Liu X, et al. Contribution of nuclease to the pathogenesis of Aeromonas hydrophila. *Virulence.* (2015) 6:515–22. doi: 10.1080/21505594.2015.1049806
2. Singh V, Chaudhary DK, Mani I, Jain R. and Mishra BN. Development of diagnostic and vaccine markers through cloning, expression, and regulation of putative virulence-protein-encoding genes of Aeromonas hydrophila. *J Microbiol.* (2013) 51:275–82. doi: 10.1007/s12275-013-2437-x
3. Bloomfield SF, Scott E. Cross-contamination and infection in the domestic environment and the role of chemical disinfectants. *J Appl Microbiol.* (1997) 83:1–9. doi: 10.1046/j.1365-2672.1997.00199.x
4. Rasmussen-Ivey CR, Hossain MJ, Odom SE, Terhune JS, Hemstreet WG, Shoemaker CA, et al. Classification of a hypervirulent Aeromonas hydrophila pathotype responsible for epidemic outbreaks in warm-water fishes. *Front Microbiol.* (2016) 7:1615. doi: 10.3389/fmicb.2016.01615
5. Hossain MJ, Sun D, McGarey DJ, Wrenn S, Alexander LM, Martino ME, et al. An Asian origin of virulent Aeromonas hydrophila responsible for disease epidemics in United States-farmed catfish. *MBio.* (2014) 5:e00848–e00814. doi: 10.1128/mBio.00848-14
6. Tian JJ, Fu B, Yu EM Li YP, Xia Y, Li ZF. et al. Feeding Faba Beans (Vicia faba L) Reduces Myocyte Metabolic Activity in Grass Carp (Ctenopharyngodon idellus). *Front Physiol.* (2020) 11:391. doi: 10.3389/fphys.2020.00391
7. Rasmussen-Ivey CR, Figueras MJ, McGarey D, Liles M R. Virulence factors of Aeromonas hydrophila: in the wake of reclassification. *Front Microbiol.* (2016) 7:1337. doi: 10.3389/fmicb.2016.01337
8. Martino ME, Fasolato L, Montemurro F, Rosteghin M, Manfrin A, Patarnello T, et al. Determination of microbial diversity of Aeromonas strains on the basis of multilocus sequence typing, phenotype, and presence of putative virulence genes. *Appl Environ Microbiol.* (2011) 77:4986–5000. doi: 10.1128/AEM.00708-11
9. Pang M, Jiang J, Xie X, Wu Y, Dong Y, Kwok AHY, et al. Novel insights into the pathogenicity of epidemic Aeromonas hydrophila ST251 clones from comparative genomics. *Sci Rep.* (2015) 5:9833. doi: 10.1038/srep09833
10. Kaas RS, Friis C, Ussery DW. and Aarestrup FM. Estimating variation within the genes and inferring the phylogeny of 186 sequenced diverse Escherichia coli genomes. *BMC Genomic.* (2012) 13:1–13. doi: 10.1186/1471-2164-13-577
11. Mafuna T, Matle I, Magwedere K, Pierneef RE. and Reva ON. Whole genome-based characterization of listeria monocytogenes isolates recovered from the food chain in South Africa. *Front Microbiol.* (2021) 12:669287. doi: 10.3389/fmicb.2021.669287
12. Ma J, Pan Z, Huang J, Sun M, Lu C, Yao H. The Hcp proteins fused with diverse extended-toxin domains represent a novel pattern of antibacterial effectors in type VI secretion systems. *Virulence.* (2017) 8:1189–202. doi: 10.1080/21505594.2017.1279374
13. Bingle LE, Bailey CM, Pallen MJ. Type VI secretion: a beginner's guide. *Curr Opin Microbiol.* (2008) 11:3–8. doi: 10.1016/j.mib.2008.01.006
14. Brockmann SO, Piechotowski I, Kimmig P. Salmonella in sesame seed products. *J Food Prot.* (2004) 67:178–80. doi: 10.4315/0362-028X-67.1.178
15. Mougous J, Cuff M, Raunser S, Shen A, Zhou M, Gifford C, et al. A Virulence locus of pseudomonas aeruginosa encodes a protein secretion apparatus. *Science.* (2006) 312:1526–30. doi: 10.1126/science.1128393
16. Bloomfield SF, Scott EA. Developing an effective policy for home hygiene: a risk-based approach. *Int J Environ Health Res.* (2003) 13:S57–66. doi: 10.1080/0960312031000102804
17. Ho BT, Dong TG, Mekalanos JJ, A. View to a Kill: The Bacterial Type VI Secretion System. *Cell Host Microbe.* (2014) 15:9–21. doi: 10.1016/j.chom.2013.11.008
18. Pukatzki S, Ma AT, Sturtevant D, Krastins B, Sarracino D, Nelson WC, et al. Identification of a conserved bacterial protein secretion system in vibrio cholerae using the dictyostelium host model system. *Proc Natl Acad Sci U S A.* (2006) 103:1528–33. doi: 10.1073/pnas.0510322103
19. Cianfanelli FR, Monlezun L, Coulthurst SJ. Aim, load, fire: the type vi secretion system, a bacterial nanoweapon. *Trends Microbiol.* (2016) 24:51–62. doi: 10.1016/j.tim.2015.10.005
20. Grim CJ, Kozlova EV, Sha J, Fitts EC, van Lier CJ, Kirtley ML, et al. Characterization of Aeromonas hydrophila wound pathotypes by comparative genomic and functional analyses of virulence genes. *MBio.* 4:e00064. doi: 10.1128/mBio.00064-13
21. Brunet YR, Khodr A, Logger L, Aussel L, Mignot T, Rimsky S, et al. (2015) H-NS silencing of the salmonella pathogenicity island 6-encoded type vi secretion system limits salmonella enterica serovar typhimurium interbacterial killing. *Infect Immun.* (2013) 83:2738–50. doi: 10.1128/IAI.00198-15
22. Sana TG, Hachani A, Bucior I, Soscia C, Garvis S, Termine E, et al. The second type VI secretion system of Pseudomonas aeruginosa strain PAO1 is regulated by quorum sensing and fur and modulates internalization in epithelial cells. *J Biol Chem.* (2012) 287:27095–105. doi: 10.1074/jbc.M112.376368
23. Suarez G, Sierra JC, Sha J, Wang S, Erova TE, Fadl AA, et al. Molecular characterization of a functional type VI secretion system from a clinical isolate of Aeromonas hydrophila. *Microb Pathog.* (2008) 44:344–61. doi: 10.1016/j.micpath.2007.10.005
24. Blanco J, Blanco M, Wong I. Blanco JE. Haemolytic Escherichia coli strains isolated from stools of healthy cats produce cytotoxic necrotizing factor type 1 (CNF1). *Vet Microbiol.* (1993) 38:157–65. doi: 10.1016/0378-1135(93)90082-I
25. Bernard CS, Brunet YR, Gavioli M, Lloubès R, Cascales E. Regulation of type VI secretion gene clusters by sigma54 and cognate enhancer binding proteins. *J Bacteriol.* (2011) 193:2158–67. doi: 10.1128/JB.00029-11
26. Guckes KR, Cecere AG, Williams AL, McNeil AE, Miyashiro T. The Bacterial Enhancer Binding Protein VasH Promotes Expression of a Type VI Secretion System in Vibrio fischeri during Symbiosis. *J Bacteriol.* (2020) 202:e00777–19. doi: 10.1128/JB.00777-19

27. Wang N, Yang Z, Zang M, Liu Y, Lu C. Identification of Omp38 by immunoproteomic analysis and evaluation as a potential vaccine antigen against Aeromonas hydrophila in Chinese breams. *Fish Shellfish Immunol.* (2013) 34:74–81. doi: 10.1016/j.fsi.2012.10.003
28. Kennedy MJ, Yancey RJ Jr. Sanchez MS, Rzepkowski RA, Kelly SM, Curtiss R. Attenuation and immunogenicity of Δcya Δcrp derivatives of Salmonella choleraesuis in pigs. *Infect Immun.* (1999) 67:4628–36. doi: 10.1128/IAI.67.9.4628-4636.1999
29. Kang HY, Dozois CM, Tinge SA, Lee TH, Curtiss R. Transduction-mediated transfer of unmarked deletion and point mutations through use of counterselectable suicide vectors. *J Bacteriol.* (2002) 184:307–12. doi: 10.1128/JB.184.1.307-312.2002
30. Page AJ, Cummins CA, Hunt M, Wong VK, Reuter S, Holden MTG, et al. Roary: rapid large-scale prokaryote pan genome analysis. *Bioinformatics.* (2015) 31:3691–3. doi: 10.1093/bioinformatics/btv421
31. Dong X, Chao Y, Zhou Y, Zhou R, Zhang W, Fischetti VA, et al. The global emergence of a novel Streptococcus suis clade associated with human infections. *EMBO Mol Med.* (2021) 13:e13810. doi: 10.15252/emmm.202013810
32. Katoh K, Standley DM, MAFFT. Multiple Sequence Alignment Software Version 7: Improvements in Performance and Usability. *Mol Biol Evol.* (2013) 30:772–80. doi: 10.1093/molbev/mst010
33. Castresana J. Selection of conserved blocks from multiple alignments for their use in phylogenetic analysis. *Mol Biol Evol.* (2000) 17:540–52. doi: 10.1093/oxfordjournals.molbev.a026334
34. Stamatakis A. RAxML version 8: a tool for phylogenetic analysis and post-analysis of large phylogenies. *Bioinformatics.* (2014) 30:1312–3. doi: 10.1093/bioinformatics/btu033
35. Wang N, Liu J, Pang M, Wu Y, Awan F, Liles MR, et al. Diverse roles of Hcp family proteins in the environmental fitness and pathogenicity of Aeromonas hydrophila Chinese epidemic strain NJ-35. *Appl Microbiol Biotechnol.* (2018) 102:7083. doi: 10.1007/s00253-018-9116-0
36. Li J, Meng C, Ren T, Wang W, Zhang Y, Yuan W, et al. Production, characterization, and epitope mapping of a monoclonal antibody against genotype VII Newcastle disease virus V protein. *J Virol Methods.* (2018) 260:88–97. doi: 10.1016/j.jviromet.2018.07.009
37. Xie Q, Mei W, Ye X, Zhou P, Islam MS, Elbassiony KRA, et al. The two-component regulatory system CpxA/R is required for the pathogenesis of Aeromonas hydrophila. *FEMS Microbiol Lett.* (2018) 365:218. doi: 10.1093/femsle/fny218
38. Dong X, Li Z, Wang X, Zhou M, Lin L, Zhou Y, et al. Characteristics of Vibrio parahaemolyticus isolates obtained from crayfish (Procambarus clarkii) in freshwater. *Int J Food Microbiol.* (2016) 238:132–8. doi: 10.1016/j.ijfoodmicro.2016.09.004
39. Dou Y, Wang X, Yu G, Wang S, Tian M, Qi J, et al. Disruption of the M949_RS01915 gene changed the bacterial lipopolysaccharide pattern, pathogenicity and gene expression of Riemerella anatipestifer. *Vet Res.* (2017) 48:1–11. doi: 10.1186/s13567-017-0409-6
40. Reed LJ. and Muench H. A simple method of estimating fifty per cent endpoints. *Am J Epidemiol.* (1938) 27:493–7. doi: 10.1093/oxfordjournals.aje.a118408
41. MacIntyre DL, Miyata ST, Kitaoka M, Pukatzki S. The Vibrio cholerae type VI secretion system displays antimicrobial properties. *Proc Natl Acad Sci U S A.* (2010) 107:19520–4. doi: 10.1073/pnas.1012931107
42. Wang S, Yang D, Wu X, Yi Z, Wang Y, Xin S, et al. The ferric uptake regulator represses type vi secretion system function by Binding Directly to the clpV Promoter in Salmonella enterica Serovar Typhimurium. *Infect Immun.* (2019) 87:e00562–19. doi: 10.1128/IAI.00562-19
43. Rowe HM, Withey JH, Neely MN. Zebrafish as a model for zoonotic aquatic pathogens. *Develop Comparat Immunol.* (2014) 46:96–107. doi: 10.1016/j.dci.2014.02.014
44. Ma J, Sun M, Pan Z, Song W, Lu C, Yao H. Three Hcp homologs with divergent extended loop regions exhibit different functions in avian pathogenic Escherichia coli article. *Emerging Microb Infect.* (2018) 7:49. doi: 10.1038/s41426-018-0042-0
45. Ma S, Dong Y, Wang N, Liu J, Lu C, Liu Y. Identification of a new effector-immunity pair of Aeromonas hydrophila type VI secretion system. *Vet Res.* (2020) 51:71. doi: 10.1186/s13567-020-00794-w
46. Elmassry MM, Mudaliar NS, Kottapalli KR, Dissanaike S, Griswold JA, San Francisco MJ, et al. Pseudomonas aeruginosa alters its transcriptome related to carbon metabolism and virulence as a possible survival strategy in blood from trauma patients. *Msystems.* 4:e00312–18. doi: 10.1128/mSystems.00312-18
47. Kirov SM, Tassell BC, Semmler ABT, O'Donovan LA, Rabaan AA, Shaw J G. (2002) Lateral flagella and swarming motility in aeromonas species. *J Bacteriol.* (2019) 184:547–55. doi: 10.1128/JB.184.2.547-555.2002
48. Janda JM, Abbott SL. The genus Aeromonas: taxonomy, pathogenicity, and infection. *Clin Microbiol Rev.* (2010) 23:35–73. doi: 10.1128/CMR.00039-09
49. Wang S-T, Meng X-Z, Li L-S, Dang Y-F, Fang Y, Shen Y, et al. Biological parameters, immune enzymes, and histological alterations in the livers of grass carp infected with Aeromonas hydrophila. *Fish and Shellfish Immunology.* (2017) 70:121–8. doi: 10.1016/j.fsi.2017.08.039
50. Josenhans C, Suerbaum S. The role of motility as a virulence factor in bacteria. *Int J Med Microbiol.* (2002) 291:605–14. doi: 10.1078/1438-4221-00173
51. Hossain S, Heo GJ. Ornamental fish: a potential source of pathogenic and multidrug-resistant motile Aeromonas spp. *Lett Appl Microbiol.* (2021) 72:2–12. doi: 10.1111/lam.13373
52. Awan F, Dong Y, Liu J, Wang N, Mushtaq MH, Lu C, et al. Comparative genome analysis provides deep insights into Aeromonas hydrophila taxonomy and virulence-related factors. *BMC Genomics.* (2018) 19:712. doi: 10.1186/s12864-018-5100-4
53. Lim Y-L, Roberts R, Ee R, Yin W-F. and Chan K-G. Complete genome sequence and methylome analysis of Aeromonas hydrophila strain YL17, isolated from a compost pile. *Genome Announc.* (2016) 4:e00060–16. doi: 10.1128/genomeA.00060-16
54. Chakraborty S, Mukhopadhyay AK, Bhadra RK, Ghosh AN, Mitra R, Shimada T, et al. Virulence genes in environmental strains of Vibrio cholerae. *Appl Environ Microbiol.* (2000) 66:4022–8. doi: 10.1128/AEM.66.9.4022-4028.2000
55. Schwartz K, Hammerl JA, Göllner C, Strauch E. Environmental and Clinical Strains of Vibrio cholerae Non-O1, Non-O139 From Germany Possess Similar Virulence Gene Profiles. *Front Microbiol.* (2019) 10:733. doi: 10.3389/fmicb.2019.00733
56. Tao Z, Zhou T, Zhou S, Wang G. Temperature-regulated expression of type VI secretion systems in fish pathogen Pseudomonas plecoglossicida revealed by comparative secretome analysis. *FEMS Microbiol Lett.* (2016) 363:fnw261 doi: 10.1093/femsle/fnw261
57. Fernández-Bravo A, Kilgore PB, Andersson JA, Blears E, Figueras MJ, Hasan NA, et al. T6SS and ExoA of flesh-eating Aeromonas hydrophila in peritonitis and necrotizing fasciitis during mono- And polymicrobial infections. *Proceed Nat Acad Sci USA* 116:24084–92. doi: 10.1073/pnas.1914395116
58. Galindo CL, Fadl AA, Sha J, Gutierrez C, Popov VL, Boldogh I, et al. (2004) Aeromonas hydrophila cytotoxic enterotoxin activates mitogen-activated protein kinases and induces apoptosis in murine macrophages and human intestinal epithelial cells. *J Biol Chem.* (2019) 279:37597–612. doi: 10.1074/jbc.M404641200
59. Black KSS, Freeman NC, Jimenez M, Donnelly KC, Calvin JA. Children's mouthing and food-handling behavior in an agricultural community on the US/Mexico border. *J Expos Anal Environ Epidemiol.* (2005) 15:244–51. doi: 10.1038/sj.jea.7500398
60. Folkesson A, Löfdahl S, Normark S. The Salmonella enterica subspecies I specific centisome 7 genomic island encodes novel protein families present in bacteria living in close contact with eukaryotic cells. *Res Microbiol.* (2002) 153:537–45. doi: 10.1016/S0923-2508(02)01348-7

61. Nano FE, Zhang N, Cowley SC, Klose KE, Cheung KKM, Roberts MJ, et al. A Francisella tularensis pathogenicity island required for intramacrophage growth. *J Bacteriol.* (2004) 186:6430–6. doi: 10.1128/JB.186.19.6430-6436.2004
62. Rao PSS, Yamada Y, Tan YP, Leung K Y. Use of proteomics to identify novel virulence determinants that are required for Edwardsiella tarda pathogenesis. *Mol Microbiol.* (2004) 53:573–86. doi: 10.1111/j.1365-2958.2004.04123.x
63. Seibt H, Aung KM, Ishikawa T, Sjöström A, Gullberg M, Atkinson GC, et al. Elevated levels of VCA0117 (VasH) in response to external signals activate the type VI secretion system of Vibrio cholerae O1 El Tor A1552. *Environ Microbiol.* (2020) 22:4409–23. doi: 10.1111/1462-2920.15141

Conflict of Interest: The authors declare that the research was conducted in the absence of any commercial or financial relationships that could be construed as a potential conflict of interest.

Publisher's Note: All claims expressed in this article are solely those of the authors and do not necessarily represent those of their affiliated organizations, or those of the publisher, the editors and the reviewers. Any product that may be evaluated in this article, or claim that may be made by its manufacturer, is not guaranteed or endorsed by the publisher.

frontiers in Veterinary Science

ORIGINAL RESEARCH
published: 24 December 2021
doi: 10.3389/fvets.2021.806653

Antimicrobial Resistance of *Escherichia coli* From Aquaculture Farms and Their Environment in Zhanjiang, China

Cui-Yi Liao[1†], *Balamuralikrishnan Balasubramanian*[2†], *Jin-Ju Peng*[1], *Song-Ruo Tao*[1], *Wen-Chao Liu*[1*] *and Yi Ma*[1*]

[1] College of Coastal Agricultural Sciences, Guangdong Ocean University, Zhanjiang, China, [2] Department of Food Science and Biotechnology, College of Life Science, Sejong University, Seoul, South Korea

OPEN ACCESS

Edited by:
Lixing Huang,
Jimei University, China

Reviewed by:
Wei Xu,
State Oceanic Administration, China
Wanxin Li,
Fujian Medical University, China

***Correspondence:**
Wen-Chao Liu
liuwc@gdou.edu.cn
Yi Ma
mayi761@163.com

[†] These authors have contributed equally to this work and share first authorship

Specialty section:
This article was submitted to Veterinary Infectious Diseases, a section of the journal Frontiers in Veterinary Science

Received: 01 November 2021
Accepted: 24 November 2021
Published: 24 December 2021

Citation:
Liao C-Y, Balasubramanian B, Peng J-J, Tao S-R, Liu W-C and Ma Y (2021) Antimicrobial Resistance of Escherichia coli From Aquaculture Farms and Their Environment in Zhanjiang, China. Front. Vet. Sci. 8:806653. doi: 10.3389/fvets.2021.806653

Antimicrobial resistance (AMR) has become a major concern worldwide. To evaluate the AMR of *Escherichia coli* in aquaculture farms of Zhanjiang, China, a total of 90 samples from the water, soil, and sediment of three aquaculture farms (farms I, II, and III) in Zhanjiang were collected, and 90 strains of *E. coli* were isolated for drug resistance analysis and AMR gene detection. The results indicated that the isolated 90 strains of *E. coli* have high resistance rates to penicillin, amoxicillin, ampicillin, tetracycline, compound sulfamethoxazole, sulfisoxazole, chloramphenicol, florfenicol, and rifampin (≥70%). Among these antimicrobial drugs, the resistance rate to rifampicin is as high as 100%. Among the isolated 90 strains of *E. coli*, all of them were resistant to more than two kinds of antimicrobial drugs, the number of strains resistant to nine kinds of drugs was the largest (19 strains), and the most resistant strain showed resistance to 16 kinds of antibacterial drugs. Regarding the AMR genes, among the three aquaculture farms, the most resistance genes were detected in farm II (28 species). The detection rate of bla_{TEM}, bla_{CIT}, bla_{NDM}, *floR*, *OptrA*, *cmlA*, *aphA1*, *Sul2*, *oqxA*, and *qnrS* in 90 isolates of *E. coli* was high (≥50%). The detection rate of carbapenem-resistant genes, such as bla_{KPC}, bla_{IMP}, and *cfr*, was relatively lower (≤30%), and the detection rate of *mcr2* was the lowest (0). At least four AMR genes were detected for each strain, and 15 AMR genes were detected at most. Among them, the number of strains that carried 10 AMR genes was the largest (15 strains). Finally, a correlation analysis found that the AMR genes including bla_{TEM}, bla_{CIT}, *floR*, *OptrA*, *cmlA*, *aac(3)-II*, *Sul2*, *ereA*, *ermB*, *oqxB*, *qnrA*, *mcr1*, and *mcr2* had a high correlation rate with drug resistance (≥50%). To summarize, the 90 strains of *E. coli* isolated from water, surrounding soil, and sediment samples showed resistance to multi-antimicrobial drugs and carried various antimicrobial resistance genes. Thus, it is essential to strengthen the rational use of antimicrobial drugs, especially the amide alcohol drugs, and control the AMR in the aquaculture industry of Zhanjiang, China.

Keywords: antimicrobial resistance, aquaculture farm, *Escherichia coli*, multi-drug resistance, resistance genes

INTRODUCTION

Currently, due to human demand for a variety of animal proteins, the aquaculture industry is developing rapidly (1). China has been one of the largest producers of aquatic products, and the coastal area is the main aquaculture base, including the coastal city of Zhanjiang (2). Because of poor resistance and susceptibility to disease of aquatic animals, antibiotics are widely used in aquaculture to prevent and treat bacterial diseases (1). As a result, the residual antibiotics in aquatic products pose a potential risk to food safety, and antibiotics excreted from aquatic animals are dispersed in the water and sediments, thus leading to the emergence of drug-resistant bacteria and antimicrobial resistance (AMR) genes in aquaculture farms and the surrounding environment (3, 4). Under the pressure of excessive use of antibiotics, the drug-resistant bacteria even appeared to demonstrate multi-drug resistance, which causes serious negative impacts on public health (5). Besides this, according to the report of Pruden et al. (6), the AMR genes are novel environmental pollutants. The existence of drug resistance genes is the key to the development of drug resistance in bacteria. The AMR genes not only spread vertically but also spread to other bacteria horizontally through genetic elements, increasing the number of drug-resistant strains and causing difficulties in the treatment of clinical diseases and infection in both humans and animals (7, 8).

Escherichia coli is a gram-negative and common conditional pathogenic bacteria in the intestines and environment of humans and animals (9). Pathogenic *Escherichia coli* results in intestinal diseases and infections of farm animals (10, 11). *Escherichia coli* also induces diseases in various aquatic animals, thereby causing serious economic losses for the aquaculture industry. In this context, the excessive use of antibacterial drugs in aquaculture has become inevitable, and aquaculture has become an important source of antibiotic-resistant strains and AMR genes of *E. coli* (1). However, the terrible thing is that the antibiotic-resistant bacteria can infect humans through the food chain or transfer AMR genes to human pathogens, leading to serious diseases such as meningitis, sepsis, and enterotoxemia in humans (12). Furthermore, the frequent application of similar antimicrobial drugs in the treatment of *E. coli* induced the diseases of animals (including aquatic animals) and humans nowadays, which makes it difficult to find an effective antimicrobial agent in case of bacterial infections in humans (13). However, little is known about the drug resistance and the distribution of AMR genes of *E. coli* isolates from aquaculture farms and their surroundings in Zhanjiang, China. Therefore, to provide basic data for a better understanding of AMR in aquaculture, the present study was conducted to evaluate the distribution of AMR genes and analyze the drug resistance of *E. coli* in aquaculture farms of Zhanjiang, China.

MATERIALS AND METHODS

Sampling

The water, surrounding soil, and sediment samples were randomly collected from three aquaculture farms in Zhanjiang, China (farms I, II, and III). The sampling locations are shown in **Figure 1**. The water samples were collected at 1–10 cm in the water surface, the soil samples were collected at 1–3 cm on the surface of the surrounding aquaculture farms, and the sediment samples were collected at 1–5 cm from the surface of the sediment. There were 10 samples of water, soil, and sediment from each aquaculture farm, respectively, and a total of 90 samples were collected in this study.

Reagents, Antibacterial Drugs, and Strains

MacConkey agar medium, Eosin Meilan agar medium, and ordinary nutrient broth were purchased from Beijing Luqiao Technology Co., Ltd. (Beijing, China); 5 × TBE buffers were obtained from Shenggong Bioengineering (Shanghai) Co., Ltd. (Shanghai, China); Premix EX TaqTM version 2.0 and DL1000 DNA Marker were both purchased from TaKaRa Bioengineering (Dalian) Co., Ltd. (Dalian, China); agarose (produced in Spain) was purchased from Beijing Kaioudi Biotechnology Co., Ltd. (Beijing, China); and the Goldview nucleic acid stains were from Vazyme Nanjing Biotech Co., Ltd. (Nanjing, China).

There was a total of 23 kinds of antibacterial drug sensitivity reagent tablets, including penicillin, amoxicillin, cefotaxime, ceftriaxone, aztreonam, gentamicin, amikacin, azithromycin, tetracycline, doxycycline, ciprofloxacin, ofloxacin, compound sulfamethoxazole, chloramphenicol, polymyxin B, nitrofurantoin, rifampicin, florfenicol, ampicillin, streptomycin, lomefloxacin, sulfisoxazole, and fosfomycin, which were from Chicheng Pharmaceutical Technology Co., Ltd. (Hangzhou, China). The quality control bacterial strain is *E. coli* ATCC 25922 (from the Laboratory of Basic Veterinary Medicine, Guangdong Ocean University, Zhanjiang, China).

Isolation and Identification of *E. coli*

The collected 90 samples (water, soil, and sediment) were diluted with sterile water to a suitable quantity. Then, 100 μl was taken and spread evenly on MacConkey agar medium and incubated at 37°C for 18–24 h. A single colony with a smooth, moist, pink surface was selected and placed on eosin. Streak purification was done on blue agar medium, and the sample was cultured at 37°C for 18–24 h. A single colony with metallic luster, black or brown-green, was selected and inoculated on eosin melan agar medium for streak purification again; finally, the suspected *E. coli* was removed. The strains were inoculated into nutrient broth medium, cultivated at 37°C for 24 h, and then stored at −20°C with 30% glycerol for later analysis.

PCR method was used for the identification of isolated *E. coli* strains from the samples. The PCR primers were designed based on the specific *phoA* gene sequence of *E. coli*—upstream primer: 5′-TACAGGTGACTGCGGGCTTATC-3′, downstream primer: 5′-CTTACCGGGCAATACACTCACTA-3′–and the primers were synthesized and produced by Shenggong Bioengineering Co., Ltd. (Shanghai, China). The length of the product is 622 bp. The DNA of the isolated strains was extracted by using DNA extraction kits (Tiangen Biochemical Technology Co., Ltd., Beijing, China). The PCR reaction system is 15 μl: DNA template 1 μl, each 0.5 μl of upstream and downstream primers (25 μmol/L), and Taq 13 μl. The PCR reaction conditions were

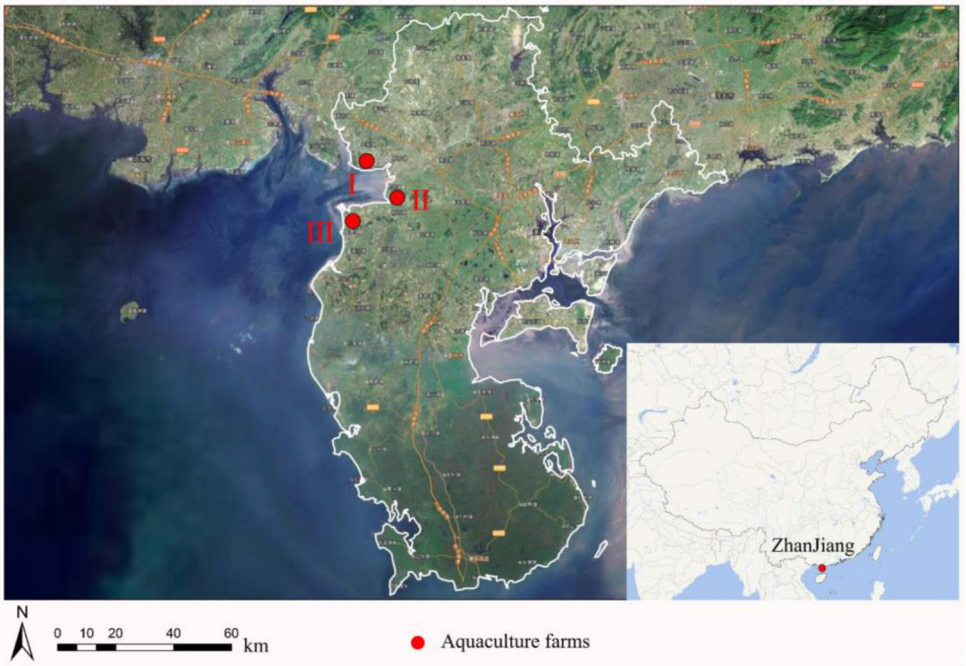

FIGURE 1 | Map of the sampling locations.

as follows: pre-denaturation at 94°C for 7 min, denaturation at 94°C for 30 s, annealing at 55°C for 30 s, and extension at 72°C for 30 s—for a total of 30 cycles, and final extension at 72°C for 5 min. The PCR products were electrophoresed on 1% agarose gel, and *E. coli* ATCC 25922 was used as standard bacteria and positive control; ddH_2O was used as the blank negative control.

Antimicrobial Drug Resistance Analysis of Isolated *E. coli* Strains

The drug susceptibility reagent tablet (test strips) method, which was recommended by the Clinical and Laboratory Standards Institute, was performed to detect and analyze the drug resistance of the isolated *E. coli* strains. Briefly, 90 strains of *E. coli* isolated from 90 samples were resuscitated, and 100 μl bacterial liquid was evenly spread on a common nutrient agar medium, and 23 kinds of antimicrobial drug-sensitive reagent tablets were used on the surface of the medium and then incubated at 37°C for 18–24 h. The diameter of the inhibition zone was observed and recorded, and the results were determined for drug resistance (14). There were three replicates for each antibacterial drug resistance analysis. *Escherichia coli* ATCC 25922 was used as the quality control bacteria. Finally, the resistance to each antimicrobial drug and the multi-drug resistance of the isolated *E. coli* strains from water, soil, and sediment were statistically analyzed by using Excel 2012.

AMR Gene Detection of Isolated *E. coli* Strains

The PCR method was used to detect 29 kinds of AMR genes carried in the 90 isolated strains of *E. coli* from the water, soil, and sediment samples of the aquaculture farms. The primers are presented in **Table 1** and designed according to previous studies (the reference details are described in **Table 1**). The PCR reaction system is 15 μl, which contained 1 μl of DNA template, 0.5 μl of upstream and downstream primers, and 13 μl of Premix EX Taq^{TM}. ddH_2O was used as blank negative control. The PCR reaction procedure was as follows: pre-denaturation at 94°C for 5 min, denaturation at 94°C for 30 s, annealing for 30 s at melting temperature (Tm, °C) (the Tm of each AMR gene is listed in **Table 1**), extension at 72°C for 1 min for 30 cycles, and a final extension at 72°C for 10 min. The PCR products were stored at 4°C. The PCR products were analyzed by 1% agarose gel electrophoresis, and the results were recorded.

Positive fragments of the target gene were randomly picked and recovered using Poly-Gel DNA Extraction Kit (OMEGE) and cloned according to vector ligation (pMD19-T vector, TaKaRa) and competent cells (DH-5α, TaKaRa). The plasmid (Plasmid DNA Kit, OMEGE) was extracted and then sent to Shanghai Biotech, China for sequencing. The sequences were compared using BLAST (http://www.ncbi.nlm.nih.gov/blast) on the National Center for Biotechnology Information (NCBI) website. The homology between the obtained sequences and the corresponding target genes on NCBI was very high, and the matching degree was more than 98%. Ultimately, the AMR gene

TABLE 1 | PCR primers of *Escherichia coli* antimicrobial resistance genes.

Category	Genes	Primer sequences (5′-3′)	Product size (bp)	Tm (°C)	References
β-Lactams	bla_{CTX-M}	F: GGGCTGAGATGGTGACAAAGAG	876	55	(15)
		R: CGTGCGAGTTCGATTTATTCAAC			
	bla_{TEM}	F: TCGCCGCATACACTATTCTCAGAATGA	445	50	(16)
		R: ACGCTCACCGGCTCCAGATTTAT			
	bla_{CIT}	F: TGGCCAGAACTGACAGGCAAA	462	55	(17)
		R: TTTCTCCTGAACGTGGCTGGC			
Carbapenems	bla_{KPC}	F: TCGCTAAACTCGAACAGG	785	63	(18)
		R: TTACTGCCCGTTGACGCCCAATCC			
	bla_{DHA}	F: AACTTTCACAGGTGTGCTGGGT	405	55	(19)
		R: CCGTACGCATACTGGCTTTGC			
	bla_{NDM}	F: GGGCAGTCGCTTCCAACGGT	475	63	(20)
		R: GTAGTGCTCAGTGTCGGCAT			
	bla_{IMP}	F: CTACCGCAGCAGAGTCTTTG	587	58	
		R: AACCAGTTTTGCCTTACCAT			
Amido alcohols	*floR*	F: CTGAACACGACGCCCGCTAT	751	60	(21)
		R: GGACCGCTCCGCAAACAA			
	cfr	F: TGAAGTATAAAGCAGGTTGGGAGTCA	746	55	(22)
		R: ACCATATAATTGACCACAAGCAGC			
	fexA	F: CTCTTCTGGACAGGCTGGAA	332	57	(23)
		R: CCAGTTCCTGCTCCAAGGTA			
	fexB	F: ACTGGACAGGCAGGCTTAAT	320	57	
		R: CCTGCCCCAAGATACATTGC			
	cat1	F: AGTTGCTCAATGTACCTATAACC	547	51	(24)
		R: TTGTAATTCATTAAGCATTCTGCC			
	OptrA	F: CTTATGGATGGTGTGGCAGC	310	59	(25)
		R: CCATGTGGTTTGTCGGTTCA			
	cmlA	F: TACGACAGCGAGCACAATTC	764	54	(26)
		R: CGGTGATGGCAAGCAATACT			
Aminoglycosides	*aphA1*	F: ATGGGCTCGCGATAATGTC	634	60	(27)
		R: CTCACCGAGGCAGTTCCAT			
	aac(3)- II	F: GGCGACTTCACCGTTTCT	412	54	(28)
		R: GGACCGATCACCCTACGAG			
Sulfonamides	*Sul1*	F: GTGACGGTGTTCGGCATTCT	779	58	(29)
		R: CCGAGAAGGTGATTGCGCT			
	Sul2	F: CGGCATCGTCAACATAACCT	721	66	(30)
		R: TGTGCGGATGAAGTCAGCTC			
Tetracyclines	*tetM*	F: GAGGTCCGTCTGAACTTTGCG	915	56	(31)
		R: AGAAAGGATTTGGCGGCACT			
	tetC	F: CTGGGCTGCTTCCTAATGC	580	56	
		R: AGCTGTCCCTGATGGTCGT			
	tetA	F: GGCACCGAATGCGTATGAT	480	56	
		R: AAGCGAGCGGGTTGAGAG			
Macrolides	*ereA*	F: GCCGGTGCTCATGAACTTGAG	419	60	(32)
		R: CGACTCTATTCGATCAGAGGC			
	ermB	F: CGAGTGAAAAAGTACTCAACC	557	52	(33)
		R: GCCGTGTTTCATTGCTTGATG			
Quinolones	*oqxA*	F: GATCAGTCAGTGGGATAGTTT	670	51	(34)
		R: TACTCGGCGTTAACTGATTA			

(Continued)

TABLE 1 | Continued

Category	Genes	Primer sequences (5′-3′)	Product size (bp)	Tm (°C)	References
	oqxB	F: TTCTCCCCCGGCGGGAAGTAC	512	65	(35)
		R: CTCGGCCATTTTGGCGCGTA			
	qnrA	F: TTCAGCAAGAGGATTTCTCA	500	55	(36)
		R: GGCAGCACTATTACTCCCAA			
	qnrS	F: ACGACATTCGTCAACTGCAA	417	53	(37)
		R: TAAATTGGCACCCTGTAGGC			
Colistin	*mcr1*	F: CGGTCAGTCCGTTTGTTC	309	53	(38)
		R: CTTGGTCGGTCTGTAGGG			
	mcr2	F: TGTTGCTTGTGCCGATTGGA	563	65	(39)
		R: AGATGGTATTGTTGGTTGCTG			

detection rates of the isolated *E. coli* strains from water, soil, and sediment were statistically analyzed by using Excel 2012.

Correlation Analysis of AMR Genes and Drug Resistance in Isolated *E. coli* Strains

A correlation analysis between the results of AMR genes and drug resistance was performed, and the correlation rate of AMR genes and drug resistance was calculated. The correlation rate of AMR genes and drug resistance was calculated as to the following formula: (number of resistant strains with positive genes + number of sensitive strains with negative genes) / total number of strains × 100% (40).

RESULTS

Isolation and Identification of the Isolated *E. coli* Strains

One *E. coli* strain was isolated from each sample of water, soil, and sediment, totaling to 90 strains. The colonies of the isolated strains grown on Macconkey agar medium have a smooth, moist, and pink surface, and the colonies grown on eosin melan agar medium have a metallic luster, either black or brown-green. Besides this, the PCR products of *E. coli*-specific *phoA* gene can be observed by gel electrophoresis and showed that 90 strains of bacteria have an amplified 622-bp band, and it is determined that the isolated and cultured 90 strains are *E. coli*.

Antimicrobial Drug Resistance of Isolated *E. coli* Strains

The results of antimicrobial drug resistance of the isolated *E. coli* strains are presented in **Table 2**. Overall, the isolated *E. coli* strains from the three aquaculture farms all have high antimicrobial drug resistance rates to penicillin and rifampicin, and the resistance rate to rifampicin reaches 100%. The *E. coli* isolates of the water, soil, and sediment samples of the three aquaculture farms all have relatively low resistance to β-lactam aztreonam, aminoglycosides gentamicin, amikacin, streptomycin, macrolide azithromycin, doxycycline, ciprofloxacin, ofloxacin, lomefloxacin, polymyxin B, nitrofurantoin, and fosfomycin (≤50%). Specifically, the *E. coli* isolates from the water samples of aquaculture farm I have a low resistance rate to amoxicillin, ampicillin, tetracyclines, sulfonamides, and amide alcohol drugs (≤30%), but the *E. coli* isolates of the soil and sediment samples from aquaculture farms I, II, and III have high resistance rates to the above-mentioned drugs (≥60%). In addition, there is high resistance to cefotaxime and ceftriaxone for the *E. coli* isolates of the water and soil samples from aquaculture farm II (≥70%).

The resistance of the 90 isolates of *E. coli* to 23 antibacterial drugs is shown in **Table 3**. The resistance rate of the 90 isolates of *E. coli* to penicillin, amoxicillin, ampicillin, tetracycline, compound sulfamethoxazole, sulfisoxazole, chloramphenicol, florfenicol, and rifampin is high (≥70%), and the resistance rate to rifampicin is 100%. The resistance rates to aztreonam, gentamicin, amikacin, streptomycin, azithromycin, ciprofloxacin, ofloxacin, lomefloxacin, polymyxin B, nitrofurantoin, and fosfomycin were low (≤30%), and the resistance rate to polymyxin B and fosfomycin was 0.

As shown in **Figure 2**, all 90 isolated *E. coli* strains exhibited varying degrees of multi-drug resistance, with resistance to at least two drugs and resistance to at most 16 kinds of antibacterial drugs. Meanwhile, 60% or more isolated *E. coli* strains are resistant to more than nine drugs; especially the number of strains resistant to nine kinds of antibacterial drugs is the largest (19 strains, 21.11%), and the number of strains resistant to four, five, and 16 kinds of antibacterial drugs is the least (one strain, 1.11%).

AMR Gene Distributions of Isolated *E. coli* Strains

The detection results of 90 strains of *E. coli* isolated from the water, soil, and sediment samples of aquaculture farms for carrying 29 kinds of AMR genes are shown in **Supplementary Table 1**. Regarding aquaculture farm I, the detection rate of the following AMR genes of the *E. coli* isolates from the water samples was high: bla_{CTX-M} (80%), bla_{CIT} (100%), bla_{DHA} (80%), *fexA* (70%), *OptrA* (90%), *aphA1* (90%) and *mcr1* (70%). The AMR genes with a high detection rate of *E. coli* isolates in soil samples include bla_{CIT} (100%), bla_{DHA} (70%), *floR* (100%), *fexB* (60%), *OptrA* (70%), *Sul2* (60%), *tetM* (90%),

TABLE 2 | Drug resistance rate of isolated strains of *Escherichia coli* from three aquaculture farms in Zhanjiang, China.

Drug category	Drugs	Drug resistance rate of farm I, %			Drug resistance rate of farm II, %			Drug resistance rate of farm III, %		
		Water	Soil	Sediment	Water	Soil	Sediment	Water	Soil	Sediment
β-Lactams	Penicillin	100	100	70	100	100	70	100	100	70
	Amoxicillin	30	90	70	100	100	90	100	90	90
	Ampicillin	0	100	60	100	90	90	90	80	90
	Aztreonam	0	0	0	30	0	10	10	0	10
Cephalosporins	Cefotaxime	0	0	40	90	90	40	40	10	0
	Ceftriaxone	0	10	0	90	70	40	40	0	0
Aminoglycosides	Gentamicin	0	0	0	10	30	20	20	0	0
	Amikacin	0	0	0	10	0	0	0	0	0
	Streptomycin	0	10	10	30	30	20	10	0	0
Macrolides	Azithromycin	20	20	0	30	10	10	20	0	20
Tetracyclines	Tetracycline	20	100	60	80	100	80	90	100	100
	Doxycycline	20	30	0	40	30	40	30	40	60
Quinolones	Ciprofloxacin	0	0	0	20	30	10	0	0	0
	Ofloxacin	0	0	0	10	0	10	0	0	0
	Lomefloxacin	0	10	0	20	50	20	10	0	0
Sulfonamides	Compound Sulfamethoxazole	20	80	80	80	90	100	80	90	100
	Sulfisoxazole	40	100	100	100	90	100	90	90	100
Amide alcohols	Chloramphenicol	20	100	60	90	90	100	100	100	100
	Florfenicol	20	100	80	100	90	90	100	90	100
Polymyxins	Polymyxin B	0	0	0	0	0	0	0	0	0
Nitrofurans	Nitrofurantoin	0	0	0	10	0	0	0	0	0
Rifamycins	Rifampin	100	100	100	100	100	100	100	100	100
Fosfomycins	Fosfomycin	0	0	0	0	0	0	0	0	0

TABLE 3 | Resistance of 90 isolated strains of *Escherichia coli* from three aquaculture farms in Zhanjiang, China, to 23 kinds of antimicrobial drugs.

Antimicrobial drugs	Number of resistance isolates	Percentage, %	Antimicrobial drugs	Number of resistance isolates	Percentage, %
Penicillin	81	90.00	Ciprofloxacin	6	6.67
Amoxicillin	74	82.22	Ofloxacin	2	2.22
Ampicillin	70	77.78	Lomefloxacin	11	12.22
Aztreonam	6	6.67	Compound Sulfamethoxazole	72	80.00
Cefotaxime	31	34.44			
Ceftriaxone	25	27.78	Sulfisoxazole	81	90.00
Gentamicin	8	8.89	Chloramphenicol	76	84.44
Amikacin	1	1.11	Florfenicol	77	85.56
Streptomycin	11	12.22	Polymyxin B	0	0.00
Azithromycin	13	14.44	Nitrofurantoin	1	1.11
Tetracycline	73	81.11	Rifampicin	90	100
Doxycycline	29	32.22	Fosfomycin	0	0.00

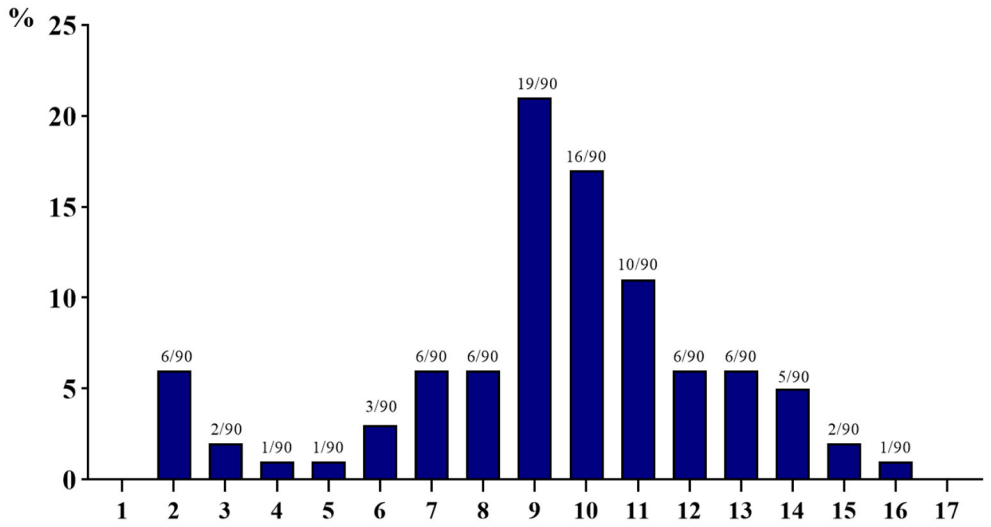

FIGURE 2 | Multi-drug resistance of 90 isolated strains of *Escherichia coli* from aquaculture farms in Zhanjiang, China (the X-axis shows the number of drug resistance, while the Y-axis shows the percentage of multi-drug-resistant strains among 90 isolates).

oqxA (60%), *qnrS* (100%), and *mcr1* (60%). The high detection rates of the AMR genes of *E. coli* isolates in the sediment samples are as follows: bla_{TEM}(60%), bla_{NDM} (80%), *fexB* (60%), *OptrA* (90%), *cmlA* (70%), *aphA1* (70%), *Sul2* (60%), *oqxA* (90%), and *qnrS* (80%).

In aquaculture farm II, 28 kinds of AMR genes were detected, which was the largest number of detected AMR genes among the three farms. Specifically, the high detection rates of the AMR genes of *E. coli* isolates from water samples are bla_{CIT} (70%), bla_{DHA} (60%), *floR* (80%), *OptrA* (70%), *cmlA* (80%), *aphA1* (80%), *Sul2* (80%), *tetA* (70%), *qnrS* (90%), and *mcr1* (70%). The high detection rates of AMR genes of *E. coli* isolates from soil samples include bla_{CTX-M} (70%), bla_{TEM} (60%), bla_{CIT} (90%), bla_{NDM} (90%), bla_{IMP} (70%), *floR* (90%), *fexB* (60%), *OptrA* (80%), *cmlA* (90%), *aphA1* (60%), *Sul2* (70%), *tetC* (60%), *oqxA* (100%), *qnrS* (70%), and *mcr1* (70%). High detection rates of *E. coli* isolates in sediment samples are demonstrated for the following AMR genes: bla_{TEM} (90%), bla_{CIT} (60%), bla_{NDM} (70%), *floR* (90%), *OptrA* (70%), *Sul2* (70%), *oqxA* (80%), and *qnrS* (80%).

Regarding aquaculture farm III, high detection rates of *E. coli* isolates in water samples are observed for the following AMR genes: bla_{DHA} (70%), *floR* (80%), *fexB* (60%), *OptrA* (80%), *cmlA* (70%), *Sul2* (90%), and *qnrS* (70%). The high detection rates of AMR genes of *E. coli* isolates from soil samples include bla_{CTX-M} (80%), bla_{TEM} (80%), bla_{CIT} (60%), bla_{NDM} (100%), *floR* (90%), *fexA* (80%), *cmlA* (70%), *oqxA* (90%), and *qnrS* (80%). High detection rates of AMR genes of *E. coli* isolates from sediment samples are observed as follows: bla_{TEM} (70%), bla_{NDM} (100%), *floR* (100%), *OptrA* (100%), *Sul2* (90%), *oqxA* (90%), and *qnrS* (80%).

As shown in **Table 4**, on the whole, among the carried AMR genes in 90 strains of *E. coli* isolates, β-lactams (bla_{TEM} and bla_{CIT}), amide alcohols (*floR*, *OptrA*, and *cmlA*), aminoglycosides (*aphA1*), sulfonamides (*Sul2*), and quinolones (*oqxA* and *qnrS*) have a high detection rate (≥50%). The detection rate of AMR genes of carbapenems (bla_{KPC} and bla_{IMP}), amide alcohols (*cfr* and *cat1*), aminoglycosides (*aac(3)-II*), sulfonamides (*Sul1*), tetracyclines (*tetM* and *tetA*), macrolides (*ereA* and *ermB*), quinolones (*oqxA* and *qnrB*), and colistins (*mcr2*) is relatively low (≤30%), and the detection rate of *mcr2* is 0.

The number and detection rate of 29 AMR genes in 90 isolated *E. coli* strains are shown in **Figure 3**. AMR genes of at least four species were detected, and a maximum of 15 AMR genes were detected in each strain of isolated *E. coli*. More than 60% of the isolated *E. coli* strains carried more than 10 kinds of AMR genes, of which the number of isolated *E. coli* strains carrying 10 kinds of AMR genes is the largest (15 strains, 15.56%), and the number of isolated *E. coli* strains carrying four kinds of AMR genes is the least (one strain, 1.11%).

Correlation Analysis of AMR Genes and Drug Resistance

As described in **Table 5**, the following AMR genes have a high correlation rate with the drug resistance of the isolated *E. coli* strains: bla_{TEM} (55.56%), bla_{CIT} (67.78%), *floR* (85.56%), *OptrA* (71.11%), *cmlA* (64.44%), *aac(3)-II* (81.11%), *Sul2* (70 %), *ereA* (84.44%), *ermB* (73.33%), *oqxB* (85.56%), *qnrA* (83.33%), *mcr1* (56.67%), and *mcr2* (95.56%). The correlation rate of other AMR genes with drug resistance is relatively low (<50%).

DISCUSSION

China is a huge market for animal product consumption. With the increase in consumer demand for meat products other than livestock products, the scale of aquaculture has significantly increased in recent years, and Zhanjiang is an important place

TABLE 4 | Detection of antimicrobial resistance genes in a total of 90 isolated strains of *Escherichia coli* from aquaculture farms in Zhanjiang, China.

Antimicrobial resistance genes	Number of resistance isolates	Detection rate %	Antimicrobial resistance genes	Number of resistance isolates	Detection rate %
bla_{CTX-M}	40	44.44	*aac(3)- II*	10	11.11
bla_{TEM}	50	55.55	*Sul1*	5	5.56
bla_{CIT}	61	67.77	*Sul2*	59	65.56
bla_{KPC}	4	4.44	*tetM*	14	15.56
bla_{DHA}	41	45.55	*tetC*	28	31.11
bla_{NDM}	54	60.00	*tetA*	20	22.22
bla_{IMP}	22	24.44	*ereA*	1	1.11
floR	74	82.22	*ermB*	17	18.89
Cfr	10	11.11	*oqxA*	53	58.89
fexA	27	30.00	*oqxB*	8	8.89
fexB	32	35.56	*qnrA*	6	6.67
cat1	19	21.11	*qnrS*	66	73.33
OptrA	70	77.78	*mcr1*	41	45.56
cmlA	55	61.11	*mcr2*	0	0.00
aphA1	51	56.67			

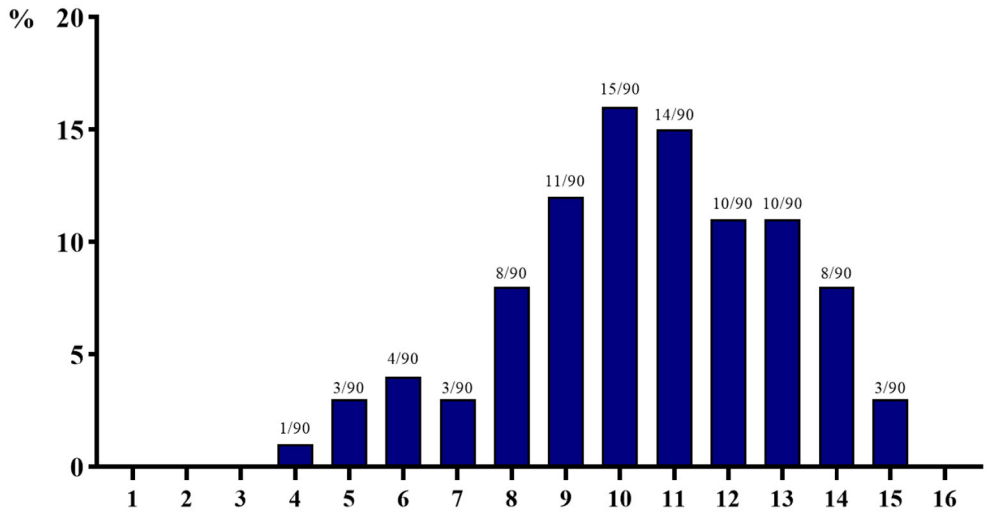

FIGURE 3 | The number of 29 antimicrobial resistance genes detected in 90 isolated strains of *Escherichia coli* from aquaculture farms in Zhanjiang, China (the X-axis indicates the number of resistance genes, while the Y-axis indicates the percentage of bacteria carrying multi-drug resistance genes among 90 isolates).

for aquatic product production in China (2). However, in order to improve the economic benefits of aquaculture, antimicrobial drugs (including preventive and therapeutic drugs) are widely used in the aquaculture industry to prevent and treat bacterial diseases (1). The overuse and/or abuse of antimicrobial drugs in animal production leads to the generation of AMR genes and drug-resistant bacteria, thus threatening to complicate the treatment of bacterial infections in humans (8, 9). Due to the fact that *E. coli* is a common pathogen in both humans and animals, the AMR issue of *E. coli* has been a prominent concern in public health (10, 11). Accordingly, the application of antibiotics for growth promotion in farm animals was banned entirely in the European Union since 2000 and in South Korea and Japan after 2011 (41). Recently, China also completely banned the preventive antibiotics for promoting the growth performance of animals to mitigate the deleterious consequences of AMR to public health and encouraged research on alternatives to preventive antibiotics (42–45). Nevertheless, in large-scale aquaculture, the extensive use of therapeutic antibacterial drugs induced the AMR issues and was still a major concern. In this context, the present study investigated the distribution of AMR genes and analyzed the drug resistance of *E. coli* in aquaculture farms of Zhanjiang and their surrounding environments, and the findings have positive implications for public health.

Through the drug resistance analysis of the present study, it was found that the *E. coli* strains isolated from three

TABLE 5 | Correlation analysis between antimicrobial resistance genes and drug resistance of *Escherichia coli* isolates from aquaculture farms in Zhanjiang, China.

Category	Test of antimicrobial resistance genes		Test of drug resistance		Correlation rate, %
	Genes	Negative (N)/positive (P)	Number of detections	Sensitive strain	
β-lactams	bla_{TEM}	P	50	0	55.56
		N	40	0	
	bla_{CIT}	P	61	0	67.78
		N	29	0	
Amide alcohols	*floR*	P	70	4	85.56
		N	9	7	
	OptrA	P	62	9	71.11
		N	17	2	
	cmlA	P	51	4	64.44
		N	28	7	
Aminoglycosides	*aac(3)- II*	P	7	3	81.11
		N	14	66	
Sulfonamides	*Sul2*	P	56	3	70.00
		N	24	7	
Macrolides	*ereA*	P	0	1	84.44
		N	13	76	
	ermB	P	3	14	73.33
		N	10	63	
Quinolones	*oqxB*	P	3	5	85.56
		N	8	74	
	qnrA	P	1	5	83.33
		N	10	74	
Colistin	*mcr1*	P	3	38	56.67
		N	1	48	
	mcr2	P	0	0	95.56
		N	4	86	

Only the data with a correlation rate of >50% are presented.

aquaculture farms in Zhanjiang, China, have different levels of resistance to various antimicrobial drugs. The *E. coli* isolates from aquaculture environments are highly resistant to β-lactams (except aztreonam), tetracycline, sulfonamides, amide alcohols, and rifamycin but have a relatively low resistance rate to aztreonam, aminoglycosides, macrolides, doxycycline, quinolones, polymyxins, nitrofurans, and fosfomycins. It is worth noting that the 90 isolated *E. coli* strains in this study were resistant to at least two drugs and at most 16 drugs, indicating that the multi-drug resistance of *E. coli* was a serious concern in the aquaculture farms of Zhanjiang, China. Similarly, Saharan et al. (46) reported that the majority of the *E. coli* isolates from a fish farm in India were found to be resistant to more than three antibiotics (>89%), suggesting that there was multi-drug resistance for *E. coli* in the fish farm. According to the study of Ng et al. (47), it was found that 33 multi-drug-resistant *E. coli* were isolated from surface waters in aquaculture sites of Singapore. Lihan et al. (48) investigated the antibiotic-resistant *E. coli* from Sarawak rivers and aquaculture farms in northwest of Borneo. They found that resistance to piperacillin (100%) was observed in all *E. coli* isolates, resistance to amoxicillin (100%) and ampicillin (100%) was observed in *E. coli* isolated from aquaculture farms, and resistance to streptomycin (93%) was observed in *E. coli* isolated from rivers. The rivers and aquaculture farms showed similar partial drug resistance, indicating that the drug-resistant *E. coli* produced by aquaculture can be transferred to surrounding waters. On the other hand, compared to these previous reports, different aquaculture farms showed different degrees of resistance to various antibacterial drugs. This may be due to a variety of feed formulas and various medication regimes of the aquaculture farms in different regions.

Nowadays, the AMR genes are considered as new environmental pollutants; the AMR genes not only spread to surrounding environments (such as water) and the food chain but also spread to other bacteria horizontally through genetic elements, leading to antibiotic-resistant bacteria and causing difficulties in therapy. Therefore, the AMR in bacteria associated with food and water has been a global concern (7, 8). Previously, it has been reported that multiple AMR genes (mainly *sul1*, *sul2*, and *tetM*) were detected in *E. coli* isolates from surface water

samples of aquaculture farms in America (49). Hassan et al. (50) also found that around five strains of *E. coli* isolated from a rainbow trout farm carried the *mcr-1* gene. In this study, the 90 strains of *E. coli* isolates from three aquaculture farms in Zhanjiang, China, mainly carried the AMR genes of β-lactams (bla_{TEM} and bla_{CIT}), carbapenems (bla_{NDM}), amide alcohols (*floR*, *OptrA*, and *cmlA*), aminoglycosides (*aphA1*), sulfonamides (*sul2*), and quinolones (*oqxA* and *qnrS*), among which *floR* has the highest carrying rate (82.2%). It was consistently found that the *floR* gene detection rate in the isolates from aquaculture farms in coastal areas of Jiangsu, China, was 76.67% (51). By contrast, Ng *et al.* (47) demonstrated that there was high relative abundance of *sul1*, *qnrA*, and *intI1* genes in the sediments of aquaculture farms in Singapore. Changkaew et al. (52) suggested that the *tet(A)* gene was the most common AMR gene (69.1%) in the 55 *E. coli* isolates from shrimp farms and their surrounding environment in Thailand. Ng et al. (53) isolated 19 strains of *E. coli* from 10 aquaculture farms and their environment in Malaysia, and they found that the AMR gene of *Cat I* has the highest detection rate (100%, 19 of 19). On the basis of these reports, we can clearly realize that there were various AMR genes carried by *E. coli* in aquaculture farms of different regions. This may be because of the different epidemic diseases of aquatic animals and the variety of medication regimens that were executed in these regions, thus resulting in the generation of inconsistent AMR genes. Therefore, the contamination of AMR genes in the aquaculture industry of different regions requires investigation case by case. Most notably, the *floR* gene had the highest detection rate in this experiment, which has been confirmed to be the main AMR gene that mediates drug resistance in *E. coli* (54). Thus, the aquaculture farms in Zhanjiang area should avoid the overuse of amide alcohol drugs. Besides this, the 90 strains of *E. coli* isolates in this study have a low carrying rate of tetracycline (*tetM*, *tetC*, and *tetA*), macrolide (*ereA* and *ermB*), and colistin (*mcr1* and *mcr2*), and none of the AMR genes was detected in the 90 *E. coli* isolates at the same time. Bacteria have different resistance mechanisms to different antimicrobial drugs, for instance, tetracycline-resistant bacteria usually produce a protein that interacts with ribosomes; thereby, protein synthesis is not affected by the antimicrobial drugs, which is called ribosome protection (36). *Escherichia coli* can produce macrolide phosphotransferase, which destroys the lactone ring of macrolide antibiotics, resulting in a high degree of resistance to macrolide drugs (27). Moreover, the detection rate of *mcr1* was not high (45.56%), and the *mcr2* gene was not detected among the 90 *E. coli* isolates from aquaculture farms. The possible reasons are as follows: (1) *mcr1* is a relatively universal AMR gene in animals, but the *mcr2* gene was carried by a rare plasmid (IncX4 type), and (2) the colistin drugs are one of the "last resorts" for the treatment of multi-drug resistant gram-negative bacterial infections; therefore, the aquaculture farms use this type of drug less.

In this study, the AMR genes of β-lactams (bla_{TEM} and bla_{CIT}), amide alcohols (*floR*, *OptrA*, and *cmlA*), aminoglycosides [*aac(3)-II*], sulfonamides (*sul2*), macrolides (*ereA* and *ermB*), quinolones (*oqxB* and *qnrA*), and colistin (*mcr1* and *mcr2*) are highly correlated with their drug resistance (>55%), while the other AMR genes are relatively less related to their drug resistance. *E. coli* has a strong ability to accumulate AMR genes. Previous studies have shown that *E. coli* from animals often carry multiple AMR genes, but not every AMR gene exhibits corresponding resistance (34, 55). There are many reasons for the development of drug resistance in bacteria, which are related to the characteristics of the bacteria, the spread of AMR genes, and the use of drugs (1, 3). Among them, although the most important factor of the AMR gene, the expression of AMR genes was associated with the complex regulation by multiple substances (5–7). Therefore, the AMR genes are detected in some bacteria, but the related drug resistance phenotypes may not be shown because the AMR genes are not expressed or are expressed in low abundance (7, 55). Exploring the intrinsic relationship between AMR genes and drug resistance and reducing the spread of AMR genes from the inner roots to curb the trend of drug resistance still require further in-depth research.

CONCLUSION

Collectively, the *E. coli* isolated from the aquaculture farms and their environment in Zhanjiang, China, showed multi-drug resistance and carried a large number of AMR genes. Among them, the *floR* gene had the highest detection rate. Meanwhile, there was a high correlation between some of the AMR genes and the drug resistance phenotypes. Therefore, in order to reduce the spread of AMR genes and the production of drug-resistant bacteria, the present study suggests for aquaculture practitioners in Zhanjiang area to decrease the use of amide alcohol drugs and regulate the use of various antibacterial drugs. The current findings persuade the prudent use of antimicrobial agents in aquatic animal farming and also provide basic information for better understanding of AMR in aquaculture farms in Zhanjiang, China, thus being beneficial to public health.

DATA AVAILABILITY STATEMENT

The original contributions presented in the study are included in the article/**Supplementary Material**, further inquiries can be directed to the corresponding authors.

AUTHOR CONTRIBUTIONS

W-CL, YM, and BB: conceptualization, writing—review, and editing. C-YL and J-JP: methodology and data curation. C-YL, J-JP, and S-RT: analysis. W-CL, C-YL, and BB: writing—original draft preparation. YM: supervision, project administration, and funding acquisition. All authors contributed to the article and approved the submitted version.

FUNDING

This research was supported by the 2019 Guangdong University Features Innovation Project by the Department of Education in

Guangdong Province, China (2019KTSCX057), the Project of Innovation and Strengthening of Guangdong Ocean University (Q18290), and Guangdong Provincial Department of Education 2021 Special Project for Key Fields of Ordinary Colleges and Universities (2021ZDZX4003).

SUPPLEMENTARY MATERIAL

The Supplementary Material for this article can be found online at: https://www.frontiersin.org/articles/10.3389/fvets.2021.806653/full#supplementary-material

REFERENCES

1. Shao Y, Wang Y, Yuan Y, Xie Y. A systematic review on antibiotics misuse in livestock and aquaculture and regulation implications in China. *Sci Total Environ.* (2021) 798:149205. doi: 10.1016/j.scitotenv.2021.149205
2. Liu WC, Zhou SH, Balasubramanian B, Zeng FY, Sun CB, Pang HY. Dietary seaweed (*Enteromorpha*) polysaccharides improves growth performance involved in regulation of immune responses, intestinal morphology and microbial community in banana shrimp *Fenneropenaeus merguiensis*. *Fish Shellfish Immun.* (2020) 104:202–12. doi: 10.1016/j.fsi.2020.05.079
3. Jindal P, Bedi J, Singh R, Aulakh R, Gill J. Phenotypic and genotypic antimicrobial resistance patterns of *Escherichia coli* and *Klebsiella* isolated from dairy farm milk, farm slurry and water in Punjab, India. *Environ Sci Pollut Res.* (2021) 28:28556–70. doi: 10.1007/s11356-021-12514-8
4. Samuel O, Olalekan F, Beatrice O, Olatunda O. Veterinary pharmaceuticals in aqueous systems and associated effects: an update. *Environ Sci Pollut Res Int.* (2017) 24:3274–97. doi: 10.1007/s11356-016-7757-z
5. Zhang T, Ling B. Antibiotic resistance in water environment: Frontiers of fundamental research, risk assessment and control strategies. *Chin Sci Bull.* (2020) 65:2543–54. doi: 10.1360/TB-2020-0110
6. Pruden A, Pei R, Storteboom H, Carlson KH. Antibiotic resistance genes as emerging contaminants: Studies in Northern Colorado. *Environ Sci Technol.* (2006) 40:7445–50. doi: 10.1021/es060413l
7. Scott AB, Mark JW. Tracking antibiotic resistance. *Science.* (2014) 345:1454–5. doi: 10.1126/science.1260471
8. Al-Tawfiq JA, Rabaan AA, Saunar JV, Bazzi AM. Antimicrobial resistance of gram-negative bacteria: a six-year longitudinal study in a hospital in Saudi Arabia. *J Infect Public Health.* (2020) 13:737–45. doi: 10.1016/j.jiph.2020.01.004
9. Mariani M, Medici C, Ugolotti E, Losurdo G, Mesini A, Castagnola E. Colonization by *Escherichia coli* strains with increased minimal inhibitory concentration for cefiderocol: when resistance anticipates drug use. *J Infect Public Health.* (2021) 14:749–50. doi: 10.1016/j.jiph.2021.03.002
10. Lippolis JD, Holman DB, Brunelle BW, Thacker TC, Bearson BL, Reinhardt TA, et al. Genomic and transcriptomic analysis of *Escherichia coli* strains associated with persistent and transient bovine mastitis and the role of colanic acid. *Infect Immun.* (2017) 86:e00566. doi: 10.1128/IAI.00566-17
11. Sarwar A, Butt MA, Hafeez S, Danish MZ. Rapid emergence of antibacterial resistance by bacterial isolates from patients of gynecological infections in Punjab, Pakistan. *J Infect Public Health.* (2020) 13:1972–80. doi: 10.1016/j.jiph.2020.06.011
12. Mujeeb UR, Zhang H, Wang YJ, Khalid M, Huang SC, Muhammad KI, et al. Experimental mouse lethality of *Escherichia coli* strains isolated from free ranging Tibetan yaks. *Microb Pathog.* (2017) 109:15–9. doi: 10.1016/j.micpath.2017.05.020
13. McNally A, Cheng L, Harris SR, Corander J. The evolutionary path to extraintestinal pathogenic, drug-resistant *Escherichia coli* is marked by drastic reduction in detectable recombination within the core genome. *Genome Biol Evol.* (2013) 5:699–710. doi: 10.1093/gbe/evt038
14. CLSI. *Performance Standards For Antimicrobial Susceptibility Testing. Clinical and laboratory standards institute*. (2018). Available online at https://www.academia.edu/41587236/M100_Performance_Standards_for_Antimicrobial_Susceptibility_Testing_A_CLSI_supplement_for_global_application_28th_Edition
15. Sun YJ, Wu YJ, Liu ZY, Hu M, Zhao YC, Huang K, et al. Antibacterial Effect of aqueous extract of Chrysanthemum indicum L. combined with antibiotics on extended spectrump β-lactamases-producing Escherichia coli. *Chin Anim Hus Vet Med.* (2016) 43:2170–5. doi: 10.16431/j.cnki.1671-7236.2016.08.033
16. Monstein HJ, Ostholm BA, Nilsson MV, Nilsson M, Dornbusch K, Nilsson LE. Multiplex PCR amplification assay for the detection of *blaSHV, blaTEM* and *blaCTX-M* genes in *Enterobacteriaceae*. *APMIS.* (2007) 115:1–6. doi: 10.1111/j.1600-0463.2007.00722.x
17. Ma QL, Wei DJ, Liu M, Men K. Detection of common genotypes CIT and DHA of plasmid mediated AmpC enzyme in *Escherichia coli*. *Tianjin Med J.* (2009) 37:308–9. doi: 10.1111/CNKI:SUN:TJYZ.0.2009-04-035
18. van der Zee A, Roorda L, Bosman G, Fluit AC, Hermans M, Smits PHM, et al. Multi-centre evaluation of real-time multiplex PCR for detection of carbapenemase genes *OXA-48, VIM, IMP, NDM* and *KPC*. *BMC Infect Dis.* (2014) 14:27. doi: 10.1186/1471-2334-14-27
19. Ma HY. *Acquired resistance-related genes and clinical characteristic in Extensively drug-resistant Klebsella pneumoniae*. (ph.D. Thesis). Suzhou: Soochow University (2017).
20. Wang SM, Zhang JD, Wang YF, Liu SY. Typing of drug resistance genes in carbapenem-resistant *Enterobacteriaceae*. *Chin J Nosocomiol.* (2019) 29:2566–70. doi: 10.11816/cn.ni.2019-182135
21. Yu XH, Li XL, Yang FL, Hai Q. Cloning and sequence analysis of *floR* genes of pathogenic *Escherichia coli* in ducks. *Chin Anim Hus Vet Med.* (2010) 37:84–7. doi: 10.11816/CNKI:SUN:GWXK.0.2010-03-023
22. Kehrenberg C, Schwarz S. Distribution of florfenicol resistance genes *fexA* and *cfr* among chloramphenicol-resistant *Staphylococcus* isolates. *Antimicrob Agents Chemother.* (2006) 50:1156. doi: 10.1128/AAC.50.4.1156-1163.2006
23. Ying YY, Wu F, Wu CY, Jiang Y, Yin M, Zhao WX, et al. Florfenicol resistance in *Enterobacteriaceae* and whole-genome sequence analysis of florfenicol-resistant *Leclercia adecarboxylata* strain R25. *Int J Genomics.* (2019) 2019:9828504. doi: 10.1155/2019/9828504
24. Zhao FJ, Guan M, Li QZ, Li JC, Liang Q, Gu GB. Detection and analysis of chloramphenicols resistance genes in *Escherichia coli* from Swine. *Prog Vet Med.* (2017) 38:49–51. doi: 10.16437/j.cnki.1007-5038.2017.07.011
25. Zhou Q, Zhang XY, Ma YP, Chen DW, Tang XJ, Lu JX, et al. Changes of drug resistance and detection of florfenicol resistance genes in *Escherichia coli* isolated from laying hens after florfenicol administration. *China Poultry.* (2020) 42:40–6. doi: 10.16372/j.issn.1004-6364.2020.09.007
26. Ming YY. Study on drug resistance gene detection and *FexB* gene transmission in pig farm environment in Zhanjiang area. (Ph.D. thesis). Zhanjiang: Guangdong Ocean University (2020).
27. Sáenz Y, Briñas L, Domínguez E, Ruiz J, Zarazaga M, Vila J, et al. Mechanisms of resistance in multiple-antibiotic-resistant *Escherichia coli* strains of human, animal, and food origins. *Antimicrob Agents Chemother.* (2004) 48:3996–4001. doi: 10.1128/AAC.48.10.3996-4001.2004
28. Liu ZM, Li JQ, Huang DH, Hao XW, Hao PG, Wu LC, et al. Study on the drug-resistance of *Escherichia coli* isolated from sheep in Inner Mongolia. *Chin Anim Hus Vet Med.* (2017) 44:839–46. doi: 10.16431/j.cnki.1671-7236.2017.03.031
29. Boerlin P, Travis R, Gyles CL, Reid SR, Janecko N, Lim H, et al. Antimicrobial resistance and virulence genes of *Escherichia coli* isolates from swine in Ontario. *Appl Environ Microbiol.* (2005) 71:6753–61. doi: 10.1128/AEM.71.11.6753-6761.2005
30. Lv WF, Jiang HQ, Yu L. Detection of sulfanilamide sensitivity and sulfonamide resistant related genes in clinical *Escherichia coli* isolates. *J Jilin Agri Univ.* (2010) 32:340–4. doi: 10.13327/j.jjlau.2010.03.026
31. Xia QQ, Wang HN, Zhang AY. Detection of tetracycline resistant genes in bacterial by using a triple-PCR method. *J Sichuan Univ.* (2013) 50:171–6. doi: 10.13327/CNKI:SUN:SCDX.0.2013-01-033

32. Lopardo HA, Vidal P, Jeric P, Centron D, Paganini H, Facklam RR, et al. Six-month multicenter study on invasive infections due to group B *Streptococci* in Argentina. *J Clin Microbiol.* (2003) 41:4688–94. doi: 10.1128/JCM.41.10.4688-4694.2003
33. He KL. *Characteristics and fate of antibiotics and antibiotic resistance genes in manure application soil.* (Ph.D. thesis). Beijing: University of Chinese Academy of Sciences (2018).
34. Feng SW, Li J, Li CT, Xu LS, Pan Y, Hu S, et al. Detection and correlation analysis on the antibiotic resistance phenotype and resistance genes of swine *Escherichia coli* in Guangxi province. *Chin J Vet Sci.* (2020) 40:1170–8. doi: 10.16303/j.cnki.1005-4545.2020.06.17
35. Hansen LH, Johannesen E, Burmølle M, Sørensen AH, Sørensen SJ. Plasmid-encoded multidrug efflux pump conferring resistance to olaquindox in *Escherichia coli*. *Antimicrob Agents Chemother.* (2004) 48:3332–7. doi: 10.1128/AAC.48.9.3332-3337.2004
36. Hansen LH, Jensen LB, Sørensen HI, Sørensen SJ. Substrate specificity of the *OqxAB* multidrug resistance pump in *Escherichia coli* and selected enteric bacteria. *J Antimicrob Chemother.* (2007) 60:145–7. doi: 10.1093/jac/dkm167
37. Gay K, Robicsek A, Strahilevitz J, Park CH, Jacoby G, Barrett TJ, et al. Plasmid-mediated quinolone resistance in non-Typhi serotypes of *Salmonella enterica*. *Clin Infect Dis.* (2006) 43:297–304. doi: 10.1086/505397
38. Liu YY, Wang Y, Walsh TR, Yi LX, Zhang R, Spencer J, et al. Emergence of plasmid-mediated colistin resistance mechanism MCR-1 in animals and human beings in China: a microbiological and molecular biological study. *Lancet Infect Dis.* (2016) 16:161–8. doi: 10.1016/S1473-3099(15)00424-7
39. Basil BX, Christine L, Rohit R, Samir KS, Patrick B, Herman G, et al. Identification of a novel plasmid-mediated colistin-resistance gene, *mcr-2*, in *Escherichia coli*, Belgium, June 2016. *Eurosurveillance.* (2016) 21:30280. doi: 10.2807/1560-7917.ES.2016.21.27.30280
40. Shen XY, Li JM, Cheng X, Liu M, Dai YB. Detection of drug-resistant genes and their correlation with drug sensitivity in *Salmonella* pullorum isolates. *China Poultry.* (2018) 40:15–8. doi: 10.16372/j.issn.1004-6364.2018.03.004
41. Cully M. Public health: The politics of antibiotics. *Nature.* (2014) 509:S16–7. doi: 10.1038/509S16a
42. Liu WC, Guo Y, Zhao ZH, Jha R, Balasubramanian B. Algae-derived polysaccharides promote growth performance by improving antioxidant capacity and intestinal barrier function in broiler chickens. *Front Vet Sci.* (2020) 7:601336. doi: 10.3389/fvets.2020.601336
43. Liu WC, Ou BH, Liang ZL, Zhang R, Zhao ZH. Algae-derived polysaccharides supplementation ameliorates heat stress-induced impairment of bursa of Fabricius via modulating NF-κB signaling pathway in broilers. *Poult Sci.* (2021) 100:101139. doi: 10.1016/j.psj.2021.101139
44. Zhao Y, Balasubramanian B, Guo Y, Qiu SJ, Jha R, Liu WC. Dietary *Enteromorpha* polysaccharides supplementation improves breast muscle yield and is associated with modification of mRNA transcriptome in broiler chickens. *Front Vet Sci.* (2021) 8:663988. doi: 10.3389/fvets.2021.663988
45. Liu WC, Zhu YR, Zhao ZH, Jiang P, Yin FQ. Effects of dietary supplementation of algae-derived polysaccharides on morphology, tight junctions, antioxidant capacity and immune response of duodenum in broilers under heat stress. *Animals.* (2021) 11:2279. doi: 10.3390/ani11082279
46. Saharan VV, Verma P, Singh AP. High prevalence of antimicrobial resistance in *Escherichia coli, Salmonella spp*. and staphylococcus aureus isolated from fish samples in India. *Aqua Res.* (2020) 51:1200–10. doi: 10.1111/are.14471
47. Ng C, Chen H, Goh SG, Haller L, Wu Z, Charles FR, et al. Microbial water quality and the detection of multidrug resistant *E.* coli and antibiotic resistance genes in aquaculture sites of Singapore. *Mar Pollut Bull.* (2018) 135:475–80. doi: 10.1016/j.marpolbul.2018.07.055
48. Lihan S, Lee SY, Toh SC, Leong SS. Plasmid-mediated antibiotic resistant *Escherichia coli* in Sarawak rivers and aquaculture farms, Northwest of Borneo. *Antibiotics.* (2021) 10:776. doi: 10.3390/antibiotics10070776
49. Huang Y, Zhang L, Tiu L, Wang HH. Characterization of antibiotic resistance in commensal bacteria from an aquaculture ecosystem. *Front Microbiol.* (2015) 6:914. doi: 10.3389/fmicb.2015.00914
50. Hassan J, Eddine RZ, Mann D, Li S, Deng X, Saoud IP, et al. The mobile colistin resistance gene, mcr-11, is carried on IncX4 plasmids in multidrug resistant E coli isolated from Rainbow trout aquaculture. *Microorganisms.* (2020) 8:1636. doi: 10.3390/microorganisms8111636
51. Qiao Y. *Study on the major pathogenic bacteria resistance of aquaculture in the coastal regions of Jiangsu province.* (Ph.D. thesis). Shanghai: Shanghai Ocean University (2015).
52. Changkaew K, Utrarachkij F, Siripanichgon K, Nakajima C, Suthienkul O, Suzuki Y. Characterization of antibiotic resistance in *Escherichia coli* isolated from shrimps and their environment. *J Food Prot.* (2014) 77:1394–401. doi: 10.4315/0362-028X.JFP-13-510
53. Ng KH, Samuel L, Kathleen MM, Leong SS, Felecia C. Distribution and prevalence of chloramphenicol-resistance gene in *Escherichia coli* isolated from aquaculture and other environment. *Int Food Res J.* (2014) 21:1321–5.
54. Li YY. *Preliminary study on the detection of florfenicol resistance gene floR in avian Escherichia coli isolates and mechanism of transmission.* (Ph.D. thesis). Yangzhou: Yangzhou University (2016).
55. Poirel L, Madec JY, Lupo A, Schink AK, Kieffer N, Nordmann P, et al. Antimicrobial resistance in *Escherichia coli*. *Microbiol Spectr.* (2018) 6:14. doi: 10.1128/microbiolspec.ARBA-0026-2017

Conflict of Interest: The authors declare that the research was conducted in the absence of any commercial or financial relationships that could be construed as a potential conflict of interest.

Publisher's Note: All claims expressed in this article are solely those of the authors and do not necessarily represent those of their affiliated organizations, or those of the publisher, the editors and the reviewers. Any product that may be evaluated in this article, or claim that may be made by its manufacturer, is not guaranteed or endorsed by the publisher.

frontiers in Veterinary Science

ORIGINAL RESEARCH
published: 12 January 2022
doi: 10.3389/fvets.2021.801990

Function and Characterization of an Alanine Dehydrogenase Homolog From *Nocardia seriolae*

Guoquan Chen[1,2†], *Ziyang Tan*[1], *Yansheng Liu*[1,2], *Tingting Weng*[1,2], *Liqun Xia*[1,2*†] and *Yishan Lu*[1,2*]

[1] Guangdong Provincial Key Laboratory of Pathogenic Biology and Epidemiology for Aquatic Economic Animals, Fisheries College of Guangdong Ocean University, Zhanjiang, China, [2] Guangdong Provincial Engineering Research Center for Aquatic Animal Health Assessment, Shenzhen Public Service Platform for Evaluation of Marine Economic Animal Seedings, Shenzhen Institute of Guangdong Ocean University, Shenzhen, China

OPEN ACCESS

Edited by:
Lixing Huang,
Jimei University, China

Reviewed by:
Jie Li,
Chinese Academy of Fishery Sciences (CAFS), China
Weiwei Zhang,
Ningbo University, China

***Correspondence:**
Liqun Xia
xialq@gdou.edu.cn
Yishan Lu
fishdis@163.com

†ORCID:
Guoquan Chen
orcid.org/0000-0002-0847-0408
Liqun Xia
orcid.org/0000-0001-6244-8060

Specialty section:
This article was submitted to Veterinary Infectious Diseases, a section of the journal Frontiers in Veterinary Science

Received: *26 October 2021*
Accepted: *22 November 2021*
Published: *12 January 2022*

Citation:
Chen G, Tan Z, Liu Y, Weng T, Xia L and Lu Y (2022) Function and Characterization of an Alanine Dehydrogenase Homolog From Nocardia seriolae. Front. Vet. Sci. 8:801990. doi: 10.3389/fvets.2021.801990

Fish nocardiosis is a chronic, systemic, granulomatous disease in aquaculture. *Nocardia seriolae* has been reported to be one of the main pathogenic bacteria of fish nocardiosis. There are few studies on the associated virulence factors and pathogenesis of *N. seriolae*. Alanine dehydrogenase (ALD), which may be a secreted protein, was discovered by analysis using bioinformatics methods throughout the whole genomic sequence of *N. seriolae*. Nevertheless, the roles of ALD and its homologs in the pathogenesis of *N. seriolae* are not demonstrated. In this study, the function of *N. seriolae* ALD (NsALD) was preliminarily investigated by gene cloning, host cell subcellular localization, secreted protein identification, and cell apoptosis detection. Identification of the extracellular products of *N. seriolae via* mass spectrometry (MS) analysis revealed that NsALD is a secreted protein. In addition, subcellular localization of NsALD-GFP recombinant protein in fathead minnow (FHM) cells showed that the strong green fluorescence co-localized with the mitochondria. Moreover, apoptosis assays demonstrated that the overexpression of NsALD induces apoptosis in FHM cells. This study may lay the foundation for further exploration of the function of NsALD and facilitate further understanding of the pathogenic mechanism and the associated virulence factors of *N. seriolae*.

Keywords: ***Nocardia seriolae*, alanine dehydrogenase, secreted protein, mitochondrial localization, apoptosis**

INTRODUCTION

Fish nocardiosis, a chronic systemic granulomatous disease, has great influence on both marine and freshwater aquaculture industry (1, 2). *Nocardia salmonicida*, *Nocardia asteroids*, and *Nocardia seriolae* have been isolated from diseased fish and confirmed as the pathogenic bacteria of fish nocardiosis (3). Remarkably, *N. seriolae* has been most frequently reported as the main pathogen in the last 30 years. *Nocardia seriolae* can infect the immunodeficient fish *via* wounds, the gills, and feeds (4). The symptoms of diseased fish include skin ulceration and serious sarcoidosis caused by a mass of white nodules in the gills, spleen, liver, head kidney, and trunk kidney (5). According to reports, *N. seriolae* was able to infect about 42 kinds of marine and freshwater fish, such as blotched snakehead (*Channa maculata*), amberjack (*Seriola dumerili*), yellowtail (*Seriola quinqueradiata*), snubnose pompano (*Trachinotus blochii*), golden pompano (*Trachinotus ovatus*),

largemouth bass (*Micropterus salmoides*), large yellow croaker (*Larimichthys crocea*), and red drum (*Sciaenops ocellatus*) (3, 6–8).

The virulence factors and pathogenic mechanisms of *N. seriolae*–host interaction are not fully studied. It was reported that the virulence of *Nocardia* species is related to their resistivity to oxidative damage of macrophages, inhibition of a combination of phagosomes and lysosomes, alteration of lysosomal enzymes in phagocytes, and neutralization of the acidification of the phagosome, and some extracellular products seemed to participate in the above processes in *Nocardia asteroide*s (9–12). Our previous studies also indicated that the MTSP3141, GluNS, NsHLP, PLC, SOD, robl/LC7, PTP, and NlpC/P60 of *N. seriolae* are able to lead to apoptosis in fish cells and are the potential virulence factors of *N. seriolae*. MTSP3141 and GluNS were also confirmed to be secreted proteins and mitochondrial targeting secretory proteins (MTSPs) (7, 13–15). The disease mechanisms of *Nocardia* sp. have been demonstrated to be varied and complicated and needed further clarification.

In this study, an alanine dehydrogenase (*ALD*) homolog of *N. seriolae* (*NsALD*) was amplified by gene cloning. Then, the secreted proteins were identified and the subcellular localization of NsALD and its involvement in disease mechanisms were evaluated. This study will put forward further clarification of the role of NsALD during infection and facilitate new insights into the molecular pathogenicity of *N. seriolae*.

TABLE 1 | Primers used for gene cloning in this study.

Primer name	Sequence (5′-3′)	Restriction enzyme
pEGFP-ALD-F	GGAATTCATGCTGTTCGATAGCGGCATC	EcoR I
pEGFP-ALD-R	CCGACGTCGACTGGGAGGCGATGCGGGTCAC	Sal I
pcDNA-ALD-F	GGAATTCATGCTGTTCGATAGCGGCATC	EcoR I
pcDNA-ALD-R	CCGCTCGAGGGAGGCGATGCGGGTCACC	Xho I

TABLE 2 | Primers used for qRT-PCR in this study.

Primer name	Sequence (5′-3′)	Gene name
Bad-F	TGATCCTTTCAGGCGGAGATCTCGC	Bad
Bad-R	CAGACTCTTTGTGACTCCAAAGGAA	
Bid-F	CTGCTTCTCCTTTCCTTCTTTGAGC	Bid
Bid-R	GATCAACTCAGCAGCCATATCCCTT	
Bax-F	TGGCACTGTTTCACCTCG	Bax
Bax-R	ATCCTCCTTGCTGTCTGATC	
Bcl-2-F	TGGGACTGTTTGCCTTCG	Bcl-2
Bcl-2-R	TCTGCCGCTGCATCTTTT	
β-actin-F	ACAATCAATACGGCTGCCATGG	β-actin
β-actin-R	TTGGCATACAGGTCCTTACTTACGT	

MATERIALS AND METHODS

Bacterial Strains, Cell Line, and Plasmids

Nocardia seriolae ZJ0503 strain (16), fathead minnow (FHM) cells (17), plasmid PEGFP-N1, plasmid PCDNA3.1-His A, and *Escherichia coli* DH5α were conserved in our laboratory. *Nocardia seriolae* ZJ0503 isolated from diseased fish was cultured in optimal medium to clone the *ALD* gene. *Escherichia coli* DH5α transformed by plasmid DNA was cultured to extract large numbers of endotoxin-free plasmids. FHM cells (17) transformed by endotoxin-free plasmids were cultured in Leibovitz's L15 medium with 10% fetal bovine serum for apoptosis assays. The endotoxin-free plasmids pEGFP-N1 and pCDNA3.1-His A were used for subcellular localization and overexpression, respectively.

Gene Cloning and Sequence Bioinformatics Analysis of *NsALD*

Nocardia seriolae ZJ0503 was collected after 5 days of cultivation in optimal medium to extract genomic DNA using TIANamp Bacteria DNA Kit (Tiangen, Beijing, China). *NsALD* was cloned *via* PCR with two pairs of primers designed using Primer Premier 5.0 software, pEGFP-ALD-F/R and pcDNA-ALD-F/R, shown in **Table 1**. Based on the whole-genome sequence data of the *N. seriolae* strain ZJ0503 (accession no. NZ_JNCT01000022), BLAST sequence analysis was carried out through NCBI (http://www.ncbi.nlm.nih.gov/BLAST/). The amino acid sequence for NsALD was predicted and the physicochemical property predicted using ExPASy software (http://www.expasy.org/). Multiple sequence alignment was done with DNAMAN software. A biological evolutionary tree was constructed using the evolutionary analysis software MEGA 6.0. LocTree 3 (https://rostlab.org/services/loctree3/) and PSORT II Prediction (https://psort.hgc.jp/form2.html) were utilized to predict the subcellular localization and signal peptides.

Plasmid Construction

Using the two pairs of primers listed in **Table 1**, the gene *NsALD* was cloned into pcDNA3.1/His A and pEGFP-N1 vectors to explore the molecular function and subcellular localization of NsALD *in vitro*. The constructed recombinant plasmids were subsequently confirmed by sequencing.

PCR was performed with TaKaRa Ex Taq® polymerase using the following PCR program: pre-denaturation at 95°C for 5 min, 34 cycles at 95°C for 30 s, 55°C for 30 s, 72°C for 1 min, and a final extension at 72°C for 3 min. The PCR products of *NsALD* were electrophoresed on 1% agarose gel and purified using EasyPure PCR Purification Kit (TransGen, Beijing, China). The purified PCR products were digested by the corresponding restriction enzymes, ligated into the eukaryotic vectors pEGFP-N1 and pcDNA3.1/His A, and then transformed into competent *E. coli* DH5α cells. The different constructs were confirmed by corresponding restriction enzyme digestion (**Table 1**) and DNA sequencing by Guangzhou Sangon Biological Engineering & Technology and Service Co. Ltd. Finally, the recombinant plasmids named as pEGFP-ALD and pcDNA-ALD.

Preparation and Identification of Extracellular Products

After culturing in optimal medium for 3–5 days, single colonies were selected to prepare bacterial suspension. Sterilized

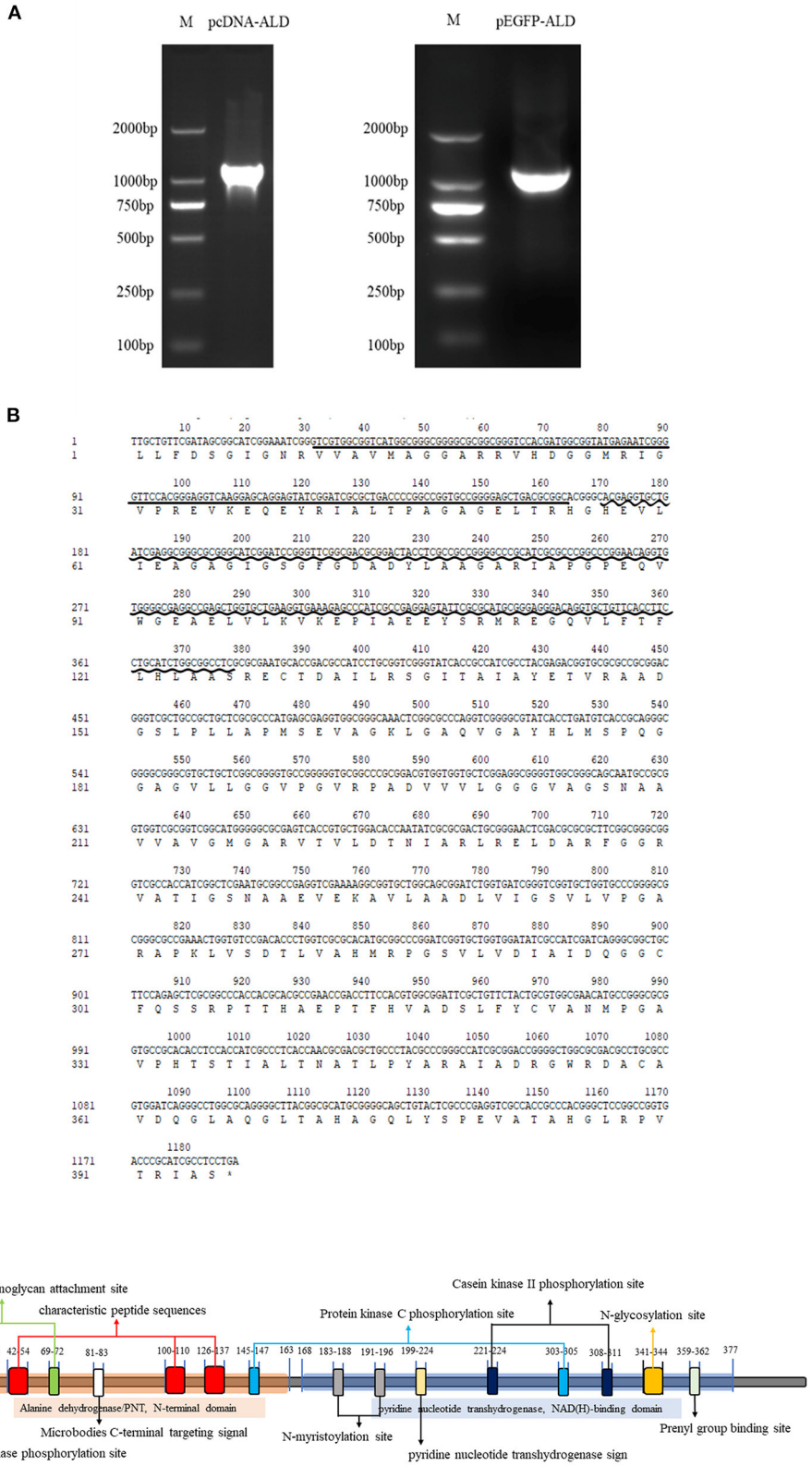

FIGURE 1 | Sequence and structure analysis of the alanine dehydrogenase of *Nocardia seriolae* (NsALD). **(A)** NsALD was amplified *via* PCR using the primers pEGFP-ALD-F/R and pcDNA-ALD-F/R. **(B)** NsALD nucleic acid sequence and its derived amino acid sequence. The *straight line* indicates the ALD/PNT, N-terminal domain and the *wavy line* shows the ALD NAD-binding and catalytic domains. **(C)** Schematic representation of the prosites of protein NsALD. The NsALD protein comprised two complexity domains (30–163 and 168–377) and nine kinds of functional sites.

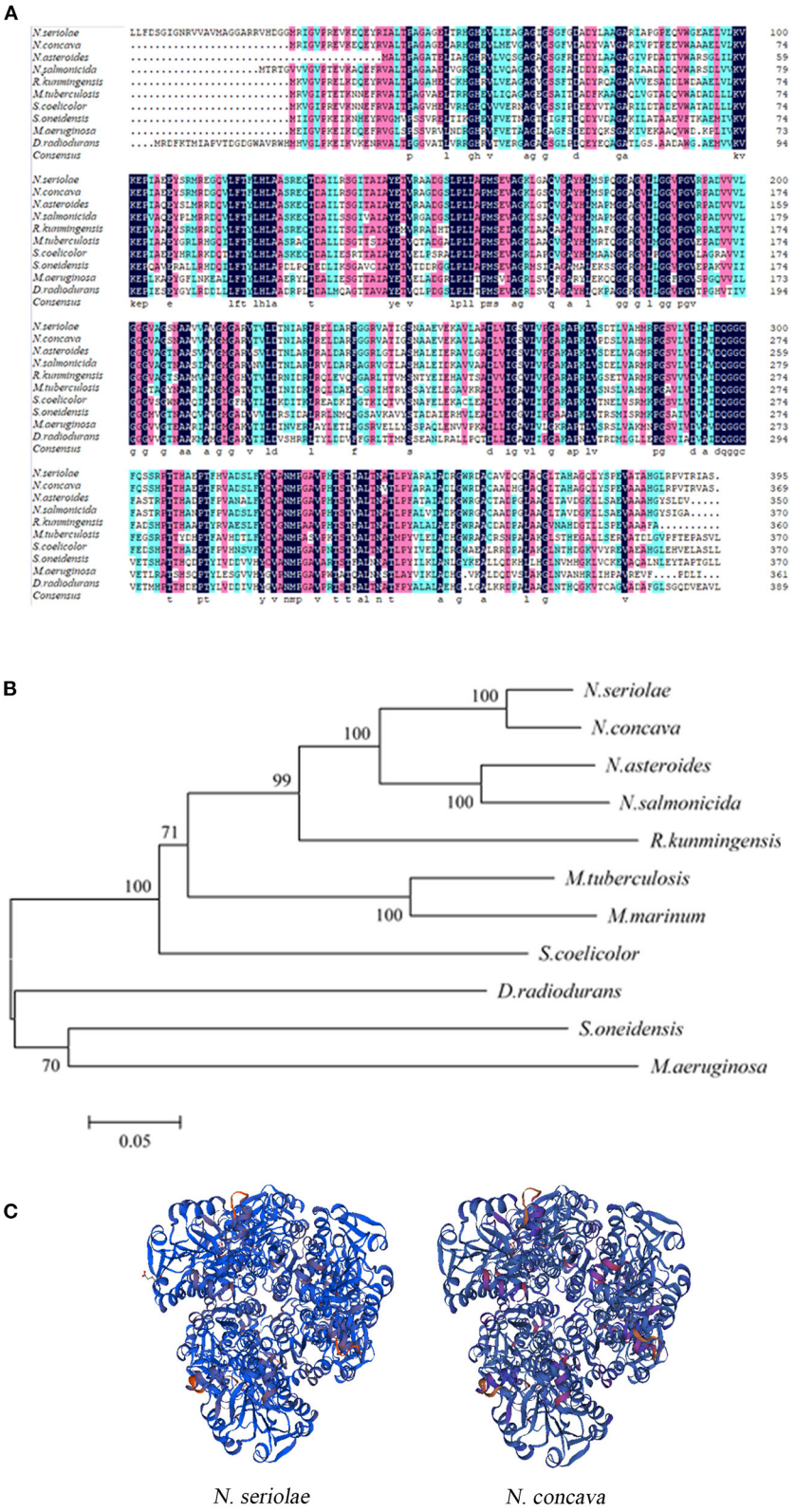

FIGURE 2 | Multiple sequence alignment, construction of a phylogenetic tree, and the three-dimensional structure of *Nocardia seriolae* alanine dehydrogenase (NsALD) protein. **(A)** Multiple alignment of the deduced amino acid sequences of NsALD protein among different species. *Black shaded backgrounds* indicate 100%

(Continued)

FIGURE 2 | homology, *pink shaded backgrounds* indicate >75% homology, and *blue shaded backgrounds* indicate >50% homology. **(B)** Construction of a phylogenetic tree among *N. seriolae* and other species with protein NsALD homologous sequences. The protein sequences were aligned using DNAMAN software, and the non-rooted neighbor joining tree was generated by the MEGA 5.0 program. *Number at branch points* indicates bootstrap support. **(C)** Structure analysis of NsALD from *N. seriolae*. The predicted three-dimensional structure of NsALD protein from *N. seriolae* (*left*) and *Nocardia concava* (*right*). The diagrams were generated using SWISS-MODEL online. GenBank accession numbers are shown as follows: *N. seriolae* ZJ0503, WP_033090406.1; *N. concava*, WP_040806553.1; *Nocardia asteroides*, SFM85941.1; *Nocardia salmonicida*, WP_062992005.1; *Rhodococcus kunmingensis*, WP_068269631.1; *Mycobacterium tuberculosis* H37Rv, NP_217296.1; *Mycobacterium marinum*, WP_020728350.1; *Streptomyces coelicolor* A3(2), NP_626044.1; *Shewanella oneidensis* MR-1, YP_007001355.1; *Microcystis aeruginosa*, WP_012268249.1; and *Deinococcus radiodurans* R1, NP_295618.1.

cellophane was laid flat on the modified medium plate as close to the medium as possible. Of the bacterial suspension, 100 μl was spread evenly on the medium covered with cellophane and incubated at 28°C for 3–5 days. The cellophane with colonies from the medium was removed with tweezers and the colonies on the cellophane rinsed into a sterile beaker with sterile phosphate-buffered saline (PBS). The collected liquid was transferred into a 50-ml centrifuge tube at 8,000 × *g* at 4°C for 20 min. After centrifugation, the supernatant was sterilized using a 0.22-μm microporous membrane and then transferred into a dialysis bag. Dialysis was performed at 4°C for 10–16 h in ultrapure water, during which the dialysate was changed 3 times. After dialysis, the samples were transferred into a 50-ml centrifuge tube and the liquid was frozen into solid at −80°C before freeze drying in a vacuum freeze dryer. The freeze-dried extracellular product samples were sent to a related biological company for protein shotgun LC-MS identification.

Cell Transfection and Subcellular Localization

Plasmids pEGFP-ALD and pEGFP-N1 were extracted in large quantities *via* Endo-Free Plasmid Mini Kit I D6948 (Omega Bio-Tek, Norcross, GA, USA). Cell transfection was carried out to explore the subcellular localization of *NsALD* in host cells using the Lipofectamine 3000 reagent. At 48 h post-transfection (hpt), pEGFP-ALD-transfected FHM cells and pEGFP-N1-transfected cells were both stained with 4′,6-diamidino-2-phenylindole (DAPI) and Mito Tracker Red according to the protocols. After staining and washing with sterilized PBS, the cells were examined under a fluorescence microscope.

Detection of Cell Apoptosis Induced by Overexpression of *NsALD* Protein

To determine whether the overexpression of NsALD induces apoptosis in fish cells, transient transfection of FHM cells was carried out using pcDNA-ALD as an experimental group or plasmid pcDNA3.1/His A as a control group. The overexpression of *NsALD* in FHM cells was verified by Western blot. Then, FHM cells were dyed with DAPI at 48 hpt and observed using a fluorescence microscope. Furthermore, the caspase-3 activity and mitochondrial membrane potential ($\Delta\Psi_m$) of the transfected cells were detected, respectively (18) with a caspase-3 colorimetric assay kit K106-25 (BioVision, Milpitas, CA, USA) and a mitochondrial membrane potential assay kit with JC-1 (Beyotime, Shanghai, China).

Quantitative Analysis of the mRNA Expression of Apoptosis-Related Genes

Quantitative PCR primers (**Table 2**) for the genes *Bcl-2*, *Bax*, *Bid*, and *Bad* of FHM cells were designed using Primer Premier 5.0 software. FHM cells transfected with pcDNA-ALD and pcDNA3.1/His A were collected at 0, 24, 48, and 72 hpt. Total RNA was extracted using the TransZol Up Plus RNA Kit (TransGen) and cDNA was synthesized with the EasyScript® One-Step gDNA Removal and cDNA Synthesis SuperMix (TransGen) for real-time quantitative PCR (RT-qPCR) with PerfectStart® Green qPCR SuperMix (TransGen). The effect of transfection on the expressions of apoptosis-related genes was calculated by LightCycler 96 software for RT-qPCR. Each test was performed with the *β-actin* gene as the internal control, and there were 3 replicates. The PCR reaction volume was 10 μl, 1 μl for each primer (10 μM), 1 μl for cDNA, 2 μl for PCR grade water, and 5 μl for Green qPCR SuperMix. The PCR procedures for the four apoptosis-related genes and *β-actin* were as follows: 95°C for 2 min, 40 cycles of 95°C for 75 s, and 55°C for 1 min.

Data Analysis

The comparative $2^{(-\Delta\Delta Ct)}$ method was used to calculate the relative expression levels of the four apoptosis-related genes. The data obtained were analyzed with one-way ANOVA using GraphPad Prism 8.0 software. The data were edited and plotted into histograms, and the expression of each apoptosis-related gene at 0 hpt was calculated as 1. Asterisks show statistical significance, as follows: $p > 0.05$, not significant; $^{*}p < 0.05$, significant; and $^{**}p < 0.01$, extremely significant.

RESULTS

Sequence Characterization and Bioinformatics Analysis of *NsALD*

NsALD was cloned *via* PCR using pEGFP-ALD-F/R and pcDNA-ALD-F/R (**Figure 1A**). Sequencing analysis showed that the total length of the open reading frame (ORF) of *NsALD* was successfully acquired, which encoded an alanine dehydrogenase homolog. The results of sequencing analysis revealed that the ORF of the *NsALD* gene (GenBank: 61148960) was 1,188 bp encoding 395 amino acid sequences, with alanine dehydrogenase/PNT, N-terminal domain, and alanine dehydrogenase NAD-binding and catalytic domains, which belong to the NADB-Rossmann superfamily (**Figure 1B**). For subcellular localization, NsALD was predicted to locate in the mitochondria with 81% expected accuracy using LocTree 3, while

it was predicted to locate in the cytoplasm with 94.1% expected accuracy using PSORT II Prediction. No signal peptide or transit peptide was found. Schematic representation of the prosites demonstrated the protein NsALD to comprise two complexity domains (30–163 and 168–377) and nine kinds of functional sites (**Figure 1C**).

BLAST protein analysis showed that the NsALD amino acid sequence had high homology with other ALD sequences in actinomycetes, with 92.41, 79.05, 76.15, 68.29, 66.67, 62.60, 52.30, 50.68, and 53.66% identity to the ALDs of *Nocardia concava*, *N. asteroides*, *N. salmonicida*, *Rhodococcus kunmingensis*, *Mycobacterium tuberculosis* H37Rv, *Streptomyces coelicolor* A3(2), *Shewanella oneidensis* MR-1, *Microcystis aeruginosa*, and *Deinococcus radiodurans* R1, respectively (**Figure 2A**). A biological evolutionary tree was constructed with the amino acid sequences of 12 bacterial ALDs, which shows that NsALD had a rather high homology among the *Nocardia* species (**Figure 2B**). Structure analysis showed a high similarity between the ALDs from *N. seriolae* and *Nocardia concave* (**Figure 2C**).

Detection of Subcellular Localization of NsALD in Transfected Cells

To explore the subcellular localization of the NsALD protein, the recombinant plasmid pEGFP-ALD was transfected into FHM cells, which was tested by green fluorescence signals. The nucleus was shown as blue fluorescence and the mitochondria was displayed as red fluorescence. In pEGFP-N1-transfected cells, the green fluorescence was dispersed in the whole cell of FHM cells, the mitochondria were distributed in the perinuclear cytoplasm, and the nucleus margin was smooth and had no apoptosis feature (**Figure 3**, right). Differently, in pEGFP-ALD-transfected cells, nuclear shrinkage appeared, the mitochondria aggregated near the nucleus, and a strong green fluorescence of ALD-GFP exhibited an aggregated distribution near the nucleus and overlapped with the location of the mitochondria, which indicated that the protein NsALD was co-localized with the mitochondria (**Figure 3**, left).

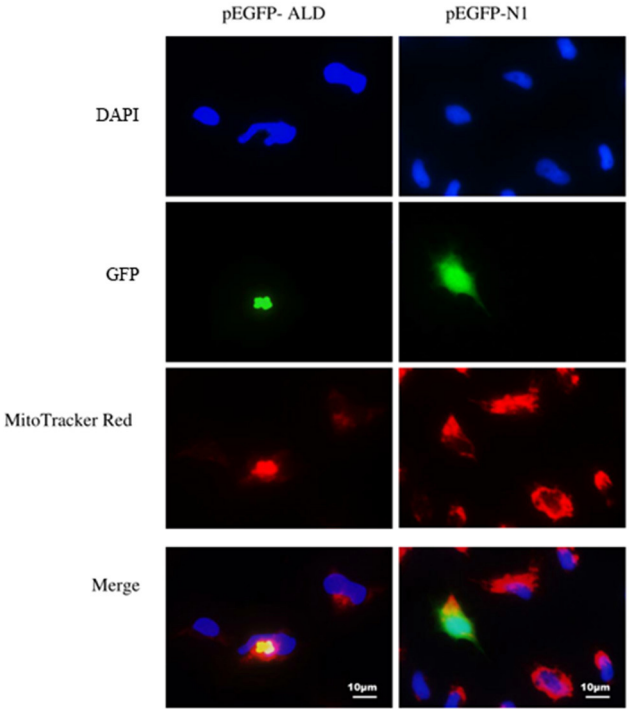

FIGURE 3 | Subcellular localization of the *Nocardia seriolae* alanine dehydrogenase (NsALD) protein in fathead minnow (FHM) cells. Green fluorescence shows ALD-GFP or GFP, red fluorescence shows the mitochondria, and blue fluorescence shows the nucleus. *Left panels* are pEGFP-ALD and *right panels* are pEGFP-N1. In pEGFP-N1-transfected cells, the green fluorescence was dispersed in the whole cell of FHM cells, the mitochondria were distributed in the perinuclear cytoplasm, and the edge of the nucleus was smooth and had no apoptosis characteristics. In pEGFP-ALD-transfected cells, nuclear shrinkage appeared, the mitochondria aggregated near the nucleus, and a strong green fluorescenc of ALD-GFP exhibited an aggregated distribution near the nucleus and overlapped with the distribution of the mitochondria.

Secreted Protein Identification to NsALD

The secreted proteins of *N. seriolae* were acquired and identified with shotgun mass spectrometry. The results revealed that three characteristic peptide sequences of NsALD (IALTPAGAGELTR, SGITAIAYETVR, and VKEPIAEEYSR) were tested with a confidence ≥99%, which demonstrated that NsALD is a secreted protein of *Nocardia seriolae*.

Apoptosis Detection Induced by the Overexpression of *NsALD*

To explore whether the NsALD protein has an influence on the apoptosis of fish cells, the control plasmid and the recombinant plasmid pcDNA-ALD were transfected into FHM cells. At 48 hpt, several apoptotic bodies can be observed in the transfected FHM cells (**Figure 4A**), and Western blot showed that the NsALD protein was expressed (**Figure 4B**). Apoptotic bodies were counted to calculate the apoptosis rate. The result revealed that there were highly significant differences between the experimental group and the control group (**Figure 4C**). As exhibited in **Figure 4D**, detection of caspase-3 activity revealed that the maximum value appeared at 48 hpt, which was a 1.63-fold increase compared to that of the control group. Furthermore, the $\Delta\Psi_m$ values of NsALD-overexpressing cells compared with those of control cells were reduced remarkably. The $\Delta\Psi_m$ values of NsALD-overexpressing cells decreased to minimum values at 48 hpt, a decrease of 0.43-fold compared to the control group (**Figure 4E**).

Quantitative Detection of Apoptosis-Related Genes in FHM Cells

The expression level of each apoptosis-related gene at 0 hpt was considered as the control group. The expressions of *Bad* and *Bax* genes increased significantly at 24–72 hpt, with peak values of 10.5-fold at 72 hpt and 2.9-fold at 48 hpt, respectively. The *Bid* gene increased significantly at 48–72 hpt, reaching a peak value of 2.5-fold at 72 hpt. Interestingly, the expression of *Bcl-2*, which is an anti-apoptotic gene, showed no change during 0–48 hpt, while it increased significantly at 72 hpt. Since a high *Bax*/*Bcl-2*

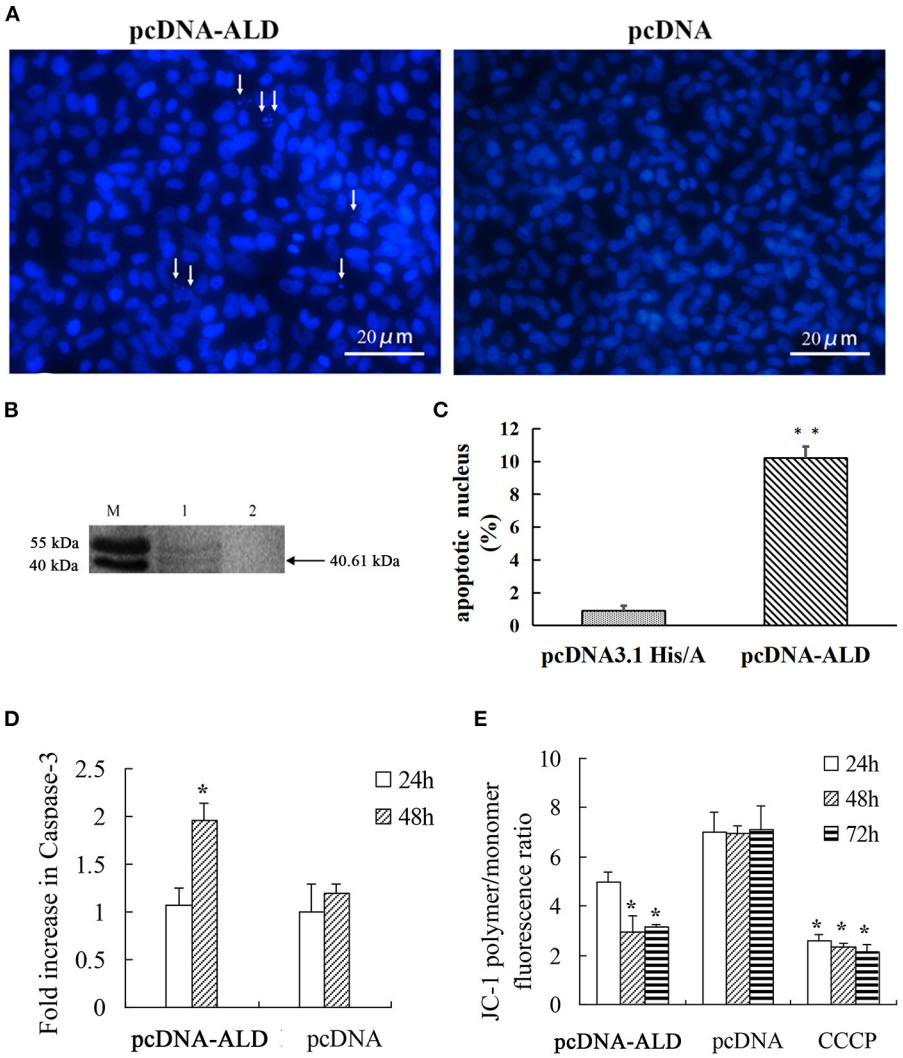

FIGURE 4 | Apoptosis characteristics in pcDNA-ALD-transfected fathead minnow (FHM) cells. **(A)** Overexpression of protein NsALD (*Nocardia seriolae* alanine dehydrogenase) in FHM cells. *White arrows* indicate apoptotic bodies. **(B)** Confirmation of NsALD expression in FHM cells by Western blot. *M*, marker. *1*, NsALD; *2*, pcDNA. **(C)** Percentage of apoptotic body in plasmid pcDNA-ALD- or pcDNA-transfected cells. *Error bars* indicate SD (**$p < 0.01$). **(D)** Fold increase in caspase-3 after plasmid pcDNA-ALD or pcDNA transfection of FHM cells. FHM cells transfected with plasmids were collected at indicated points after transfection and the levels of cleaved caspase-3 measured. *Error bars* indicate SD (*$p < 0.05$). **(E)** Detection of $\Delta\Psi_m$ values. FHM cells transfected with plasmid pcDNA-ALD or pcDNA were collected at indicated time points after transfection and the values accessed using JC-1. Untransfected cells treated with carbonyl cyanide *m*-chlorophenylhydrazone (CCCP) were positive controls. Data are expressed as the JC-1 polymer/monomer fluorescence ratio. *Error bars* indicate SD (*$p < 0.05$).

ratio is related to cell apoptosis, the *Bax*/*Bcl-2* ratio was calculated according to their expressions. The *Bax*/*Bcl-2* ratio increased significantly at 24–48 hpt, with a peak value of 10.5-fold at 48 hpt, and then it decreased to 0.5 times that of the control group at 72 hpt (**Figure 5**). This meant that, although the expression of *Bcl-2* increased significantly, the *Bax*/*Bcl-2* ratio is still low at 72 hpt.

DISCUSSION

Alanine dehydrogenase (ALD) is a microbial enzyme that catalyzes the reversible oxidation of the deamination of alanine to pyruvate. ALD interconversion between alanine and pyruvate is the core of microbial metabolism (19). ALD was firstly found in *Bacillus subtilis* by Wiame and Pierard (20). The pathogenicity of bacteria is closely associated with its pathogenic factors. However, only a few studies have been conducted on the virulence factor of *N. seriolae*. Interestingly, in some bacteria, ALD was found to be an antigen-secreting protein *in vitro* and was regarded as a virulence factor of pathogenic bacteria. For instance, ALD was found in *M. tuberculosis* culture filtrate and identified as one of its main antigens (21). Transcriptional induction of the *ALD* gene has been observed upon infection of leopard frogs with *Mycobacterium marinum*, which indicated that ALD may be crucial during *M. marinum* infection (22). So far, information about the regulation of ALD and its possible role in pathogenesis

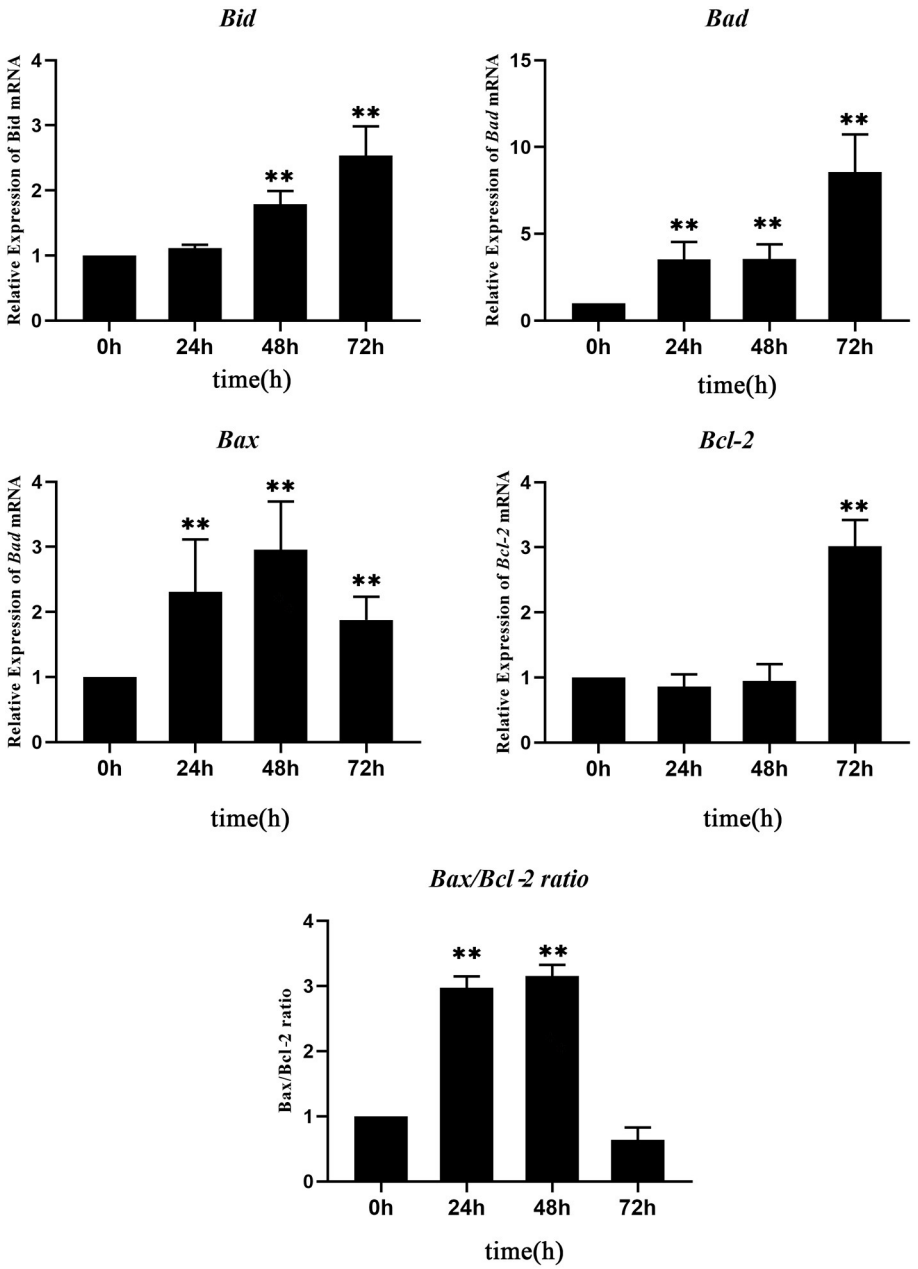

FIGURE 5 | Real-time quantitative PCR (RT-qPCR) analysis of the expressions of apoptosis-related genes in *Nocardia seriolae* alanine dehydrogenase (NsALD)-overexpressing fathead minnow (FHM) cells. Significant differences are indicated by $^{**}p < 0.01$.

is limited (18), and no study related to the ALD of *N. seriolae* (NsALD) has been reported.

In this study, NsALD was obtained and identified as a secreted protein without a signal peptide. It has been reported that the ALD of *M. tuberculosis* is a predominant antigen in its culture filtrate, which means that ALD is a secreted protein of *M. tuberculosis*; the ALD of *M. tuberculosis* also lacks a signal peptide (23). NsALD was found to co-localize with the mitochondria in this research. Some proteins targeting the mitochondria contain a transit peptide, while no transit peptide was found in the NsALD protein by bioinformatic prediction. Mitochondrial targeting of bacterial proteins has been reported. Some proteins from parasitic microorganisms such as rickettsial postulated peptidase (RPP) have been discovered to be similar to the protein subunit of mitochondrial processing peptidase (MPP) (24). Additionally, some bacterial virulence factors contain N-terminal mitochondrial targeting signals (25, 26). The host cells are invaded by certain proteins of Gram-negative bacteria through the type 3 secretion system (TTSS) and are co-positioned with the mitochondria of host cells (25–27). *Helicobacter pylori*

VacA-targeted mitochondria was associated with the formation of anion-selective channels in mitochondrial membranes (28). Further research on the mitochondria-targeting mechanism of NsALD is needed.

The mitochondria is an important organelle with various important functions, such as participating in innate and adaptive immunity and acting as the signal center in cell apoptosis (29), and is also the key target of bacterial invasion (30). Most of the identified bacterial proteins targeting the mitochondria are involved in cell apoptosis, which is consistent with the core effect of the mitochondria in apoptosis regulation (31). For example, the *hlyA* gene of enteropathogenic *E. coli* (EPEC) encodes hemolysin, which is targeted to the mitochondria and triggers the apoptosis of host cells *via* mitochondrial pathways (25). In the process of infection with macrophages, the secreted SopA protein of *Salmonella enterica* locates in the mitochondria to activate the caspase-1 independent pathway *via* the TTSS and leads to macrophage death (32). Cytotoxin VacA related to gastric epithelial lesions is a virulence factor of pathogenic *H. pylori* (33). It was found that p34, a subunit of VacA, specifically locates in host mitochondria and induces the release of host cytochrome C, which activates caspase-3 and leads to cell death (34). In this study, typical apoptosis characteristics, such as apoptotic bodies, $\Delta\Psi_m$ values dropping, and caspase-3 activation, were examined in NsALD-expressed cells, which indicated that NsALD induces apoptosis in host cells.

In our previous work, the secreted virulence factors of *N. seriolae* have also been identified to induce cell apoptosis. The phospholipase C of *N. seriolae* was a secreted protein and induced apoptosis in FHM cells (15). The MTSP3141 of *N. seriolae* was proven to be a secreted protein, co-located with the mitochondria, and had a 30-amino acid transit peptide at the N-terminal (35). Glutamyl endopeptidase was a secreted protein without a transit peptide, localized in the mitochondria, and was also a virulence factor of *N. seriolae* that induced apoptosis (36). In addition, the superoxide dismutase (SOD) and histone-like DNA-binding protein (HLP) of *N. seriolae* was also identified as secreted proteins that lead to apoptosis in host cells (7, 13). Taken together, secreted protein-induced apoptosis is associated with *N. seriolae* infection.

According to relevant articles, the main apoptosis pathways in fish are the extrinsic/death receptor pathway (37) and the intrinsic/Bcl-2-regulated/mitochondrial pathway (38). In addition, like mammals, fish have similar functions of conserved members of the Bcl-2 family and inherent apoptosis pathways. Among them, the Bax/Bak-like proteins (Bax, Bak, Bok, Bcl-xs, and Mtd) and the BH3-only proteins (Bad, Bid, Bik, Bim, Bmf, and Noxa) are pro-apoptotic molecules (39). According to the results of the RT-qPCR of the four apoptosis-related genes, three pro-apoptotic genes (*Bax*, *Bad*, and *Bid*) and the *Bax*/*Bcl-2* ratio were significantly activated at 24–48 hpt, suggesting that NsALD could induce the apoptosis of host cells through the intrinsic/Bcl-2-regulated/mitochondrial pathway.

In this study, NsALD was verified to be a secreted protein of *N. seriolae* by shotgun mass spectrometry and target the mitochondria in fish cells. The overexpression of the NsALD protein caused obvious apoptotic characteristics, such as the increase of the activity of caspase-3, the decrease of the $\Delta\Psi_m$ values in FHM cells, and the significantly induced expressions of pro-apoptotic genes, indicating that NsALD can induce cell apoptosis. This study has laid the foundation for further clarification of the function of NsALD and provided new insights into the understanding of the molecular pathogenicity of *N. seriolae.*

DATA AVAILABILITY STATEMENT

The original contributions presented in the study are included in the article/**Supplementary Material**, further inquiries can be directed to the corresponding author/s.

ETHICS STATEMENT

This research did not include live animals. All animal experimental procedures involved were carried out in accordance with the Regulations for Animal Experimentation of GuangDong Ocean University, and the animal facility was based on the National Institutes of Health guide for the care and use of the Laboratory (NIH Publications No. 8023).

AUTHOR CONTRIBUTIONS

LX and YLiu designed the experiments. GC, LX, ZT, YLu, and TW performed the experiments. GC, LX, and ZT contributed to analysis. GC and LX wrote the paper. YLiu polished the paper. All authors contributed to the article and approved the submitted version.

FUNDING

This work was supported by the National Key Research and Development Project (2020YFD0900201), the Natural Science Foundation of Guangdong Province (2021A1515011222), the Key Research and Development Projects in Guangdong Province (2020B0202010009), and the Shenzhen Dapeng New District special fund for industry development (KJYF202001-08).

ACKNOWLEDGMENTS

We are grateful to all the laboratory members for their constructive suggestions to improve the manuscript.

SUPPLEMENTARY MATERIAL

The Supplementary Material for this article can be found online at: https://www.frontiersin.org/articles/10.3389/fvets.2021.801990/full#supplementary-material

REFERENCES

1. Valdez IE, Conroy DA. The study of a tuberculosis-like condition in neon tetras (hyphessobrycon innesi). II. Characteristics of the bacterium isolated. *Microbiol Espanola*. (1963) 16:249–53.
2. Ho PY, Byadgi O, Wang PC, Tsai MA, Liaw LL, Chen SC. Identification, molecular cloning of il-1 beta and its expression profile during Nocardia seriolae infection in largemouth bass, Micropterus salmoides. *Int J Mol Sci.* (2016) 17:1670. doi: 10.3390/ijms17101670
3. Xia L, Cai J, Wang B, Huang Y, Jian J, Lu Y. Draft genome sequence of Nocardia seriolae ZJ0503, a fish pathogen isolated from *Trachinotus ovatus* in China. *Genome Announcements*. (2015) 3:e01223-14. doi: 10.1128/genomeA.01223-14
4. Manrique WG, Da SCG, de Castro MP, Petrillo TR, Figueiredo MA, Belo MA, et al. Expression of cellular compo nents in granulomatous inflammatory response in piaractus mesopotamicus model. *PLoS ONE.* (2015) 10:e0121625. doi: 10.1371/journal.pone.0121625
5. Maekawa S, Yoshida T, Wang PC, Chen SC. Current knowledge of nocardiosis in teleost fish. *J Fish Dis.* (2018) 41:413–9. doi: 10.1111/jfd.12782
6. Shimahara Y, Nakamura A, Nomoto R, Itami T, Chen SC, Yoshida T. Genetic and phenotypic comparison of Nocardia seriolae isolated from fish in Japan. *J Fish Dis.* (2008) 31:481–8. doi: 10.1111/j.1365-2761.2008.00920.x
7. Wang W, Chen J, Liao B, Xia L, Hou S, Wang Z, et al. Identification and functional characterization of Histone-like DNA-binding protein in Nocardia seriolae (NsHLP) involved in cell apoptosis. *J Fish Dis.* (2019) 42:657–66. doi: 10.1111/jfd.12962
8. Rio-Odriguez RE, Ramirez-Paredes JG, Soto-Rodriguez SA, Shapira Y, Haydon DJ. First evidence of fish nocardiosis in mexico caused by *Nocardia seriolae* in farmed red drum (*Sciaenops ocellatus, Linnaeus*). *J Fish Dis.* (2021) 44:1117–30. doi: 10.1111/jfd.13373
9. Barry DP, Beaman BL. Nocardia asteroides strain GUH-2 induces proteasome inhibition and apoptotic death of cultured cells. *Res Microbiol.* (2007) 158:86–96. doi: 10.1016/j.resmic.2006.11.001
10. Camp DM, Loeffler DA, Razoky BA, Tam S, Beaman BL, LeWitt PA. Nocardia asteroides culture filtrates cause dopamine depletion and cytotoxicity in PC12 cells. *Neurochem Res.* (2003) 28:1359–67. doi: 10.1023/A:1024944431725
11. Beaman BL, Beaman L. Nocardia species: host-parasite relationships. *Clin Microbiol Rev.* (1994) 7:213–64. doi: 10.1128/cmr.7.2.213
12. Loeffler DA, Camp DM, Qu S, Beaman BL, LeWitt PA. Characterization of dopamine-depleting activity of Nocardia asteroides strain GUH-2 culture filtrate on PC12 cells. *Microb Pathog.* (2004) 37:73–85. doi: 10.1016/j.micpath.2004.05.001
13. Hou S, Chen G, Wang W, Xia L, Wang Z, Lu Y. Identification of a cell-wall peptidase (NlpC/P60) from Nocardia seriolae which induces apoptosis in fathead minnow cells. *J Fish Dis.* (2020) 43:571–81. doi: 10.1111/jfd.13154
14. Hou S, Wang W, Chen G, Xia L, Wang Z, Lu Y. Identification of a secreted superoxide dismutase (SOD) from Nocardia seriolae which induces apoptosis in fathead minnow (FHM) cells. *J Fish Dis.* (2021) 44:63–72. doi: 10.1111/jfd.13268
15. Xia L, Liang H, Xu L, Chen J, Bekaert M, Zhang H, et al. Subcellular localization and function study of a secreted phospholipase C from Nocardia seriolae. *Fems Microbiol Lett.* (2017) 364:fnx143. doi: 10.1093/femsle/fnx143
16. Huang YC, Jian JC, Wu ZH, Lu YS, Yu TJ. Isolation and identification of the pathogen causing sarcoidosis of *Trachinotus ovatus*. *J Guangdong Ocean Univ.* (2008) 4:49–53. doi: 10.3969/j.issn.1673-9159.2008.04.011
17. Gravell M, Malsberger RG. A permanent cell line from the fathead minnow (*Pimephales promelas*). *Ann N Y Acad Sci.* (1965) 126:555–65. doi: 10.1111/j.1749-6632.1965.tb14302.x
18. Feng Z, Cáceres NE, Sarath G, Barletta RG. Mycobacterium smegmatis L-alanine dehydrogenase (Ald) is required for proficient utilization of alanine as a sole nitrogen source and sustained anaerobic growth. *J Bacteriol.* (2002) 184:5001–10. doi: 10.1128/jb.184.18.5001-5010.2002
19. Dave UC, Kadeppagari RK. Alanine dehydrogenase and its applications-A review. *Crit Rev Biotechnol.* (2019) 39:648–64. doi: 10.1080/07388551.2019.1594153
20. Wiame JM, Pierard A. Occurrence of an L(+)-alanine-dehydrogenase in *Bacillus subtilis*. *Nature.* (1955) 176:1073–5. doi: 10.1038/1761073b0
21. Hutter B, Singh M. Properties of the 40 kDa antigen of *Mycobacterium tuberculosis*, a functional L-alanine dehydrogenase. *Biochem J.* (1999) 343:669–72. doi: 10.1042/0264-6021:3430669
22. Chan K, Knaak T, Satkamp L, Humbert O, Falkow S, Ramakrishnan L. Complex pattern of Mycobacterium marinum gene expression during long-term granulomatous infection. *Proc Nat Acad Sci.* (2002) 99:3920–5. doi: 10.1073/pnas.002024599
23. Andersen AB, Andersen P, Ljungqvist L. Structure and function of a 40,000-molecular-weight protein antigen of *Mycobacterium tuberculosis*. *Infect Immun.* (1992) 60:2317–23. doi: 10.1128/IAI.60.6.2317-2323.1992
24. Kitada S, Uchiyama T, Funatsu T, Kitada Y, Ogishima T, Ito A, et al. protein from a parasitic microorganism, Rickettsia prowazekii, can cleave the signal sequences of proteins targeting mitochondria. *J Bacteriol.* (2007) 189:844–50. doi: 10.1128/JB.01261-06
25. Kenny B, Jepson M. Targeting of an enteropathogenic *Escherichia coli* (EPEC) effector protein to host mitochondria. *Cell Microbiol.* (2000) 2:579–90. doi: 10.1046/j.1462-5822.2000.00082.x
26. Nougayrède JP, Donnenberg MS. Enteropathogenic *Escherichia coli* EspF is targeted to mitochondria and is required to initiate the mitochondrial death pathway. *Cell Microbiol.* (2004) 6:1097–111. doi: 10.1111/j.1462-5822.2004.00421.x
27. Papatheodorou P, Domańska G, Öxle M, Mathieu J, Selchow O, Kenny B, et al. The enteropathogenic *Escherichia coli* (EPEC) Map effector is imported into the mitochondrial matrix by the TOM/Hsp70 system and alters organelle morphology. *Cell Microbiol.* (2006) 8:677–89. doi: 10.1111/j.1462-5822.2005.00660.x
28. Palframan SL, Kwok T, Gabriel K. Vacuolating cytotoxin A (VacA), a key toxin for *Helicobacter pylori* pathogenesis. *Front Cell Infect Microbiol.* (2012) 2:92. doi: 10.3389/fcimb.2012.00092
29. Galluzzi L, Kepp O, Kroemer G. Mitochondria: master regulators of danger signalling. *Nat Rev Mol Cell Biol.* (2012) 13:780–8. doi: 10.1038/nrm3479
30. Lobet E, Letesson JJ, Arnould T. Mitochondria: a target for bacteria. *Biochem Pharmacol.* (2015) 94:173–85. doi: 10.1016/j.bcp.2015.02.007
31. Kozjak-Pavlovic V, Ross K, Rudel T. Import of bacterial pathogenicity factors into mitochondria. *Curr Opin Microbiol.* (2008) 11:9–14. doi: 10.1016/j.mib.2007.12.004
32. Layton AN, Brown PJ, Galyov EE. The Salmonella translocated effector SopA is targeted to the mitochondria of infected cells. *J Bacteriol.* (2005) 187:3565–71. doi: 10.1128/JB.187.10.3565-3571.2005
33. Galmiche A, Rassow J. Targeting of *Helicobacter pylori* VacA to mitochondria. *Gut Microbes.* (2010) 1:392–5. doi: 10.4161/gmic.1.6.13894
34. Galmiche A, Rassow J, Doye A, Cagnol S, Chambard JC, Contamin S, et al. The N-terminal 34 kDa fragment of *Helicobacter pylori* vacuolating cytotoxin targets mitochondria and induces cytochrome c release. *EMBO J.* (2000) 19:6361–70. doi: 10.1093/emboj/19.23.6361
35. Chen J, Xia L, Wang W, Wang Z, Hou S, Xie C, et al. Identification of a mitochondrial-targeting secretory protein from *Nocardia seriolae* which induces apoptosis in fathead minnow cells. *J Fish Dis.* (2019) 42:1493–507. doi: 10.1111/jfd.13062
36. Wang W, Hou S, Chen G, Xia L, Chen J, Wang Z, et al. Characterization and function study of a glutamyl endopeptidase homolog from *Nocardia seriolae*. *J Fish Dis.* (2021) 44:813–21. doi: 10.1111/jfd.13311
37. Mehlen P, Bredesen DE. The dependence receptor hypothesis. *Apoptosis Int J Programmed Cell Death.* (2004) 9:37–49. doi: 10.1023/B:APPT.0000012120.66221.b2
38. Reed JC. Cytochrome c: Can't live with it - can't live without it. *Cell.* (1997) 91:559–62. doi: 10.1016/S0092-8674(00)80442-0

39. Tischner D, Woess C, Ottina E, Villunger A. Bcl-2-regulated cell death signalling in the prevention of autoimmunity. *Cell Death Dis.* (2010) 1:e48. doi: 10.1038/cddis.2010.27

Conflict of Interest: The authors declare that the research was conducted in the absence of any commercial or financial relationships that could be construed as a potential conflict of interest.

Publisher's Note: All claims expressed in this article are solely those of the authors and do not necessarily represent those of their affiliated organizations, or those of the publisher, the editors and the reviewers. Any product that may be evaluated in this article, or claim that may be made by its manufacturer, is not guaranteed or endorsed by the publisher.

frontiers in Veterinary Science

ORIGINAL RESEARCH
published: 25 January 2022
doi: 10.3389/fvets.2021.819681

CRISPR/Cas12a Based Rapid Molecular Detection of Acute Hepatopancreatic Necrosis Disease in Shrimp

Chenglong Li[1†], Nan Lin[2†], Zhihua Feng[1], Minhua Lin[1], Biyun Guan[1], Kunsen Chen[1], Wangwang Liang[1], Qiaohuang Wang[2], Miaomiao Li[2], Yu You[2] and Qi Chen[1*]*

[1] Fujian Key Laboratory of Innate Immune Biology, Biomedical Research Center of South China, College of Life Science, Fujian Normal University, Fuzhou, China, [2] Fujian Provincial Fisheries Technology Extension Center, Fuzhou, China

Acute hepatopancreatic necrosis disease (AHPND), formerly called early mortality syndrome (EMS), causes high mortality in cultured penaeid shrimp, particularly *Penaeus vannamei* and *Penaeus monodon*. AHPND is mainly caused by *Vibrio* species carrying the pVA1 plasmid encoding the virulence genes Photorhabdus insect-related (*pir*) $pir^{VP}A$ and $pir^{VP}B$. We developed a new molecular assay that combines recombinase polymerase amplification (RPA) and CRISPR/Cas12a technology (RPA-CRISPR/Cas12a) to detect $pir^{VP}A$ and $pir^{VP}B$, with a fluorescent signal result. The fluorescence RPA-CRISPR/Cas12a assay had a detection limit of 20 copies/μL for $pir^{VP}A$ and $pir^{VP}B$. To improve usability and visualize RPA-CRISPR/Cas12a assay results, a lateral flow strip readout was added. With the lateral flow strip, the RPA-CRISPR/Cas12a assay had a lower limit of detection of 200 copies/μL (0.3 fmol/L). The lateral flow assay can be completed in 2 h and showed no cross-reactivity with pathogens causing other shrimp diseases. In a field test of 60 shrimp samples, the RPA-CRISPR/Cas12a lateral flow assay showed 92.5% positive predictive agreement and 100% negative predictive agreement. As the new RPA-CRISPR/Cas12a assay is rapid, specific, and does not require complicated experimental equipment, it may have important field applications for detecting AHPND in farmed shrimp.

Keywords: acute hepatopancreatic necrosis disease (AHPND), CRISPR/Cas12a, recombinase polymerase amplification (RPA), lateral flow strip (LFS), shrimp

OPEN ACCESS

Edited by:
Lixing Huang,
Jimei University, China

Reviewed by:
Yaoguo Li,
Hunan Agricultural University, China
Youyu Zhang,
Xiamen University, China

***Correspondence:**
Yu You
fpftec@163.com
Qi Chen
chenqi@fjnu.edu.cn

†These authors share first authorship

Specialty section:
This article was submitted to Veterinary Infectious Diseases, a section of the journal Frontiers in Veterinary Science

Received: *22 November 2021*
Accepted: *29 December 2021*
Published: *25 January 2022*

Citation:
Li C, Lin N, Feng Z, Lin M, Guan B, Chen K, Liang W, Wang Q, Li M, You Y and Chen Q (2022) CRISPR/Cas12a Based Rapid Molecular Detection of Acute Hepatopancreatic Necrosis Disease in Shrimp. Front. Vet. Sci. 8:819681. doi: 10.3389/fvets.2021.819681

INTRODUCTION

As the demand for shrimp continues to increase worldwide, Asia has become a dominant supplier of farmed penaeid shrimp, in particular *Penaeus vannamei* (*P. vannamei*) and *Penaeus monodon* (*P. monodon*). In 2018, the production of aquaculture in Asia totaled 73 million tons, accounting for 88.7% of the world's total production (1). In Southeast Asia alone, production was 5.37 million tons, with *P. vannamei* and *P. monodon* accounting for the majority of total penaeid production (1, 2). The primary threat to the Asian shrimp supply is disease caused by viruses, bacteria, and parasites (3), which have led to losses of nearly 80% in recent years. Acute hepatopancreatic necrosis disease (AHPND), formerly called early mortality syndrome (EMS), is caused by infection with *Vibrio* species and leads to high mortality rates in cultured penaeid shrimp. Shrimp with AHPND show

slow growth, massive sloughing of hepatopancreatic tubule epithelial cells, and an empty stomach and midgut (4, 5). The first outbreak of AHPND in China occurred in 2009, and quickly spread to Vietnam, Malaysia, Thailand, and Mexico (4, 6, 7). In Asia, the economic loss associated with AHPND in cultured penaeid shrimp was ∼US$44 billion in 2010–2016 (6). In Vietnam, the losses due to the outbreak peaked in 2015 at US$97.96 million; in Thailand, losses from 2012 to 2015 totaled US$5.01 billion, including 100,000 in lost jobs (6). With poor management and reliance on time-consuming detection methods, infections with *Vibrio* and other pathogens, such as the white spot syndrome virus (WSSV, a member of the Nimaviridae family) (8–10) and the parasite enterocytozoon hepatopenaei (EHP) (11), will continue to cause serious economic losses in the shrimp culture industry. Timely detection and prevention of AHPND spread in farmed shrimp is thus critical to mitigate the associated economic losses.

Many *Vibrio* species have been isolated from AHPND-infected shrimp, including *Vibrio parahaemolyticus* (12–14), *Vibrio harveyi* (15), *Vibrio owensii* (16), and *Vibrio campbellii* (17). These pathogens all carry an AHPND-related plasmid encoding the Photorhabdus insect-related (*pir*) $pir^{VP}A$ and $pir^{VP}B$ genes (GenBank Accession No. KM067908.1) (18). Several groups have pursued molecular testing to detect AHPND by targeting $pir^{VP}A$ and $pir^{VP}B$, using methods including polymerase chain reaction (PCR), nested PCR, loop-mediated isothermal amplification (LAMP), recombinase polymerase amplification (RPA), and real-time quantitative PCR (qPCR) (19–22). The limit of detection (LOD) of PCR is 10 pg and nested PCR is 100 fg. With their high sensitivity and specificity, nested PCR and qPCR have been accepted by many agencies as the gold standard tests to diagnose AHPND (20, 23). Unlike PCR and nested PCR, isothermal amplification methods such as LAMP and RPA amplify nucleotides at a constant temperature and thus do not require thermocyclers. The RPA reaction comprises a recombinase, a single-stranded DNA-binding protein (SSB), a strand-displacing polymerase, two primers, and a constant temperature of 37–42°C (24). The LAMP reaction needs 4–6 primers and is run at 65°C to amplify target DNA (25). Isothermal amplification methods are rapid and sensitive and are often combined lateral flow strip technology to simplify its use in field-based assays, with test results read directly by the user (26). LAMP may produce non-specific amplicons that lead to false positive test results, and maintaining the test temperature at 65°C can be difficult. Therefore, RPA may be the better choice for developing rapid, sensitive, and simple molecular tests for field use (27).

In recent years, the CRISPR (Clustered Regularly Interspaced Short Palindromic Repeats)/Cas9 (CRISPR-associated protein) system has emerged as a powerful tool for gene editing. In the type II CRISPR/Cas system, a guide crRNA (CRISPR RNA) binds with Cas9 to form a Cas9-crRNA complex that then binds to target DNA. Cas9 recognizes a protospacer adjacent motif (PAM) sequence near the target DNA sequence, and activated Cas9 cleaves the target DNA to produce a double strand break (DSB) (28–30). Based on this, Cas9 has been applied to genome-scale screening (31) and deactivated Cas9 (dCas9) with gene activation/repression elements has been used to regulate gene transcription (32). Cas12 and Cas13 have an extra enzymatic activity called collateral cleavage that has implications for molecular assay development. Activated Cas12 possesses single-stranded DNA (ssDNA) cleavage activity (33), while Cas13 possesses single-stranded RNA (ssRNA) cleavage activity (34). ssDNA with a linked fluorophore and quencher at either end (called an FQ reporter, FAM-TTATT-TAMRA) can be cleaved by Cas12 in the presence of target DNA (35). Alternatively, the labeled reporter can be linked with biotin (called an FB reporter, FAM-TTATT-Biotin), which can been detected using lateral flow test strip. The technologies based on Cas12 and Cas13 collateral cleavage activity have been used to detect nCOV-2019, African swine fever virus (ASFV), Zika virus (ZIKV), and Dengue virus (DENV) (36–38).

In this study, we developed a novel molecular assay that combines the CRISPR/Cas12a system with RPA and lateral flow technology to detect AHPND virulence genes in cultured penaeid shrimp (*P. vannamei* and *P. monodon*). We found that a CRISPR/Cas12a based assay alone did not achieve a sufficiently low LOD for the $pir^{VP}A$ and $pir^{VP}B$ target genes. Thus, we added RPA to pre-amplify the target genes. Furthermore, to visualize the assay results, we combined our RPA-CRISPR/Cas12a assay with lateral flow strip (LFS) technology. Our new molecular assay (LFS-based RPA-CRISPR/Cas12a) has the potential to detect AHPND with high accuracy without the need for lab equipment, providing a convenient and simple method that can be deployed to the field for rapid AHPND detection in cultured shrimp.

MATERIALS AND METHODS

Primers and crRNAs Design

PCR and RPA primers targeting the AHPND virulence genes $pir^{VP}A$ and $pir^{VP}B$ were designed based on the published sequence of pVA1 plasmid (GenBank Accession No. KM067908.1) in the National Center for Biotechnology Information (NCBI) database.

Cas12a crRNA consists of a 21 bp spacer and a 20 bp direct repeat (DR). For the T-rich (5′-TTTN-3′) protospacer adjacent motif (PAM) restriction, four crRNAs targeting the genes $pir^{VP}A$ and $pir^{VP}B$ were designed and validated. All primers and probes were purchased and synthesized by Sangon Biotech (Shanghai, China). The primers and DNA oligos used in this study were listed in **Supplementary Tables 1, 2**.

Vibrio Culture and Plasmid Construction

AHPND-causing *Vibrio* was gifted from Fujian Provincial Fisheries Technology Extension Center (Fujian, China). *Vibrio* was cultured in Tryptic Soy Broth (TSB), at 37°C, 180 rpm overnight. *Vibrio* total DNA was extracted using the TaKaRa MiniBEST Viral RNA/DNA Extraction Kit (TaKaRa, China) according to the manufacturer's protocol. PCR primers (**Supplementary Table 1**) PirAB-F1 and PirAB-R1 were used to amplify the virulence genes, with an amplicon size of 1,794 bp. This amplicon was cloned into pMD19-T vector (TaKaRa, China) to create the recombinant plasmid pUC19-PirAB. After transformation into *E. coli* DH5α, the recombinant plasmid was

extracted using a kit (DP118-02) purchased from TIANGEN BIOTECH (Beijing, China). The plasmid was measured with NanoDrop 2000C (Thermo Fisher, United States) at A260/280 and stored at −20°C.

Preparation of Cas12a crRNA

The DNA templates for *in vitro* T7 transcription were synthesized by Sangon (Shanghai, China), and listed in **Supplementary Table 2**. The DNA template was comprised of T7 promoter and crRNA. crRNA was transcribed following the manufacturer's protocol with a T7 *in vitro* transcription kit (VK010) purchased from VIEWSOLID (Beijing, China). After transcribing at 37°C for 6 h, the products were mixed with 75% ethanol and incubated at −20°C overnight. Following centrifugation at 13,000 rpm for 30 min, the supernatant was discarded and RNA products were dissolved in RNase-free ddH_2O and stored at −80°C for subsequent tests.

CRISPR/Cas12a *in vitro* Cleavage Assay

Cas12a cleavage assays were performed in a PCR tube in a total reaction volume of 20 μL. One microlitre Cas12a (20 μM) and 1 μL crRNA (10 μM) were pre-mixed and incubated at 37°C for 15 min. Cas buffer, 100 ng of PCR products (primers: PirAB-F1 and PirAB-R1, products: 1,794 bp), and RNase-free ddH_2O were then added to the reaction tube and incubated at 37°C for an additional 15 min. To stop the reaction, 3 μL DNA Loading Buffer was added and the tube was heated to 65°C for 5 min. Reaction products were verified by 2% agarose gel electrophoresis.

CRISPR/Cas12a Fluorescence Assay and Optimization

The Cas12a fluorescence assay was performed by mixing Cas12a, crRNA, FQ reporter, and Cas buffer in a 384-well plate and incubating at 37°C for 45 min. The fluorescence signal was detected by QuantStudio 6 Flex (Applied Biosystems, USA) in the FAM channel every 60 s, with three replicates run in each reaction. The reaction conditions were optimized based on the assay performance using various concentrations of Cas12a and crRNA.

Recombinase Polymerase Amplification and Primers Optimization

RPA was performed in a 50 μL tube containing the forward primer, reverse primer, primer-free rehydration buffer, DNA template, and magnesium acetate and using the Twistamp™ Basic Kit following the manufacturer's instructions (Babraham, UK). RPA products were purified and verified by 2% agarose gel electrophoresis. Various pairs of RPA primers (**Supplementary Table 1**) were tested to optimize the assay.

Sensitivity of RPA-CRISPR/Cas12a Assay and qPCR

The sensitivity of our new RPA-CRISPR/Cas12a assay was tested using a 10-fold serial dilution panel of plasmid pUC19-PirAB (from 2 copies/μL to 2×10^7 copies/μL). RPA products were used as the DNA template in the subsequent CRISPR/Cas12a fluorescence assay.

The performance of the assay was also compared to real-time qPCR as the current gold standard for detection of AHPND. qPCR primers (**Supplementary Table 1**) were PirAB-qPCR-F and PirAB-qPCR-R. The reaction was performed using FastStart™ Universal SYBR® Green Master (ROX) purchased from Roche (Roche, China) following the manufacturer's instruction. The qPCR reaction and readout of fluorescence were run on the StepOne system (Applied Biosystems, USA) with following the cycle conditions: 95°C for 5 min; 40 cycles of denaturation at 95°C for 10 s; annealing and amplification at 60°C for 30 s.

RPA-CRISPR/Cas12a Assay With Lateral Flow Strip Technology

For direct readout of the assay result, we coupled LFS technology with the new RPA-CRISPR/Cas12a assay to create the LFS-based RPA-CRISPR/Cas12a assay. The LFS-based assay used the same reagents as the fluorescence-based assay except for the replacement of the FQ reporter with an FB reporter. The reaction was performed in a 1.5 mL tube containing Cas12a and crRNA. After a 10-min incubation, the reaction was mixed with FB reporter, Cas buffer, and DNA template, and incubated at 37°C for 30 min. Then, a lateral flow strip was added to the tube and the result was read in 10 min. The control band is close to the sample pad, while the test band appears at the top of the strip, away from the sample pad. Appearance of a red test band indicated a positive result; any other result was considered negative.

Specificity of the RPA-CRISPR/Cas12a Assay

Several shrimp pathogens including WSSV and EHP were used to test cross-reactivity in the new RPA-CRISPR/Cas12a assays (fluorescence and LFS-based). All pathogens were gifted from Fujian Provincial Fisheries Technology Extension Center (Fujian, China). After RPA amplification of target DNA, the RPA products were directly used in subsequent fluorescence and lateral flow assays.

Detection of AHPND in Field Samples

To assess the field performance of the new LFS-based RPA-CRISPR/Cas12a assay to detect AHPND-causing *Vibrio* strains, 60 shrimp samples were tested and the results were compared to the real-time qPCR assay. Total DNA was extracted from hepatopancreas (HP) tissues of shrimp samples using the TaKaRa MiniBEST viral RNA/DNA extraction kit (TaKaRa, China) following the manufacturer's protocols. Briefly, 800 μL of PBS solution was added to the shrimp sample in a 2 mL lysing matrix tube, the tissue was disrupted for 40 s using an MP Biomedical Fast-Prep®-24, and 200 μL of lysate was used for DNA extraction.

Statistical Analysis

Software GraphPad Prism 6.01 (GraphPad Software, San Diego, CA) was used for statistical analyses and graphing. Student *t*-tests were performed and data were presented as mean ± SD, with

error bars representing the standard deviation of at least three independent experiments.

RESULTS

Cas12a *in vitro* Cleavage

As the first step in establishing the new CRISPR/Cas12a assay for AHPND (**Figure 1**), Cas12a cleavage activity was assessed in an *in vitro* cleavage assay. Cas12a protein was expressed in *E. coli* BL21 and purified with Ni-NTA resin (**Supplementary Figure 2**). Virulence genes $Pir^{VP}A$ and $Pir^{VP}B$ were cloned into pMD19-T vector (pUC19-PirAB) and verified *via* sequencing (**Supplementary Figure 1**). Four crRNAs were tested to target the virulence genes $Pir^{VP}A$ and $Pir^{VP}B$. The results of the *in vitro* cleavage assay are shown in **Figure 1B**, intact dsDNA template (1,794 bp) was cleaved by Cas12a in the presence of crRNA, indicated that all four crRNAs enable Cas12a to cleave the target DNA template, crRNA3 induced a specific on-target cleavage with the expected cleave products of 1,142 and 652 bp, respectively, while the other crRNAs did not.

CRISPR/Cas12a Reaction Optimization

We next assessed Cas12a collateral cleavage activity, specifically, its single-stranded DNase activity. A ssDNA labeled with fluorophore (FAM) and quencher (TAMRA) at each end, called an FQ reporter, was used to assess Cas12a collateral cleavage based on a fluorescent signal readout. The concentration of FQ reporter was 250 nM (**Supplementary Figure 3**). The plasmid pUC19-PirAB was used as a positive template, the blank vector pUC19 was used as a negative template, and no DNA template (reporter-only group) served as a negative control. The results (**Figure 1C**) showed that pUC19-PirAB produced a significant fluorescence signal ($p < 0.001$) whereas the blank vector pUC19 template showed no significant signal relative to the reporter-only group.

Because the four crRNAs target different sites on $Pir^{VP}A$ and $Pir^{VP}B$, they may induce different levels of fluorescence intensity in the CRISPR/Cas12a assay. To optimize the assay, we compared the activity with each of the four crRNAs. **Figure 1D** indicates that crRNA1 and crRNA3 outperformed the other crRNAs in terms of fluorescence readout. Based upon the results of Cas12a *in vitro* cleavage (**Figure 1B**), thus, we selected crRNA3 for further assay development. We then optimized the concentration ratio of Cas12a to crRNA3; as shown in the heatmap (**Figure 1E**), a ratio of 40 μM Cas12a to 5 μM crRNA induced the highest fluorescence intensity.

RPA-CRISPR/Cas12a Fluorescence Assay Development

We then evaluated the sensitivity of the new CRISPR/Cas12a assay compared with real-time qPCR to detect a dilution series of plasmid pUC19-PirAB. The limit of detection (LOD) of real-time qPCR was 200 copies/μL (**Figure 2A**) and of the CRISPR/Cas12a assay was 2×10^9 copies/μL (**Figure 2C**). Thus, the CRISPR/Cas12a assay alone would be unable to detect *Vibrio* gene targets when present in low copy numbers.

To improve the LOD of the CRISPR/Cas12a assay, we added a recombinase polymerase amplification (RPA) step to pre-amplify the target DNA. Six RPA primers (**Supplementary Table 1**) were tested and run on 2% agarose gel (**Figure 2B**). Except for the PirAB-RPA-F4/PirAB-RPA-R4 primer set, all other RPA primers successfully amplified the target DNA. The PirAB-RPA-F3/PirAB-RPA-R3 primer set was chosen for further assay development since this pair of primer can induce more specific amplification products.

The LOD of the CRISPR/Cas12a assay was compared with and without RPA pre-amplification using the same serial dilution panel of plasmid pUC19-PirAB. Two microliter of RPA product was used as the template for RPA-CRISPR/Cas12a assay. The LOD of the RPA-CRISPR/Cas12a assay reached 20 copies/μL, lower than that achieved with real-time qPCR (**Figure 2C**).

To make the RPA-CRISPR/Cas12a assay useful for rapid detection of AHPND in field-based settings, we combined it with lateral flow strip (LFS) technology to create the LFS-based RPA-CRISPR/Cas12a assay (**Figure 3**). We switched the FQ reporter with an FB reporter as the target for Cas12a collateral cleavage. Using the pUC19-PirAB plasmid dilution panel, the LFS-based RPA-CRISPR/Cas12a assay had an LOD of 200 copies/μL, comparable to real-time qPCR (**Figure 2D**).

Field Performance of the New RPA-CRISPR/Cas12a Assay for AHPND

We evaluated the specificity of the new RPA-CRISPR/Cas12a assay by examining cross-reactivity with two other pathogens that commonly affect penaeid shrimp, WSSV and EHP. As seen in **Figures 4B,C**, it showed positive results with significant fluorescence signal in **Figure 4B** and red line at the test band in **Figure 4C** when the reaction existed pathogen DNA with matched crRNA, both the fluorescence-based and LFS-based RPA-CRISPR/Cas12a assays did not cross-react with these two shrimp pathogens, demonstrating specificity for the *Vibrio* virulence genes target.

To evaluate the accuracy of the LFS-based RPA-CRISPR/Cas12a assay, we compared results with the real-time qPCR assay on 60 field samples of shrimp. qPCR detected 40 AHPND-positive and 20 AHPND-negative shrimp samples (**Figure 4D**). The LFS-based RPA-CRISPR/Cas12a assay detected 37 of the 40 AHPND-positive samples and all 20 of the AHPND-negative samples (**Figure 4E**). As seen in **Table 1**, the test results showed 92.5% positive predictive agreement (PPA) and 100% negative predictive agreement (NPA), respectively.

DISCUSSION

While improvement of water quality and oxygen levels can reduce the concentration of AHPND-causing *Vibrio* (39), and farmers have used broad-spectrum antibiotics to inhibit gram-negative bacteria and parasites (40), these measures cannot prevent outbreaks of pathogenic bacteria. Furthermore, inappropriate use of broad-spectrum antibiotics may result in

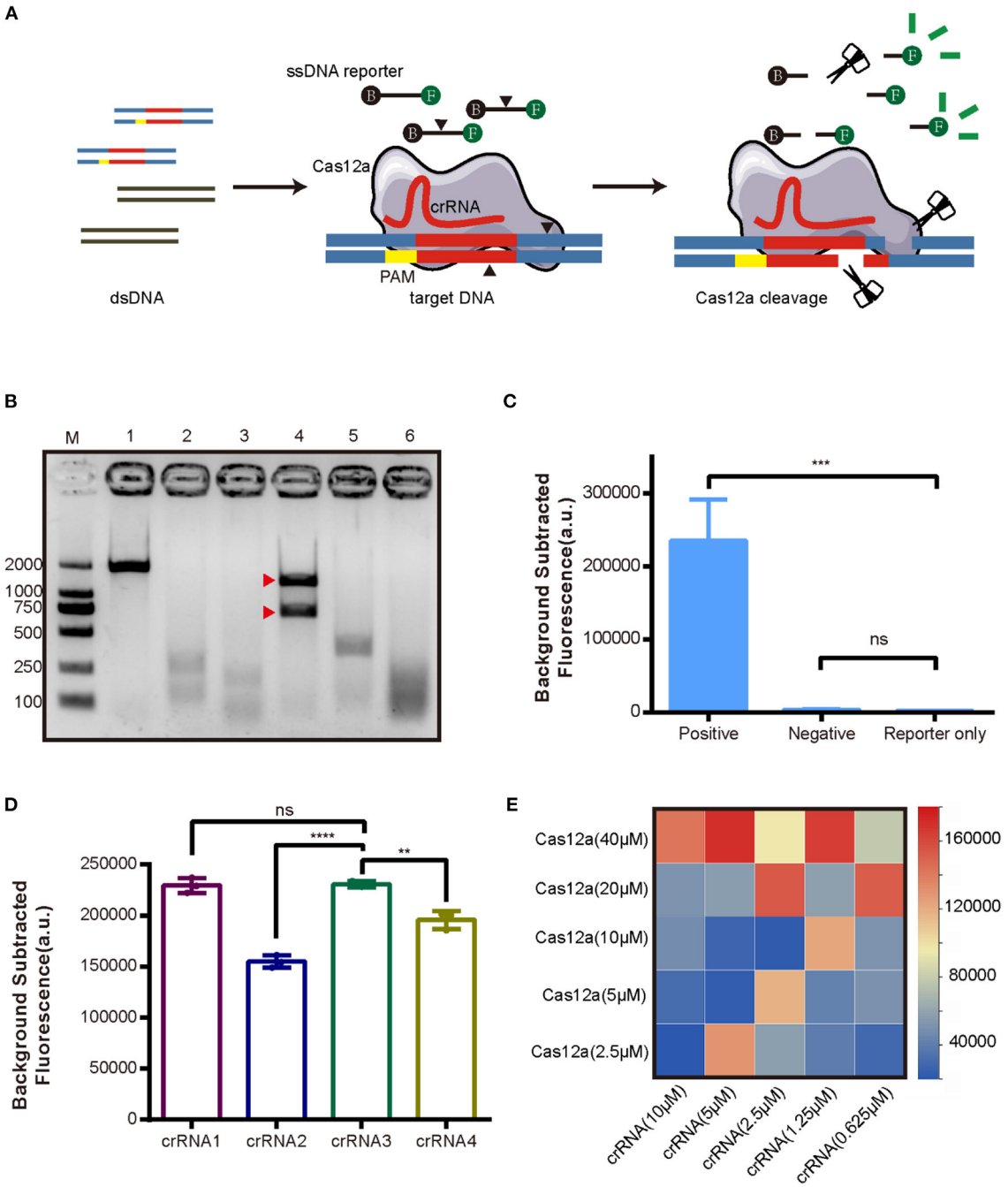

FIGURE 1 | Development of the CRISPR/Cas12a assay for detection of AHPND virulence genes *Pir*^{VP}*A* and *Pir*^{VP}*B*. **(A)** Schematic diagram of the CRISPR/Cas12a. **(B)** Cleavage activity of crRNA-guided Cas12a. M: DL 2000 DNA marker; 1: intact dsDNA template (1794 bp); 2-5: The cleavage products of dsDNA template induced by crRNA1, crRNA2, crRNA3, crRNA4; 6: The cleavage products of dsDNA template induced by mixture of crRNA1 to crRNA4. The expected cleavage products are marked by red arrows. **(C)** Validation of collateral cleavage activity of Cas12a by fluorescence assay. The DNA template in positive group was plasmid pUC19-PirAB, and negative group was blank vector pUC19, while reporter only group was reaction without DNA template. **(D)** Comparison of different crRNAs targeting *Pir*^{VP}*A* and *Pir*^{VP}*B* by fluorescence assay. **(E)** Heatmap showing the optimal concentrations of Cas12a and crRNA based on fluorescence intensity. Each row presents the concentration of Cas12a used, each column presents the concentration of crRNA used. Error bars represent the standard deviation from three independent experiments. $^{**}p < 0.01$, $^{***}p < 0.001$, $^{****}p < 0.0001$ and *ns,* not significant.

multidrug-resistant bacteria that exacerbate the risk of outbreaks. Therefore, timely and rapid detection of shrimp diseases at early stages of the infection is urgent to prevent outbreaks that have devastating economic consequences. Current AHPND tests include molecular assays (such as qPCR and nested PCR) and histological analysis [hematoxylin and eosin (H&E) staining].

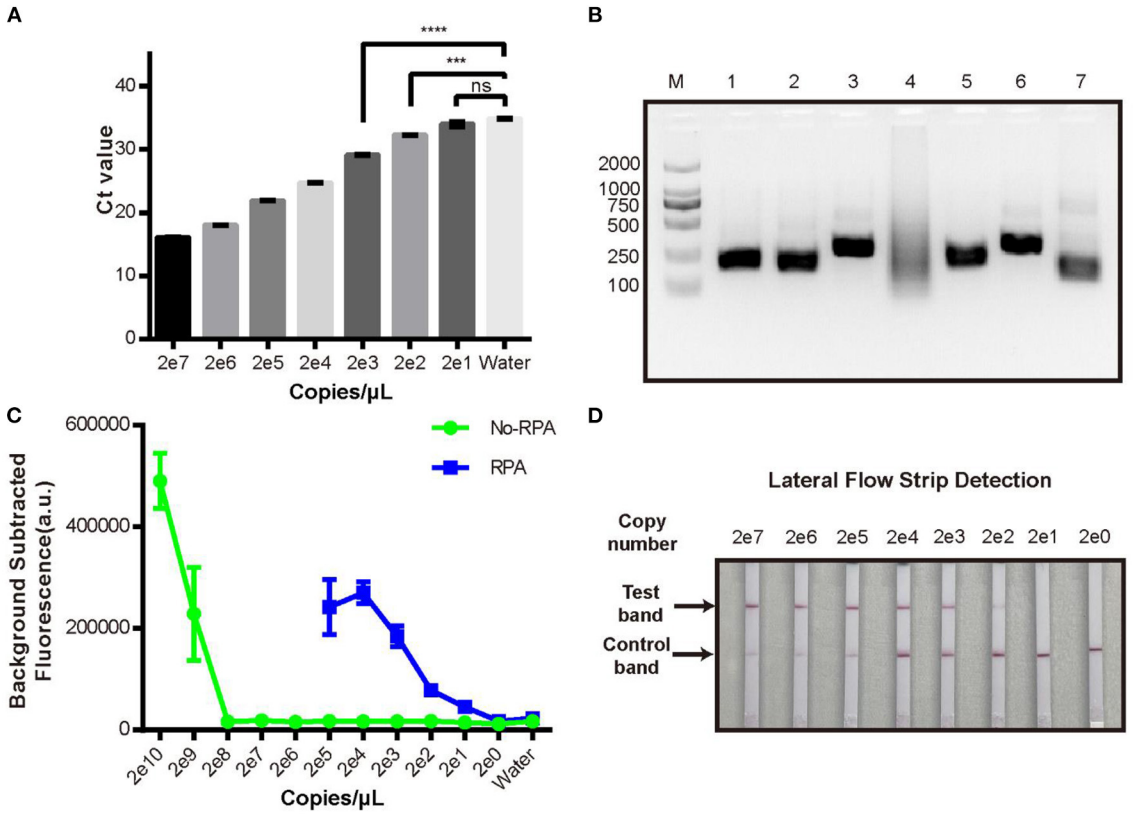

FIGURE 2 | Limit of detection analysis of the new RPA-CRISPR/Cas12a fluorescence assay. **(A)** qPCR detection of pUC19-PirAB plasmid at various concentrations from 2 copies/μL to 2 × 10^7 copies/μL. **(B)** Analysis of different RPA primers for pre-amplification of the target DNA. M: DL 2000 DNA marker; 1-6: the RPA product derived by using each of PirAB-RPA-F1/R1 to PirAB-RPA-F6/R6 primers; 7: RPA positive control. **(C)** Limit of detection of the pUC19-PirAB plasmid with or without RPA prior to the CRISPR/Cas12a fluorescence assay. **(D)** Limit of detection when lateral flow strip technology was combined with the RPA-CRISPR/Cas12a assay for detection of pUC19-PirAB plasmid from 2 copies to 2 × 10^7 copies. Error bars represent the standard deviation from three independent experiments. ***$p < 0.001$, ****$p < 0.0001$ and *ns,* not significant.

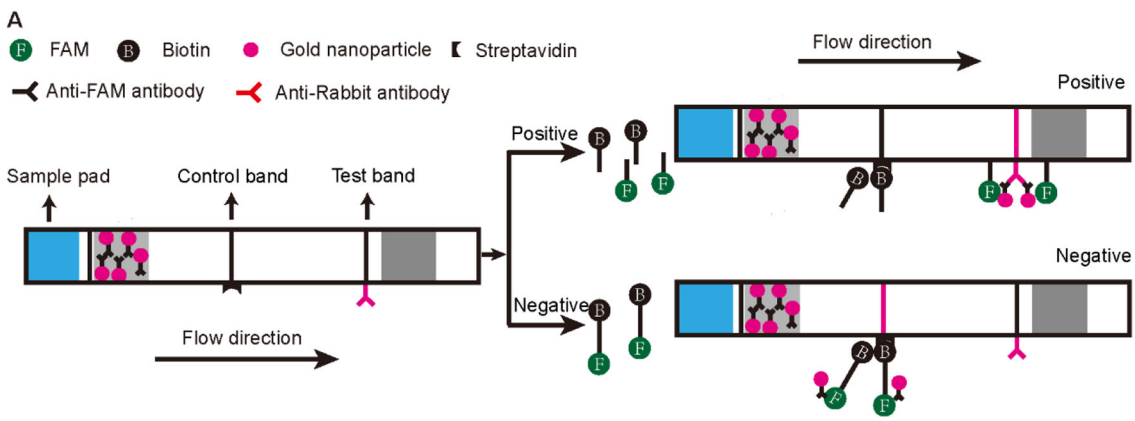

FIGURE 3 | Schematic diagram of the lateral flow test strip technology applied to the RPA-CRISPR/Cas12a assay. The first line on the strip (Control band) is fixed with streptavidin, which can bind biotin. The second line on the strip (Test band) is fixed with Anti-Rabbit antibody that binds Anti-FAM antibody. Appearance of a red color test band indicates a positive result. Any other result is considered negative.

qPCR can detect low levels of pathogens both qualitatively and quantitatively, and H&E staining is helpful for distinguishing between normal and necrotic tissues in photomicrographs. However, qPCR requires laboratory equipment and H&E staining is not useful for catching early-stage infections in shrimp samples, and both approaches are time consuming (41). Thus,

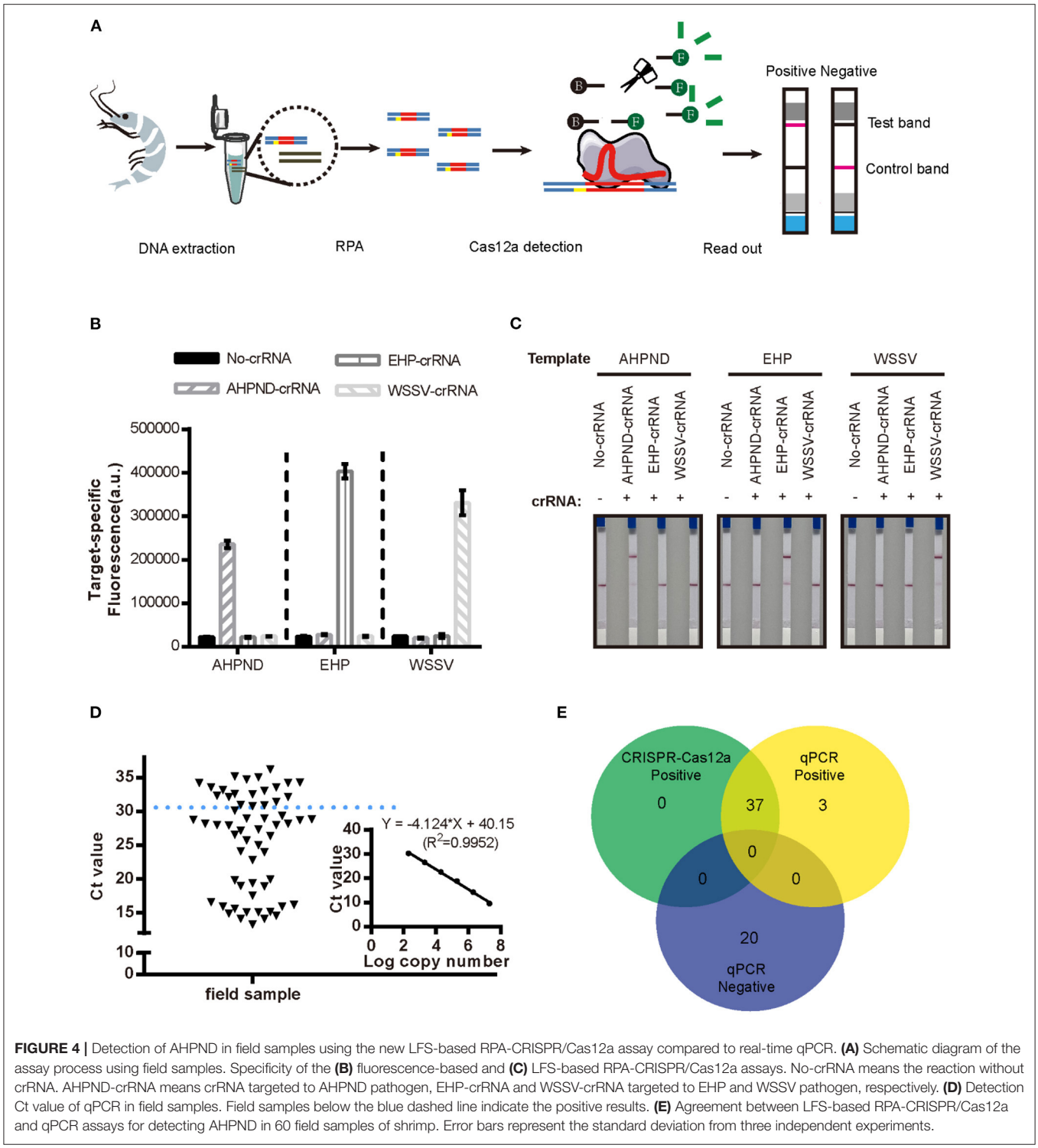

FIGURE 4 | Detection of AHPND in field samples using the new LFS-based RPA-CRISPR/Cas12a assay compared to real-time qPCR. **(A)** Schematic diagram of the assay process using field samples. Specificity of the **(B)** fluorescence-based and **(C)** LFS-based RPA-CRISPR/Cas12a assays. No-crRNA means the reaction without crRNA. AHPND-crRNA means crRNA targeted to AHPND pathogen, EHP-crRNA and WSSV-crRNA targeted to EHP and WSSV pathogen, respectively. **(D)** Detection Ct value of qPCR in field samples. Field samples below the blue dashed line indicate the positive results. **(E)** Agreement between LFS-based RPA-CRISPR/Cas12a and qPCR assays for detecting AHPND in 60 field samples of shrimp. Error bars represent the standard deviation from three independent experiments.

there is a need for simpler, rapid tests that are suitable for use in a field setting and can detect low levels of pathogen prior to an AHPND outbreak.

To address this problem, we developed a new assay, the LFS-based RPA-CRISPR/Cas12a assay, by combining CRISPR/Cas12a with RPA and a rapid LFS-based readout that can be used for the field detection of shrimp AHPND (**Figure 4A**). The new assay includes three steps that take ∼2 h: (1) DNA extraction from shrimp; (2) RPA amplification of target DNA; and (3) CRISPR/Cas12a reaction with LFS readout within 10 min. Compared with qPCR, RPA amplifies target DNA in 20–30 min at a constant temperature 37–42°C and

TABLE 1 | Correlation of AHPND field-testing results for the LFS-based RPA-CRISPR/Cas12a assay and real-time qPCR.

		Real-time qPCR	
		Positive	**Negative**
LFS-based RPA-CRISPR/Cas12a	Positive	37	0
	Negative	3	20
		PPA: 92.5%	NPA: 100%

PPA, positive predictive agreement; NPA, negative predictive agreement.

thus does not require a thermocycler. In addition, the results of our assay can be visualized on LFS, making it a convenient and rapid alternative that can be translated to the field.

The advantage of our LFS-based RPA-CRISPR/Cas12a assay is apparent since it only requires three steps without using any complicated equipment. Additionally, more pathogens could be detected through the modification of crRNA sequences, which widen the detection scope. Furthermore, the crRNA used in the CRISPR/Cas12a reaction can trigger different cleavage activities of Cas12a, so careful selection of the crRNA is crucial for achieving robust cleavage activity to use in an assay (33).

To achieve high accuracy with our RPA-CRISPR/Cas12a assay, a few design factors needed to be taken into consideration. For instance, RPA is a crucial step that can pre-amplify low levels of target DNA present early in the course of an infection. Compared with PCR, the amplicon size of RPA may be constrained to under 1,000 bp, since its optimal amplification size is between 100 and 300 bp (42). The length of RPA primers is typically 30–35 bp. Thus, an amplicon size larger than 300 bp or primers smaller than 25 bp can reduce the efficiency of amplification. With these limitations, both target DNA sequence and primer length need to be taken into account to achieve the best performance. In addition, the test results derived from our CRISPR-based assay are more reliable when used in field assay of AHPND where the field conditions could be variable. For instance, RPA reaction works in the presence of three core enzymes. To avoid the RPA core enzymes and other reagents become inactive in transportation and longtime storage, the commercially purchased RPA components were lyophilized and all reagents used (antibodies on the test strips, Cas12a, crRNA and ssDNA reporters) were transported through cold-chain.

As for economic cost, compared with the qPCR—high-throughput at low cost (such as US$1-$5/test), our LFS-based RPA-CRISPR/Cas12a assay requires high expenditure of the reagents (RPA at the price of US$2/test and lateral flow strip at the price of US$3/test) and cold-chain transportation. However, instrument-dependent qPCR method can be expensive with equipment acquisition and maintenance. Besides, the laboratory method like qPCR cannot fulfill the instant detection of the field assay with drawbacks in the requirement of complicated equipment and technical expertise. Our LFS-based RPA-CRISPR/Cas12a assay provides the advantages of rapid, specific and portable which can fill this gap in first-line detection, thus, it may have important field applications for detecting AHPND in farmed shrimp.

In this study, We tested cross-reactivity with two other shrimp pathogens—WSSV and EHP—and showed high specificity of our RPA-CRISPR/Cas12a assay. Compared with qPCR, the LFS-based RPA-CRISPR/Cas12a assay also displayed high concordance with real-time qPCR results on field samples of shrimp, with 92.5% PPA and 100% NPA. The lower PPA between the LFS-based RPA-CRISPR/Cas12a assay and real-time qPCR may be due to the differences in the two amplification methods. Particularly, the amplification efficiency is highly affected by the primers used. The optimal length of RPA primers is 30–35 bp, but 20 bp for qPCR primers. The amplification of qPCR is driven by one key enzyme and thermocycling between 95 and 60°C, whereas RPA requires three enzymes and a constant temperature of 37°C (24). The quality of the field test samples may also have led to inconsistencies between test results. *Vibrio* DNA isolated from the field shrimp samples may have been fragmented that primer binding sites were lost, thus affecting the RPA reaction step. Sample preparation may need to be further optimized.

In summary, taking advantage of the high specificity of crRNA to target DNA, and the collateral cleavage activity of Cas12a, we developed a new AHPND molecular assay that combines CRISPR/Cas12a with RPA and readout by LFS. This new assay requires minimal equipment and involves a simple three-step process. Advantages relevant to field use include amplification at a constant temperature at 37–42°C and visualization of results by LFS. The LOD of the new RPA-CRISPR/Cas12a assay can reach the attomole level: 20 copies/μL for the fluorescence assay and 200 copies/μL for the lateral flow strip assay. This is comparable to the 200 copies/μL LOD of the current gold standard qPCR assays used to detect AHPND infection. Thus, our new LFS-based RPA-CRISPR/Cas12a assay is rapid, specific, and portable, and may be suitable for use for the field detection of shrimp AHPND.

DATA AVAILABILITY STATEMENT

The original contributions presented in the study are included in the article/**Supplementary Material**, further inquiries can be directed to the corresponding author/s.

AUTHOR CONTRIBUTIONS

QC, CL, and NL conceptualized and designed research. CL, ZF, MLin, BG, KC, and WL performed the experiments. NL, QW, MLi, and YY provided shrimp samples. QC and CL analyzed data and wrote the manuscript. All authors have read and approved the final manuscript.

FUNDING

This work was supported by the Natural Science Foundation of Fujian Province, China (Grant No. 2021J01202).

ACKNOWLEDGMENTS

We would like to thank Fujian Provincial Fisheries Technology Extension Center (Fujian, China) for the gift of infected penaeid shrimp samples and the members of Chen's Laboratory for technical assistance and helpful discussion.

SUPPLEMENTARY MATERIAL

The Supplementary Material for this article can be found online at: https://www.frontiersin.org/articles/10.3389/fvets.2021.819681/full#supplementary-material

REFERENCES

1. FAO. *FAO Yearbook. Fishery and Aquaculture Statistics 2018*. (2020). Available online at: https://www.fao.org/fishery/statistics/yearbook/en (accessed July 11, 2021).
2. Liao IC, Chien Y-H. The pacific white shrimp, Litopenaeus vannamei, in Asia: the world's most widely cultured alien crustacean. In: *The Wrong Place-Alien Marine Crustaceans: Distribution, Biology and Impacts*. Dordrecht: Springer (2011), p. 489–519. doi: 10.1007/978-94-007-0591-3_17
3. Flegel TW. Historic emergence, impact and current status of shrimp pathogens in Asia. *J Invertebr Pathol.* (2012) 110:166–73. doi: 10.1016/j.jip.2012.03.004
4. Nunan L, Lightner D, Pantoja C, Gomez-Jimenez S. Detection of acute hepatopancreatic necrosis disease (AHPND) in Mexico. *Dis Aquat Organ.* (2014) 111:81–6. doi: 10.3354/dao02776
5. Leobert D, Cabillon NAR, Catedral DD, Amar EC, Usero RC, Monotilla WD, et al. Acute hepatopancreatic necrosis disease (AHPND) outbreaks in *Penaeus vannamei* and *P. monodon* cultured in the Philippines. *Dis Aquat Organ.* (2015) 116:251–4. doi: 10.3354/dao02919
6. Tang KFJ, Bondad-Reantaso MG. Impacts of acute hepatopancreatic necrosis disease on commercial shrimp aquaculture. *Revue Sci Tech (Int Office Epizoo).* (2019) 38:477–90. doi: 10.20506/rst.38.2.2999
7. Tran L, Nunan L, Redman RM, Mohney LL, Pantoja CR, Fitzsimmons K, et al. Determination of the infectious nature of the agent of acute hepatopancreatic necrosis syndrome affecting penaeid shrimp. *Dis Aquat Organ.* (2013) 105:45–55. doi: 10.3354/dao02621
8. Flegel TW. Detection of major penaeid shrimp viruses in Asia, a historical perspective with emphasis on Thailand. *Aquaculture.* (2006) 258:1–33. doi: 10.1016/j.aquaculture.2006.05.013
9. Mathew S, Kumar KA, Anandan R, Nair PGV, Devadasan K. Changes in tissue defence system in white spot syndrome virus (WSSV) infected Penaeus monodon. *Comparat Biochem Physiol C Toxicol Pharmacol.* (2007) 145:315–20. doi: 10.1016/j.cbpc.2007.01.001
10. Mayo Ma. A summary of taxonomic changes recently approved by ICTV. *Arch Virol.* (2002) 147:1655–6. doi: 10.1007/s007050200039
11. Shen H, Qiao Y, Wan X, Jiang G, Fan X, Li H, et al. Prevalence of shrimp microsporidian parasite Enterocytozoon hepatopenaei in Jiangsu Province, China. *Aquacult Int.* (2019) 27:675–83. doi: 10.1007/s10499-019-00358-6
12. Joshi J, Srisala J, Truong VH, Chen I-T, Nuangsaeng B, Suthienkul O, et al. Variation in *Vibrio parahaemolyticus* isolates from a single Thai shrimp farm experiencing an outbreak of acute hepatopancreatic necrosis disease (AHPND). *Aquaculture.* (2014) 428:297–302. doi: 10.1016/j.aquaculture.2014.03.030
13. Mai HN, Caro LFA, Cruz-Flores R, Dhar AK. Development of a recombinase polymerase amplification (RPA) assay for acute hepatopancreatic necrosis disease (AHPND) detection in Pacific white shrimp (Penaeus vannamei). *Mol Cell Probes.* (2021) 57:101710. doi: 10.1016/j.mcp.2021.101710
14. Han JE, Tang KFJ, Pantoja CR, White BL, Lightner DV. qPCR assay for detecting and quantifying a virulence plasmid in acute hepatopancreatic necrosis disease (AHPND) due to pathogenic *Vibrio parahaemolyticus*. *Aquaculture.* (2015) 442:12–5. doi: 10.1016/j.aquaculture.2015.02.024
15. Kondo H, Van PT, Dang LT, Hirono I. Draft genome sequence of non-*Vibrio parahaemolyticus* acute hepatopancreatic necrosis disease strain KC13.175, isolated from diseased shrimp in Vietnam. *Genome Announc.* (2015) 3:e00978–15. doi: 10.1128/genomeA.00978-15
16. Liu L, Xiao J, Xia X, Pan Y, Yan S, Wang Y. Draft genome sequence of Vibrio owensii strain SH-14, which causes shrimp acute hepatopancreatic necrosis disease. *Genome Announc.* (2015) 3:e01395–15. doi: 10.1128/genomeA.01395-15
17. Dong X, Wang H, Xie G, Zou P, Guo C, Liang Y, et al. An isolate of Vibrio campbellii carrying the pirVP gene causes acute hepatopancreatic necrosis disease. *Emerg Microbes Infect.* (2017) 6:1–3. doi: 10.1038/emi.2016.131
18. Han JE, Tang KFJ, Tran LH, Lightner DV. Photorhabdus insect-related (Pir) toxin-like genes in a plasmid of *Vibrio parahaemolyticus*, the causative agent of acute hepatopancreatic necrosis disease (AHPND) of shrimp. *Dis Aquatic Organ.* (2015) 113:33–40. doi: 10.3354/dao02830
19. Sirikharin R, Taengchaiyaphum S, Sanguanrut P, Chi TD, Mavichak R, Proespraiwong P, et al. Characterization and PCR detection of binary, Pir-like toxins from *Vibrio parahaemolyticus* isolates that cause acute hepatopancreatic necrosis disease (AHPND) in shrimp. *PLoS ONE.* (2015) 10:e0126987. doi: 10.1371/journal.pone.0126987
20. Dangtip S, Sirikharin R, Sanguanrut P, Thitamadee S, Sritunyalucksana K, Taengchaiyaphum S, et al. AP4 method for two-tube nested PCR detection of AHPND isolates of *Vibrio parahaemolyticus*. *Aquacult Rep.* (2015) 2:158–62. doi: 10.1016/j.aqrep.2015.10.002
21. Arunrut N, Kampeera J, Sirithammajak S, Sanguanrut P, Proespraiwong P, Suebsing R, et al. Sensitive visual detection of AHPND bacteria using loop-mediated isothermal amplification combined with DNA-functionalized gold nanoparticles as probes. *PLoS One.* (2016) 11:e0151769. doi: 10.1371/journal.pone.0151769
22. Santos HM, Tsai C-Y, Maquiling KRA, Tayo LL, Mariatulqabtiah AR, Lee C-W, et al. Diagnosis and potential treatments for acute hepatopancreatic necrosis disease (AHPND): a review. *Aquacult Int.* (2020) 28:169–85. doi: 10.1007/s10499-019-00451-w
23. Dhar AK, Piamsomboon P, Caro LFA, Kanrar S, Adami R, Jr.,, Juan Y-S. First report of acute hepatopancreatic necrosis disease (AHPND) occurring in the USA. *Dis Aquat Organ.* (2019) 132:241–7. doi: 10.3354/dao03330
24. Daher RK, Stewart G, Boissinot M, Bergeron MG. Recombinase polymerase amplification for diagnostic applications. *Clin Chem.* (2016) 62:947–58. doi: 10.1373/clinchem.2015.245829
25. Suebsing R, Prombun P, Srisala J, Kiatpathomchai W. Loop-mediated isothermal amplification combined with colorimetric nanogold for detection of the microsporidian E nterocytozoon hepatopenaei in penaeid shrimp. *J Appl Microbiol.* (2013) 114:1254–63. doi: 10.1111/jam.12160
26. Prompamorn P, Sithigorngul P, Rukpratanporn S, Longyant S, Sridulyakul P, Chaivisuthangkura P. The development of loop-mediated isothermal amplification combined with lateral flow dipstick for detection of *Vibrio parahaemolyticus*. *Lett Appl Microbiol.* (2011) 52:344–51. doi: 10.1111/j.1472-765X.2011.03007.x
27. Kanitchinda S, Srisala J, Suebsing R, Prachumwat A, Chaijarasphong T. CRISPR-Cas fluorescent cleavage assay coupled with recombinase polymerase amplification for sensitive and specific detection of Enterocytozoon hepatopenaei. *Biotechnol Rep.* (2020) 27:e00485. doi: 10.1016/j.btre.2020.e00485
28. Jinek M, Chylinski K, Fonfara I, Hauer M, Doudna JA, Charpentier E, et al. programmable dual-RNA–guided DNA endonuclease in adaptive bacterial immunity. *Science.* (2012) 337:816–21. doi: 10.1126/science.1225829

29. Wiedenheft B, Sternberg SH, Doudna JA. RNA-guided genetic silencing systems in bacteria and archaea. *Nature.* (2012) 482:331–8. doi: 10.1038/nature10886
30. Bhaya D, Davison M, Barrangou R. CRISPR-Cas systems in bacteria and archaea: versatile small RNAs for adaptive defense and regulation. *Annu Rev Genet.* (2011) 45:273–97. doi: 10.1146/annurev-genet-110410-132430
31. Joung J, Konermann S, Gootenberg JS, Abudayyeh OO, Platt RJ, Brigham MD, et al. Genome-scale CRISPR-Cas9 knockout and transcriptional activation screening. *Nat Protoc.* (2017) 12:828–63. doi: 10.1038/nprot.2017.016
32. Li Y, Li S, Wang J, Liu G. CRISPR/Cas systems towards next-generation biosensing. *Trends Biotechnol.* (2019) 37:730–43. doi: 10.1016/j.tibtech.2018.12.005
33. Chen JS, Ma E, Harrington LB, da Costa M, Tian X, Palefsky JM, et al. CRISPR-Cas12a target binding unleashes indiscriminate single-stranded DNase activity. *Science.* (2018) 360:436–9. doi: 10.1126/science.aar6245
34. Abudayyeh OO, Gootenberg JS, Konermann S, Joung J, Slaymaker IM, Cox DBT, et al. C2c2 is a single-component programmable RNA-guided RNA-targeting CRISPR effector. *Science.* (2016) 353:eaaf5573. doi: 10.1126/science.aaf5573
35. Gootenberg JS, Abudayyeh OO, Kellner MJ, Joung J, Collins JJ, Zhang F. Multiplexed and portable nucleic acid detection platform with Cas13, Cas12a, and Csm6. *Science.* (2018) 360:439–44. doi: 10.1126/science.aaq0179
36. Broughton JP, Deng X, Yu G, Fasching CL, Servellita V, Singh J, et al. CRISPR–Cas12-based detection of SARS-CoV-2. *Nat Biotechnol.* (2020) 38:870–4. doi: 10.1038/s41587-020-0513-4
37. Bai J, Lin H, Li H, Zhou Y, Liu J, Zhong G, et al. Cas12a-based on-site and rapid nucleic acid detection of African swine fever. *Front Microbiol.* (2019) 10:2830. doi: 10.3389/fmicb.2019.02830
38. Myhrvold C, Freije CA, Gootenberg JS, Abudayyeh OO, Metsky HC, Durbin AF, et al. Field-deployable viral diagnostics using CRISPR-Cas13. *Science.* (2018) 360:444–8. doi: 10.1126/science.aas8836
39. Nghia NH, Van PT, Giang PT, Hanh NT, St-Hilaire S, Domingos JA. Control of *Vibrio parahaemolyticus* (AHPND strain) and improvement of water quality using nanobubble technology. *Aquac Res.* (2021) 52:2727–39. doi: 10.1111/are.15124
40. Chopra I, Roberts M. Tetracycline antibiotics: mode of action, applications, molecular biology, and epidemiology of bacterial resistance. *Microbiol Mol Biol Rev.* (2001) 65:232–60. doi: 10.1128/MMBR.65.2.232-260.2001
41. Jun JW, Han JE, Giri SS, Tang KFJ, Zhou X, Aranguren LF, et al. Phage application for the protection from acute hepatopancreatic necrosis disease (AHPND) in Penaeus vannamei. *Indian J Microbiol.* (2018) 58:114–7. doi: 10.1007/s12088-017-0694-9
42. Lobato IM, O'Sullivan CK. Recombinase polymerase amplification: basics, applications and recent advances. *Trac Trends Analyt Chem.* (2018) 98:19–35. doi: 10.1016/j.trac.2017.10.015

Conflict of Interest: The authors declare that the research was conducted in the absence of any commercial or financial relationships that could be construed as a potential conflict of interest.

Publisher's Note: All claims expressed in this article are solely those of the authors and do not necessarily represent those of their affiliated organizations, or those of the publisher, the editors and the reviewers. Any product that may be evaluated in this article, or claim that may be made by its manufacturer, is not guaranteed or endorsed by the publisher.

frontiers in Veterinary Science

ORIGINAL RESEARCH
published: 28 January 2022
doi: 10.3389/fvets.2021.823332

Selection of the Amino Acid and Saccharide That Increase the Tetracycline Susceptibility of *Vibrio splendidus*

Guohua Jiang[1,2], *Yanan Li*[1,2], *Ya Li*[1,2], *Weiwei Zhang*[1,2]* *and Chenghua Li*[1,2,3]*

[1] *Collaborative Innovation Center for Zhejiang Marine High-efficiency and Healthy Aquaculture, Ningbo University, Ningbo, China,* [2] *State Key Laboratory for Quality and Safety of Agro-products, Ningbo University, Ningbo, China,* [3] *Laboratory for Marine Fisheries Science and Food Production Processes, Qingdao National Laboratory for Marine Science and Technology, Qingdao, China*

Bacterial persister cells are a subpopulation of isogenic bacteria with characteristics of reduced metabolic activity and multidrug antibiotic resistance. Our lab had previously proved that *Vibrio splendidus* could form persister cells both naturally and after stimulation. However, the conditions for the waking up of *V. splendidus* persister cells remain marginal. In this study, the carbon sources that could wake up *V. splendidus* persister cells were selected from 20 amino acids and eight saccharides. The result showed that L-glutamic acid, L-aspartic acid, L-arginine, L-phenylalanine, L-leucine, maltose, D-galactose, sorbitol, mannose, N-acetyl-D-glucosamine, D-glucose, and D-fructose could wake up the *V. splendidus* persister cells. The chemotaxis activity of both exponential cells and regrown persister cells on plate containing each of the selected carbon source are also high. The existence of the selected carbon source can affect the antibiotic susceptibility of *V. splendidus*. When L-glutamic acid, L-aspartic acid, L-phenylalanine, and D-glucose were separately added into the cultured *V. splendidus* simultaneously with tetracycline, *V. splendidus* could be completely eliminated, while the addition of L-alanine and D-galactose could not. Our study suggested that *V. splendidus* persister cells could revive in the presence of specific carbon sources, and the addition of these exogenous nutrients could increase the tetracycline susceptibility of *V. splendidus*.

Keywords: *Vibrio splendidus*, persister cells, carbon source, chemotaxis, antibiotic susceptibility

OPEN ACCESS

Edited by:
Lixing Huang,
Jimei University, China

Reviewed by:
Zhe Zhao,
Hohai University, China
Qingpi Yan,
Jimei University, China

***Correspondence:**
Weiwei Zhang
zhangweiwei1@nbu.edu.cn
Chenghua Li
lichenghua@nbu.edu.cn

Specialty section:
This article was submitted to Veterinary Infectious Diseases, a section of the journal Frontiers in Veterinary Science

Received: *27 November 2021*
Accepted: *17 December 2021*
Published: *28 January 2022*

Citation:
Jiang G, Li Y, Li Y, Zhang W and Li C (2022) Selection of the Amino Acid and Saccharide That Increase the Tetracycline Susceptibility of Vibrio splendidus. Front. Vet. Sci. 8:823332. doi: 10.3389/fvets.2021.823332

INTRODUCTION

Persister cells are a little potion of bacterial cells which are temporarily resistant to multidrug on account of a metabolic transient alteration (1). In the 1940s, it was found that some bacteria were not killed completely after treatment with antibiotics (2). In 1944, Bigger named these surviving subpopulation "persister cells" (3). Both groups determine that persister cells are dormant, and this conclusion has been corroborated from that time on (4, 5). Unlike resistant cells, the genes of the persister cells did not alter (6, 7), but they are a little potion of bacterial cells with a transient state of hypometabolic or dormancy that can help bacteria to survive the exterior stresses, such as antibiotic treatment and nutrient deficiency (8–11). Till now, this phenotype has been commonly found in *Staphylococcus aureus*, *Pseudomonas aeruginosa, Escherichia coli*, Vibrio splendidus and Archaea (12–14) during *in vitro* growth as well as infection in the host.

Up to now, more and more studies have shown that persister cells play an important part in the resuscitation of infection diseases. Persister cells avoid antibiotic killing by reducing metabolism, and when the level of antibiotics in the external environment drops, the persister cells resume growing (3, 12, 15, 16). Therefore, the persister cells lead to low efficacy of antibiotic treatment and high occurance of repeated infection. Different kinds of persister cells use specific carbon sources to wake up. For example, the persister cells of *P. aeruginosa* resuscitated in the condition of L-proline (17), while the persister cells of *E. coli* revived in the presence of L-alanine (18). Furthermore, the carbon sources that wake up the persister cells affect the antibiotic susceptibility of persister cells. The changes in antibiotic susceptibility triggered by glucose are documented in *E. coli*, *Vibrio cholerae*, *P. aeruginosa*, and *S. aureus* (19–22). The antibiotic sensitivity of *E. coli*, *S. aureus*, *Edwardsiella tarda*, *Edwardsiella piscicida*, and *P. aeruginosa* are also affected by fructose, maltose, sucrose, leucine, glycine, and alanine (19–21, 23–25).

V. splendidus is a gram-negative bacterium that is ubiquitously presented in marine ecosystems (26), and it is a significant opportunistic bacterial pathogen which causes infection of marine shellfish and sea cucumber *Apostichopus japonicus* (27–30). Our previous study showed that *V. splendidus* could form persister cells (14). To further know more about *V. splendidus* persister cells, the carbon sources that could wake up *V. splendidus* persister cells were selected in this study, and furthermore, a strategy for completely eliminating *V. splendidus* was proposed.

MATERIALS

Bacterial Strains and Culture Conditions

V. splendidus was cultured in 2216E medium at 28°C (1 g yeast extract; 5 g tryptone; and 0.01 g $FePO_4$, 1 L seawater). M9 minimal medium was prepared as follows: 10 ml 0.1 M $CaCl_2$, 10 ml 0.1 M $MgSO_4$, 840 ml ddH_2O, 100 ml sterilized 10 × salt (20 g NaCl, 30 g KH_2PO_4, 70 g Na_2HPO_4, 10 g NH_4Cl in 1 L ddH_2O). The concentration of each saccharide was 0.4%, which was used to wake up *V. splendidus* persister cells. The amino acids and their corresponding levels used to wake up *V. splendidus* persister cells are listed in **Table 1** (31). Tetracycline was dissolved in pure ethanol to make a stock solution of 10 mg·ml^{-1}.

Selection of Persister Cells

V. splendidus persister cells were prepared by lysing active cells with high concentration of tetracycline 400 μg·ml^{-1}, according to our previous study (14). Briefly, 10 ml of overnight *V. splendidus* culture was mixed with 40 ml 2216E containing 2,000 μl of tetracycline stock solution, and the culture was incubated 4 h in a shaker with a shaking speed of 150 rpm. The remaining bacteria were washed with 2% NaCl three times. To verify whether these remaining cells were persister cells, we observed their status on agarose gel pads without any carbon sources as described by Kim et al. (32). In short, agarose was put into 44 ml ddH_2O at 1.5% and sterilized by autoclaving; then, 5 ml 10 × M9 salt solution, 0.5 ml 0.01 M $CaCl_2$, and 0.5 ml 0.1 M $MgSO_4$ solution were subsequently added before the gel was solidified. The cells were observed under the optical microscope (ZEISS) maintained at 28°C.

TABLE 1 | Levels (5× concentration) of amino acids in M9 minimal medium.

Amino acid	Final concentration (μg/ml)	Stock	Amount per liter
L-alanine	75	1%	7.5 ml
L-arginine	145	2%	7.25 ml
L-asparagine	75	1%	7.5 ml
L-aspartic acid	75	1%	7.5 ml
L-cysteine	50	2%	2.5 ml
L-histidine	42	2%	2.1 ml
L-glutamic acid	75	1%	7.5 ml
L-glutamine	75	1%	7.5 ml
L-glycine	110	2%	5.5 ml
L-isoleucine	42	1%	4.2 ml
L-leucine	41	1%	4.1 ml
L-lysine	75	1%	7.5 ml
L-methionine	25	2%	1.25 ml
L-phenylalanine	75	1%	7.5 ml
L-proline	164	4%	4.1 ml
L-serine	42	2%	2.1 ml
L-threonine	82	2%	4.1 ml
L-tryptophan	18	0.25%	7.1 ml
L-tyrosine	75	1%	7.5 ml
L-valine	42	1%	4.2 ml

V. splendidus Persister Cells Revived on Amino Acids

The selection of amino acid for the resuscitation of *V. splendidus* persister cells was determined as reported previously (17). Twenty amino acids were divided into four combinations, and five amino acids were in one group; #1: Phe, Ala, Cys, Ser, and Arg, #2: Tyr, Val, Gly, Thr, and His, #3: Trp, Ile, Pro, Asn, and Lys, and #4: Met, Leu, Gln, Glu, and Asp. To explore the recovery of persister cells on a single amino acid, we separately tested 15 amino acids in combination #1, #3, and #4. *V. splendidus* persister cells were 10-fold serially diluted, and 100 μl of diluent were spread onto M9 minimal plates containing each kind of amino acid as carbon source, and the plates were incubated at 28°C for 96 h.

V. splendidus Persister Cells Revived on Saccharides

Persister cells were also woken up by recognizing saccharides (18). To explore whether saccharides could be used as carbon source to resuscitate *V. splendidus* persister cells, eight saccharides, including maltose, D-glucose, D-ribose, mannose, D-galactose, sorbitol, N-acetyl-D-glucosamine and D-fructose, were separately added into M9 minimal medium. These saccharides are chosen because they are usually good carbon

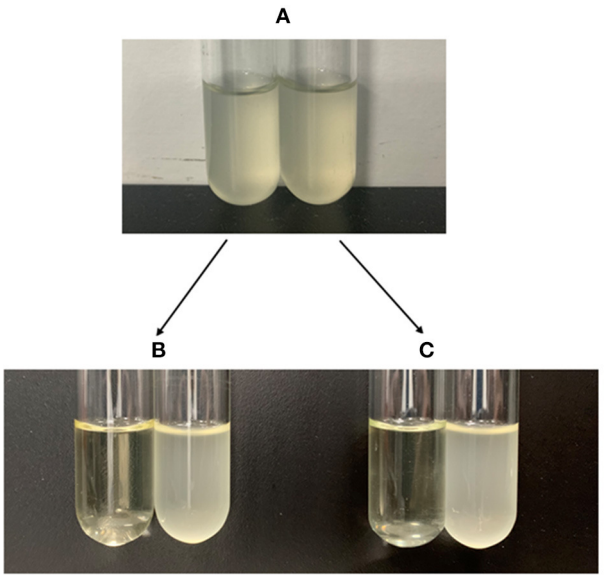

FIGURE 1 | The antibiotic susceptibility of the tetracycline-selected *V. splendidus* persister cells and *V. splendidus* cells. **(A)** The growth of *V. splendidus* exponential cells (left) and regrowth of *V. splendidus* persister cells (right); **(B)** the exponential cells of *V. splendidus* with (left) and without (right) 40 μg·ml^{-1} tetracycline treatment; **(C)** the regrown cells of *V. splendidus* persister cells with (left) and without (right) 40 μg·ml^{-1} tetracycline treatment.

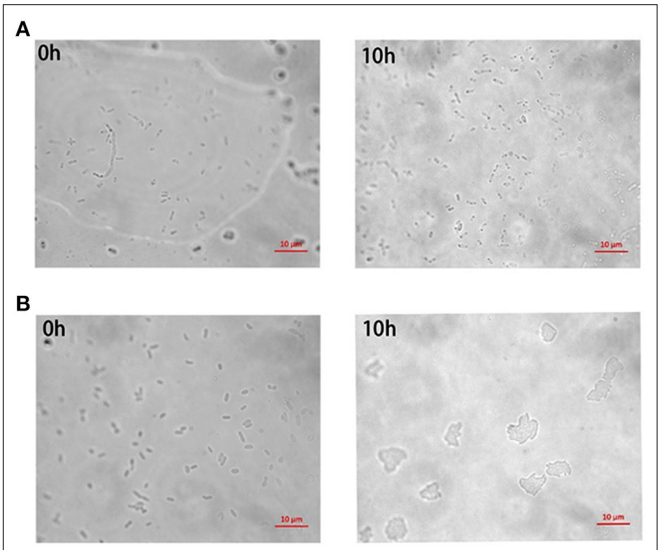

FIGURE 2 | The division of *V. splendidus* persister cells and *V. splendidus* exponential cells in the lack of nutrition. **(A)** Division of *V. splendidus* persister cells on M9 minimal gel pads that without nutrition at the time points of 0 h and 10 h, respectively. **(B)** Division of *V. splendidus* exponential cells at time points of 0 h and 10 h in the lack of nutrition. Scale bar indicates 10 μm.

sources for bacteria, especially *N*-acetyl-D-glucosamine which is used as principal source of carbon and nitrogen by marine bacteria (33). *V. splendidus* persister cells were 10-fold serially diluted, and 100 μl of diluent were spread onto M9 minimal plates containing each kind of saccharide as carbon source, and the plates were incubated at 28°C for 48 h.

Chemotaxis Assays

The chemotaxis of both exponential cells and regrown persister cells were performed as reported previously by Weng et al. (34). Briefly, *V. splendidus* were cultured until an optical density at 600 nm (OD_{600}) of 1.0 and washed twice with M9 minimal medium. *V. splendidus* persister cells were obtained as previously described, and the persister cells were put into 1 ml M9 minimal medium. Amino acid or saccharide solutions were separately added onto M9 minimal plates containing 0.2% (w/v) agar. Ten microliter of bacterial suspensions were dropped on the M9 minimal plates containing each kind of individual carbon source, respectively, and the plates were incubated at 28°C for 96 h.

Antibiotic Susceptibility

The overnight grown stationary phase culture was supplemented with each exogenous carbon source at levels of 0, 1, 5, 10, 15, 20, 30, and 40 mM, respectively, and tetracycline stock solution was added into the medium at a concentration of 400 μg·ml^{-1} immediately. The culture without addition of any exogenous carbon sources was used as a control. All the cultures were incubated at 28°C for 6 h with shaking at 150 rpm. After treatment, the cells were collected by centrifugation, diluted in 10-fold serially, and 10 μl of each diluent was dropped on 2216E plates. After incubation at 28°C for 24 h, the colonies that emerged on the plates were counted. The relative percent of survival was determined as follows: the cell number after tetracycline plus exogenous carbon source challenge/the cell number after tetracycline solo challenge.

Strain Number and Statistical Analysis

The isolates of *V. splendidus* were deposited into the China General Microbiological Culture Collection (CGMCC, Beijing, China) with strain No. 7.242. Statistical analyses were performed by using the two tailed *t*-test. Statistical significance was determined by one-way ANOVA. In all cases, the significance level was defined as $^{*}p < 0.05$ and $^{**}p < 0.01$.

RESULTS

Tetracycline-Selected *V. splendidus* Persister Cells

A portion of antibiotic-resistant *V. splendidus* cells emerged after 400 μg·ml^{-1} tetracycline was treated for 4 h at 28°C. These cells were confirmed as persister cells by measuring their antibiotic sensitivity and cell division. The result showed that the regrown cells from persister cells had equal susceptibility to the tetracycline, and 40 μg·ml^{-1} tetracycline could completely lyse both the regrown cells from persister cells and the exponential cells (**Figure 1**). The division of cells in the absence of nutrients was observed under microscope. It showed that the persister cells did not resuscitate within 10 h on agarose gel pads without nutrients (**Figure 2A**), while exponential cells of *V. splendidus* showed several divisions on agarose gel pads (**Figure 2B**). All

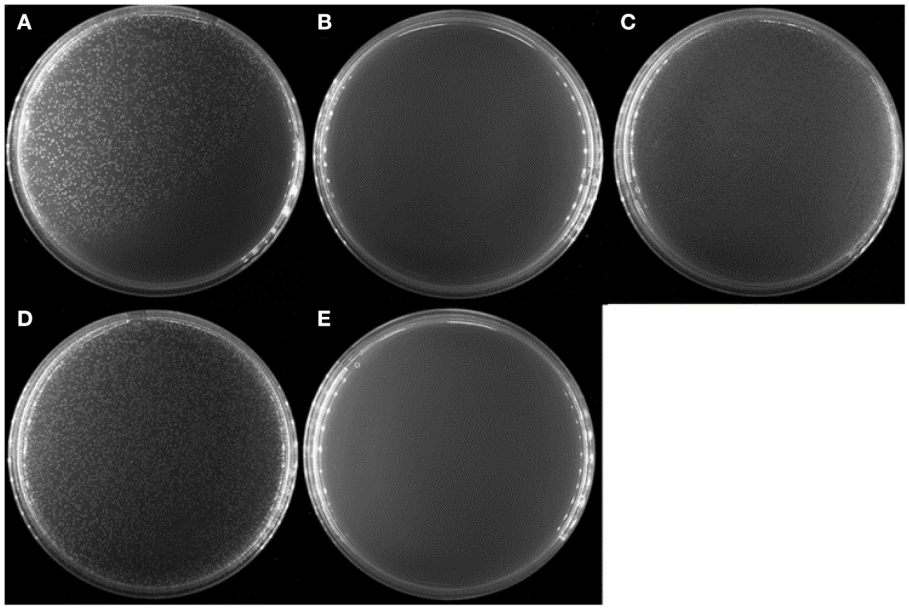

FIGURE 3 | Persister cells wake up on amino acids combination plate agar. *V. splendidus* persister cells were incubated at 28°C for 96 h on M9 minimal plate agar with four different amino acid combinations, respectively: **(A)** #1: Phe, Ala, Cys, Ser, and Arg; **(B)** #2: Tyr, Val, Gly, Thr, and His; **(C)** #3: Trp, Ile, Pro, Asn, and Lys; **(D)** #4: Met, Leu, Gln, Glu, and Asp; **(E)** without amino acid. All amino acids in the experiment were 5×concentration as listed in **Table 1**.

these results showed that the cells obtained after treatment with high concentration of tetracycline were persister cells. In addition, the persister cells in the stationary culture of *V. splendidus* were determined to be at a potion of approximately 0.1%-1% determined by the colony that emerged on the plates.

V. splendidus Persister Cells Resuscitated on Specific Amino Acid

To see whether *V. splendidus* persister cells could resuscitate on specific carbon source like the spores of *Bacillus subtilis*, a total of 20 amino acids were separately used as carbon source to wake up *V. splendidus* persister cells. For the first assay, we divided 20 amino acids into four groups as four kinds of carbon sources. The result showed that *V. splendidus* persister cells did not resuscitate on combination #2, but they could resuscitate on combinations #1, #3, and #4 (**Figure 3**). The 15 amino acids in combinations #1, #3, and #4 were further chosen to detect the single amino acid to wake up *V. splendidus* persister cells. Result showed that *V. splendidus* persister cells woke up at 17 h when L-glutamic acid was used as the only carbon source, which was the fastest among all the 20 amino acids (**Figure 4**). *V. splendidus* persister cells revived on M9 minimal plate with L-aspartic acid at 24 h, and they revived on M9 minimal plates with solo L-leucine, L-phenylalanine, and L-arginine when the resuscitation time increased to 40 h (**Figure 4**).

V. splendidus Persister Cells Resuscitated on Specific Saccharide

To see whether *V. splendidus* persister cells could resuscitate on saccharides, eight different kinds of saccharides were separately used as carbon source for *V. splendidus* persister cells to revive. Our result showed that *V. splendidus* persister cells revived on M9 minimal plate supplemented with D-galactose and maltose at 24 h and they revived on mannose and sorbitol at 36 h, but *V. splendidus* persister cells slowly revived on M9 agar plate with separate D-fructose, N-acetyl-D-glucosamine, and D-glucose when the resuscitation time increased to 48 h. Less colony numbers were obtained when the persister cells were revived on D-fructose and D-glucose, but larger colonies were obtained when they were revived on D-fructose and D-glucose compared with N-acetyl-D-glucosamine. However, *V. splendidus* persister cells did not revive with D-ribose at all within 48 h (**Figure 5**).

V. splendidus Showed Chemotaxis in Different Carbon Sources

In the experiment to assess the chemotaxis ability of exponential cells and regrown cells of *V. splendidus* persister cells in the context of various carbon sources, three amino acids of L-glutamic acid, L-aspartic acid, and L-phenylalanine and two saccharides of D-galactose and D-glucose were chosen. L-alaine that could not revive the persister cells was selected to be used as a control. Ten microliters of each kind of cells was dropped on 0.2% M9 minimal plate containing each carbon source. We found that both exponential cells and regrown persister cells of *V. splendidus* showed obvious chemotaxis to 400 $mg{\cdot}l^{-1}$ L-glutamic acid, L-aspartic acid, L-phenylalanine, D-galactose, and D-glucose. After 96 h of treatment, the diameters of the *V. splendidus* on the plates containing L-alanine, L-aspartic acid, L-glutamic acid, L-phenylalanine, D-galactose, and D-glucose were,

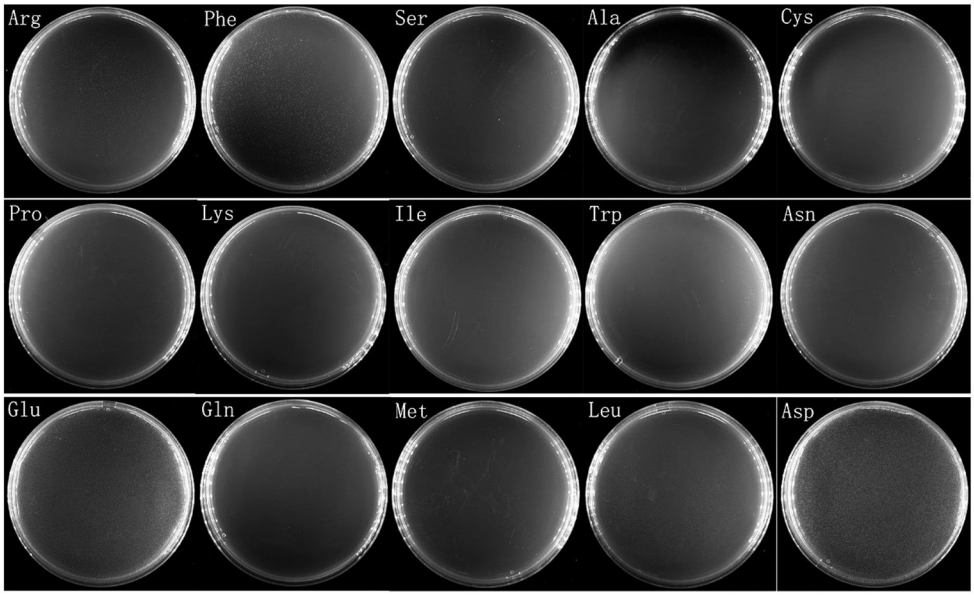

FIGURE 4 | Persister cells wake up on plate containing single amino acid. *V. splendidus* persister cells were incubated at 28°C for 96 h on M9 minimal plate with 15 individual amino acids (L-alanine, L-serine, L-cystine, L-arginine, L-lysine, L-phenylalanine, L-asparagine, L-proline, L-isoleucine, L-tryptophan, L-glutamine, L-leucine, L-aspartic acid, L-methionine, and L-glutamic acid). The concentrations of the amino acids in the experiment were 5×concentration as listed in **Table 1**.

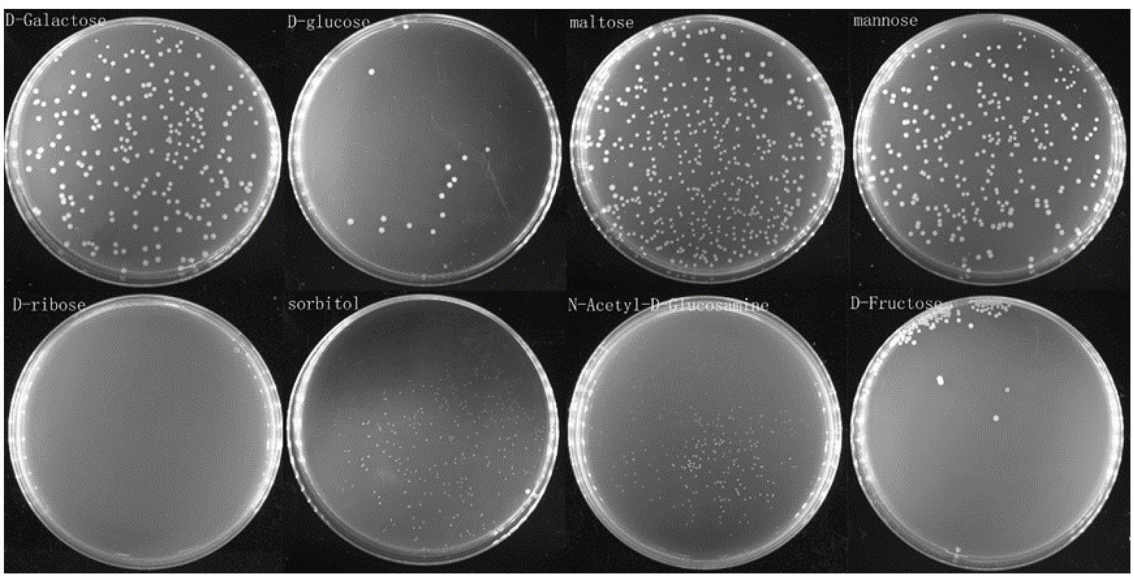

FIGURE 5 | Persister cells wake up on plate containing single saccharide. Persister cells were spread on M9 minimal plates with D-glucose, D-fructose, D-ribose, N-acetyl-D-glucosamine, D-galactose, mannose, maltose, and sorbitol, respectively. The concentration of each saccharide on the plate was 0.4%, and the plates were incubated at 28°C for 48 h.

respectively, 3.13, 8.67, 8.65, 4.06, 9.93, and 8.74 cm, respectively (**Figure 6**), and the diameters of the regrown *V. splendidus* persister cells on the L-alanine, L-aspartic acid, L-glutamic acid, L-phenylalanine, D-galactose, and D-glucose plates were 1.93, 6.69, 8.15, 3.17, 8.57, and 5.48 cm, respectively (**Figure 7**). The chemotaxis of both exponential cells and regrown persister cells of *V. splendidus* showed the highest chemotaxis ability toward D-galactose and L-glutamic acid. On the contrary, the regrown cells of *V. splendidus* persister cells were not attracted by L-alanine within the 72 h.

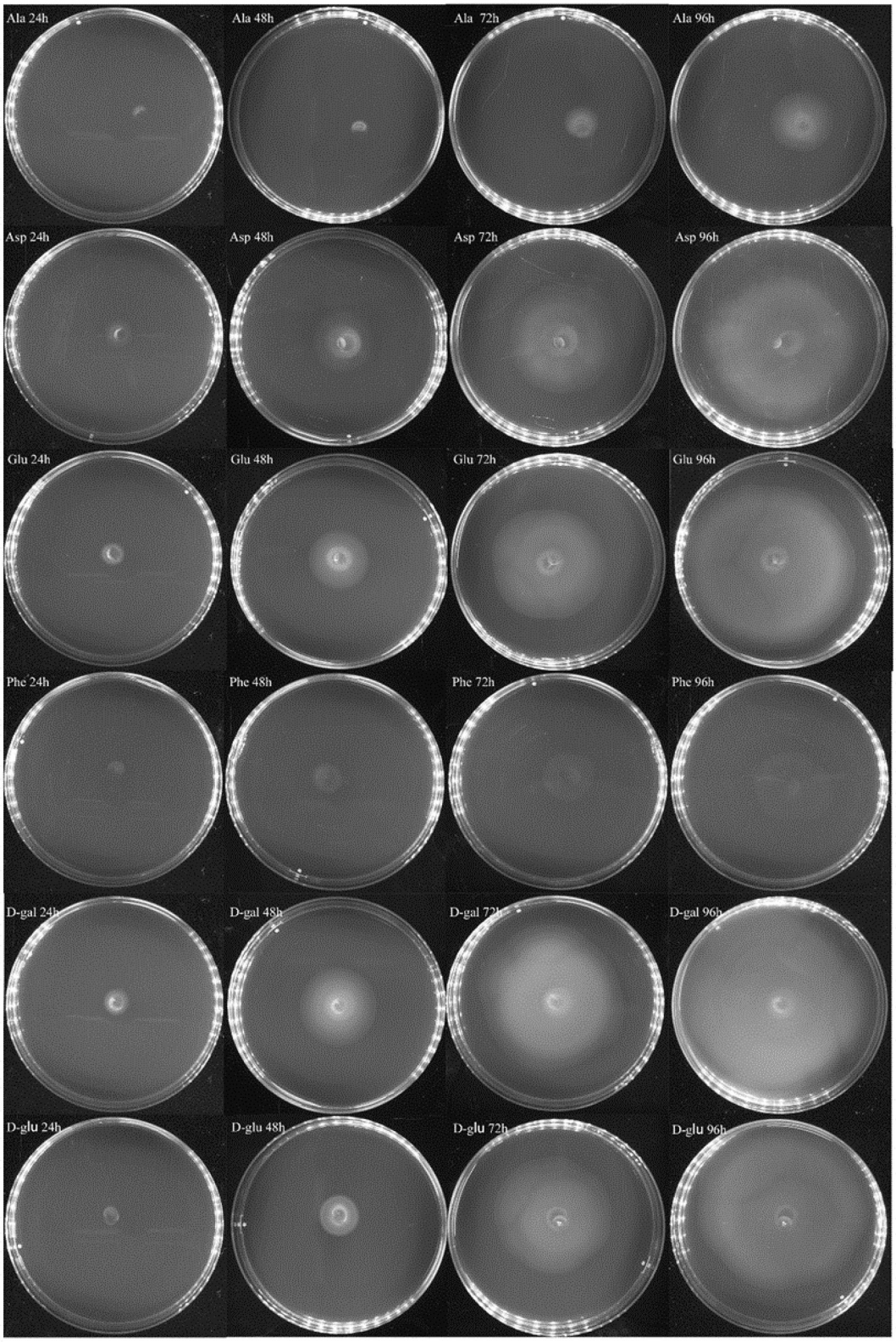

FIGURE 6 | Chemotaxis of *V. splendidus* exponential cells. Each exogenous carbon source at a concentration of 400 mg·L^{-1} was separately added into M9 minimal plates containing 0.20% (w/v) agar; 1 ml M9 minimal medium was used to resuspend persister cells, and 10 μl cell suspensions was dropped on the M9 minimal plate containing each carbon source, and the plates were incubated at 28°C for 96 h.

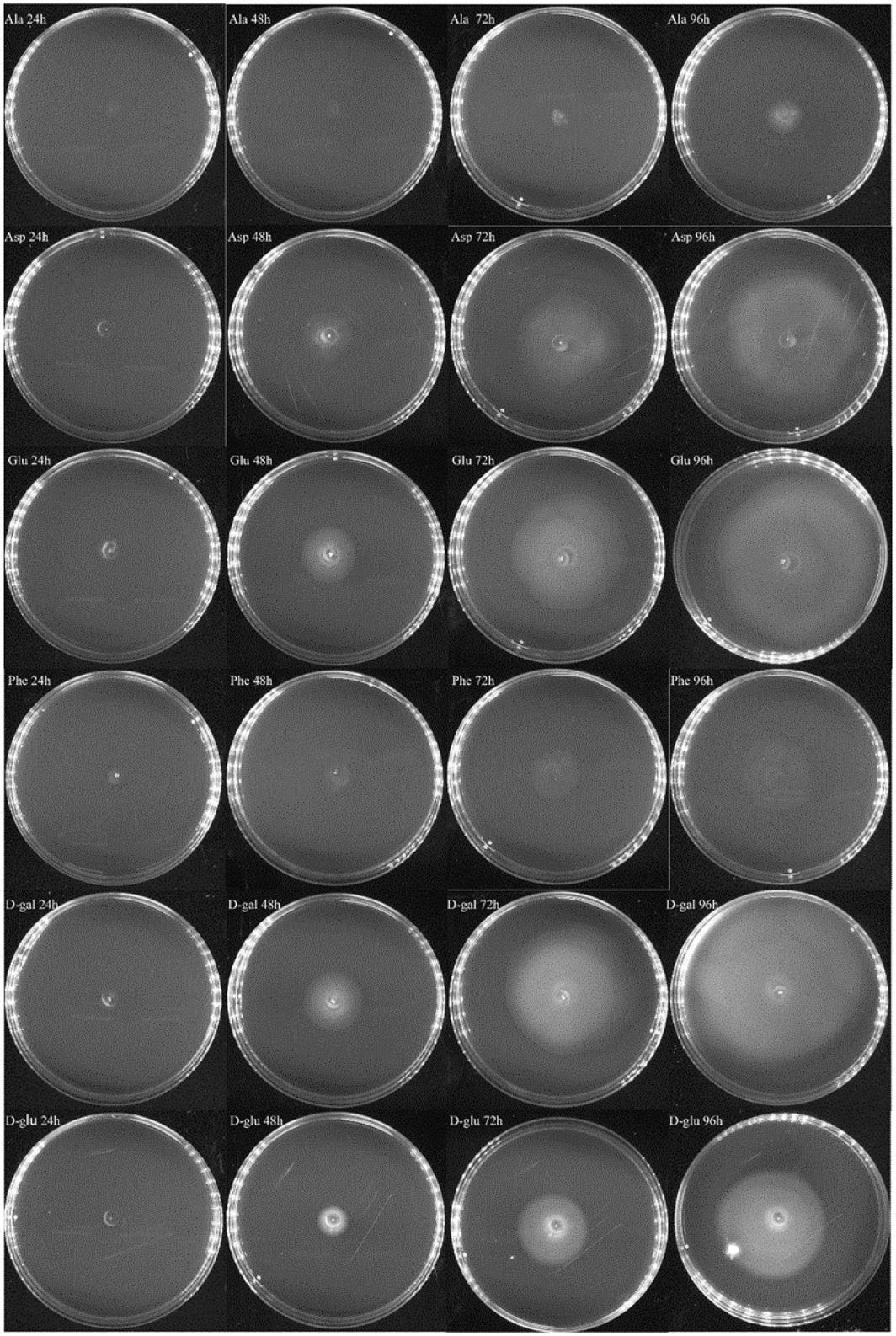

FIGURE 7 | Chemotaxis of the regrown cells of *V. splendidus* persister cells. Each exogenous carbon source at a concentration of 400 mg·L^{-1} was separately added into M9 minimal plates containing 0.20% (w/v) agar; 1 ml M9 minimal medium was used to resuspend persister cells, and 10 μl bacterial suspension was dropped on M9 plate containing each carbon source, and the plates were incubated at 28°C for 96 h.

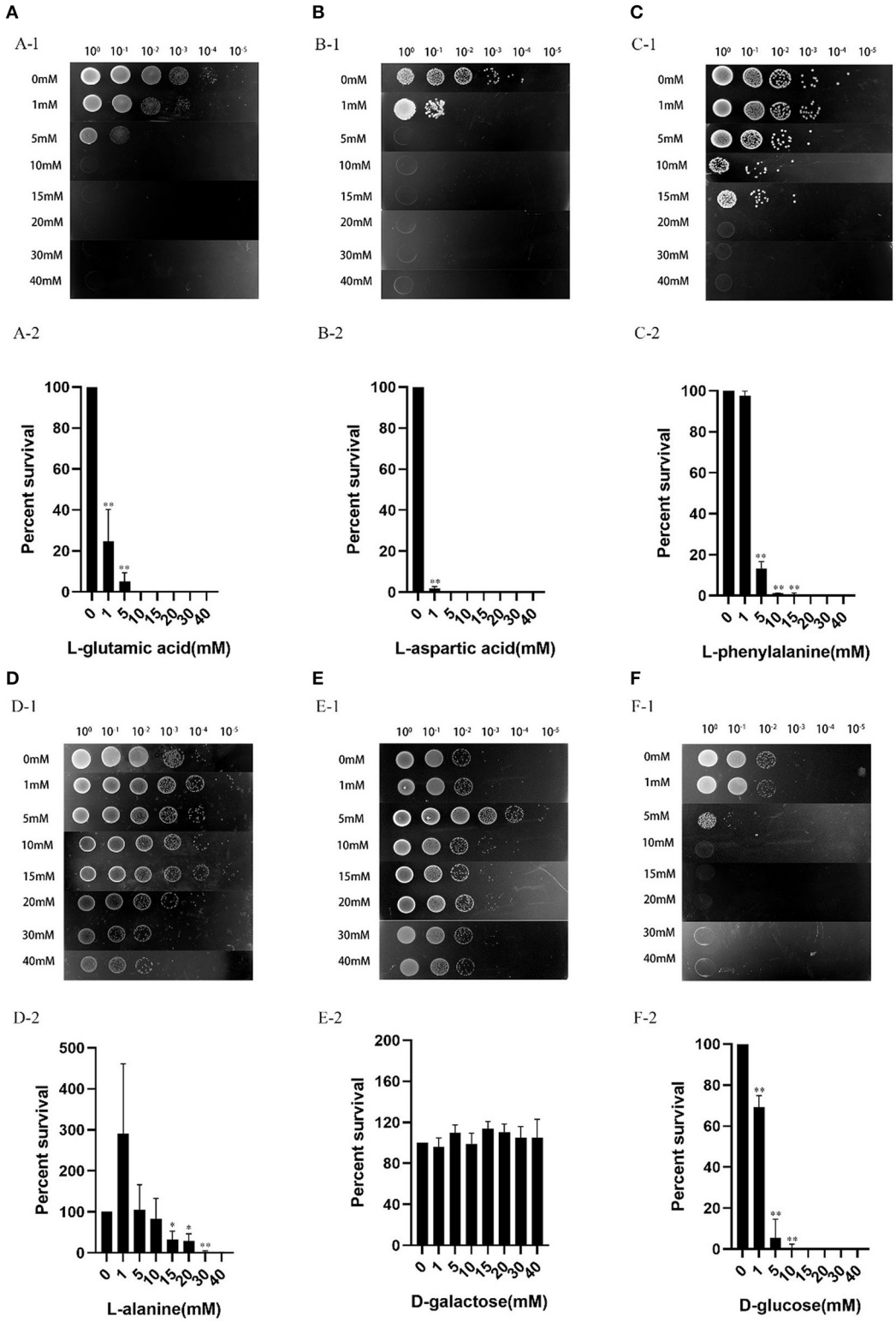

FIGURE 8 | Effects of exogenous carbon sources on antibiotic susceptibility of *V. splendidus*. The overnight grown stationary phase culture was supplemented with the following concentrations of exogenous metabolites: **(A)** L-glutamic acid, **(B)** L-aspartic acid, **(C)** L-phenylalanine, **(D)** L-alanine, **(E)** D-galactose, and **(F)** D-glucose. The cultures without addition of any exogenous carbon sources were used as a control. The antibiotics and exogenous carbon sources were simultaneously added to the culture and incubated for 6 h, and the survived cells in different dilutions was represented by the colony formed on the plates (10^0, 10^{-1}, 10^{-2}, 10^{-3}, 10^{-4}, and 10^{-5} meant no dilution, 10-, 100-, 1,000-, 10,000- and 100,000- dilutions). The relative percent of survival was calculated as follows: the cell number after tetracycline plus exogenous carbon source challenge/the cell number after tetracycline challenge alone. $^*p < 0.05$ and $^{**}p < 0.01$.

Exogenous Carbon Source Increased Tetracycline Susceptibility of *V. splendidus*

Studies have proved that the sensitivity of *E. coli* persister cells to aminoglycoside antibiotics is affected by exogenous glucose (23). In our present study, we tested whether the selected six metabolites, L-glutamic acid, L-aspartic acid, L-phenylalanine, L-alanine, D-galactose, and D-glucose could be used to increase the tetracycline susceptibility of *V. splendidus*. The results showed that the percentage of survived cells decreased with increased dose of L-glutamic acid, L-aspartic acid, L-phenylalanine, L-alanine, and D-glucose, with simultaneous addition of tetracycline (**Figure 8**). *V. splendidus* cells that were incubated with 400 $\mu g{\cdot}ml^{-1}$ tetracycline alone for 6 h were used as a control sample, and approximately 0.1%-1% cells survived after tetracycline treatment. Compared to *V. splendidus* grown in 400 $\mu g{\cdot}ml^{-1}$ tetracycline alone, the potion of the survived cells with the addition of carbon sources decreased significantly. The effect of exogenous carbon sources on the antibiotic sensitivity of *V. splendidus* was determined to be dose-dependent. The antibiotic sensitivity of *V. splendidus* also enhances when the concentrations rose from 0 to 40 mM. When the concentrations of L-aspartic acid, L-glutamic acid, D-glucose, and L-phenylalanine were 5, 10, 15, and 20 mM, *V. splendidus* cells were completely killed by 400 $\mu g{\cdot}ml^{-1}$ tetracycline; however, compared to *V. splendidus* in the control sample, the percentage of cell survival in the sample supplemented with 40 mM D-galactose showed no obvious change. These results suggested that the antibiotic susceptibility could be increased by addition of exogenous carbon sources.

DISCUSSION

Persister cells refer to a state of reduced metabolic activity that endows a subpopulation of isogenic bacteria with temporary multi-drug resistance, and they are able to revive the growth after the external stress is relieved. The development of persister cells can affect antibiotic efficacy, leading to incomplete treatment and repeated infections (35). Different kinds of bacterial persister cells have their preferred carbon source to wake up. The persister cells of *P. aeruginosa* revived in L-proline (17), while the persister cells of *E. coli* recovered in the presence of L-alanine (18). This study is the first attempt to explore the carbon sources that could wake up *V. splendidus* persister cells. *V. splendidus* persister cells can revive in the context of the amino acids including L-glutamic acid, L-aspartic acid, L-phenylalanine, L-leucine and L-arginine, and saccharides including D-galactose, maltose, mannose, sorbitol, D-fructose, N-acetyl-D-glucosamine, and D-glucose. For amino acids, L-glutamic acid revived *V. splendidus* persister cells used for the shortest time, and for saccharides, D-galactose, maltose, mannose, and sorbitol woke up *V. splendidus* persister cells better than D-fructose, N-acetyl-D-glucosamine, and D-glucose. The different numbers of colonies emerged on the specific carbon source probably attributed to the high heterogeneity of *V. splendidus* persister cells in dormancy (14), which resulted in their heterogeneous waking up on different carbon sources, probably due to different metabolism of various carbon sources in *V. splendidus*. Consequently, the results of this study indicated that (1) *V. splendidus* persister cells woke up responding to nutrient incentives similar to *P. aeruginosa* and *E. coli* (17, 18, 36) (2) L-glutamic acid is the best amino acid to revive *V. splendidus* persister cells, which is specific to this bacterial species; this further strengthened the concept that different bacterial persister cells preferred to use different carbon sources to wake up (17, 18).

Chemotaxis is the response to the stimulation of chemical substances in the external environment (37). Bacteria receive signals from external stimuli through chemoreceptors and process them through signal transduction systems to make corresponding movements (38). Chemotaxis plays an important role in the recovery of *E. coli* persister cells. Once persister cells resuscitated, the cells use chemotaxis to gain nutrients (18). In this study, we found that both exponential cells and persister cells of *V. splendidus* showed obvious chemotaxis to L-glutamic acid, L-aspartic acid, L-phenylalanine, D-galactose, and D-glucose; but relative to L-glutamic acid, L-aspartic acid, D-galactose, and D-glucose *V. splendidus* showed lower chemotaxis to L-phenylalanine, and L-alaine. The carbon sources that persister cells showed stronger chemotaxis were consist with the carbon sources that were suitable for the revival of persister cells, which suggested that the chemotaxis system may also play important roles in recognizing nutritional signals and resuscitation in *V. splendidus* persister cells, similarly to that in *E. coli* persister cells (18).

Further, we tested the effect of these exogenous carbon sources on the antibiotic susceptibility of *V. splendidus*. The addition of exogenous nutrients increases the antibiotic susceptibility of bacteria and has been reported in various pathogens. For example, glucose can alter cell metabolism, which leads to increased sensitivity to kanamycin and ciprofloxacin (22, 24) and aminoglycosides (21, 23), and this phenomenon is also found in *V. parahaemolyticus*, *K. peneumoniae*, *S. aureus*, and *P. aeruginosa* (39–44). In the present study, we found that addition of exogenous carbon sources, L-glutamic acid, L-aspartic acid, L-phenylalanine, and D-glucose could also increase the tetracycline susceptibility of *V. splendidus* persister cells and this led us to speculate that these exogenous additions might trigger the little potion of persister cells at stationary phase to secede the persister state and enter into an active metabolic state. Compared with other methods to eliminate persister cells, such as development of new drugs, this method shows more effectiveness in combating antibiotic-resistant bacteria (24). Thus, we can surely believe that adding of the selected exogenous carbon sources combined with proper antibiotics will be a useful strategy to completely eliminate *V. splendidus*.

DATA AVAILABILITY STATEMENT

The original contributions presented in the study are included in the article/supplementary material, further inquiries can be directed to the corresponding authors.

AUTHOR CONTRIBUTIONS

GJ conducted the experiments, analyzed the data, and wrote the original manuscript. YanL conducted parts of the experiments and analyzed the data. YaL conducted parts of the experiments. WZ conceived and planned the research, supervised the research, revised the manuscript, and acquired funding. CL supervised the research and acquired funding. All authors reviewed the manuscript.

FUNDING

This study was funded by the Zhejiang Provincial Natural Science Foundation for Distinguished Young Scholar (LR20C190001), the National Natural Science Foundation of China (31972833), the Zhejiang Provincial Natural Science Foundation (LZ19C190001), the Fundamental Research Funds for the Provincial Universities of Zhejiang (SJLZ2020001), and the K.C. Wong Magna Fund at Ningbo University.

REFERENCES

1. Helaine S, Kugelberg E. Bacterial persisters: formation, eradication, and experimental systems. *Trends Microbiol.* (2014) 22:417–24. doi: 10.1016/j.tim.2014.03.008
2. Hobby GL, Meyer K, Chaffee E. Observations on the mechanism of action of penicillin. *Exp Biol Med.* (1942) 50:281–5. doi: 10.3181/00379727-50-13773
3. Bigger JW. Treatment of staphylococcal infections with penicillin-by intermittent sterilisation. *Lancet.* (1944) 2:497–500. doi: 10.1016/S0140-6736(00)74210-3
4. Shah D, Zhang ZG, Khodursky A, Kaldalu N, Kurg K, Lewis K. Persisters: a distinct physiological state of *E. coli BMC Microbiol.* (2006) 6:53. doi: 10.1186/1471-2180-6-53
5. Kwan BW, Valenta JA, Benedik MJ, Wood TK. Arrested protein synthesis increases persister-like cell formation. *Antimicrob Agents Ch.* (2013) 57:1468–73. doi: 10.1128/AAC.02135-12
6. Kwan BW, Chowdhury N, Wood TK. Combatting bacterial infections by killing persister cells with mitomycin C. *Environ Microbiol.* (2015) 17:4406–14. doi: 10.1111/1462-2920.12873
7. Chowdhury N, Wood TL, Martinez-Vazquez M, Garcia-Contreras R, Wood TK. DNA-crosslinker cisplatin eradicates bacterial persister cells. *Biotechnol Bioeng.* (2016) 113:1984–92. doi: 10.1002/bit.25963
8. Bernier SP, Létoffé S, Delepierre M, Ghigo JM. Biogenic ammonia modifies antibiotic resistance at a distance in physically separated bacteria. *Mol Microbiol.* (2011) 81:705–16. doi: 10.1111/j.1365-2958.2011.07724.x
9. Maisonneuve E, Gerdes K. Molecular mechanisms underlying bacterial persisters. *Cell.* (2014) 157:539–48. doi: 10.1016/j.cell.2014.02.050
10. Martins PMM, Merfa MV, Takita MA, De Souza AA. Persistence in phytopathogenic bacteria: do we know enough? *Front Microbiol.* (2018) 9:1099. doi: 10.3389/fmicb.2018.01099
11. Song S, Wood TK. Post-segregational killing and phage inhibition are not mediated by cell death through toxin/antitoxin systems. *Front Microbiol.* (2018) 9:814. doi: 10.3389/fmicb.2018.00814
12. Fisher RA, Gollan B, Helaine S. Persistent bacterial infections and persister cells. *Nat Rev Microbiol.* (2017) 15:453–64. doi: 10.1038/nrmicro.2017.42
13. Megaw J, Gilmore BF. Archaeal persisters: persister cell formation as a stress response in *Haloferax volcanii*. *Front Microbiol.* (2017) 8:1589. doi: 10.3389/fmicb.2017.01589
14. Li YN, Wood TK, Zhang WW, Li CH. Vibrio splendidus persister cells induced by host coelomic fluids show a similar phenotype to antibiotic-induced counterparts. *Environ Microbiol.* (2021) 23:5605–20. doi: 10.1111/1462-2920.15717
15. Lewis K. Persister cells. *Annu Rev Microbiol.* (2010) 64:357–72. doi: 10.1146/annurev.micro.112408.134306
16. Van den Bergh B, Fauvart M, Michiels J. Formation, physiology, ecology, evolution and clinical importance of bacterial persisters. *FEMS Microbiol Rev.* (2017) 41:219–51. doi: 10.1093/femsre/fux001
17. Zhang WW, Yamasaki R, Song S, Wood TK. Interkingdom signal indole inhibits *Pseudomonas aeruginosa* persister cell waking. *J App Microbiol.* (2019) 127:1768–72. doi: 10.1111/jam.14434
18. Yamasaki R, Song S, Benedik MJ, Wood TK. Persister cells resuscitate using membrane sensors that activate chemotaxis, lower cAMP levels, and revive ribosomes. *iScience.* (2019) 23:100792. doi: 10.1016/j.isci.2019.100792
19. Thorsing M, Bentin T, Givskov M, Tolker-Nielsen T, Goltermann L. The bactericidal activity of β-lactam antibiotics is increased by metabolizable sugar species. *Microbiology.* (2015) 161:1999–2007. 2 doi: 10.1099/mic.0.000152
20. Prax M, Mechler L, Weidenmaier C, Bertram R. Glucose augments killing efficiency of daptomycin challenged *Staphylococcus aureus* persisters. *PLoS ONE.* (2016) 11:e0150907. doi: 10.1371/journal.pone.0150907
21. Meylan S, Porter CBM, Yang JH, Belenky P, Gutierrez A, Lobritz MA. Carbon sources tune antibiotic susceptibility in *Pseudomonas aeruginosa* via tricarboxylic acid cycle control. *Cell Chem Biol.* (2017) 24:195–206. doi: 10.1016/j.chembiol.2016.12.015
22. Paranjape SS, Shashidhar R. Glucose sensitizes the stationary and persistent population of *Vibrio cholerae* to ciprofloxacin. *Arch Microbiol.* (2020) 202:343–9. doi: 10.1007/s00203-019-01751-8
23. Allison KR, Brynildsen MP, Collins JJ. Metabolite-enabled eradication of bacterial persisters by aminoglycosides. *Nature.* (2011) 473:216–20. doi: 10.1038/nature10069
24. Peng B, Su Y, Li H, Han Y, Guo C, Tian Y, et al. Exogenous alanine and/or glucose plus kanamycin kills antibiotic-resistant bacteria. *Cell Metab.* (2015) 21:249–62. doi: 10.1016/j.cmet.2015.01.008
25. Ye J, Lin X, Cheng Z, Su Y, Li W, Ali F, et al. Identification and efficacy of glycine, serine and threonine metabolism in potentiating kanamycin-mediated killing of *Edwardsiella piscicida*. *J Proteomics.* (2018) 183:34–44. doi: 10.1016/j.jprot.2018.05.006
26. Macián MC, Garay E, González-Candelas F, Pujalte MJ, Aznar R. Ribotyping of *Vibrio* populations associated with cultured oysters (Ostrea edulis). Syst Appl Microbiol. (2020) 23:409–17.—2020(00)80072-7 doi: 10.1016/S0723-2020(00)80072-7
27. Beaz-Hidalgo R, Balboa S, Romalde JL, Figueras MJ. Diversity and pathogenecity of *Vibrio* species in cultured bivalve molluscs. *Environ Microbiol Rep.* (2010) 2:34–43. doi: 10.1111/j.1758-2229.2010.00135.x
28. Lemire A, Goudenège D, Versigny T, Petton B, Calteau A, Labreuche Y, et al. Populations, not clones, are the unit of *vibrio* pathogenesis in naturally infected oysters. *ISME J.* (2015) 9:1523–31. doi: 10.1038/ismej.2014.233
29. Travers MA, Miller BK, Roque A, Friedman CS. Bacterial diseases in marine bivalves. *J Invertebr Pathol.* (2015) 131:11–31. doi: 10.1016/j.jip.2015.07.010
30. Zhang WW, Li CH. Virulence mechanisms of vibrios belonging to the Splendidus clade as aquaculture pathogens, from case studies and genome data. *Rev Aquacult*. (2021) 13:2004–026. doi: 10.1111/raq.12555
31. Rodriguez R, Tait RC. *Recombinant DNA Techniques: An Introduction.* Menlo Park, CA: Benjamin Cummings Publishing Company. (1983)
32. Kim JS, Chowdhury N, Yamasaki R, Wood TK. Viable but non-culturable and persistence describe the same bacterial stress state. *Environ Microbiol.* (2018) 20:2038–48. doi: 10.1111/1462-2920.14075
33. Keyhani NO, Roseman S. Physiological aspects of chitin catabolism in marine bacteria. *Biochim Biophys Acta.* (1999) 1473:108–22. doi: 10.1016/S0304-4165(99)00172-5
34. Weng Y, Jiang JD, Deng HH, Lan H, Li SP. Effect of mutation of chemotaxis signal transduction gene cheA in *Pseudomonas putida* DLL-1 on its chemotaxis and methyl parathion biodegradation. *Wei Sheng Wu Xue Bao.* (2007) 47:471–6.

35. Lewis K. Platforms for antibiotic discovery. *Nat Rev Drug Discov.* (2013) 12:371–87. doi: 10.1038/nrd3975
36. Kim JS, Yamasaki R, Song S, Zhang W, Wood TK. Single cell observations show persister cells wake based on ribosome content. *Environ Microbiol.* (2018) 20:2085–98. doi: 10.1111/1462-2920.14093
37. Karmakar R. State of the art of bacterial chemotaxis. *J Basic Microbiol.* (2021) 61:366–79. doi: 10.1002/jobm.202000661
38. Porter SL, Wadhams GH, Armitage JP. Signal processing in complex chemotaxis pathways. *Nat Rev Microbiol.* (2011) 9:153–65. doi: 10.1038/nrmicro2505
39. Gusarov I, Shatalin K, Starodubtseva M, Nudler E. Endogenous nitric oxide protects bacteria against a wide spectrum of antibiotics. *Science.* (2009) 325:1380–4. doi: 10.1126/science.1175439
40. Lee HH, Molla MN, Cantor CR, Collins JJ. Bacterial charity work leads to population-wide resistance. *Nature.* (2010) 467:82–5. doi: 10.1038/nature09354
41. Barbieri E, Falzano L, Fiorentini C, Pianetti A, Baffone W, Fabbri A, et al. Occurrence, diversity, and pathogenicity of halophilic *Vibrio* spp. and Non-O1 Vibrio cholerae from estuarine waters along the Italian Adriatic coast. *App Environ Microbiol.* (1999) 65:2748–53. doi: 10.1128/AEM.65.6.2748-2753.1999
42. Shatalin K, Shatalina E, Mironov A, Nudler E. H_2S: a universal defense against antibiotics in bacteria. *Science.* (2011) 334:986–90. doi: 10.1126/science.1209855
43. Vega NM, Allison KR, Khalil AS, Collins JJ. Signaling-mediated bacterial persister formation. *Nat Chem Biol.* (2012) 8:431–3. doi: 10.1038/nchembio.915
44. Vega NM, Allison KR, Samuels AN, Klempner MS, Collins JJ. *Salmonella typhimurium* intercepts *Escherichia coli* signaling to enhance antibiotic tolerance. *PNAS USA.* (2013) 110:14420–5. doi: 10.1073/pnas.1308085110

Conflict of Interest: The authors declare that the research was conducted in the absence of any commercial or financial relationships that could be construed as a potential conflict of interest.

Publisher's Note: All claims expressed in this article are solely those of the authors and do not necessarily represent those of their affiliated organizations, or those of the publisher, the editors and the reviewers. Any product that may be evaluated in this article, or claim that may be made by its manufacturer, is not guaranteed or endorsed by the publisher.

frontiers in Veterinary Science

ORIGINAL RESEARCH
published: 31 January 2022
doi: 10.3389/fvets.2021.813988

RNA-Sequencing Analysis of the Spleen and Gill of *Takifugu rubripes* in Response to *Vibrio harveyi* Infection

Dongxu Gao[1†], *Wei Lei*[2†], *Chenshi Wang*[1], *Ping Ni*[1], *Xiaoyu Cui*[1], *Xindi Huang*[1] *and Shigen Ye*[1*]

[1] *Key Laboratory of Mariculture and Stock Enhancement in North China's Sea, Ministry of Agriculture and Rural Affairs, College of Fisheries and Life Science, Dalian Ocean University, Dalian, China,* [2] *State Environmental Protection Key Laboratory of Marine Ecosystem Restoration, National Marine Environmental Monitoring Center, Dalian, China*

Takifugu rubripes is commonly subjected to the disease-causing bacterium, *Vibrio harveyi*. However, the mechanism involved in the immune response of *T. rubripes* to *V. harveyi* infection is unclear. We conducted a transcriptomic analysis of the spleen and gill from *T. rubripes* infected with *V. harveyi*. We obtained 60,981,357 and 60,760,550 clean reads from the control and infected spleens, and 57,407,586 and 57,536,651 clean reads from the control and infected gills, respectively. We also identified 1,560 and 1,213 differentially expressed genes in the spleen and gill, respectively. Gene ontology analysis revealed that the most enriched biological process in both the spleen and gill was "immune response". The most enriched Kyoto Encyclopedia of Genes and Genomes immune response–related pathways were the NOD-like receptor signaling pathway in the spleen and cytokine–cytokine receptor interaction in the gill. We found 10 candidate immune-related genes in the spleen and gill. These putative immune pathways and candidate genes will provide insight into the immune response mechanisms of *T. rubripes* against *V. harveyi*.

Keywords: *Takifugu rubripes*, *Vibrio harveyi*, RNA-sequencing, immune response, aquacultural species

OPEN ACCESS

Edited by:
Lixing Huang,
Jimei University, China

Reviewed by:
Jiaojiao Guo,
Inner Mongolia University, China
Lingbin Sun,
Peking University Shenzhen Hospital, China

****Correspondence:***
Shigen Ye
Shgye@dlou.edu.cn

[†] These authors have contributed equally to this work and share first authorship

Specialty section:
This article was submitted to Veterinary Infectious Diseases, a section of the journal Frontiers in Veterinary Science

Received: *12 November 2021*
Accepted: *20 December 2021*
Published: *31 January 2022*

Citation:
Gao D, Lei W, Wang C, Ni P, Cui X, Huang X and Ye S (2022) RNA-Sequencing Analysis of the Spleen and Gill of Takifugu rubripes in Response to Vibrio harveyi Infection. Front. Vet. Sci. 8:813988. doi: 10.3389/fvets.2021.813988

INTRODUCTION

Takifugu rubripes is becoming one of the most economic aquatic fish species in East Asia (1–3). The total aquacultural yield of *T. rubripes* in China reached 17,473 tons in 2019 (4). In Japan, these aquacultural species is considered one of the most valuable commercial finfish in recent decades (5). However, the aquacultural industry for *T. rubripes* is restricted by several serious aquatic diseases (6, 7). Specifically, high mortality resulting from *Vibrio harveyi* infections leads to enormous economic losses (8, 9). *V. harveyi* is an important luminous marine bacterium (10, 11) that is pathogenic to many aquatic animals (12, 13).

Fish immunology has received much attention for its important and unique role in understanding the evolution of immune system. Investigating the effects of bacterial infections on fish immune organs is important for understanding the immune response mechanisms to bacterial diseases (14, 15). The spleen and gill are important immune organs in fish. The spleen is the primary hematopoietic and peripheral lymphoid organ (16, 17) and is important for antigen (e.g., bacteria) presentation and initiation of adaptive immune responses (18, 19). The gill is a type of mucosal

surface and a mucosal immune organ in fish (14, 20), and is an important site of bacterial exposure and host defense mechanisms (14).

Sequencing technology is widely applied in aquaculture (21–24). RNA-sequencing technology can effectively reveal genes that are engaged in immune responses and expressed in response to the presence of toxicants or infection (25–27). Many studies have focused on the transcriptomic changes in different fish tissues after bacterial infection (15, 28). However, few studies have reported the combined analysis of RNA-sequencing in the spleen and gill of *T. rubripes* after *V. harveyi* infection.

Here, we used RNA-sequencing technology to detect genome-wide transcriptional changes in the spleen and gill of *V. harveyi*–infected *T. rubripes*. These results may help identify the immune-relevant genes and mechanisms during *V. harveyi* infection. Our study provides a novel strategy for understanding the mechanisms of action of *V. harveyi*–induced aquacultural diseases in fish and developing genetic markers for *V. harveyi* disease resistance.

MATERIALS AND METHODS

Experimental Animals and Tissue Collection

The Animal Care and Use Committee of the Key Laboratory of Mariculture and Stock Enhancement in North China's Sea at Dalian Ocean University approved all fish-related procedures in this study. *T. rubripes* (weighing 118 ± 7.5 g) were obtained from a local supplier (Tianzheng Industrial, Dalian, China) and acclimated for approximately 7 days in seawater at 19 ± 1°C.

Fish were challenged in six seawater tanks with three control and three treatment groups. The identified *V. harveyi* were reisolated from a symptomatic *T. rubripes* with skin and visceral lesions. Fifteen fish were put into each tank with 2.5×10^7 colony-forming units per milliliter of *V. harveyi*, exposed to the bacteria for 12 h, then transferred to clean seawater and maintained for 7 days. The same number of fish was used as controls. Fish in the control group stayed in clean seawater throughout the experiment. One-third of the seawater was replaced every 2 days throughout the experiment. On day 7 post-challenge, some fish in the treatment group showed slow movement, decreased vitality, and cell necrosis in their spleens and gills. The control fish displayed no abnormalities in their movement, vitality, or visceral organs [see more details in **Supplementary Figure 1**; (29)]. The spleen and gill were collected from both the symptomatic *V. harveyi*–treated fish and control fish on day 7. Samples were frozen in liquid nitrogen prior to RNA extraction.

Library Preparation for Transcriptome Sequencing

Sequencing analysis was performed to evaluate the effects of *V. harveyi* on global transcription in the spleen and gill. In both the control and treatment groups, the fish from the three tanks were firstly mixed, and then the four fish were randomly selected from the mixed fish. The selected samples were taken for sequencing analysis. RNA-sequencing and library preparation were performed by Novo Genomic Services Lab (Qingdao, Shandong, China). RNA (3 μg per sample) was used as the input material for the RNA sample preparation. Sequencing libraries were generated using the NEBNext Ultra RNA Library Prep Kit for Illumina (NEB, Ipswich, MA, USA) per the manufacturer's recommendations, and index codes were added to attribute sequences to each sample.

The index-coded samples were clustered using a cBot Cluster Generation System with a TruSeq PE Cluster Kit v3-cBot-HS (Illumina; NEB) per the manufacturer's instructions. After cluster generation, the library preparations were sequenced on an Illumina HiSeq platform, and 125/150-bp paired-end reads were generated.

RNA Extraction and Reverse Transcription

Total RNA was extracted from the spleens and gills using TRIzol reagent (Invitrogen, Carlsbad, CA, USA) per the manufacturer's protocol. First-strand cDNA was synthesized from 1 μg of total RNA using a MonScript RTIII All-in-One Mix kit (Monad, Shanghai, China) per the manufacturer's protocol.

Real-Time Quantitative PCR

Real-time quantitative (RT-q) PCR was performed to validate the sequencing analysis results on a StepOnePlus Real-Time PCR system (ABI, USA) using SYBR green I fluorescent dye. Gene expression levels were normalized to *T. rubripes β-actin* (30). Relative gene expression was calculated using the $2^{-\Delta\Delta CT}$ method (31). The primer sequences were designed using software Primers Premier 5.0 (**Supplementary Table 1**). Eight genes were randomly selected for RT-qPCR verification.

Data Analysis

High-quality clean reads were obtained from raw reads. The reference genome and gene model annotation files were directly downloaded from the genome website (ftp.ensembl.org/pub/release-92/fasta/takifugu_rubripes/). Hisat2 v2.0.5 was used to build the index of the reference genome and align the paired-end clean reads to the reference genome (*Takifugu_rubripes_Ensemble_92*) (32). FeatureCounts v1.5.0-p3 was used to count the read numbers mapped to each gene (33). The fragments per kilobase of transcript sequence per millions base pairs sequenced of each gene was then calculated based on the gene length, and read counts were mapped to the gene. Differential expression analysis of two conditions was performed using the DESeq2 R package (1.16.1) (34), which provides statistical routines for determining differential expression in digital gene expression data using a model based on the negative binomial distribution. The resulting *p*-values were adjusted using the Benjamini and Hochberg approach for controlling the false discovery rate. Genes with an adjusted *p*-value < 0.05 in DESeq2 were assigned as differentially expressed genes (DEGs). Gene ontology (GO) enrichment analysis of the DEGs was implemented by the clusterProfiler R package, which corrects for gene length bias. GO terms with corrected $p < 0.05$ were considered significantly enriched by DEGs (35). The Kyoto Encyclopedia of Genes and Genomes (KEGG) database

enables understanding high-level functions and utilities of biological systems, such as cells, organisms, and ecosystems, from molecular-level information, especially large-scale molecular datasets generated *via* genome sequencing and other high-throughput experimental technologies (http://www.genome.jp/kegg/). We used clusterProfiler R to test the statistical enrichment of the DEGs in the KEGG pathways (36). The top GO categories and KEGG pathways were selected according to their *p*-values.

RESULTS

Differential Gene Expression in the Spleen After *V. harveyi* Infection

The RNA-sequencing data were submitted to Gene Expression Omnibus (accession number: GSE155911). The four control spleens (CS1–4) yielded 60,298,712; 59,160,768; 61,669,660 and 62,796,286 clean reads, respectively. The four *V. harveyi*–infected spleens (VhS1–4) yielded 61,129,742; 67,177,292; 55,859,620; and 58,875,544 clean reads, respectively. The mapping rates were 88.94%, 87.47%, 88.88%, and 88.87% for the four control spleens (CS1–4), respectively. The mapping rates were 89.50%, 89.24%, 89.29%, and 89.61% for the four infected spleens (VhS1–4), respectively. Compared with the controls, the spleens of the *V. harveyi*–infected fish contained 1,560 DEGs ($p < 0.05$, fold difference >1). Of these, 726 genes were significantly upregulated, and 834 were significantly downregulated (**Figure 1A**). **Figure 1B** shows the volcano plot of the DEG distribution.

GO analysis results for the spleen tissue showed that these DEGs were clustered into predicted functional groups. The effects of *V. harveyi* were demonstrated in 1,939 groups, including 1,344 biological process (BP) terms (69.31%), 205 cellular component (CC) terms (10.57%), and 390 molecular function (MF) terms (20.12%). In the BP category, "immune response" (GO:0006955), "response to external biotic stimulus" (GO:0043207), and "regulation of immune response" (GO:0050776) were most noteworthy. The most highly represented CC term was "extracellular region" (GO:0005576). The most highly enriched MF terms were "enzyme regulator activity" (GO:0030234) and "enzyme inhibitor activity" (GO:0004857; **Figure 2A**).

Using KEGG functional annotations, the 1,560 DEGs were classified to identify the pathways in which they participate. The DEGs were mapped to 115 KEGG pathways, and the top 20 most common pathways were identified, among which, the most significant and highly enriched pathway was the NOD-like receptor signaling pathway (**Figure 2B**).

Differential Gene Expression in the Gill After *V. harveyi* Infection

The four control gills (CG1–4) yielded 57,172,556; 58,742,866; 57,255,304; and 56,459,618 clean reads, with mapping rates of 88.04%, 88.13%, 88.65%, and 88.09%, respectively. The four *V. harveyi*–infected gills (VhG1–4) yielded 58,236,430; 63,555,364; 54,010,958; and 54,343,850 clean reads, with mapping rates of 88.34%, 88.58%, 88.69%, and 88.41%, respectively. The RNA-sequencing results yielded 1,213 DEGs, including 602 upregulated and 611 downregulated genes ($p < 0.05$, fold difference >1) in the gills after *V. harveyi* treatment relative to the controls (**Figure 3A**). These 1,213 genes were hierarchically clustered to produce a volcano plot (**Figure 3B**).

V. harveyi significantly altered the GO analysis results for the gills, yielding 1,743 GO terms, including 1,235 BP terms (70.85%), 159 CC terms (9.12%), and 349 MF terms (20.03%). In the GO term for BP, much more attention was paid to "immune response" (GO:0006955), "immune system process" (GO:0002376), "regulation of immune system process" (GO:0002682), "regulation of immune response" (GO:0050776), and "positive regulation of immune system process" (GO:0002684). The most enriched CC term was "integrin complex" (GO:0008305); the most enriched MF term was "extracellular matrix structural constituent" (GO:0005201; **Figure 4A**).

In the gills, the DEGs were mapped to 116 KEGG pathways, and the top 20 representative enriched KEGG pathways were identified. Cytokine–cytokine receptor interaction, which is related to immune response, was highly enriched (**Figure 4B**).

Combined RNA-Sequencing Analysis of the Spleen and Gill

To investigate the effects of *V. harveyi* infection in both the spleen and gill, we constructed a Venn diagram to find the common genes from significant DEGs in the spleen and gill (with $p < 0.05$, fold change > 1). We found 288 overlapping genes in these organs (**Figure 5A**), which were then assigned to 619 GO terms: 413 BP terms (66.72%), 66 CC terms (10.66%), and 140 MF terms (22.62%). For the BP terms, "immune system process" (GO:0002376), "immune response" (GO:0006955), and "immune effector process" (GO:0002252) were highly enriched. "Integral component of plasma membrane" (GO:0005887) was the most significantly enriched CC term, and "transferase activity, transferring glycosyl groups" (GO:0016757) was the most significantly enriched MF term (**Figure 5B**). Overlapping DEGs were mapped to 29 KEGG pathways. In the top 20 representative enriched KEGG pathways, much more attention was paid to the C-type lectin receptor signaling pathway and the Cellular senescence which were related to immune response (**Figure 5C**). These findings indicate that *V. harveyi* infection could lead to abnormal gene expression and trigger immune responses in both the spleen and gill.

To better understand the mechanisms of action of *V. harveyi*–induced disease in *T. rubripes*, we analyzed 23 immune-related DEGs from our transcriptomic dataset of the spleen and gill. Ten of these 23 DEGs were found in both the spleen and gill (**Table 1**).

DEG Validation *via* RT-qPCR

Constitutive changes in the DEGs identified *via* RNA-sequencing were consistent with the RT-qPCR results from the spleen and gill samples. The RNA-sequencing data for the spleen showed that *V. harveyi* infection significantly upregulated the expressions of *IL-1b* (by 4.05-fold) and *nppc* (by 10.46-fold) compared with those of the controls. The expression changes of *IL-1b*

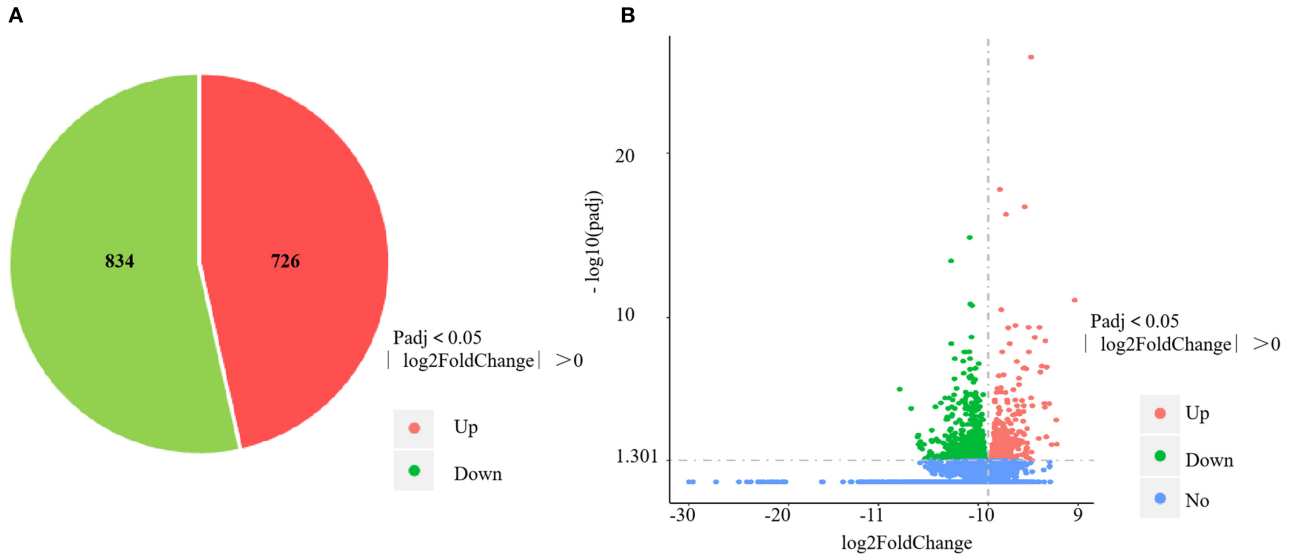

FIGURE 1 | DEGs identified in the spleen infected by *V. harveyi*. The number of DEGs in spleen is shown in **(A)**, and the volcano plot of DEGs in spleen is shown in **(B)**.

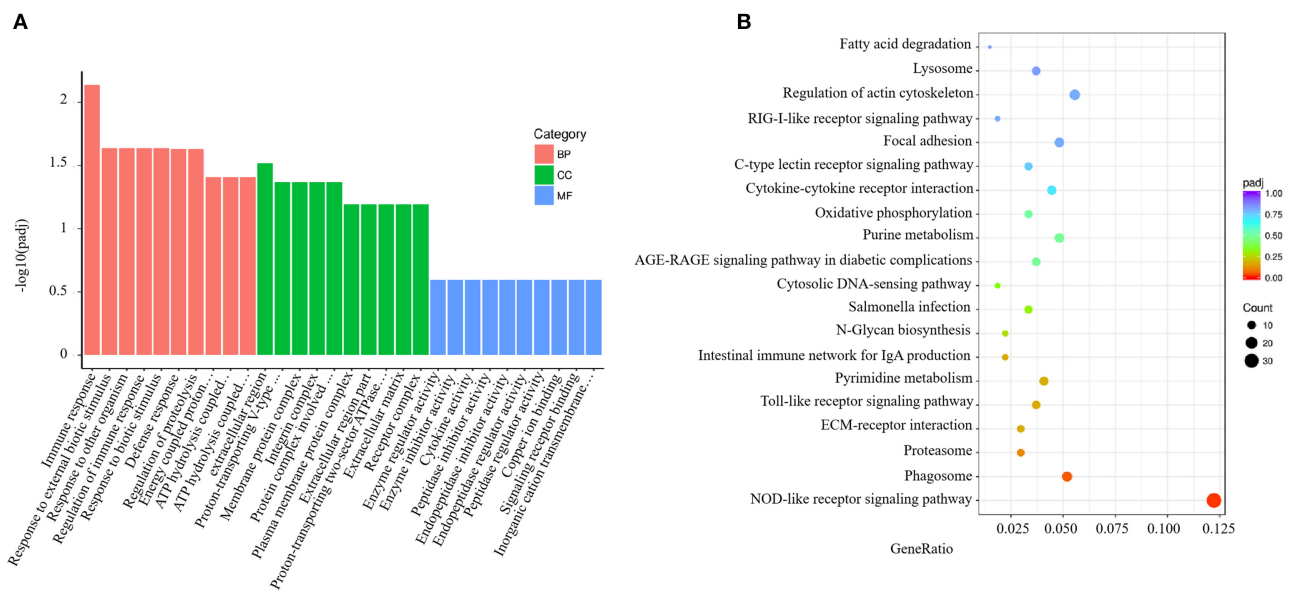

FIGURE 2 | Enrichment GO and KEGG annotation in the spleen infected by *V. harveyi*. Top GO categories in the spleen are shown in **(A)**. KEGG category of DEGs in the spleen infected by *V. harveyi* is shown in **(B)**.

(by 2.68-fold) and *nppc* (by 1.81-fold) were confirmed *via* RT-qPCR (**Figure 6A**). The significantly downregulated genes, *cd74* (by 1.48-fold) and *IL-2* (by 2.43-fold), were also validated *via* RT-qPCR (downregulated by 3.42- and 3.12-fold, respectively; **Figure 6A**). The RNA-sequencing data for the gill showed that *V. harveyi* infection significantly upregulated the expressions of *scpp3b* (by 14.54-fold) and *IL-8* (by 6.39-fold) compared with those of the controls. The expression changes in *scpp3b* (by 3.91-fold) and *IL-8* (by 1.89-fold) were confirmed *via* RT-qPCR (**Figure 6B**). The significantly downregulated genes, *IL-21* (by 1.93-fold) and *b3gat1* (by 5.02-fold), were also validated *via* RT-qPCR (downregulated by 1.68- and 3.60-fold, respectively; **Figure 6B**).

DISCUSSION

T. rubripes is becoming a very important economic aquacultural species. Large-scale breeding of *T. rubripes* can easily result in disease outbreaks, which would thus reduce the food quality and economic benefits. Therefore, researchers should determine the

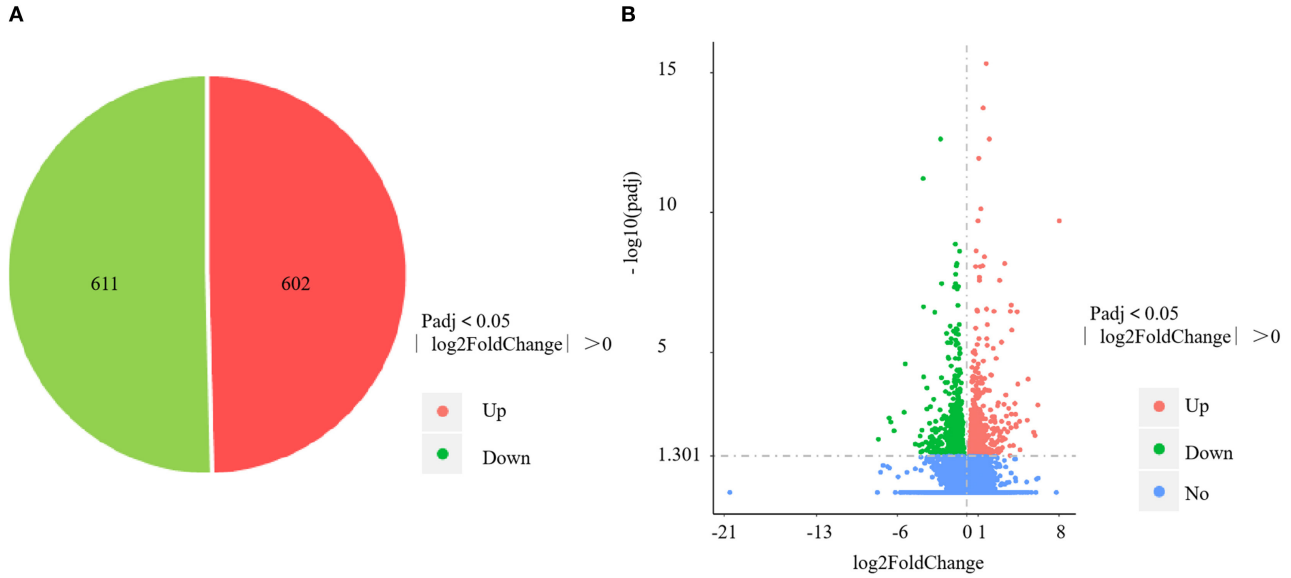

FIGURE 3 | DEGs identified in the gill infected by *V. harveyi*. The number of DEGs in gill is shown in **(A)**, and the volcano plot of DEGs in gill is shown in **(B)**.

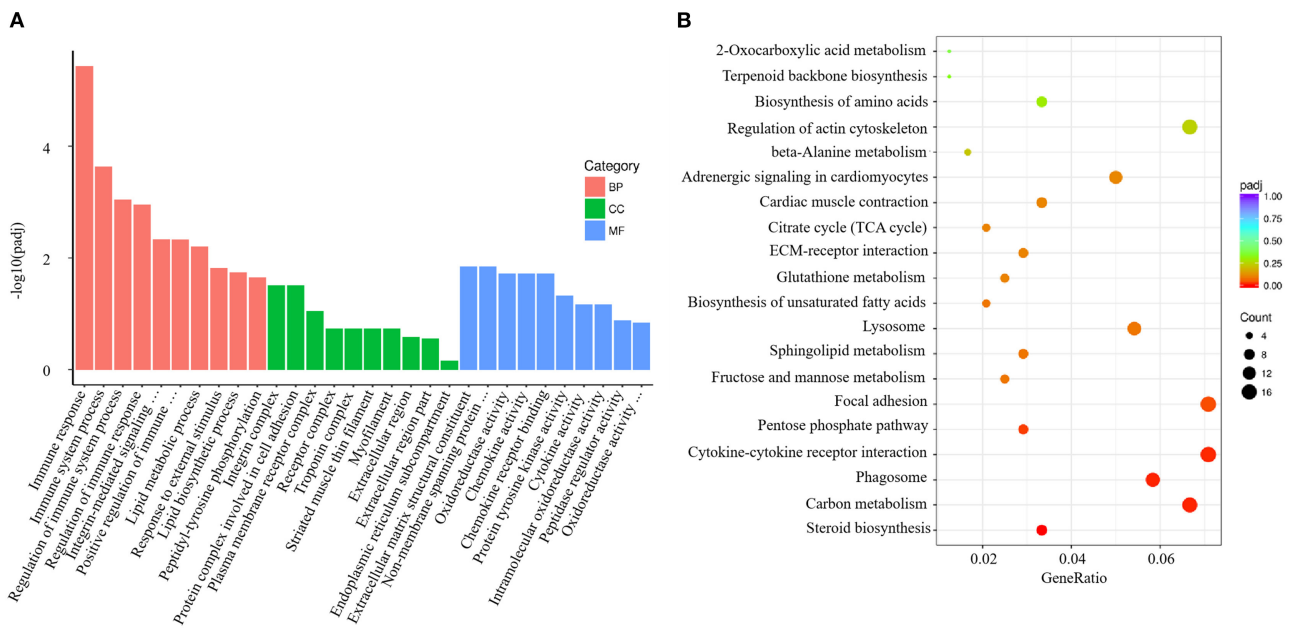

FIGURE 4 | Enrichment GO and KEGG annotation in the gill infected by *V. harveyi*. Top GO categories in the gill are shown in **(A)**. KEGG category of DEGs in the gill infected by *V. harveyi* is shown in **(B)**.

molecular mechanisms of disease resistance in *T. rubripes*. Here, we performed RNA-sequencing analysis of *T. rubripes* spleen and gill responding to *V. harveyi* infection. Peng et al. (30) demonstrated that *V. harveyi* can alter the splenic transcriptome of *T. rubripes*; however, the effect of *V. harveyi* on the *T. rubripes* gill transcriptome remains unknown. Our study is the first to report the changes in the *T. rubripes* gill transcriptome after *V. harveyi* infection. The results of this study enrich our knowledge of the *T. rubripes* transcriptome.

Several studies have identified immune-related genes in *T. rubripes* spleen and gill (6, 37). However, few studies have reported combined analysis of immune-related DEGs in *T. rubripes* spleen and gill after *V. harveyi* infection. Our analysis yielded 1,560 and 1,213 DEGs in the spleen and gill, respectively.

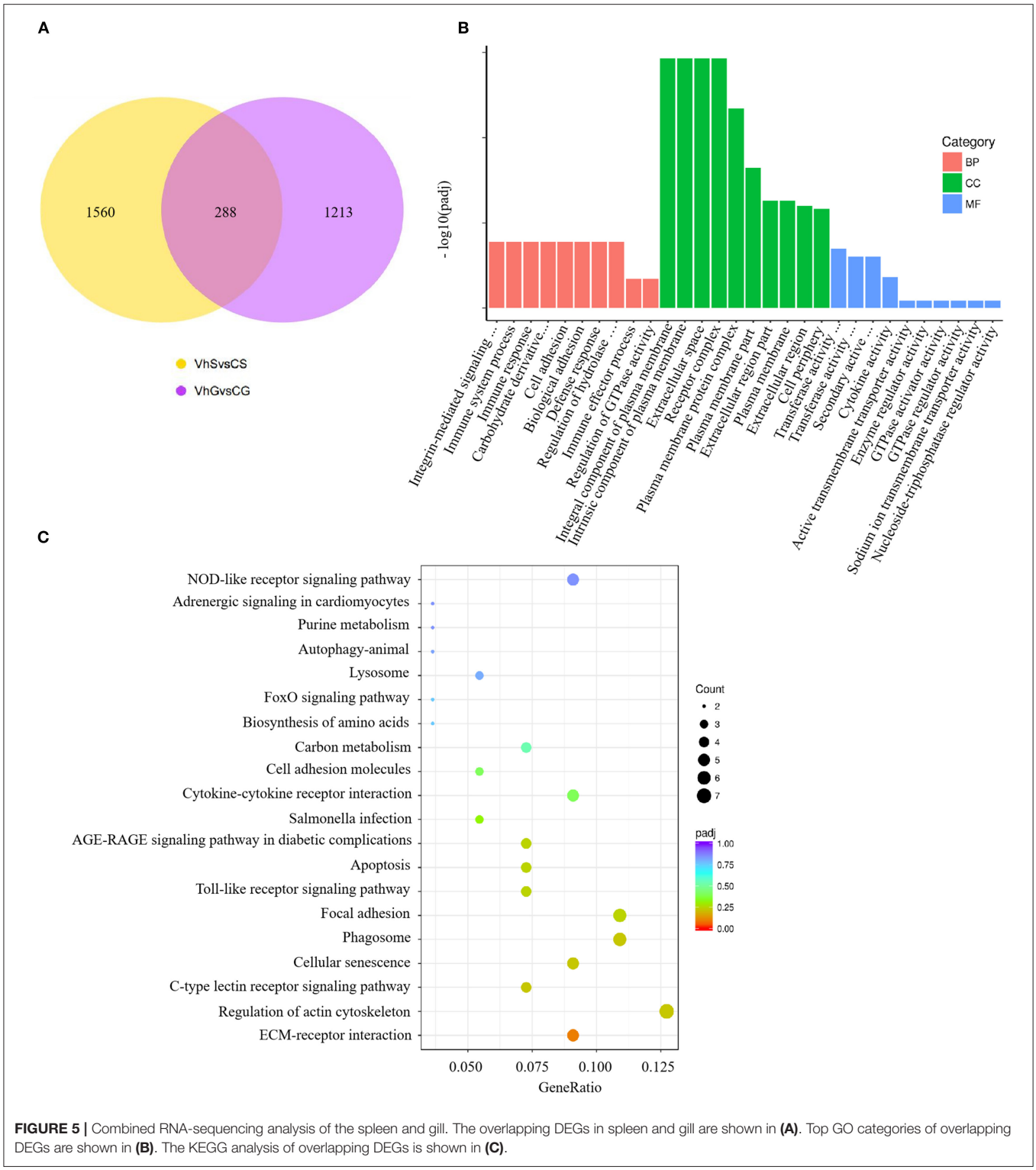

FIGURE 5 | Combined RNA-sequencing analysis of the spleen and gill. The overlapping DEGs in spleen and gill are shown in **(A)**. Top GO categories of overlapping DEGs are shown in **(B)**. The KEGG analysis of overlapping DEGs is shown in **(C)**.

We performed functional enrichment analysis to further study the role of DEGs in immune-related disorders. GO and KEGG pathway analyses showed that many immune-related terms and pathways were highly enriched in the spleen and gill (**Figures 2**, **4**, **5**). To determine the common GO terms, KEGG pathways and target DEGs in the spleen and gill after *V. harveyi* infection, we conducted the first reported combined analysis of the transcriptomic changes in the spleen and gill. In the common GO category, three immune-related BP terms were highly enriched: immune system process, immune response,

TABLE 1 | Partial differentially expressed immune-related genes in *T. rubripes* after *V. harveyi* infection.

	Gene catalog	Organ	Fold change
Interleukin	Interleukin-1b	Spleen	4.05
	interleukin-2	Spleen	−2.43
	interleukin-6	Spleen/gill	2.44/5.16
	Interleukin-8	Spleen/gill	2.37/6.39
	Interleukin-16	Gill	−1.33
	interleukin-21	Gill	−1.93
Complement component	complement component 7a	Spleen/gill	−1.97/−1.96
	complement component 7b	Spleen/gill	34.82/258.31
	complement component 6	Gill	3.38
Toll-like receptor	toll-like receptor 5	Spleen	−3.83
	toll-like receptor 7	Spleen/gill	−1.97/−1.43
	toll-like receptor 2	Gill	−1.66
Interferon regulatory factor	interferon regulatory factor 7	Spleen	−2.09
	interferon regulatory factor 1b	Spleen/gill	−1.59/−1.53
	interferon regulatory factor 8	Gill	−1.37
Other genes related to immune response	NK-lysin tandem duplicate 4	Spleen/gill	−2.79/−1.94
	carnitine palmitoyltransferase 1B (muscle)	Spleen	2.09
	isocitrate dehydrogenase 1	Gill	1.35
	coagulation factor II (thrombin) receptor	Spleen/gill	2.09
	transcription factor 7	Spleen/gill	−1.68
	tryptophan hydroxylase 1	Gill	3.25
	wingless-type MMTV integration site family, member 4a	Gill	−2.10
	SATB homeobox 1b	Spleen/gill	−2.32

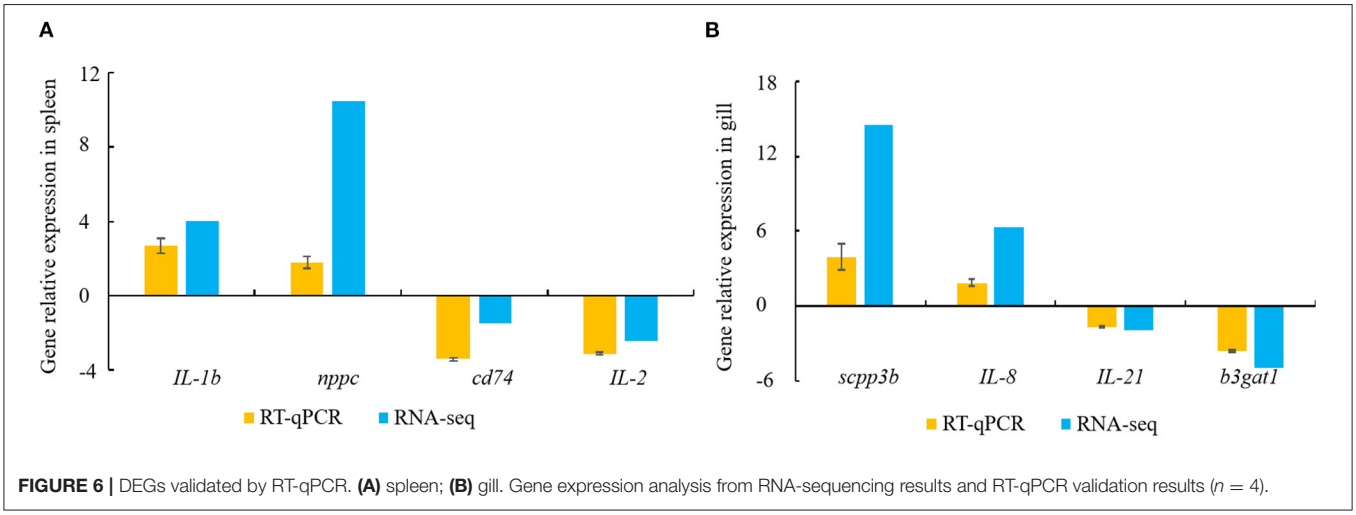

FIGURE 6 | DEGs validated by RT-qPCR. **(A)** spleen; **(B)** gill. Gene expression analysis from RNA-sequencing results and RT-qPCR validation results ($n = 4$).

and immune effector process (**Figure 5B**). Two immune-related pathways were significantly enriched among the common KEGG annotations.

The GO and KEGG analyses revealed several important immune-related genes in the transcriptome, including genes for interleukin (IL), complement components, toll-like receptors (TLRs), interferon regulatory factors (IRFs), and others (**Table 1**). *IL-6*, *IL-8*, *c7a*, *c7b*, *tlr7*, *irf1b*, *NK-lysin tandem duplicate 4*, *coagulation factor II (thrombin) receptor*, *transcription factor 7*, and *SATB homeobox 1b* were differentially expressed in both the spleen and gill. Of these, *IL-6*, *IL-8*, *c7a*, *c7b*, *tlr7*, and *irf1b* caught our attention.

IL is an important cytokine involved in inflammatory and immune responses. *IL-6* is among the most important multifunctional cytokines owing to its essential roles in both innate and adaptive immune responses, and in defending against pathogenic microbial invasion (38, 39). *IL-8* plays a key role in the inflammatory responses toward bacterial infections in

some fish [e.g., *Cynoglossus semilaevis* (40), *Ictalurus punctatus* (41), and *Siniperca chuatsi* (42)]. RNA-sequencing analysis results suggested that the *IL-6* and *IL-8* expression levels were highly upregulated after *V. harveyi* infection in both the spleen and gill, indicating that *IL-6* and *IL-8* are involved in anti-*V. harveyi* defenses. The complement system, activated by bacteria, is part of the innate immune system and can be recruited and activated by the adaptive immune system (26, 43). Complement component 7 (c7) plays a significant role in assembling the cytolytically active membrane attack complex within target cell membranes and performs its main function in host defenses against pathogens and promoting inflammation (44, 45). Although the complement system has been studied extensively in mammals, considerably less is known about complement in teleost fish (45–47). In addition, the functions of *c7a* and *c7b* (*c7* subtypes) in teleosts remain unclear, particularly in *T. rubripes* (48–50). Our data revealed that *c7a* was significantly downregulated, and *c7b* was significantly upregulated in both the spleen and gill. *c7a* and *c7b* were differentially expressed suggesting that the complement system might play an important role in response to *V. harveyi* infection. Why these two complement components were differentially altered remains uncertain. However, our findings may help reveal the molecular function of *c7*. TLRs are a group of pattern-recognition receptors in the innate immune system (51). Here, we identified DEGs mapped to the TLR signaling pathway, including *tlr7* in both the spleen and gill. *tlr7*, a member of the TLR family, plays an essential role in fish antibacterial immunity (52). Here, *tlr7* was significantly downregulated in both the spleen and gill, implying that innate immune genes could be altered at 7 days after *V. harveyi* infection. IRFs mediate host responses against pathogen infection and other important biological processes. Zhan et al. (53) showed that *irf1* plays an important role in defending blunt snout bream against *Aeromonas hydrophila* infection. Here, *irf1b* expression was downregulated after *V. harveyi* challenge in the spleen and gill, indicating that *irf1b* is involved in *V. harveyi*–induced immune regulation.

In this study, we performed the first reported combined RNA-sequencing analysis of the spleen and gill in *T. rubripes* infected with *V. harveyi* and screened many immune-related DEGs, GO terms, and KEGG pathways. Several immune-related genes were altered in both the spleen and gill and might play important roles in the immune response of *T. rubripes* to *V. harveyi* infection. Our results provide an important basis for further studies on the mechanisms of action of *V. harveyi*–induced aquacultural fish disease and enable better understanding this severe disease.

DATA AVAILABILITY STATEMENT

The datasets presented in this study can be found in online repositories. The names of the repository/repositories and accession number(s) can be found at: https://www.ncbi.nlm.nih.gov/geo/, GSE155911.

ETHICS STATEMENT

The animal study was reviewed and approved by all procedures of fish used during this study were approved by the Animal Care and Use Committee of Key Laboratory of Mariculture and Stock Enhancement in North China's Sea at Dalian Ocean University.

AUTHOR CONTRIBUTIONS

DG, WL, and SY conceived the whole project. CW and PN carried out the animal preparation and participated in the bioinformatics analysis. XC and XH participated in the RNA extraction, reverse transcription, and real-time quantitative PCR. DG and WL wrote the article and all authors participated in the discussion. All authors approved the final article.

FUNDING

This work was funded by the National Natural Science Foundation of China (Grant Nos. 42006126 and 41806187), the Doctoral Start-up Foundations of both Liaoning Province (20180540023), Dalian Ocean University (HDYJ201809), and the Major Special Project of Science and Technology of Liaoning Province (2020JH1/10200002).

SUPPLEMENTARY MATERIAL

The Supplementary Material for this article can be found online at: https://www.frontiersin.org/articles/10.3389/fvets.2021.813988/full#supplementary-material

REFERENCES

1. Cui JZ, Shen XY, Gong QL, Yang GP, Gu QQ. Identification of sex markers by cDNA-AFLP in *Takifugu rubripes*. *Aquaculture.* (2006) 257:30–6. doi: 10.1016/j.aquaculture.2006.03.003
2. Hwang SM, Oh KS. Comparisons of food component characteristics of wild and cultured edible pufferfishes in Korea. *Korean J Fish Aquat Sci.* (2013) 46:725–32. doi: 10.5657/KFAS.2013.0725
3. Jiang JL, Xu J, Ye L, Sun ML, Jiang ZQ, Mao MG. Identification of differentially expressed genes in gills of tiger puffer (*Takifugu rubripes*) in response to low-salinity stress. *Comp Biochem Physiol B Biochem Mol Biol.* (2020) 243–244:110437. doi: 10.1016/j.cbpb.2020.110437
4. Ministry of Agriculture and Rural Affairs of China. China Fishery Statistical Yearbook (2020). Available online at: http://www.moa.gov.cn/ (accessed November 5, 2021).
5. International Union for Conservation of Nature. IUCN red list of threatened species. Available online at: https://www.iucnredlist.org/ (accessed November 2, 2021).
6. Cui J, Liu SK, Zhang B, Wang HD, Sun HJ, Song SH, et al. Transcriptome analysis of the gill and swimbladder of *Takifugu rubripes* by RNA-Seq. *PLoS ONE.* (2014) 9:e85505. doi: 10.1371/journal.pone.0085505
7. Liu XH, Jiao CL, Ma Y, Wang QY, Zhang YX. A live attenuated *Vibrio anguillarum* vaccine induces efficient immunoprotection in Tiger puffer (*Takifugu rubripes*). *Vaccine.* (2018) 36:1460–6. doi: 10.1016/j.vaccine.2018.01.067

8. Wang B, Yu LP, Hu L, Li Y, Liu SF, Jiang ZQ. Isolation and identification of bacteriosis pathogen from cultured *Fugu obscurus* with canker of skin. *J Fish Sci China.* (2008) 15:352–8. doi: 10.3724/SP.J.1005.2008.01008
9. Mohi MM, Kuratani M, Miyazaki T, Yoshida T. Histopathological studies on *Vibrio harveyi*-infected tiger puffer, *Takifugu rubripes* (Temminck et Schlegel), cultured in Japan. *J Fish Dis.* (2010) 33:833–40. doi: 10.1111/j.1365-2761.2010.01184.x
10. LaVilla-Pitogo CR, Albright LJ, Paner MG, Sunaz NA. Previous studies on the sources of luminescent *Vibrio harveyi* in Penaeus monodon hatcheries. In: *Diseases in Asian Aquaculture* (1992). Available online at: http://hdl.handle.net/10862/354 (accessed January 15, 2022).
11. Owens L, Muir P, Sutton D, Wingfield M. The pathology of microbial diseases in tropical Australian crustacean. In: *Diseases in Asian Aquaculture*. Fish Health Section, Asian Fisheries Society, Manila, Philippines (1992). p. 165–72.
12. Alvarez JD, Austin B. Alvarez, AM, Reyes H. *Vibrio harveyi:* a pathogen of penaeid shrimps and fish in Venezuela. *J Fish Dis.* (1998) 21:313–16. doi: 10.1046/j.1365-2761.1998.00101.x
13. Soto-Rodriguez SA, Gomez-Gil B, Lozano R, Rio-Rodríguez R, Diéguez AL, Romalde JL. Virulence of *Vibrio harveyi* responsible for the "Bright-red" Syndrome in the Pacific white shrimp *Litopenaeus vannamei*. *J Invertebr Pathol.* (2012) 109:307–17. doi: 10.1016/j.jip.2012.01.006
14. Li C, Zhang Y, Wang RJ, Lu JG, Nandi S, Mohanty S, et al. RNA-Seq analysis of mucosal immune responses reveals signatures of intestinal barrier disruption and pathogen entry following *Edwardsiella ictaluri* infection in channel catfish, *Ictalurus punctatus*. *Fish Shellfish Immunol.* (2012) 32:816–27. doi: 10.1016/j.fsi.2012.02.004
15. Zhao C, Fu MJ, Wang CY, Jiao ZY, Qiu LH. RNA-seq analysis of immune-relevant genes in *Lateolabrax japonicus* during *vibrio anguillarum* infection. *Fish Shellfish Immunol.* (2016) 52:57–64. doi: 10.1016/j.fsi.2016.02.032
16. Zapata A, Diez B, Cejalvo T. Gutiérrez-de Frías C, Cortés A. Ontogeny of the immune system of fish. *Fish Shellfish Immunol.* (2006) 20:126–36. doi: 10.1016/j.fsi.2004.09.005
17. Mahabady M, Morovvati H, Arefi A, Karamifar M. Anatomical and histomorphological study of spleen and pancreas in berzem (*barbus pectoralis*). *World J Fish Mar Sci.* (2012) 4:263–7. doi: 10.5829/idosi.wjfms.2012.04.03.61283
18. Zapata A, Chibá A, Vara A. Cells and tissues of the immune system of fish. In: Iwama G, Nakanishi T, editors. *The Fish Immune System: Organism, Pathogen, and Environment*. San Diego, CA: Academic Press (1997).
19. Alvarez-Pellitero P. Fish immunity and parasite infections: from innate immunity to immunoprophylactic prospects. *Vet Immunol Immunopathol.* (2008) 126:171–98. doi: 10.1016/j.vetimm.2008.07.013
20. Lazado CC, Caipang CMA. Mucosal immunity and probiotics in fish. *Fish Shellfish Immunol.* (2014) 39:78–89. doi: 10.1016/j.fsi.2014.04.015
21. Dehler CE, Secombes CJ. Martin SA. Environmental and physiological factors shape the gut microbiota of Atlantic salmon parr *(Salmo salar L). Aquaculture.* (2017) 467:149–57. doi: 10.1016/j.aquaculture.2016.07.017
22. Nie HT, Wang HM, Jiang KY, Yan XW. Transcriptome analysis reveals differential immune related genes expression in *Ruditapes philippinarum* under hypoxia stress: potential HIF and NF-κB crosstalk in immune responses in clam. *BMC Genomics.* (2020) 21:318. doi: 10.1186/s12864-020-6734-6
23. Miao L, Zhang Y, Lin Y, Liu B, Ge X. Appropriate leucine supplementation promotes glucose metabolism and enhances energy homeostasis in juvenile crucian carp (*Carassius auratus gibelio var*. CAS III). *Comp Biochem Physiol Part D Genomics Proteomics.* (2021) 40:100907. doi: 10.1016/j.cbd.2021.100907
24. Seibel H, Baßmann B, Rebl A. Blood will tell: what hematological analyses can reveal about fish welfare. *Front Vet Sci.* (2021) 8:616955. doi: 10.3389/fvets.2021.616955
25. Pereiro P, Balseiro P, Romero A, Dios S, Forn-Cuni G, Fuste B, et al. High-throughput sequence analysis of turbot (*Scophthalmus maximus*) transcriptome using 454-pyrosequencing for the discovery of antiviral immune genes. *PLoS ONE.* (2012) 7:e35369. doi: 10.1371/journal.pone.0035369
26. Zhang X, Wang S, Chen S, Chen Y, Liu Y, Shao C, et al. Transcriptome analysis revealed changes of multiple genes involved in immunity in *Cynoglossus semilaevis* during *Vibrio anguillarum* infection. *Fish Shellfish Immunol.* (2015) 43:209–18. doi: 10.1016/j.fsi.2014.11.018
27. Chen S, Chen K, Xu J, Li F, Ding J, Ma Z, et al. Insights into mRNA and long non-coding RNA profiling RNA sequencing in uterus of chickens with pink and blue eggshell colors. *Front Vet Sci.* (2021) 8:736387. doi: 10.3389/fvets.2021.736387
28. Zhou X, Zhang GR, Ji W, Shi ZC, Ma XF, Luo ZL, et al. The dynamic immune response of yellow catfish (*Pelteobagrus fulvidraco*) infected with *Edwardsiella ictaluri* presenting the inflammation process. *Front Immunol.* (2021) 12:625928. doi: 10.3389/fimmu.2021.625928
29. Wang CS, Huang XD, Cui XY, Ni P, Ye SH, Wang H, et al. Effects of *Vibrio harveyi* infection on DNA methylation of the IL-6 gene in *Takifugu rubripes*. *J Dalian Med Univ*. [Preprint].(2021). doi: 10.16535/j.cnki.dlhyxb.2021-115
30. Peng HY, Yang BX, Li BY, Cai ZL, Cui QJ, Chen MK, et al. Comparative transcriptomic analysis reveals the gene expression profiles in the liver and spleen of Japanese pufferfish (*Takifugu rubripes*) in response to *Vibrio harveyi* infection. *Fish Shellfish Immunol.* (2019) 90:308–16. doi: 10.1016/j.fsi.2019.04.304
31. Livak KJ, Schmittgen TD. Analysis of relative gene expression data using real-time quantitative PCR and the $2^{-\Delta\Delta Ct}$ method. *Methods.* (2001) 25:402–48. doi: 10.1006/meth.2001.1262
32. Kim D, Langmead B, Salzberg SL, HISAT. a fast spliced aligner with low memory requirements. *Nat Methods.* (2015) 12:357–60. doi: 10.1038/nmeth.3317
33. Liao Y, Smyth GK, Shi W. featureCounts: an efficient general purpose program for assigning sequence reads to genomic features. *Bioinformatics.* (2014) 30:923–30. doi: 10.1093/bioinformatics/btt656
34. Love MI, Huber W, Anders S. Moderated estimation of fold change and dispersion for RNA-Seq data with DESeq2. *Genome Biol.* (2014) 15:550. doi: 10.1186/s13059-014-0550-8
35. Tarazona S, García-Alcalde F, Dopazo J, Ferrer A, Conesa A. Differential expression in RNA-Seq: a matter of depth. *Genome Res.* (2011) 21:2213–23. doi: 10.1101/gr.124321.111
36. Kanehisa M, Goto S, KEGG. Kyoto encyclopedia of genes and genomes. *Nucleic Acids Res.* (2000) 28:27–30. doi: 10.1093/nar/28.1.27
37. Fu SL, Ding MM, Liang QJ, Yang YJ, Chen M, Wei XF, et al. The key differentially expressed genes and proteins related to immune response in the spleen of pufferfish (*Takifugu obscurus*) infected by *Aeromonas hydrophila*. *Fish Shellfish Immunol.* (2019) 91:1–11. doi: 10.1016/j.fsi.2019.05.016
38. Choy EHS, Isenberg DA, Garrood T, Farrow S, Ioannou Y, Bird H, et al. Therapeutic benefit of blocking interleukin-6 activity with an anti–interleukin-6 receptor monoclonal antibody in rheumatoid arthritis: a randomized, double-blind, placebo-controlled, dose-escalation trial. *Arthritis Rheumatol.* (2002) 46:3143–50. doi: 10.1002/art.10623
39. Tsukamoto H, Fujieda K, Senju S, Ikeda T, Oshiumi H, Nishimura Y. Immune-suppressive effects of interleukin-6 on T-cell-mediated anti-tumor immunity. *Cancer Sci.* (2018) 109:523–30. doi: 10.1111/cas.13433
40. Sun JS, Zhao L, Sun L. Interleukin-8 of *Cynoglossus semilaevis* is a chemoattractant with immunoregulatory property. *Fish Shellfish Immunol.* (2011) 30:1362–7. doi: 10.1016/j.fsi.2011.03.023
41. Wang EL, Wang J, Long B, Wang KY, He Y, Yang Q, et al. Molecular cloning, expression and the adjuvant effects of interleukin-8 of channel catfish (*Ictalurus Punctatus*) against *Streptococcus iniae*. *Sci Rep*. (2016) 6:29310. doi: 10.1038/srep29310
42. Wang GL, Wang MC, Zhang XC, Chang MX, Xie HX, Nie P. Molecular cloning, biological effect, and tissue distribution of interleukin-8 protein in mandarin fish (*Siniperca chuasti*) upon *Flavobacterium columnare* infection. *Fish Shellfish Immunol.* (2017) 66:112–19. doi: 10.1016/j.fsi.2017.05.016
43. Janeway CA, TraversP, Walport M, Shlomchik MJ. The complement system and innate immunity, Texas, TX: Garland Science (2001).
44. Bossi F, Rizzi L, Bulla R, Debeus A, Tripodo C, Picotti P, et al. C7 is expressed on endothelial cells as a trap for the assembling terminal complement complex and may exert anti-inflammatory function. *Blood.* (2009) 113:3640–8. doi: 10.1182/blood-2008-03-146472
45. Shen Y, Zhang J, Xu X, Fu J, Li J. Expression of complement component C7 and involvement in innate immune responses to bacteria in grass carp. *Fish Shellfish Immunol.* (2012) 33:448–54. doi: 10.1016/j.fsi.2012.05.016
46. Liyanage DS, Omeka WKM, Godahewa GI, Lee S, Nam BH, Lee J. Membrane attack complex-associated molecules from redlip mullet (*Liza*

haematocheila): Molecular characterization and transcriptional evidence of C6, C7, C8β, and C9 in innate immunity. *Fish Shellfish Immunol.* (2018) 81:1–9. doi: 10.1016/j.fsi.2018.07.006
47. Wickramaarachchi WD, Whang I, Kim E, Lim BS, Jeong HB, De Zoysa M, et al. Genomic characterization and transcriptional evidence for the involvement of complement component 7 in immune response of rock bream (*Oplegnathus fasciatus*). *Dev Comp Immunol.* (2013) 41:44–9. doi: 10.1016/j.dci.2013.04.007
48. Løvoll M, Dalmo RA, Bøgwald J. Extrahepatic synthesis of complement components in the rainbow trout (*Oncorhynchus mykiss*). *Fish Shellfish Immunol.* (2007) 23:721–31. doi: 10.1016/j.fsi.2007.01.019
49. Matsumoto T, Ishizaki S, Nagashima Y. Differential gene expression profile in the liver of the marine puffer fish *Takifugu rubripes* induced by intramuscular administration of tetrodotoxin. *Toxicon.* (2011) 57:304–10. doi: 10.1016/j.toxicon.2010.12.007
50. Wang S, Gao Y, Shu C, Xu T. Characterization and evolutionary analysis of duplicated C7 in miiuy croaker. *Fish Shellfish Immunol.* (2015) 45:672–9. doi: 10.1016/j.fsi.2015.05.042
51. Aderem A, Ulevitch RJ. Toll-like receptors in the induction of the innate immune response. *Nature.* (2000) 406:782. doi: 10.1038/35021228
52. Li XP, Sun L. TLR7 is required for optimal immune defense against bacterial infection in tongue sole (*Cynoglossus semilaevis*). *Fish Shellfish Immunol.* (2015) 47:93–9. doi: 10.1016/j.fsi.2015.08.025
53. Zhan FB, Liu H, Lai RF, Jakovlić I, Wang WB, Wang WM. Molecular identification and functional characterisation of the interferon regulatory factor 1 in the blunt snout bream (*Megalobrama amblycephala*). *Fish Shellfish Immunol.* (2016) 54:456–65. doi: 10.1016/j.fsi.2016.05.002

Conflict of Interest: The authors declare that the research was conducted in the absence of any commercial or financial relationships that could be construed as a potential conflict of interest.

Publisher's Note: All claims expressed in this article are solely those of the authors and do not necessarily represent those of their affiliated organizations, or those of the publisher, the editors and the reviewers. Any product that may be evaluated in this article, or claim that may be made by its manufacturer, is not guaranteed or endorsed by the publisher.

frontiers in Veterinary Science

ORIGINAL RESEARCH
published: 08 February 2022
doi: 10.3389/fvets.2022.799414

Quorum Sensing Controls the CRISPR and Type VI Secretion Systems in *Aliivibrio wodanis* 06/09/139

Amudha Deepalakshmi Maharajan[1]*, *Erik Hjerde*[1,2], *Hilde Hansen*[1] and *Nils Peder Willassen*[1,2]*

[1] Norwegian Structural Biology Center and Department of Chemistry, Faculty of Science and Technology, UiT The Arctic University of Norway, Tromsø, Norway, [2] Centre for Bioinformatics, Department of Chemistry, Faculty of Science and Technology, UiT The Arctic University of Norway, Tromsø, Norway

For bacteria to thrive in an environment with competitors, phages and environmental cues, they use different strategies, including Type VI Secretion Systems (T6SSs) and Clustered Regularly Interspaced Short Palindromic Repeats (CRISPR) to compete for space. Bacteria often use quorum sensing (QS), to coordinate their behavior as the cell density increases. Like other aliivibrios, *Aliivibrio wodanis* 06/09/139 harbors two QS systems, the main LuxS/LuxPQ system and an N-acyl homoserine lactone (AHL)-mediated AinS/AinR system and a master QS regulator, LitR. To explore the QS and survival strategies, we performed genome analysis and gene expression profiling on *A. wodanis* and two QS mutants (Δ*ainS* and Δ*litR*) at two cell densities (OD600 2.0 and 6.0) and temperatures (6 and 12°C). Genome analysis of *A. wodanis* revealed two CRISPR systems, one without a *cas* loci (CRISPR system 1) and a type I-F CRISPR system (CRISPR system 2). Our analysis also identified three main T6SS clusters (T6SS1, T6SS2, and T6SS3) and four auxiliary clusters, as well about 80 potential Type VI secretion effectors (T6SEs). When comparing the wildtype transcriptome data at different cell densities and temperatures, 13–18% of the genes were differentially expressed. The CRISPR system 2 was cell density and temperature-independent, whereas the CRISPR system 1 was temperature-dependent and cell density-independent. The primary and auxiliary clusters of T6SSs were both cell density and temperature-dependent. In the Δ*litR* and Δ*ainS* mutants, several CRISPR and T6SS related genes were differentially expressed. Deletion of *litR* resulted in decreased expression of CRISPR system 1 and increased expression of CRISPR system 2. The T6SS1 and T6SS2 gene clusters were less expressed while the T6SS3 cluster was highly expressed in Δ*litR*. Moreover, in Δ*litR*, the *hcp1* gene was strongly activated at 6°C compared to 12°C. AinS positively affected the *csy* genes in the CRISPR system 2 but did not affect the CRISPR arrays. Although AinS did not significantly affect the expression of T6SSs, the hallmark genes of T6SS (*hcp* and *vgrG*) were AinS-dependent. The work demonstrates that T6SSs and CRISPR systems in *A. wodanis* are QS dependent and may play an essential role in survival in its natural environment.

Keywords: CRISPR, T6SS, QS, *Aliivibrio wodanis* 06/09/139, LitR and AinS

OPEN ACCESS

Edited by:
Najiah Musa,
University of Malaysia Terengganu, Malaysia

Reviewed by:
Natrah Fatin Mohd Ikhsan,
Putra Malaysia University, Malaysia
Qingpi Yan,
Jimei University, China

***Correspondence:**
Amudha Deepalakshmi Maharajan
amudha.d.maharajan@uit.no
Nils Peder Willassen
nils-peder.willassen@uit.no

Specialty section:
This article was submitted to Veterinary Infectious Diseases, a section of the journal Frontiers in Veterinary Science

Received: *21 October 2021*
Accepted: *12 January 2022*
Published: *08 February 2022*

Citation:
Maharajan AD, Hjerde E, Hansen H and Willassen NP (2022) Quorum Sensing Controls the CRISPR and Type VI Secretion Systems in Aliivibrio wodanis 06/09/139. Front. Vet. Sci. 9:799414. doi: 10.3389/fvets.2022.799414

INTRODUCTION

Quorum sensing (QS) is a cell density-dependent cell-to-cell communication system in which bacteria produce and respond to signaling molecules called autoinducers (AIs), which subsequently activates the QS transcriptional regulator to control specific functions such as bioluminescence, motility, biofilm, secretion and virulence (1–5). Multiple QS systems have been described in several *Vibrio* species (6). Two QS systems, AinS/AinR and LuxS/LuxPQ that are believed to work through phosphorelay mechanism have been identified in the genome of *Aliivibrio wodanis* (7). The AinS/AinR QS system produces AI-1 known as N-acyl homoserine lactones (AHLs) and is present in many Gram-negative bacteria (2, 8). These AHL-mediated QS systems are used for intra-species communication (8, 9). The LuxS/LuxPQ QS system is present in a wide variety of Gram-negative and Gram-positive bacteria, and produces the AI-2 called furanosyl borate diester and is involved in inter-species communication (10, 11). These two QS systems are known to work in parallel in *Vibrio harveyi, Aliivibrio fischeri* and *Vibrio cholerae* (12–14). At low cell density, when the AI concentrations are low, the AI receptors act as kinases and relay phosphate to the RpoN (σ54)-dependent activator LuxO via phosphotransferase LuxU. This, in turn, activates the expression of *qrr* sRNAs, which together with RNA chaperone Hfq represses translation of the mRNA encoding the master regulator *LitR* (9, 14, 15). At high cell density, the signaling molecules reach a threshold concentration and bind to the receptors to dephosphorylate LuxO, which terminates the *qrr* sRNA transcription. In the absence of Qrr sRNA, *litR* is activated to regulate hundreds of genes (1, 14, 16).

In the environment, bacteria co-exist in communities with multiple competitors, including other bacterial species and phages, and have to respond to various cues such as changes in temperature, nutrient and iron availability, pH, osmolarity and salinity (17–22). Hence, bacteria have developed various strategies such as protein secretion, contact-dependent growth inhibition, bacteriocin production and antibiotic production to survive and thrive (23–27). Some strategies are not necessarily harmful to competitors, such as adhesion, exopolysaccharide production, siderophore production, motility, biofilm formation, heat shock response and quorum quenching (28–34). Other strategies developed, such as defense mechanisms against phages or mobile genetic elements (MGEs), including restriction-modification, receptor modification and clustered regularly interspaced short palindromic repeats-CRISPR associated (CRISPR-Cas) are for protection (35–37).

The CRISPR-Cas system is an adaptive immune system against invading nucleic acids from phages and other MGEs and is composed of *cas* genes, a leader sequence and a CRISPR array with repeats separated by several spacer sequences (35, 38). Two CRISPR classes have been identified with six main types and several subtypes, which are categorized based on the types of *cas* genes, direct repeats and gene arrangement where class 1 includes the type I, III and IV whereas type II, V and VI belong to class 2 (39–41). Several *Vibrio* species harbor the type I CRISPR system classified into subtypes such as type I-A, I-B, I-C, I-D, I-E and I-F (40, 42, 43). QS regulation of CRISPR system has been described in bacteria like *Pseudomonas aeruginosa*, *Serratia* sp. and *Chromobacterium violaceum* (44–47).

QS regulates type VI secretion systems (T6SSs) in several vibrios such as *V. cholerae*, *Vibrio parahaemolyticus*, *Vibrio anguillarum*, *Vibrio fluvialis* and *Vibrio alginolyticus* (48–52). T6SS is one of the largest contact-dependent secretion system bacteria use to transport T6SS effectors (T6SEs) into eukaryotic hosts, bacterial competitors or the environment (53–56). In some bacteria, T6SSs are also known to be involved in the uptake of metal ion (57, 58). The T6SS was first identified in *V. cholerae* as a virulence-associated secretion (*vas*) gene cluster and later in many other bacteria (59–61). The T6SEs are toxin molecules with anti-bacterial or anti-eukaryotic activity (62–64). Several anti-bacterial effector molecules such as amidases, glycoside hydrolases, lipases, phospholipases and nucleases and anti-eukaryotic effectors such as VasX, the Multifunctional-autoprocessing repeats-in-toxin and EvpP have been identified (65–69). T6SS gene clusters often encode immunity proteins close to the effector genes in order to neutralize their effector molecules to prevent self or sibling-killing (70). For instance, immunity proteins such as antitoxin TsaB in *V. cholerae* have been reported to protect self-killing against effectors VgrG-3 and Tse2, respectively (71). In addition, immunity protein-independent mechanisms like envelope stress response and two-component systems can facilitate self-protection (72).

A. wodanis is a Gram-negative, rod-shaped, non-luminescent and motile bacterium with multiple polar flagella (73). *A. wodanis* strains grow in the range of temperatures and salt concentrations between 4–25°C and 1–4% respectively (73). The genome of *A. wodanis* 06/09/139 contains two chromosomes and 4 plasmids (7). *A. wodanis* has been repeatedly isolated together with *Moritella viscosa (M. viscosa)* from Atlantic salmon (*Salmo salar*) during outbreaks of winter ulcer that mainly occurs at a temperature below 8°C (74, 75). Infected fish can survive when the temperature rises above 8°C (74, 76). Winter ulcer causes mortality and significant losses in farming industry and is characterized by large ulcers, hemorrhages and internal tissue necrosis in the infected fish (74, 77). Although *M. viscosa* is the primary agent for the disease, the role of *A. wodanis* and the mechanism behind the co-existence with *A. wodanis* in the winter ulcers are still unclear (74, 77). Experimental study reproducing field observation reveal that *A. wodanis* affects the progression of *M. viscosa* infection and is responsible for the chronic pathogenesis in fish (78). *A. wodanis* adheres to Atlantic salmon head kidney cells and in a bath challenge, *A. wodanis* separately produces clinical symptoms such as fin rot and other internal pathological symptoms in Atlantic salmon and it can co-infect Atlantic salmon together with *M. viscosa* (78). In a co-cultivation experiment, *A. wodanis* impedes the growth of *M.*

Abbreviations: AHL, N-acyl homoserine lactone; Aux, Auxiliary; Bp, Base pair; CHSE, Chinook salmon embryo; CRISPR, Clustered Regularly Interspaced Short Palindromic Repeats; DEGs, Differentially expressed genes; FC, Fold change; HCD, High cell density; LCD, Low cell density; MGE, Mobile genetic element; Min, minutes; OD_{600}, Optical density measured at 600 nm; QS, Quorum sensing; RHS, Rearrangement hotspot protein; RPKM, reads per kilobase of gene per million reads mapped; T6SE, Type VI Secretion Effector; T6SS, Type VI Secretion System; tp, Transcriptome profile.

viscosa and when both the bacteria were implanted together in fish abdomen, *A. wodanis* alters the gene expression of *M. viscosa* (7). It has been further hypothesized that *A. wodanis* perhaps uses bacteriocin to impede the growth and virulence of *M. viscosa* (7). In our previous studies we have reported that *A. wodanis* produces one AHL and encodes two QS systems (7, 79). In the cell culture studies, *A. wodanis* is known to be cytotoxic to different salmon cell lines when treated with supernatants harvested at cell densities higher than OD_{600} (optical density measured at 600 nm) of 6.0 (78, 80). Moreover, in a HPLC-MS/MS analysis, the AHL production in *A. wodanis* begins at the early log phase and increases with increase in cell density along the growth curve (80). Hence in this transcriptomics study, we chose two cell densities one at the early log phase (OD_{600} 2.0) and the other at the cell density close to the end log phase (OD_{600} 6.0) to study the role of cell densities in gene expression. Furthermore, in our recent study, we found that the temperature 6°C which is lower than the winter ulcer disease threshold temperature 8°C, has more impact on AHL production and cytotoxicity in CHSE cell line than 12°C (80). Therefore, in this study, we wanted to analyze the effects of 6°C and 12°C in gene expression. We have also shown that *A. wodanis* uses the QS to regulate growth, motility, siderophore- and protease production, hemolysis as well as cytotoxicity in the Chinook salmon embryo (CHSE) cell line (80). Considering the importance of understanding the QS and survival strategies in *A. wodanis*, we performed genome analysis and RNA sequencing (RNA-Seq) to reveal the global gene expression in the wild type and its QS mutant strains Δ*ainS* and Δ*litR*.

MATERIALS AND METHODS

Bacterial Strains and Growth Conditions

The *A. wodanis* 06/09/139 used was originally isolated from the head kidney of an Atlantic salmon on the west coast of Norway in 2006 (78). The construction of the Δ*ainS* and Δ*litR* in-frame mutants by allelic exchange has been described in a recent study (80). *A. wodanis* 06/09/139 and the mutants from glycerol stocks were grown at 12°C for 3 days on Luria-Bertani Agar (Difco BD Diagnostics Sparks, MD, USA) with a total concentration of 1.0% (wt/vol) peptone (Sigma-Aldrich, St. Louis, MO, USA), 0.5% (wt/vol) yeast extract (Merck, Darmstadt, Germany), 2.5% NaCl (wt/vol) (Sigma-Aldrich, St. Louis, MO, USA) and 1.5% agar (Sigma-Aldrich, St. Louis, MO, USA). The pH of the media was adjusted to 7.5. Three biological replicates of pre-cultures of *A. wodanis* 06/09/139 and the mutants Δ*ainS* and Δ*litR* were grown from a single colony in 2 ml of Luria-Bertani Broth (LB2.5) overnight at 12°C, 220 rpm.

RNA Extraction and rRNA Depletion

Pre-culture biological triplicates of *A. wodanis* 06/09/139, Δ*ainS* and Δ*litR* were diluted to a start OD_{600} of 0.01 in LB2.5 in a final volume of 60 ml using a 250 ml baffled flasks. The cultures were grown further in parallel using two Infors HT Multitron incubators set at 6 and 12°C at 220 rpm. The cultures were diluted 1:10 for OD_{600} measurement and harvested at low cell density (LCD) OD_{600} of 2.0 and high cell density (HCD) OD_{600} of 6.0. A small culture volume (1 ml) was harvested and mixed with two volumes of RNAprotect Bacteria reagent (Qiagen, Hilden, Germany). The treated cultures were then incubated for 5 min at room temperature and vortexed for a few seconds before centrifuging at 13,000 rpm for 2 min in a cold Heraeus fresco 21 centrifuge (Thermo Scientific, Waltham, MA, USA). The pellets were flash-frozen with liquid nitrogen and stored at −80°C until RNA isolation. The total RNA from the cell pellets was isolated using the Masterpure^{TM} complete DNA/RNA purification kit (Epicenter, Madison, WI, USA) according to the manufacturer's instructions. The RNA concentration was measured in NanoDrop^{TM} 2000c spectrophotometer (Thermo Scientific, Waltham, MA, USA). Ribosomal RNA (rRNA) was depleted from the total RNA using a Ribo-zero rRNA removal kit for bacteria (Illumina, San Diego, CA, USA). The RNA quality before and after rRNA depletion was determined using Agilent 2100 Bioanalyzer (Agilent Technologies, Santa Clara, CA, USA).

RNA Sequencing and Data Analysis

The mRNA libraries were prepared using the TrueSeq stranded mRNA library kit (Illumina, San Diego, CA, USA) and sequenced on Nextseq 500 (Illumina, USA) using 150 cycles mid-output kit and run as a 75 bp paired-end reads at Norwegian Sequencing Center. The image analysis and base calling were performed using Illumina's RTA software version 2.4.6. Reads with low base call quality were removed using Illumina's default chastity criteria. The quality of the raw sequencing data was controlled using FastQC version 0.11.5 (https://www.bioinformatics.babraham.ac.uk/projects/fastqc/). The gene expression levels were determined using EDGE-pro v1.0.1 (81) and DESeq2 (82) with default parameters. EDGE-pro was used to align the reads to the reference genome (GCA_000953695.1) and convert the raw coverage into reads per kilobase of gene per million reads mapped (RPKM). DEseq2 was used to estimate the comparative differential gene expression values and provide the output as a log2fold change value with *p-value*. The log2fold change values were converted into fold change (FC) values, and the cutoff values of $\geq$ 2.0 or ≤ -2.0 with *p*adj values of < 0.05 were counted as significantly differentially expressed genes (DEGs). The transcriptome profiles of each strain was compared as high cell density against low cell density (tpHCD/LCD), high growth temperature 12°C against low temperature 6°C (tp12°C/6°C) and mutants against wild type (tpΔ*litR*/WT and tpΔ*ainS*/WT). These abbreviations of comparisons are used throughout this paper. The RNA sequence data of wild type *A. wodanis*, Δ*ainS* and Δ*litR* have been deposited in the European Nucleotide Archive (www.ebi.ac.uk/ena) under study accession number PRJEB34433.

Functional Gene Family and Pathway Analysis

KEGG BRITE and KEGG pathway mapper were used to map the DEGs (FC values $\geq$ 2.0 or ≤ -2.0) found when wild type was compared against cell densities (tpHCD/LCD) and temperatures (tp12°C/6°C) and also when mutants were compared against wild type (tpΔ*litR*/WT and tpΔ*ainS*/WT) at different cell

densities and temperatures against the reference organism *A. wodanis* 06/09/139 (83).

Identification of CRISPR Systems, Protospacers and Prophage

The CRISPR-Cas operon in *A. wodanis* 06/09/139 genome was identified using CRISPRCasFinder (84), and a homology search was performed using KEGG Sequence Similarity Database (SSDB) (83). An intergenic distance of < 100 bp between genes was considered as a single operon in this study. The CRISPR arrays with direct repeats and spacers were identified from the genome of *A. wodanis* using the CRISPR finder tool (85), while the protospacers were identified using CRISPR target (86). The prophages in *A. wodanis* were identified using the phage search tool (PHASTER) (87, 88).

Identification of Type VI Secretion Systems and Type VI Secretion Effectors

The T6SS gene clusters in *A. wodanis* 06/09/139 were identified using SecReT6 (89) and a homology search against other T6SS gene clusters using KEGG SSDB database (83). The naming of T6SS genes of *A. wodanis* 06/09/139 in this study follows the naming of *V. cholerae* T6SS (90). Potential T6SEs in *A. wodanis* were predicted using the Bastion 6 tool (91).

RESULTS

We have previously shown that *A. wodanis* 06/09/139 produces one AHL (3OHC10-HSL) and encodes genes for QS (7, 79). Moreover, in a recent study, the QS system in *A. wodanis* 06/09/139 was found to affect various phenotypes that are possibly linked to the winter ulcer disease development (80). Genome analysis and transcriptome profiling was therefore performed to further study the QS and survival strategies in *A. wodanis* by comparing wild type and its Δ*litR* and Δ*ainS* mutants at low (OD_{600} of 2.0) and high cell density (OD_{600} of 6.0) and two different temperatures, 6 and 12°C.

Differential Expressed Genes

The transcriptome profiles of *A. wodanis* and mutant strains Δ*litR* and Δ*ainS* at different cell densities and temperatures are listed in **Supplementary Table 1**. The average of mapped reads to the reference genome of *A. wodanis* was above 90% in all samples suggesting that the transcriptome data were sufficient for further analysis.

The total number of DEGs at all tested conditions are shown in **Figure 1**, and the complete lists of all DEGs are given in **Supplementary Table 2**. When comparing the transcriptome profiles at HCD relative to LCD (tpHCD/LCD) of the wild type after growth at 6°C, 18% of the total genes (n = 4,282) of *A. wodanis* were differentially expressed. Increasing the growth temperature to 12°C lowered this number of DEGs to 15%. Among the tested tpHCD/LCD conditions of wildtype, Δ*litR* and Δ*ainS* (**Figure 1A**), the highest numbers of DEGs were observed for the Δ*litR* mutant at 6°C, where the number of DEGs account for about 32% of the total genes in of *A. wodanis*. On the other side, the lowest number of DEGs (8% of the total 4282 genes) was observed in the Δ*litR* mutant tpHCD/LCD at 12°C. The *ainS* mutant tpHCD/LCD at 6°C and 12°C showed 15 and 18% DEGs, respectively. Further, the DEGs in tpHCD/LCD (WT_12°C) and tpHCD/LCD (WT_6°C) were sorted using KEGG BRITE and KEGG pathway mapper using *A. wodanis* 06/09/139 as a reference organism. The functional families with at least 15 DEGs were *enzymes*, *transporters, secretion system*, *bacterial motility proteins* and *ribosome* as shown in **Supplementary Figure 1A**. In addition, in the wild type tpHCD/LCD comparison, at 6°C, a few DEGs (n = 5) with FC values ≥ 2.0 were also mapped into the functional families *prokaryotic defense system*, which includes the CRISPR related genes. The KEGG pathway mapping revealed that the DEGs (n ≥ 30) in the wild type tpHCD/LCD were involved in *metabolic pathways*, *microbial metabolism in diverse environments*, *biosynthesis of secondary metabolites*, *ABC transporters, biosynthesis of antibiotics, two-component system*, *carbon metabolism* and the *ribosome*. The numbers of DEGs involved in these pathways were similar in wild type tpHCD/LCD at both temperatures except in the *ribosome* pathway. At tpHCD/LCD (6°C), 42 DEGs mapped into *the ribosome* pathway, whereas only one DEG mapped at tpHCD/LCD (12°C) (**Supplementary Figure 2A**).

Comparison of the transcriptome profiles of the wild type grown at 12°C and 6°C (tp12°C/6°C) revealed DEGs, accounting for 13 and 17% of the total 4282 *A. wodanis* genes at HCD and LCD, respectively (**Figure 1A**). In the Δ*ainS* mutant (tp12°C/6°C), 10 and 14% of total genes were differentially expressed at HCD and LCD, respectively. Compared to the wild type and the Δ*ainS* mutant, 31% of the total genes in the Δ*litR* mutant were differentially expressed (tp12°C/6°C) at LCD, whereas at HCD, 4% of the total genes were differentially expressed. Further, the DEGs in wild type (tp12°C/6°C) with FC values ≥ 2.0 and ≤−2.0 were sorted into KEGG BRITE and KEGG pathway mapper. The functional families with DEGs of ≥ 15 were *enzymes*, *transporters*, *ribosome*, *ribosome biogenesis* and *non-coding RNAs* (**Supplementary Figure 1B**). Few DEGs (n < 10) in wild type (tp12°C/6°C) mapped into families such as *secretion system* and *prokaryotic defense system*. The KEGG pathway mapping revealed that the DEGs (n ≥ 30) in the WT(tp12°C/6°C) were involved in pathways such as *metabolic pathways*, *microbial metabolism in diverse environments*, *biosynthesis of secondary metabolites*, *ABC transporters*, *biosynthesis of antibiotics*, *two-component system*, *carbon metabolism, purine metabolism*, *Aminoacyl-tRNA biosynthesis* and *ribosome*. The numbers of DEGs involved in these pathways were higher at tp12°C/6°C (LCD) than at tp12°C/6°C (HCD). For example, 43 DEGs at LCD mapped to the *ribosome pathway* while only 6 DEGs mapped at HCD (**Supplementary Figure 2B**).

When comparing the profile of the Δ*litR* mutant to the wild type tpΔ*litR*/WT at HCD, 3 and 4% of the total genes were differentially expressed at 12 and 6°C, respectively. In the tpΔ*litR*/WT (HCD_6°C), 4% of the total genes were differentially expressed. In tpΔ*litR*/WT (LCD_12°C), 5% of total genes whereas in tpΔ*litR*/WT (LCD_ 6°C), 11% of the total genes were found to be differentially expressed. The number of DEGs was two times higher at 6°C and LCD compared to 12°C and

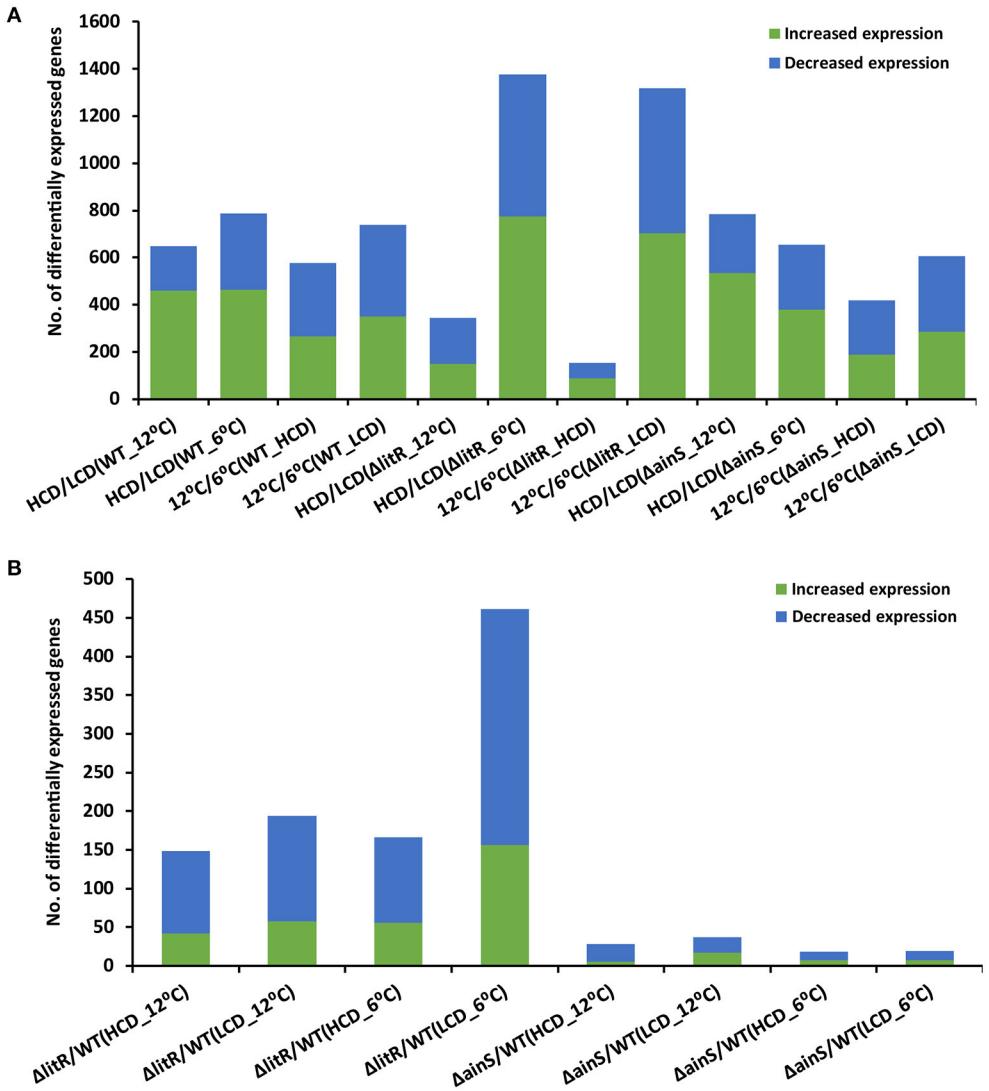

FIGURE 1 | The total number of differentially expressed genes in *A. wodanis* 06/09/139, Δ*ainS* and Δ*litR*. **(A)** The bar chart shows the number of increased (green) and decreased (blue) expression of genes when comparing high cell density (HCD) to low cell density (LCD) and growth temperature at 12 to 6°C. **(B)** The bar chart shows the number of increased and downregulated genes in comparisons Δ*litR*/WT and Δ*ainS*/WT.

HCD (**Figure 1A**). When comparing the expression profile of the Δ*ainS* mutant with the wild type (tpΔ*ainS*/WT) at HCD, 0.7 and 0.4% of the total genes were differentially expressed at 12 and 6°C, respectively. In tpΔ*ainS*/WT, during LCD and 12°C, 0.9% of the total genes and at LCD and 6°C, 0.4% of the total genes were found to be differentially expressed. The DEGs in Δ*litR* and Δ*ainS* mutants were sorted using KEGG BRITE (**Supplementary Figure 3A**) and mapped into KEGG reference pathway for *A. wodanis* 06/09/139 (**Supplementary Figure 4A**). The DEGs ($n \geq 5$) in the Δ*litR* and Δ*ainS* mutants compared to wild type with FC values of ≥ 2.0 and ≤ -2.0 were associated with functional families such as *enzymes*, *secretion system*, *bacterial motility proteins*, *transporters* and *prokaryotic defense system*. The KEGG pathway mapping revealed that the DEGs in the tpΔ*litR*/WT and tpΔ*ainS*/WT mutants affected several pathways, including *metabolic pathways*, *two-component system*, *biosynthesis of secondary metabolites*, *Quorum sensing* and *bacterial chemotaxis* (**Supplementary Figures 3B**, **4B**). Together our results suggest that, LitR is a crucial global regulator of genes at 6°C and at low cell density. As well, LitR has more impact on gene expression than AinS.

Key QS Genes of *A. wodanis* Are Cell Density and Temperature Dependent

Only a few genes known to be involved in the *A. wodanis* QS system were differentially expressed under the experimental conditions tested (**Supplementary Table 3**). When comparing the wild type transcriptome profile at HCD to LCD

(tpHCD/LCD), the AI synthase gene *ainS* (AWOD_I_1040) and master QS regulator gene *litR* (AWOD_I_0419) showed FC values of 2.01 and 2.24, at 6°C, respectively, while no significant differences were observed at 12°C.

When the wild type profile at high temperature was compared at low temperature (tp12°C/6°C), the *qrr* sRNA gene (AWOD_I_sRNA_054) was significantly higher with FC value of 2.92 at LCD, whereas no difference in its expression was observed at HCD. Temperature alone did not significantly impact other genes of the QS system at either HCD or LCD (**Supplementary Table 3**).

Comparing the profile of the Δ*litR* mutant relative to the wild type (tpΔ*litR*/WT), only the FC value of *ainS* at LCD and 12°C was significant (FC = −1.93, p_{adj} value < 0.05), although slightly lower than the cutoff FC value used in this study. The deletion of *litR* did not affect other QS related genes in *A. wodanis* under the conditions tested. On the other hand, when comparing the Δ*ainS* mutant profile to the wildtype (tpΔ*ainS*/WT), the *litR* expression was significantly lower at all conditions examined. The FC values of *litR* were notably lower at HCD compared to LCD. At HCD, the FC values for *litR* at 6°C and 12°C were −2.53 and −2.87, respectively. At LCD, the FC values at 6°C and 12°C were −1.93 and −2.04, respectively, indicating that the expression of *litR* in the Δ*ainS* mutant increases with increased density and independent of the temperature. Furthermore, the phosphorelay protein-encoding gene *luxU* (AWOD_I_0921) expression was significantly higher in the Δ*ainS* mutant at HCD (FC = 2.81) and LCD (FC = 2.17) at 6°C, whereas at 12°C no differences were observed. Hence, the *luxU* expression in the Δ*ainS* mutant was slightly higher at HCD compared to LCD and its expression was affected only at low temperature.

Differential Expression of CRISPR-Cas System in *A. wodanis*

We identified two CRISPR systems in the genome of *A. wodanis* using CRISPRCas finder (84), where CRISPR system 1, located on chromosome 1, did not contain any *cas* loci, whereas CRISPR system 2, located in chromosome 2, contains the *cas* loci (**Figure 2**). The CRISPR system 2 was classified as a Type I-F CRISPR system. A total number of 25 and 40 spacers with a length of 32-33 nucleotides were identified in CRISPR system 1 and 2, respectively (**Supplementary File S4**). When the spacers were searched against the phage databases using CRISPR Target, spacers matched to the protospacers with at least 5 single nucleotide polymorphisms. For example, spacer 11 of CRISPR system 1 matched to the *Vibrio* phage CTX plasmid pCTX-2, whereas spacer 19 of CRISPR system 2 matched to the *Staphylococcus* phage phiSP38-1 with a score of 20.

The data shows that in the wild type, the *csy3*, *cas1,* and *cas3* genes of CRISPR system 2 have significantly higher FC values (FC > 2.0) at HCD than at LCD after growth at 6°C. No significant differences in FC values of the *cas* genes were observed in wild type (tpHCD/LCD) at 12°C (**Supplementary Table 5**). Cell density had no impact on the expression of CRISPR arrays of CRISPR systems 1 and 2 at either temperature.

When the expression profile at 12°C was compared to 6°C, at LCD and HCD, the CRISPR arrays of system 1 displayed significantly lower FC values (FC value = ∼−2.0), suggesting temperature difference influences CRISPR system 1. However, temperature had no effect on the CRISPR system 2.

Further, the expression data showed that the expression of *cas* genes of CRISPR system 2 were strongly reduced in the Δ*litR* mutant at all conditions examined. The FC values of the *cas* genes in the Δ*litR* mutant increased with increasing cell density at both temperatures. Notably, in the Δ*litR* mutant at 6°C, the FC values of *csy3* and *csy1* were twice as high at HCD (FC = − approx. 10.0) compared to LCD (FC = − approx. 5.0). At LCD, the genes *csy1*, *csy2*, *csy3,* and *csy4* had lower FC values at 6°C compared to 12°C, whereas the *cas1* and *cas3* showed higher FC values (**Supplementary Table 5**). However, at HCD, the highest FC values for *cas* genes were observed at 6°C than at 12°C. The CRISPR array of system 2 in the Δ*litR* mutant showed significantly lower expression at LCD and 12°C (FC value = −1.96) and LCD and 6°C (FC value = −2.69). However, at HCD, the expression of the CRISPR array of system 2 was not significantly different. The data also showed that the CRISPR array of system 1 was highly expressed at HCD and 12°C, whereas the FC values were not significantly different at HCD and 6°C or at LCD at 6°C and 12°C. In the Δ*ainS* mutant compared to wild type, genes such as *csy2*, *csy3,* and *csy4* showed significantly lower expression at two experimental conditions, LCD, 12°C and HCD, 6°C. No significant differences were observed in expressions of the CRISPR array of system 1 and 2 in *the* Δ*ainS* mutant.

A. wodanis Harbors Three Main T6SSs and Four Auxiliary Clusters

A. wodanis was found to harbor three T6SSs, each encoding the conserved core and accessory T6SS genes. T6SS1 was located on chromosome 1, whereas the T6SS2 and T6SS3 were on chromosome 2. The T6SS1 gene clusters (AWOD_I_0981-0995) were composed of 3 operons with 15 consecutive genes, whereas the T6SS2 gene clusters consisted of 1 operon with 15 consecutive genes (AWOD_II_0111-0125) and T6SS3 gene clusters with 2 operons with 20 consecutive genes (AWOD_II_1008-1027) as shown in **Figure 3**. The main T6SS clusters comprised the core components *vasABDEFGHJKLQRS*, valine-glycine repeat protein G (*vgrG*) and Hemolysin Coregulated protein (*hcp*) and the accessory genes *vasCIUVX* (60, 92, 93). The genes *vasABEJL* and *vasDFK* may form the base-plate and membrane complex, respectively (94–96). The genes *vasRQ* and *vasC* may form the outer sheath and the FHA domain, respectively, while *vasG* is believed to act as a chaperone (97, 98). The gene *vasH* may serve as a sigma-54 dependent transcriptional regulator and *vasIS* as lysozyme-related proteins (99). The T6SS3 in *A. wodanis* does not encode the transcriptional regulator *vasH* (99). Four *vgrG* paralogous genes were identified in *A. wodanis,* and using them as markers, four auxiliary clusters were predicted, such as Aux-1 (AWOD_I_1435-1440, AWOD_I_2030), Aux-2 (AWOD_II_0126-0141), Aux-3 (AWOD_II_1028-1032) and Aux-4 (AWOD_II_1054-1060). The auxiliary clusters were

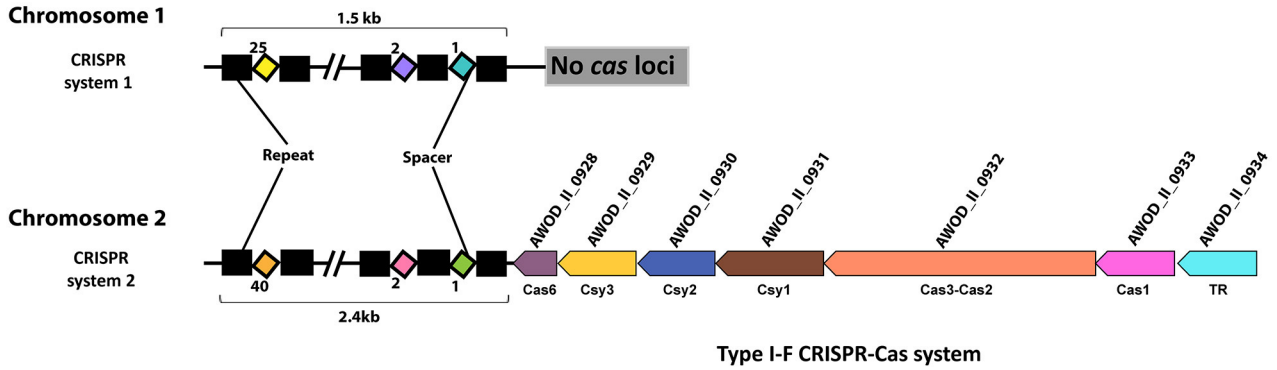

FIGURE 2 | CRISPR systems in *A. wodanis* 06/09/139. The figure shows the CRISPR arrays with repeats (black rectangle) and spacers (colored diamonds). In CRISPR system 2, the CRISPR array is located close to the *cas* operon (arrows) of the Type I-F CRISPR-Cas system. TR denotes transcriptional regulator.

located together with the core T6SS genes encoding Proline-alanine-alanine-arginine repeats (PAAR), VgrG and Hcp. The Aux-1 cluster does not encode Hcp, and Aux-4 does not encode a PAAR protein. Four genes encoding adaptor proteins of the DUF4123 family (unknown function) were identified adjacent to *vgrG1*, *vgrG2* and *vgrG4,* whereas no adaptor protein-encoding gene was present adjacent to *vgrG3*.

Differential Expression of T6SSs and Auxiliary Clusters of *A. wodanis*

In the wild type, at HCD, the main clusters T6SS1 (*vasR1Q1J1*) and T6SS2 (*vasH1I1J1K1L1*) were highly expressed at both 6 and 12°C, compared to LCD. No differential expression was observed for the T6SS3 (**Supplementary Table 6**). Furthermore, the complete auxiliary cluster Aux-1 showed higher expression at HCD at both temperatures. The Aux-2, Aux-3 and Aux-4 showed only significant differences in some genes such as AWOD_II_0126 - 0139, AWOD_II_1031 - 1032 and AWOD_II_1054 - 1059, respectively.

The temperature did not affect the expression of the T6SS1 and T6SS3 in the wild type. However, a few genes (*vasQ2, vasR2, vasS2, and vasD2*) of T6SS2 were differentially expressed at HCD, while at LCD, only *vasQ2* was differentially expressed. As for the auxiliary clusters, only the genes encoding membrane protein and DUF4123 (AWOD_I_1435 and AWOD_I_1439) of Aux-1, *hcp1* of Aux-2 and a putative uncharacterized protein (AWOD_II_1031) of Aux-3 were differentially expressed.

When the Δ*litR* mutant was compared to wild type (tpΔ*litR*/WT), the data revealed that the *vasR1Q1J1* operon of T6SS1 was differentially expressed at all tested conditions. The FC values of genes *vasR1Q1J1* were marginally higher at HCD compared to LCD. Particularly the FC values of *vasQ1* gene in Δ*litR* mutant were twice as high at HCD compared to LCD at both temperatures. The FC values of *vasR1Q1J1* operon in the Δ*litR* mutant were significantly higher at 6°C compared to 12°C at both cell densities (**Supplementary Table 6**). The genes *vasF1D1C1* showed higher FC values in Δ*litR* mutant at LCD than HCD. At 6°C, the complete T6SS2 cluster was differentially expressed in the Δ*litR* mutant at both HCD and LCD. At 12°C, differential expression was only observed in some of the genes in the T6SS2 cluster. Moreover, the FC values of T6SS2 genes were higher at low (6°C) compared to high (12°C) temperature. The T6SS3 gene cluster was only differentially expressed at LCD and 6°C with an average FC value of 2.0. In Δ*litR* mutant, some genes of Aux-1, Aux-2 and Aux-3 were differentially expressed, whereas the Aux-4 showed no differential expression (**Supplementary Table 6**). In Aux-1, the expression of *vgrG1* was lower in Δ*litR* mutant with an FC value of−4.90 at LCD and 6°C. The genes encoding Hcp1, VgrG2, PAAR motif-containing protein, a protein with ankyrin repeats and the rearrangement hotspot (RHS) protein in the Aux-2 were differentially expressed, where the FC values (FC = −22.75) of *hcp1* at HCD and 6°C was approximately thrice compared to LCD (FC = −8.32). Similarly, three times higher expression of *hcp1* was observed at 6°C compared to 12°C at both HCD and LCD. About 6 of the 16 total genes in the Aux-2 cluster showed significantly lower expression at LCD and 6°C. The Aux-3 was highly expressed in the Δ*litR* mutant, relative to wild type, at HCD and 12°C and at LCD and 6°C. When comparing the Δ*ainS* mutant with the wild type (tpΔ*ainS*/WT), only the expression of *vasR1* and *vasQ1* genes of the T6SS1 cluster were significantly reduced, whereas no differences in T6SS2 and T6SS3 gene clusters were observed. The *vgrG1* of Aux-1 showed lower expression (FC value = −2.07) at LCD and 6°C while the *hcp1* of Aux-2 showed significant lower expression (FC < −2.0) at all conditions except at LCD and 12°C. Additionally, the genes AWOD_II_1031 and *hcp3* of Aux-3 showed significant higher expression at HCD and 12°C. Other genes of auxiliary clusters in Δ*ainS* mutant did not show significant differential expression.

Potential T6SE Molecules Identified in *A. wodanis* 06/09/139

We predicted 80 potential effectors proteins using the T6SE prediction tool Bastion 6 (**Supplementary Table 7**) (91). Of the 80 potential effectors, 29 could be annotated, while 51 were identified as putative proteins. Of the potential effectors, 44 were located on chromosome 1, 33 effectors on chromosome 2 and 2 effectors were predicted to be located on plasmid p20. Among the

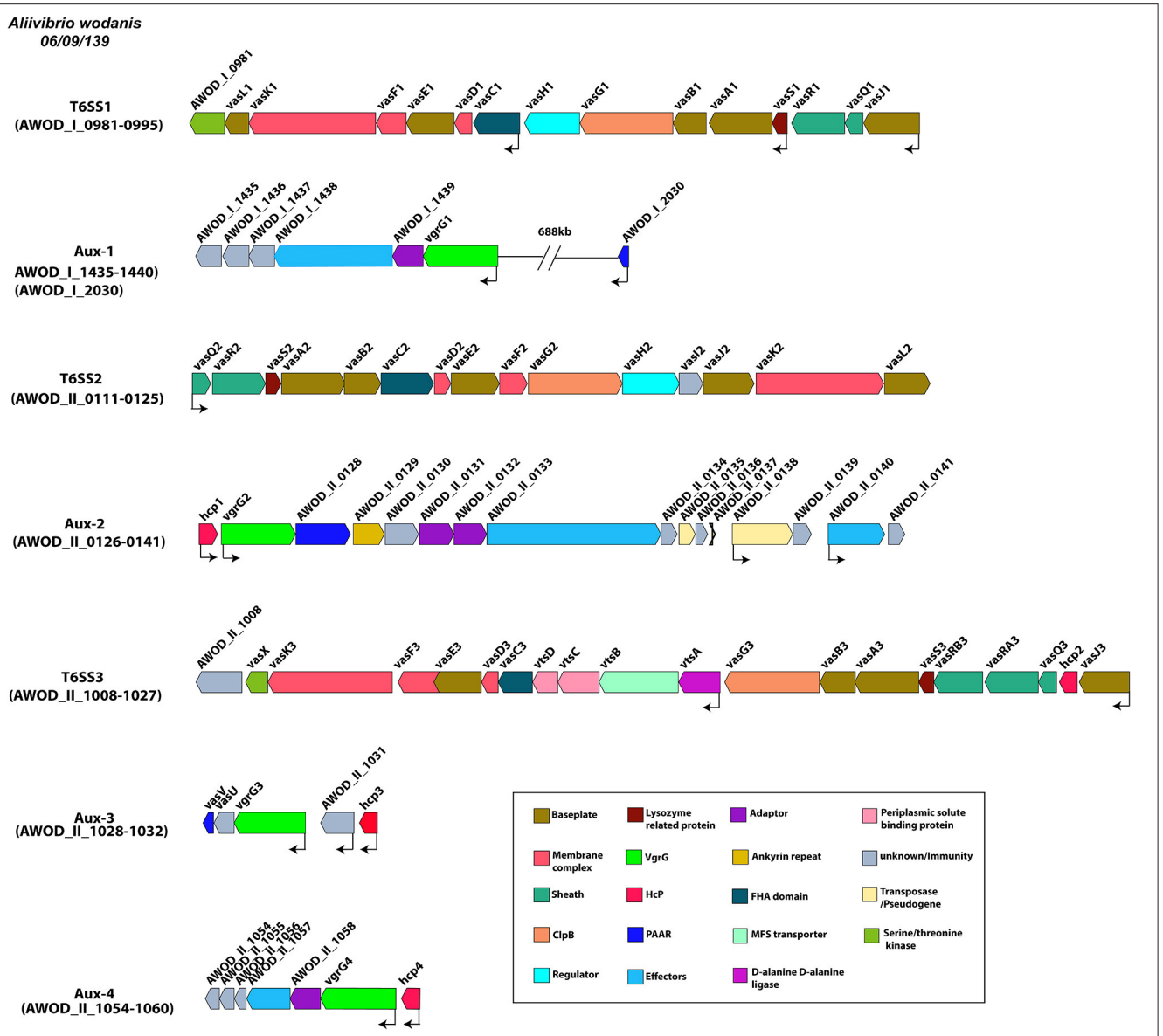

FIGURE 3 | Type VI secretion systems in *A. wodanis* 06/09/139. Graphical representation of the three main T6SSs of *A. wodanis* and the four auxiliary T6SS clusters. The thin black arrows indicate the direction and start of the transcription sites.

annotated T6SEs, we found potential cell wall degrading effectors such as N-acetylmuramoyl-L-alanine amidase and hydrolases, membrane degrading effectors including phospholipases, and several nucleotide degrading nucleases. Only a few effectors such as a porin-like protein H (AWOD_I_1000), a RHS protein (AWOD_II_0133) and type VI secretion system secreted protein Hcp (AWOD_II_1032) were located close to the main T6SS clusters, whereas the rest were located in different locations on both chromosomes.

Differential Expression of T6SEs in *A. wodanis*

In wild type, 24 effector genes were differentially expressed at HCD (tpHCD/LCD) at 6°C, while 19 effectors were differentially expressed at 12°C (**Supplementary Table 7**). These effector genes encoded several proteins including outer membrane proteins, membrane proteins, proteins with PAAR motif, lipoproteins with LysM domain, a sulfite reductase [NADPH] flavoprotein alpha-component, a secreted endonuclease I and a choline dehydrogenase. Interestingly, in the wild type at HCD and 6°C, an FC value of 173.29 was found for choline dehydrogenase (AWOD_II_1235), which was 20 times higher than at 12°C (FC = 8.99). When the wild type profiles at high and low temperatures were compared (tp12°C/6°C), 18 effectors and 22 effectors were differentially expressed at HCD and LCD, respectively. These effectors comprised putative exported protein, putative lipoprotein, putative beta-lactamase, amine oxidase and choline dehydrogenase.

In the Δ*litR* mutant, genes encoding effector molecules with significantly lower expression (FC < −2.0) were putative exported proteins (AWOD_I_0175, AWOD_I_1184, AWOD_II_0501, and AWOD_II_0656), outer membrane protein (AWOD_I_1120), putative lipoprotein (AWOD_I_1186, AWOD_II_0440, AWOD_II_0804, and AWOD_II_1206), putative polysaccharide deacetylase (AWOD_I_1338), membrane protein (AWOD_I_1567), amine oxidase (AWOD_II_0852) and phospholipase (AWOD_II_1212). The effector molecules genes differentially expressed in Δ*ainS* mutants included a putative histidine decarboxylase (AWOD_I_1509), and a secreted endonuclease (AWOD_II_0252). Additionally, genes encoding effectors such as a porin-like protein H (AWOD_I_1000), an endonuclease I precursor (AWOD_I_2248) and a 6-phospho-beta-glucosidase (AWOD_I_0029) were differentially expressed in both Δ*litR* and Δ*ainS* mutants. The differential expression of effector molecules in Δ*litR* mutant was seen more often during LCD and 6°C than at other experimental conditions like HCD and 12°C (**Supplementary Table 7**).

DISCUSSION

A. wodanis is frequently isolated together with *M. viscosa* during the winter ulcer outbreaks and believed to be involved in the progression of winter ulcer disease (7, 73, 74, 78). Although *M. viscosa* is the main agent causing the disease, the reason for its co-existence with *A. wodanis* is not yet clear. Bacteria use several strategies to compete for niche adaptions, which are known to be regulated by various mechanisms, including QS (49, 100–102). In our previous study we have shown that QS in *A. wodanis* regulates various phenotypic traits and cytotoxicity on CHSE cell line (80). In this study, we performed genome analysis and gene expression profiling of *A. wodanis* to explore the QS system and its role in regulating the survival strategies.

Total DEGs

When comparing the transcriptome profile of the *A. wodanis* wild type between cell densities (tpHCD/LCD) and temperatures (tp12°C/6°C), the strongest effect in terms of number of DEGs were at LCD (164 more genes than at HCD) and at 6°C (140 more genes than at 12°C). Furthermore, the functional mapping of DEGs revealed that families such as *secretion system, prokaryotic defense system* and *transporters* were highly expressed at HCD compared to LCD. As expected, the gene families related to protein synthesis such as *ribosomes*, *ribosome biogenesis* and *transfer RNA biogenesis* were less expressed at HCD compared to LCD (tpHCD/LCD). Similar cell density-dependent gene expression has been reported in *Aliivibrio salmonicida*, where about 1,000 genes were differentially expressed in response to increase in cell density (103). In the Δ*litR* mutant, 1.8 times more DEGs were observed at tpHCD/LCD at 6°C than for the wild type grown at the same condition, suggesting LitR is an important regulator in *A. wodanis* at low temperature. Furthermore, in *A. wodanis*, the lowly expressed genes in comparison tp12°C/6°C were related to protein synthesis such as *non-coding RNAs*, *ribosomes*, *transfer RNA biogenesis* and *ribosome biogenesis*. This suggests that genes related to protein synthesis are less expressed at 12°C compared to 6°C. Temperature is one of the major environmental stress factors that bacteria encounter in nature and many genes respond to temperature changes. In addition, the functional families such as the *secretion system* and *prokaryotic defense system* were also regulated by temperature in *A. wodanis*. For example, in *V. parahaemolyticus* 13% of DEGs were observed when the bacteria were grown at 15°C and 42°C compared to its optimal temperature 37°C, where genes related to energy metabolism were highly affected due to temperature change (104). In *A. wodanis*, more DEGs were identified in tpΔ*litR*/WT (LCD) and tpΔ*litR*/WT (6°C) compared to at HCD and 12°C, suggesting LitR is a global regulator when the temperature is low and the cells are in the early log phase. This is in contrast to *A. salmonicida*, where the numbers of DEGs in Δ*litR* mutant were higher at HCD compared to LCD at 12°C (103). The comparison between the transcriptome profiles of mutants and wildtype (tpΔ*litR*/WT and tpΔ*ainS*/WT) showed about 5 to 24 times more DEGs in tpΔ*litR*/WT compared to tpΔ*ainS*/WT at both cell densities and temperatures. This indicates that only a few genes seem to be regulated through the AinS-dependent QS system. This is similar to *A. salmonicida,* where only about 20 genes were differentially expressed in Δ*ainS* mutant when compared to wild type, whereas in *litR* mutant compared to wild type, 3 to 10 times more DEGs were found (103, 105). Moreover, in this study, the transcriptomics was performed at OD_{600} of 6.0, which is a late log phase in *A. wodanis* while it can reach an OD_{600} of ∼8.0. Therefore, the AHL-mediated gene regulation in *A. wodanis* may differ at OD_{600} higher than 6.0. The functional mapping of DEGs from comparisons tpΔ*litR*/WT and tpΔ*ainS*/WT showed that the genes affected by LitR and AinS in *A. wodanis* mainly belongs to the families such as *secretion system* and *prokaryotic defense mechanism*, which contained the T6SS and CRISPR genes, respectively. Nevertheless, other families such as *enzymes*, *bacterial motility proteins* and *transporters* were also found to be affected by LitR and AinS in this study. LitR and AinS in *A. wodanis* also influenced various pathways such as metabolic pathways, *Quorum sensing*, and *two-component systems*, *suggesting* their role in signaling mechanisms and metabolic activities. QS regulation of metabolic functions such as glucose uptake, phosphoenolpyruvate-dependent sugar and nucleotide biosynthesis are known to enhance the co-operative behavior of bacteria to survive under limited nutrient conditions (101). Similarly, the LitR and AinS regulation of metabolic pathways in *A. wodanis* may play a role in co-operative behavior under limited nutrient conditions.

QS System in *A. wodanis*

In wild type, we found that an increase in cell density resulted in a higher expression of the AHL autoinducer synthase *ainS* and the master QS regulator *litR* when grown at 6°C and not at 12°C. This demonstrates that cell density only affects the expression of *litR* and *ainS* genes at low temperature. Similar increased expression of *ainS* was also observed in the Δ*litR* mutant strain when comparing HCD to LCD (tpHCD/LCD), indicating that the *ainS* expression is not entirely LitR-dependent. These results

confirm our previous work, where we showed that the 3OHC10-HSL production is cell density- and temperature-dependent (80). Similar to AinS in *A. salmonicida* (105), the AinS in *A. wodanis* negatively affected the *luxU* expression. This suggests that the decreased expression of *luxU* could repress *qrr* and activate *litR* in *A. wodanis*. Similarly, in this study, *luxU* was affected by AinS only at 6°C, which could suggest that low temperature affects the phosphorelay function of *luxU*. On the other hand, the *qrr* gene was more expressed at 12°C compared to 6°C. Qrr sRNAs in vibrios are known to regulate several target mRNAs, including the master QS regulator LuxR (106). In *A. fischeri*, Qrr sRNAs negatively regulates the production of LitR (16). Therefore, the increased expression of *qrr* in *A. wodanis* at 12°C may negatively affect the production of LitR and, subsequently, the QS dependent gene expression. Our results illustrate that *litR*, *ainS*, *luxU*, *qrr* sRNA in the *A. wodanis* QS system were differentially expressed in a cell density and temperature-dependent manner. The proposed QS model in *A. wodanis* and its regulation of target genes are presented in **Figure 4**.

In this study, LitR in *A. wodanis* did not affect the *ainS* expression, except at LCD and 12°C (FC = −1.93) in the Δ*litR* mutant. This confirms our previous work where we showed that the 3OHC10-HSL production is not completely controlled through LitR (80). However, LitR in *A. fischeri* and *A. salmonicida* has been shown to significantly upregulate AinS (11, 107). In *A. fischeri*, several LitR-independent regulatory mechanisms have been reported to regulate *ainS*, such as *ainS* auto-regulation or cyclic AMP receptor protein- and glucose-mediated mechanisms (11, 108). Similarly, in *A. wodanis*, other regulatory mechanisms may regulate the expression of *ainS*. The deletion of *ainS* in *A. wodanis* negatively affected the *litR* expression. In the Δ*ainS* mutants, the FC values of *litR* were slightly higher at HCD compared to LCD at both temperatures, which suggests that 3OHC10-HSL partly activates *litR* independently of the temperature. Similarly, the autoinducer synthase C8-HSL in *A. fischeri* positively affected *litR* in a cell density-dependent manner (14).

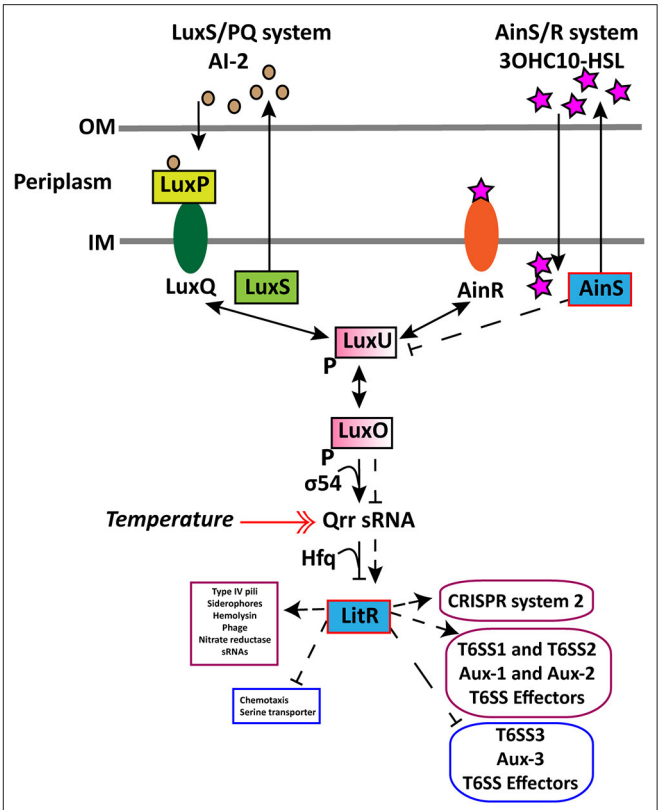

FIGURE 4 | Proposed model for regulation of CRISPR and T6SS in *A. wodanis* 06/09/139 at 6°C. The model includes the two QS systems LuxS/PQ and AinS/R in *A. wodanis*. At low cell density (LCD), when the AIs concentration is low, the receptors (AinR and LuxPQ) may act as kinases and relay phosphate to LuxO via LuxU, which activates the expression of *qrr* sRNA. The Qrr sRNA inhibits the expression of *litR*. When the AI concentration is high at high cell density (HCD), they bind to the receptors to dephosphorylate LuxO and inactivate *qrr* sRNA. Inactivation of *qrr* sRNA, in turn, activates *litR*, which regulates many genes. Arrowheads at both ends indicate phosphorylation relay, and the symbol "P" indicates the phosphorylated state. AinS seems to affect luxU negatively and the *litR* expression positively. LitR seems to positively affect the genes involved in T6SS1, T6SS2, Aux-1, Aux-2, T6SS effectors and CRISPR system 2 and, conversely, affect T6SS3, Aux-3 and T6SS effectors negatively. Thin line and dashed line with arrowhead indicate regulation at LCD and HCD, respectively, where arrowheads indicate increased expression (+) and bars indicate decreased expression (-). A double arrowhead red line indicates the increased expression of *qrr* sRNA at 12°C compared to 6°C. Genes with significantly higher and lower expression are presented in purple and blue boxes, respectively.

Regulation of CRISPRs and Spacers

A. wodanis harbors a type I-F CRISPR system and a CRISPR system without *cas* loci, the CRISPR system 1 and CRISPR system 2, respectively. CRISPR systems without *cas* loci are known as orphan arrays, where most of these are known to be non-functional (39). However, some of the orphan CRISPR arrays may function together with invading *cas* genes or the *cas* genes present in a different location within the same genome (109). In *A. wodanis*, the CRISPR system 1 consists of 25 spacers, whereas CRISPR system 2 consists of 40 spacers. The difference in the number of spacers in *A. wodanis* suggests that the CRISPR system 1 is less active than the CRISPR system 2 or is a remnant of a previously active CRISPR system. In addition, the spacers were not identical between CRISPR systems 1 and 2, indicating both are working independently of each other or that CRISPR system 2 has been introduced later than CRISPR system 1. The *cas* genes in *A. wodanis* shows ∼90% amino acid similarity to the *cas* genes in *M. viscosa*, suggesting that the CRISPR system 2 has been horizontally transferred from *M. viscosa*. We speculate here that both bacteria can defend themselves against the same agents, which may favor their co-existence during the development of the winter ulcer disease. Similarity search of the spacers in *A. wodanis* against the phage databases revealed *Vibrio* phage CTX plasmid pCTX-2 and *Staphylococcus* phage phiSP38-1.

The expressions of *cas* genes (*cas1*, *cas3,* and *csy3*) in wild type seems to be cell density-dependent at 6°C, where the *cas* genes showed increased expression at HCD compared to LCD. However, cell density had no significant effect on the expression of CRISPR arrays of CRISPR systems 1 and 2 regardless of temperatures. Therefore, the CRISPR systems are

partially dependent on cell density. Previous studies suggest that bacteria are at higher phage risk at higher cell density densities, and thus protection against phage is important at HCD (45). This suggests that *A. wodanis* positively influences *cas* genes as the cell density increases, and this might provide protection upon phage infection at HCD.

The CRISPR arrays of CRISPR system 1 in *A. wodanis*, was more highly expressed at 6°C when compared to 12°C, suggesting that the temperature 6°C plays a significant role in CRISPR array 1 expression. Temperature is known to regulate CRISPR-Cas genes in *P. aeruginosa* (45, 102). However, temperature difference did not regulate the expression of neither the *cas* operon nor the CRISPR array of the CRISPR system 2.

The complete *cas* operon of CRISPR system 2 in *A. wodanis* showed decreased expression in the Δ*litR* mutant irrespective of cell densities and temperatures, which demonstrates that the CRISPR system 2 is regulated through LitR. In the Δ*litR* mutant, the expression of the *cas* genes was higher at 6°C compared to 12°C at HCD. At LCD, only the expression values of the *cas1* and *cas3* were higher at 6°C compared to 12°C, while other genes such as *csy1234* were higher at 12°C. Although LitR in *A. wodanis* activates the CRISPR system 2, the QS regulation is not completely cell density and temperature-dependent. Furthermore, the data shows that the CRISPR system 1 was more highly expressed in Δ*litR* mutant compared to wild type, implying that LitR negatively affects CRISPR system 1.

In the Δ*ainS* mutant, although a lower expression was observed on genes *csy2*, *csy3,* and *csy4*, the expression of CRISPR arrays of CRISPR system 2 and CRISPR system 1 were not changed by inactivation of *ainS*. Hence, the activation of the CRISPR system 2 in *A. wodanis* seems to be partly dependent on the AHL-mediated QS system. The QS activation of the CRISPR system has been reported as an efficient mechanism to enhance the benefit-to-cost ratio in *P. aeruginosa* (44, 45). Although several vibrios and aliivibrios comprise both QS and CRISPR systems, the QS regulation of the CRISPR system has not been described yet. Expression of the CRISPR system can be costly to the bacteria, and in some bacteria like *Streptococcus thermophilus*, the CRISPR system is constitutively expressed and confers a fitness cost (110). Therefore, the CRISPR system may only be expressed during phage infection or due to environmental cues (111–113). Similarly, the cell density, temperature and QS dependent regulation of CRISPR may enforce a benefit for *A. wodanis* during the development of winter ulcer.

Despite exhibiting CRISPR systems, one intact prophage was identified in *A. wodanis* chromosome 1 and several incomplete prophages in both chromosomes and the plasmids. Phages that infect *P. aeruginosa* are known to escape the type I-F and I-E CRISPR systems using anti-CRISPR proteins (114, 115). Therefore, we searched for anti-CRISPR proteins in *A. wodanis* using ArcFinder (116). No anti-CRISPR proteins were predicted, suggesting no self-targeted protospacers that prevent CRISPR-Cas response in *A. wodanis*. Although defective in their function, these incomplete phages are known to have adaptive functions in their hosts (117). Several of these incomplete phages are a putative source for phage-derived molecular products such as gene transfer agents, bacteriocins, phage killer particles, and they can also interfere with assembly of other phages (117, 118). The hypothetical proteins of intact and incomplete prophages from PHASTER output were searched against non-redundant protein database using BLASTP with default parameters. The hypothetical proteins present in the intact prophage were annotated as structural phage-related proteins. However, the incomplete prophages encoded several conserved proteins (with $\geq$ 90% amino acid identity and query coverage) such as type I restriction endonuclease subunit M, ClbS/DfsB family four-helix bundle protein, DUF559 domain-containing protein, type II toxin-antitoxin system RelE/ParE family toxin and other conserved hypothetical proteins (**Supplementary Table 8**). These proteins encoded by the incomplete prophage may play a role in adaptive functions of *A. wodanis*. However, further research is required to verify this.

Regulation of T6SSs, Aux, and T6SE Molecules

Bacteria secrete many virulence factors during the host-pathogen interface, not only to overcome the host's immune system but also for inter-bacterial competition (119). T6SS is an important virulence and survival factor present in about a quarter of known Gram-negative bacteria (120). *A. wodanis* genome revealed three T6SSs and four auxiliary clusters. Many bacteria possess more than one T6SS, which likely have different functions. For example, *Burkholderia thailandensis* possesses five T6SSs copies with different functions, where T6SS1 enhances the growth in the presence of other competing bacteria and T6SS4 is involved in the manganese transport to survive under oxidative stress, and the T6SS5 is involved in virulence in the murine model of pneumonic melioidosis (121, 122). Similarly, the multiple T6SSs in *A. wodanis* may have different cellular functions.

The T6SS1 in *A. wodanis* is highly similar (71–88%) to the T6SS system 1 in *A. fischeri* MJ11, while the T6SS2 shows high similarity (54–92%) to *V. cholerae* O1E1 T6SS and *V. fluvialis* T6SS2 (90, 123, 124). The T6SS3 in *A. wodanis* shows similarity (33–84%) to *M. viscosa*, *V. anguillarum, A. salmonicida* and *Vibrio tapetis* (48, 125, 126). Hcp and VgrG are essential components for the proper functioning of T6SS (127). *A. wodanis* encodes *vgrG1* in Aux-1, however, it contains *hcp* in neither T6SS1 nor Aux-1 clusters. In *A. fischeri* MJ11, the T6SS1, which is similar to the T6SS1 of *A. wodanis*, is believed to interact with eukaryotic cells and is not involved in inter-strain killing (124). Moreover, in *A. wodanis* Aux-1 is located close to the heme uptake and utilization related genes. Metals such as iron are important for many cellular processes, and the genes located close to T6SS genes are known to be involved in iron uptake, for example, in *P. aeuroginosa* (58). Thus, the T6SS1 along with the Aux-1 may possibly be involved in iron uptake from the host or environment. Except for Hcp, the other structural T6SS proteins share low-level homology between each T6SSs. This indicates that the multiple T6SSs in *A. wodanis* is not a result of a recent duplication. Four copies of *hcp* were identified in the main and auxiliary T6SS clusters of chromosome 2. The proteins Hcp1 and Hcp4 showed 60% homology to each other, whereas Hcp3 and Hcp4 showed 100% homology to each

other. Besides the structural role of Hcp, it is involved in the inter-bacterial competition, bacterial invasion, adherence, and cytotoxicity against host cells, also known to have other functions in different bacteria (127, 128). Therefore, the multiple copies of *hcp* in *A. wodanis* may have different functions.

V. cholerae utilizes T6SS to compete against diverse eukaryotic and prokaryotic organisms (66, 129). In *V. fluvialis*, the T6SS2 is anti-bacterial and provides a better competitive fitness in the marine environment (123). The T6SS2 in *A. wodanis,* which shows higher homology to *V. fluvialis* and *V. cholerae*, may enhance *A. wodanis* through inter-bacterial competition and virulence.

The T6SS3, unlike T6SS1 and T6SS2 in addition to structural components, contains additional genes *vtsABCD* encoding transporter proteins and does not contain *vasH.* VtsA-D plays a role in stress responses, transport function and *hcp* expression in *V. anguillarum*, and VasH is essential to drive the expression of the T6SS operon by inducing *hcp* and *vgrG* expression (48, 130). The mutation in *vasH* repressed *hcp* expression and impaired its anti-bacterial activity in other vibrios (123, 131). In *V. anguillarum*, VtsA-D proteins are involved in stress responses, however, plays no role in virulence (48). Similarly, T6SS3 in *A. wodanis* is probably involved in stress responses. After *V. anguillarum*, the T6SS similar to T6SS3 in *A. wodanis* is in *M. viscosa* (mts1). The genes encoding Hcp (AWOD_II_1028 and AWOD_II_1032), which are located close to each other, shows 71% similarity to *M. viscosa hcp,* MVIS_3030 (7). This implies that the T6SS3 in *A. wodanis* might have a similar function as mts1 of *M. viscosa* during the winter ulcer disease development.

In this study, expression of the T6SS1 and T6SS2 genes and their auxiliary clusters in *A. wodanis* are dependent on cell density. Such cell density-dependent T6SS expression has been reported in *V. parahaemolyticus* (50). Some of the genes in the T6SS2 and auxiliary clusters (Aux-2 and Aux-3) were found to be altered by temperature. The expression was found to be higher at 6°C than at 12°C. In *V. fluvialis*, the T6SS2 is regulated by temperature (123). Temperature-dependent regulation of virulent factor genes may be an essential feature for many bacteria to survive in harsh environments (132).

LitR in *A. wodanis* seemed to positively affect two T6SSs (T6SS1 and T6SS2) and negatively affect the expression of T6SS3 gene cluster. This demonstrates that QS regulation of the T6SSs in *A. wodanis* is very complex. The regulation of T6SS3 by LitR in *A. wodanis* indicates T6SS3 may play different roles than T6SS1 and T6SS2. Such reciprocal regulation has also been shown in *V. parahaemolyticus*, where the QS regulator OpaR downregulates T6SS1 and upregulates T6SS2 where T6SS1 functions as anti-bacterial and T6SS2 as anti-eukaryotic (133).

LitR in *A. wodanis* seemed to positively affect only the genes encoding the outer sheath and base-plate proteins of T6SS1, suggesting these genes are QS dependent. Interestingly, LitR was involved in activating the expression of the whole apparatus of the T6SS2 system. Moreover, LitR also repressed the entire T6SS3 gene clusters but only at LCD at 6°C. Therefore, T6SS2 is ultimately QS dependent, whereas T6SS1 and T6SS3 are not completely QS dependent. Regulation of T6SS by LuxR homologs have been described in *V. cholerae* (HapR), *V. alginolyticus* (LuxR) and *V. anguillarum* (VanT) (48, 49, 51, 134). Furthermore, we observed that LitR in *A. wodanis* is a strong activator of *hcp1* expression at 6°C than at 12°C. Hence, this possibly implies that *hcp1* of T6SS2 is may be involved in the cytotoxicity in CHSE cell line (80). Temperature has been shown to influence *hcp* expression in other bacteria such as *Yersinia pestis* and *V. parahaemolyticus* (133, 135). Similarly, in *A. wodanis*, the high expression of *hcp* at 6°C indicates that the T6SS2 could be more active at low temperature (6°C).

We identified that the genes in Aux-2 encoding ankyrin repeat-containing proteins and RHS proteins were differentially expressed in tpΔ*litR*/WT at 6°C. Ankyrin repeat proteins are known to be involved in pathogenesis by imitating and impeding host function (136). RHS proteins are toxins that are exported to the cell surface through T6SS, and it mediates anti-bacterial activity (137–139). AinS had no significant effect on the main and auxiliary clusters of T6SSs like LitR. However, AinS positively influenced the expression of the *hcp1* and *vgrG1* genes and may indicate that only these T6SS genes are dependent on AHL-mediated QS. We predicted several T6SS effectors in *A. wodanis*, including lipoprotein, nucleases, membrane proteins, amidases and succinylglutamate desuccinylase. However, most of them are putative and hypothetical proteins, which require further research to confirm. From the transcriptomics data, we found that cell density regulated several predicted T6SEs in wild type. Choline dehydrogenase, an osmoprotectant enzyme that protects bacteria from adverse temperatures and other stresses, was more highly expressed at 6°C (140, 141). The temperature has affected expression of several T6SEs indicating a temperature-dependent production of effector proteins. Similar to the LitR regulation of T6SS main and auxiliary clusters, it also controlled several T6SEs. Few T6SEs were also found to be affected by AinS. This may indicate that several effectors are dependent on QS, where LitR influenced the expression higher at LCD and 6°C. Some of the known effectors included porin-like protein H (AWOD_I_1000), a molecular filter for hydrophilic compounds and bacteriocin (AWOD_p920_0063), which is a virulent factor in *A. wodanis* that modulates the growth and virulence of *M. viscosa* (7, 17). Genes encoding T6SS immunity proteins are usually located close to the genes encoding effector proteins (63). The potential immunity protein of Aux-1 (AWOD_I_1437) in *A. wodanis* shows 30% amino acid similarity to the immunity protein in *V. cholerae* strain O1E1 (90), while in Aux-2, the immunity protein (AWOD_II_0134) shows 29% amino acid similarity to *Mucilaginibacter gotjawali* (142). The immunity protein (AWOD_II_1056) in Aux-4 shows 77% amino acid similarity to a hypothetical protein in *A. fischeri* MJ11 (124).

CONCLUSION

In this present study we show that cell densities and temperatures influenced the expression of many genes in *A. wodanis*. Moreover, the QS related genes in *A. wodanis* are cell density- and temperature-dependent, where 6°C plays an essential role in activating the AHL-mediated QS system. *A. wodanis* harbors two CRISPR systems, three T6SSs and four auxiliary T6SSs in

its genome. We show that the CRISPR system 2 and T6SS3 of *A. wodanis* are similar to those in *M. viscosa*, the bacteria with which *A. wodanis* co-exists during winter ulcer disease. The low-temperature 6°C at which winter ulcer occurs exerts a significant effect on the expression pattern of *A. wodanis* than at high-temperature 12°C. We demonstrate here that LitR regulates CRISPR-Cas and T6SSs in a cell density- and temperature manner. Moreover, QS is found to regulate several potential T6SEs in *A. wodanis.* Thus, the QS regulation of T6SSs and CRISPR-Cas system of *A. wodanis* could be essential to understand the possible mechanisms used by *A. wodanis* during its co-existence with other bacteria like *M. viscosa* or the host.

DATA AVAILABILITY STATEMENT

The datasets presented in this study can be found in online repositories. The names of the repository/repositories and accession number(s) can be found in the article/**Supplementary Material**.

AUTHOR CONTRIBUTIONS

AM, EH, HH, and NW conceived and designed the experiments. AM performed the experiments. AM, EH, and NW analyzed the transcriptomics data. AM and NW wrote the manuscript. All authors contributed to reviewing and proof reading the final manuscript.

FUNDING

This work was funded by the Research council of Norway (#270068: ELIXIR2) and UiT The Arctic University of Tromsø. The publication charges for this article have been funded by UiT The Arctic University of Tromsø.

ACKNOWLEDGMENTS

The sequencing service was provided by the Norwegian Sequencing Centre (http://www.sequencing.uio.no), a national technology platform hosted by the University of Oslo and supported by the Functional Genomics and Infrastructure programs of the Research Council of Norway and the Southeastern Regional Health Authorities.

SUPPLEMENTARY MATERIAL

The Supplementary Material for this article can be found online at: https://www.frontiersin.org/articles/10.3389/fvets.2022.799414/full#supplementary-material

REFERENCES

1. Dunlap PV, Kuo A. Cell density-dependent modulation of the *Vibrio fischeri* luminescence system in the absence of autoinducer and LuxR protein. *J Bacteriol.* (1992) 174:2440–8. doi: 10.1128/jb.174.8.2440-2448.1992
2. Fuqua WC, Winans SC, Greenberg EP. Quorum sensing in bacteria: the LuxR-LuxI family of cell density-responsive transcriptional regulators. *J Bacteriol.* (1994) 176:269–75. doi: 10.1128/jb.176.2.269-275.1994
3. Davies DG, Parsek MR, Pearson JP, Iglewski BH, Costerton JW, Greenberg EP. The involvement of cell-to-cell signals in the development of a bacterial biofilm. *Science.* (1998) 280:295–8. doi: 10.1126/science.280.5361.295
4. Zhu J, Miller MB, Vance RE, Dziejman M, Bassler BL, Mekalanos JJ. Quorum-sensing regulators control virulence gene expression in *Vibrio cholerae*. *Proc Natl Acad Sci USA*. (2002) 99:3129–34. doi: 10.1073/pnas.052694299
5. Pena RT, Blasco L, Ambroa A, Gonzalez-Pedrajo B, Fernandez-Garcia L, Lopez M, et al. Relationship Between Quorum Sensing and Secretion Systems. *Front Microbiol.* (2019) 10:1100. doi: 10.3389/fmicb.2019.01100
6. Girard L. Quorum sensing in Vibrio spp.: the complexity of multiple signalling molecules in marine and aquatic environments. *Crit Rev Microbiol.* (2019) 45:451–471. doi: 10.1080/1040841X.2019.1624499
7. Hjerde E, Karlsen C, Sorum H, Parkhill J, Willassen NP, Thomson NR. Co-cultivation and transcriptome sequencing of two co-existing fish pathogens *Moritella viscosa* and *Aliivibrio wodanis*. *BMC Genomics.* (2015) 16:447. doi: 10.1186/s12864-015-1669-z
8. Greenberg EP. Quorum sensing in Gram-negative bacteria: acylhomoserine lactone signalling and cell-cell communication. *Symp Soc Gen Microbi.* (1999) 57:71–84.
9. Milton DL. Quorum sensing in vibrios: complexity for diversification. *Int J Med Microbiol.* (2006) 296:61–71. doi: 10.1016/j.ijmm.2006.01.044
10. Chen X, Schauder S, Potier N, Van Dorsselaer A, Pelczer I, Bassler BL, et al. Structural identification of a bacterial quorum-sensing signal containing boron. *Nature.* (2002) 415:545–9. doi: 10.1038/415545a
11. Lupp C, Ruby EG. *Vibrio fischeri* LuxS and AinS: Comparative study of two signal synthases. *J Bacteriol.* (2004) 186:3873–81. doi: 10.1128/JB.186.12.3873-3881.2004
12. Freeman JA, Bassler BL. Sequence and function of LuxU: a two-component phosphorelay protein that regulates quorum sensing in *Vibrio harveyi*. *J Bacteriol.* (1999) 181:899–906. doi: 10.1128/JB.181.3.899-906.1999
13. Miller MB, Skorupski K, Lenz DH, Taylor RK, Bassler BL. Parallel quorum sensing systems converge to regulate virulence in *Vibrio cholerae*. *Cell.* (2002) 110:303–14. doi: 10.1016/S0092-8674(02)00829-2
14. Lupp C, Urbanowski M, Greenberg EP, Ruby EG. The *Vibrio fischeri* quorum-sensing systems ain and lux sequentially induce luminescence gene expression and are important for persistence in the squid host. *Mol Microbiol.* (2003) 50:319–31. doi: 10.1046/j.1365-2958.2003.t01-1-03585.x
15. Millikan DS, Ruby EG. FlrA, a sigma(54)-dependent transcriptional activator in *Vibrio fischeri*, is required for motility and symbiotic light-organ colonization. *J Bacteriol.* (2003) 185:3547–57. doi: 10.1128/JB.185.12.3547-3557.2003
16. Miyashiro T, Wollenberg MS, Cao X, Oehlert D, Ruby EG. A single qrr gene is necessary and sufficient for LuxO-mediated regulation in *Vibrio fischeri*. *Mol Microbiol.* (2010) 77:1556–67. doi: 10.1111/j.1365-2958.2010.07309.x
17. Benz R, Bauer K. Permeation of Hydrophilic Molecules through the Outer-Membrane of Gram-Negative Bacteria - Review on Bacterial Porins. *Eur J Biochem.* (1988) 176:1–19. doi: 10.1111/j.1432-1033.1988.tb14245.x
18. Konkel ME, Tilly K. Temperature-regulated expression of bacterial virulence genes. *Microbes Infect.* (2000) 2:157–66. doi: 10.1016/S1286-4579(00)00272-0
19. Ramos JL, Gallegos MT, Marques S, Ramos-Gonzalez MI, Espinosa-Urgel M, Segura A. Responses of Gram-negative bacteria to certain environmental stressors. *Curr Opin Microbiol.* (2001) 4:166–71. doi: 10.1016/S1369-5274(00)00183-1
20. Sandy M, Butler A. Microbial Iron Acquisition: Marine and Terrestrial Siderophores. *Chem Rev.* (2009) 109:4580–95. doi: 10.1021/cr9002787

21. Tan HJ, Liu SH, Oliver JD, Wong HC. Role of RpoS in the susceptibility of low salinity-adapted *Vibrio vulnificus* to environmental stresses. *Int J Food Microbiol.* (2010) 137:137–42. doi: 10.1016/j.ijfoodmicro.2009.12.006
22. Quinn MJ, Resch CT, Sun J, Lind EJ, Dibrov P, Hase CC. NhaP1 is a K+(Na+)/H+ antiporter required for growth and internal pH homeostasis of *Vibrio cholerae* at low extracellular pH. *Microbiol-Sgm.* (2012) 158:1094–105. doi: 10.1099/mic.0.056119-0
23. Kohanski MA, Dwyer DJ, Collins JJ. How antibiotics kill bacteria: from targets to networks. *Nat Rev Microbiol.* (2010) 8:423–35. doi: 10.1038/nrmicro2333
24. Mercy C, Ize B, Salcedo SP, De Bentzmann S, Bigot S. Functional Characterization of Pseudomonas Contact Dependent Growth Inhibition (CDI) Systems. *PLoS ONE.* (2016) 11:e0150538. doi: 10.1371/journal.pone.0150538
25. Lasica AM, Ksiazek M, Madej M, Potempa J. The Type IX Secretion System (T9SS): Highlights and recent insights into its structure and function. *Front Cell Infect Mi.* (2017) 7:215. doi: 10.3389/fcimb.2017.00215
26. O'sullivan JN, Rea MC, O'connor PM, Hill C, Ross RP. Human skin microbiota is a rich source of bacteriocin-producing staphylococci that kill human pathogens. *Fems Microbiol Ecol.* (2019) 95:241. doi: 10.1093/femsec/fiy241
27. Yu KW, Xue P, Fu Y, Yang L. T6SS mediated stress responses for bacterial environmental survival and host adaptation. *Int J Mol Sci.* (2021) 22:478. doi: 10.3390/ijms22020478
28. West SA, Buckling A. Cooperation, virulence and siderophore production in bacterial parasites. *P Roy Soc B-Biol Sci.* (2003) 270:37–44. doi: 10.1098/rspb.2002.2209
29. Reichenbach T, Mobilia M, Frey E. Mobility promotes and jeopardizes biodiversity in rock-paper-scissors games. *Nature.* (2007) 448:1046–9. doi: 10.1038/nature06095
30. Natrah FMI, Defoirdt T, Sorgeloos P, Bossier P. Disruption of bacterial cell-to-cell communication by marine organisms and its relevance to aquaculture. *Mar Biotechnol.* (2011) 13:109–26. doi: 10.1007/s10126-010-9346-3
31. Oliveira NM, Martinez-Garcia E, Xavier J, Durham WM, Kolter R, Kim W, et al. Biofilm Formation As a Response to Ecological Competition. *PLoS Biol.* (2015) 13:e1002191. doi: 10.1371/journal.pbio.1002191
32. Schluter J, Nadell CD, Bassler BL, Foster KR. Adhesion as a weapon in microbial competition. *Isme J.* (2015) 9:139–49. doi: 10.1038/ismej.2014.174
33. Roncarati D, Scarlato V. Regulation of heat-shock genes in bacteria: from signal sensing to gene expression output. *Fems Microbiol Rev.* (2017) 41:549–74. doi: 10.1093/femsre/fux015
34. Toska J, Ho BT, Mekalanos JJ. Exopolysaccharide protects *Vibrio cholerae* from exogenous attacks by the type 6 secretion system. *Proc Natl Acad Sci USA.* (2018) 115:7997–8002. doi: 10.1073/pnas.1808469115
35. Mojica FJM, Diez-Villasenor C, Garcia-Martinez J, Soria E. Intervening sequences of regularly spaced prokaryotic repeats derive from foreign genetic elements. *J Mol Evol.* (2005) 60:174–82. doi: 10.1007/s00239-004-0046-3
36. Mruk I, Kobayashi I. To be or not to be: regulation of restriction-modification systems and other toxin-antitoxin systems. *Nucleic Acids Res.* (2014) 42:70–86. doi: 10.1093/nar/gkt711
37. Rostol JT, Marraffini L. (Ph)ighting phages: how bacteria resist their parasites. *Cell Host Microbe.* (2019) 25:184–94. doi: 10.1016/j.chom.2019.01.009
38. Makarova KS, Haft DH, Barrangou R, Brouns SJ, Charpentier E, Horvath P, et al. Evolution and classification of the CRISPR-Cas systems. *Nat Rev Microbiol.* (2011) 9:467–77. doi: 10.1038/nrmicro2577
39. Makarova KS, Wolf YI, Alkhnbashi OS, Costa F, Shah SA, Saunders SJ, et al. An updated evolutionary classification of CRISPR-Cas systems. *Nat Rev Microbiol.* (2015) 13:722–36. doi: 10.1038/nrmicro3569
40. Koonin EV, Makarova KS, Zhang F. Diversity, classification and evolution of CRISPR-Cas systems. *Curr Opin Microbiol.* (2017) 37:67–78. doi: 10.1016/j.mib.2017.05.008
41. Makarova KS, Wolf YI, Iranzo J, Shmakov SA, Alkhnbashi OS, Brouns SJJ, et al. Evolutionary classification of CRISPR-Cas systems: a burst of class 2 and derived variants. *Nat Rev Microbiol.* (2020) 18:67–83. doi: 10.1038/s41579-019-0299-x
42. Mcdonald ND, Regmi A, Morreale DP, Borowski JD, Boyd EF. CRISPR-Cas systems are present predominantly on mobile genetic elements in Vibrio species. *BMC Genomics.* (2019) 20:5439. doi: 10.1186/s12864-019-5439-1
43. Liu TY, Doudna JA. Chemistry of Class 1 CRISPR-Cas effectors: Binding, editing, and regulation. *J Biol Chem.* (2020) 295:14473–87. doi: 10.1074/jbc.REV120.007034
44. Patterson AG, Jackson SA, Taylor C, Evans GB, Salmond GPC, Przybilski R, et al. Quorum sensing controls adaptive immunity through the regulation of multiple CRISPR-Cas systems. *Mol Cell.* (2016) 64:1102–8. doi: 10.1016/j.molcel.2016.11.012
45. Hoyland-Kroghsbo NM, Paczkowski J, Mukherjee S, Broniewski J, Westra E, Bondy-Denomy J, et al. Quorum sensing controls the *Pseudomonas aeruginosa* CRISPR-Cas adaptive immune system. *Proc Natl Acad Sci USA.* (2017) 114:131–5. doi: 10.1073/pnas.1617415113
46. Mion S, Plener L, Remy B, Daude D, Chabriere E. Lactonase SsoPox modulates CRISPR-Cas expression in Gram-negative proteobacteria using AHL-based quorum sensing systems. *Res Microbiol.* (2019) 170:296–9. doi: 10.1016/j.resmic.2019.06.004
47. Broniewski JM, Chisnall M, Hoyland-Kroghsbo NM, Buckling A, Westra ER. The effect of Quorum sensing inhibitors on the evolution of CRISPR-based phage immunity in *Pseudomonas aeruginosa*. *Isme J.* (2021) 15:2465–73. doi: 10.1038/s41396-021-00946-6
48. Weber B, Hasic M, Chen C, Wai SN, Milton DL. Type VI secretion modulates quorum sensing and stress response in *Vibrio anguillarum*. *Environ Microbiol.* (2009) 11:3018–28. doi: 10.1111/j.1462-2920.2009.02005.x
49. Sheng LL, Gu D, Wang QY, Liu Q, Zhang YX. Quorum sensing and alternative sigma factor RpoN regulate type VI secretion system I (T6SSVA1) in fish pathogen *Vibrio alginolyticus*. *Arch Microbiol.* (2012) 194:379–90. doi: 10.1007/s00203-011-0780-z
50. Wang L, Zhou DS, Mao PY, Zhang YQ, Hou J, Hu Y, et al. Cell density- and quorum sensing-dependent expression of type VI secretion system 2 in *Vibrio parahaemolyticus*. *PLoS ONE.* (2013) 8:e073363. doi: 10.1371/journal.pone.0073363
51. Shao Y, Bassler BL. Quorum regulatory small RNAs repress type VI secretion in *Vibrio cholerae*. *Mol Microbiol.* (2014) 92:921–30. doi: 10.1111/mmi.12599
52. Liu X, Pan J, Gao H, Han Y, Zhang A, Huang Y, et al. CqsA/LuxS-HapR Quorum sensing circuit modulates type VI secretion system V fl T6SS2 in *Vibrio fluvialis*. *Emerg Microbes Infect.* (2021) 10:589–601. doi: 10.1080/22221751.2021.1902244
53. Leung KY, Siame BA, Snowball H, Mok YK. Type VI secretion regulation: crosstalk and intracellular communication. *Curr Opin Microbiol.* (2011) 14:9–15. doi: 10.1016/j.mib.2010.09.017
54. Ho BT, Dong TG, Mekalanos JJ. A view to a kill: the bacterial type VI secretion system. *Cell Host Microbe.* (2014) 15:9–21. doi: 10.1016/j.chom.2013.11.008
55. Cianfanelli FR, Monlezun L, Coulthurst SJ. Aim, load, fire: the type VI secretion system, a bacterial nanoweapon. *Trends Microbiol.* (2016) 24:51–62. doi: 10.1016/j.tim.2015.10.005
56. Wang J, Brodmann M, Basler M. Assembly and subcellular localization of bacterial type VI secretion systems. *Annu Rev Microbiol.* (2019) 73:621–38. doi: 10.1146/annurev-micro-020518-115420
57. Wang TT, Si MR, Song YH, Zhu WH, Gao F, Wang Y, et al. Type VI secretion system transports Zn2+ to combat multiple stresses and host immunity. *PLoS Pathog.* (2015) 11:1005020. doi: 10.1371/journal.ppat.1005020
58. Lin JS, Zhang WP, Cheng JL, Yang X, Zhu KX, Wang Y, et al. A Pseudomonas T6SS effector recruits PQS-containing outer membrane vesicles for iron acquisition. *Nat Commun.* (2017) 8:14888. doi: 10.1038/ncomms14888
59. Mougous JD, Cuff ME, Raunser S, Shen A, Zhou M, Gifford CA, et al. A virulence locus of *Pseudomonas aeruginosa* encodes a protein secretion apparatus. *Science.* (2006) 312:1526–30. doi: 10.1126/science.1128393
60. Pukatzki S, Ma AT, Sturtevant D, Krastins B, Sarracino D, Nelson WC, et al. Identification of a conserved bacterial protein secretion system in *Vibrio cholerae* using the Dictyostelium host model system. *Proc Natl Acad Sci USA.* (2006) 103:1528–33. doi: 10.1073/pnas.0510322103
61. Schell MA, Ulrich RL, Ribot WJ, Brueggemann EE, Hines HB, Chen D, et al. Type VI secretion is a major virulence determinant in *Burkholderia mallei*. *Mol Microbiol.* (2007) 64:1466–85. doi: 10.1111/j.1365-2958.2007.05734.x

62. Russell AB, Peterson SB, Mougous JD. Type VI secretion system effectors: poisons with a purpose. *Nat Rev Microbiol.* (2014) 12:137–48. doi: 10.1038/nrmicro3185
63. Lien YW, Lai EM. Type VI secretion effectors: methodologies and biology. *Front Cell Infect Microbiol.* (2017) 7:254. doi: 10.3389/fcimb.2017.00254
64. Ma J, Pan Z, Huang J, Sun M, Lu C, Yao H. The Hcp proteins fused with diverse extended-toxin domains represent a novel pattern of antibacterial effectors in type VI secretion systems. *Virulence.* (2017) 8:1189–202. doi: 10.1080/21505594.2017.1279374
65. Prochazkova K, Shuvalova LA, Minasov G, Voburka Z, Anderson WF, Satchell KJF. Structural and molecular mechanism for autoprocessing of MARTX toxin of *Vibrio cholerae* at multiple sites. *J Biol Chem.* (2009) 284:26557–68. doi: 10.1074/jbc.M109.025510
66. Miyata ST, Kitaoka M, Brooks TM, Mcauley SB, Pukatzki S. *Vibrio cholerae* requires the type VI secretion system virulence factor VasX to kill *Dictyostelium discoideum*. *Infect Immun.* (2011) 79:2941–9. doi: 10.1128/IAI.01266-10
67. Whitney JC, Chou S, Russell AB, Biboy J, Gardiner TE, Ferrin MA, et al. Identification, structure, and function of a novel type VI secretion peptidoglycan glycoside hydrolase effector-immunity pair. *J Biol Chem.* (2013) 288:26616–24. doi: 10.1074/jbc.M113.488320
68. Jiang F, Waterfield NR, Yang J, Yang GW, Jin Q. A *Pseudomonas aeruginosa* type VI secretion phospholipase D effector targets both prokaryotic and eukaryotic cells. *Cell Host Microbe.* (2014) 15:600–10. doi: 10.1016/j.chom.2014.04.010
69. Chen H, Yang DH, Han FJ, Tan JC, Zhang LZ, Xiao JF, et al. The bacterial T6SS effector EvpP prevents NLRP3 inflammasome activation by inhibiting the Ca2+-dependent MAPK-Jnk pathway. *Cell Host Microbe.* (2017) 21:47–58. doi: 10.1016/j.chom.2016.12.004
70. Hood RD, Singh P, Hsu FS, Guvener T, Carl MA, Trinidad RRS, et al. A type VI secretion system of *Pseudomonas aeruginosa* targets, a toxin to bacteria. *Cell Host Microbe.* (2010) 7:25–37. doi: 10.1016/j.chom.2009.12.007
71. Brooks TM, Unterweger D, Bachmann V, Kostiuk B, Pukatzki S. Lytic activity of the *Vibrio cholerae* type VI secretion toxin VgrG-3 is inhibited by the antitoxin TsaB. *J Biol Chem.* (2013) 288:7618–25. doi: 10.1074/jbc.M112.436725
72. Hersch SJ, Watanabe N, Stietz MS, Manera K, Kamal F, Burkinshaw B, et al. Envelope stress responses defend against type six secretion system attacks independently of immunity proteins. *Nat Microbiol.* (2020) 5:706–14. doi: 10.1038/s41564-020-0672-6
73. Lunder T, Sorum H, Holstad G, Steigerwalt AG, Mowinckel P, Brenner DJ. Phenotypic and genotypic characterization of *Vibrio viscosus* sp nov and *Vibrio wodanis* sp nov isolated from Atlantic salmon *(Salmo salar)* with 'winter ulcer'. *Int J Syst Evol Micr.* (2000) 50:427–50. doi: 10.1099/00207713-50-2-427
74. Lunder T, Evensen Ø, Holstad G, Hastein T. Winter ulcer in the atlantic salmon *salmo salar* - pathological and bacteriological investigations and transmission experiments. *Dis Aquat Organ.* (1995) 23:39–49. doi: 10.3354/dao023039
75. Benediktsdottir E, Helgason S, Sigurjonsdottir H. Vibrio spp. *i*solated from salmonids with shallow skin lesions and reared at low temperature. *J Fish Dis.* (1998) 21:19–28. doi: 10.1046/j.1365-2761.1998.00065.x
76. Lovoll M, Wiik-Nielsen CR, Tunsjo HS, Colquhoun D, Lunder T, Sorum H, et al. Atlantic salmon bath challenged with *Moritella viscosa*–pathogen invasion and host response. *Fish Shellfish Immunol.* (2009) 26:877–84. doi: 10.1016/j.fsi.2009.03.019
77. Bruno DW, Griffiths J, Petrie J, Hastings TS. *Vibrio viscosus* in farmed Atlantic salmon *Salmo salar* in Scotland: field and experimental observations. *Dis Aquat Organ.* (1998) 34:161–6. doi: 10.3354/dao034161
78. Karlsen C, Vanberg C, Mikkelsen H, Sorum H. Co-infection of Atlantic salmon *(Salmo salar)*, by *Moritella viscosa* and *Aliivibrio wodanis*, development of disease and host colonization. *Vet Microbiol.* (2014) 171:112–21. doi: 10.1016/j.vetmic.2014.03.011
79. Purohit AA, Johansen JA, Hansen H, Leiros HKS, Kashulin A, Karlsen C, et al. Presence of acyl-homoserine lactones in 57 members of the Vibrionaceae family. *J Appl Microbiol.* (2013) 115:835–47. doi: 10.1111/jam.12264
80. Maharajan A, Hansen H, Khider M, Willassen N. Quorum sensing in *Aliivibrio wodanis* 06/09/139 and its role in controlling various phenotypic traits. *Peerj.* (2021) 9:11980. doi: 10.7717/peerj.11980
81. Magoc T, Wood D, Salzberg SL. EDGE-pro: estimated degree of gene expression in prokaryotic genomes. *Evol Bioinform Online.* (2013) 9:127–36. doi: 10.4137/EBO.S11250
82. Love MI, Huber W, Anders S. Moderated estimation of fold change and dispersion for RNA-seq data with DESeq2. *Genome Biol.* (2014) 15:550. doi: 10.1186/s13059-014-0550-8
83. Kanehisa M, Goto S, Sato Y, Furumichi M, Tanabe M. KEGG for integration and interpretation of large-scale molecular data sets. *Nucleic Acids Res.* (2012) 40:D109–14. doi: 10.1093/nar/gkr988
84. Couvin D, Bernheim A, Toffano-Nioche C, Touchon M, Michalik J, Neron B, et al. CRISPRCasFinder, an update of CRISRFinder, includes a portable version, enhanced performance and integrates search for Cas proteins. *Nucleic Acids Res.* (2018) 46:W246–51. doi: 10.1093/nar/gky425
85. Grissa I, Vergnaud G, Pourcel C. CRISPRFinder: a web tool to identify clustered regularly interspaced short palindromic repeats. *Nucleic Acids Res.* (2007) 35:W52–7. doi: 10.1093/nar/gkm360
86. Biswas A, Gagnon JN, Brouns SJJ, Fineran PC, Brown CM. CRISPRTarget: Bioinformatic prediction and analysis of crRNA targets. *Rna Biol.* (2013) 10:817–27. doi: 10.4161/rna.24046
87. Zhou Y, Liang YJ, Lynch KH, Dennis JJ, Wishart DS. PHAST: A fast phage search tool. *Nucleic Acids Res.* (2011) 39:W347–52. doi: 10.1093/nar/gkr485
88. Arndt D, Grant JR, Marcu A, Sajed T, Pon A, Liang Y, et al. PHASTER: a better, faster version of the PHAST phage search tool. *Nucleic Acids Res.* (2016) 44:W16–21. doi: 10.1093/nar/gkw387
89. Li J, Yao YF, Xu HH, Hao LM, Deng ZX, Rajakumar K, et al. SecReT6: a web-based resource for type VI secretion systems found in bacteria. *Environ Microbiol.* (2015) 17:2196–202. doi: 10.1111/1462-2920.12794
90. Joshi A, Kostiuk B, Rogers A, Teschler J, Pukatzki S, Yildiz FH. Rules of engagement: The type VI secretion system in *Vibrio cholerae*. *Trends Microbiol.* (2017) 25:267–79. doi: 10.1016/j.tim.2016.12.003
91. Wang JW, Yang BJ, Leier A, Marquez-Lago TT, Hayashida M, Rocker A, et al. Bastion6: a bioinformatics approach for accurate prediction of type VI secreted effectors. *Bioinformatics.* (2018) 34:2546–55. doi: 10.1093/bioinformatics/bty155
92. Unterweger D, Kostiuk B, Otjengerdes R, Wilton A, Diaz-Satizabal L, Pukatzki S. Chimeric adaptor proteins translocate diverse type VI secretion system effectors in *Vibrio cholerae*. *EMBO J.* (2015) 34:2198–210. doi: 10.15252/embj.201591163
93. Spinola-Amilibia M, Davo-Siguero I, Ruiz FM, Santillana E, Medrano FJ, Romero A. The structure of VgrG1 from *Pseudomonas aeruginosa*, the needle tip of the bacterial type VI secretion system. *Acta Crystallogr D Struct Biol.* (2016) 72:22–33. doi: 10.1107/S2059798315021142
94. Pukatzki S, Ma AT, Revel AT, Sturtevant D, Mekalanos JJ. Type VI secretion system translocates a phage tail spike-like protein into target cells where it cross-links actin. *Proc Natl Acad Sci USA.* (2007) 104:15508–13. doi: 10.1073/pnas.0706532104
95. Zoued A, Durand E, Bebeacua C, Brunet YR, Douzi B, Cambillau C, et al. TssK is a trimeric cytoplasmic protein interacting with components of both phage-like and membrane anchoring complexes of the type VI secretion system. *J Biol Chem.* (2013) 288:27031–41. doi: 10.1074/jbc.M113.499772
96. Brunet YR, Zoued A, Boyer F, Douzi B, Cascales E. The type VI secretion TssEFGK-VgrG phage-like baseplate is recruited to the TssJLM membrane complex via multiple contacts and serves as assembly platform for tail tube/sheath polymerization. *PLoS Genet.* (2015) 11:1005545. doi: 10.1371/journal.pgen.1005545
97. Bonemann G, Pietrosiuk A, Diemand A, Zentgraf H, Mogk A. Remodelling of VipA/VipB tubules by ClpV-mediated threading is crucial for type VI protein secretion. *EMBO J.* (2009) 28:315–25. doi: 10.1038/emboj.2008.269
98. Pietrosiuk A, Lenherr ED, Falk S, Bonemann G, Kopp J, Zentgraf H, et al. Molecular basis for the unique role of the AAA+ chaperone ClpV in type VI protein secretion. *J Biol Chem.* (2011) 286:30010–21. doi: 10.1074/jbc.M111.253377
99. Kitaoka M, Miyata ST, Brooks TM, Unterweger D, Pukatzki S. VasH is a transcriptional regulator of the type VI secretion system functional

in endemic and pandemic vibrio cholerae. *J Bacteriol.* (2011) 193:6471–82. doi: 10.1128/JB.05414-11
100. Sana TG, Hachani A, Bucior I, Soscia C, Garvis S, Termine E, et al. The second type VI secretion system of *Pseudomonas aeruginosa* strain PAO1 is regulated by quorum sensing and fur and modulates internalization in epithelial cells. *J Biol Chem.* (2012) 287:27095–105. doi: 10.1074/jbc.M112.376368
101. An JH, Goo E, Kim H, Seo YS, Hwang I. Bacterial quorum sensing and metabolic slowing in a cooperative population. *P Natl Acad Sci USA.* (2014) 111:14912–7. doi: 10.1073/pnas.1412431111
102. Hoyland-Kroghsbo NM, Munoz KA, Bassler BL. Temperature, by controlling growth rate, regulates CRISPR-Cas activity in *Pseudomonas aeruginosa*. *Mbio*. (2018) 9:2184. doi: 10.1128/mBio.02184-18
103. Khider M, Hjerde E, Hansen H, Willassen NP. Differential expression profiling of litR and rpoQ mutants reveals insight into QS regulation of motility, adhesion and biofilm formation in *Aliivibrio salmonicida*. *BMC Genomics.* (2019) 20:5594. doi: 10.1186/s12864-019-5594-4
104. Urmersbach S, Aho T, Alter T, Hassan SS, Autio R, Huehn S. Changes in global gene expression of *Vibrio parahaemolyticus* induced by cold- and heat-stress. *Bmc Microbiol.* (2015) 15:565. doi: 10.1186/s12866-015-0565-7
105. Khider M, Hansen H, Hjerde E, Johansen JA, Willassen NP. Exploring the transcriptome of luxI(-) and Delta ainS mutants and the impact of N-3-oxo-hexanoyl-L- and N-3-hydroxy-decanoyl-L-homoserine lactones on biofilm formation in *Aliivibrio salmonicida*. *Peerj.* (2019) 7:6845. doi: 10.7717/peerj.6845
106. Feng L, Rutherford ST, Papenfort K, Bagert JD, Van Kessel JC, Tirrell DA, et al. A Qrr noncoding RNA deploys four different regulatory mechanisms to optimize quorum-sensing dynamics. *Cell.* (2015) 160:228–40. doi: 10.1016/j.cell.2014.11.051
107. Hansen H, Purohit AA, Leiros HKS, Johansen JA, Kellermann SJ, Bjelland AM, et al. The autoinducer synthases LuxI and AinS are responsible for temperature-dependent AHL production in the fish pathogen *Aliivibrio salmonicida*. *Bmc Microbiol.* (2015) 15:402. doi: 10.1186/s12866-015-0402-z
108. Lyell NL, Colton DM, Bose JL, Tumen-Velasquez MP, Kimbrough JH, Stabb EV. Cyclic AMP receptor protein regulates pheromone-mediated bioluminescence at multiple levels in *Vibrio fischeri* ES114. *J Bacteriol.* (2013) 195:5051–63. doi: 10.1128/JB.00751-13
109. Almendros C, Guzman NM, Garcia-Martinez J, Mojica FJM. Anti-cas spacers in orphan CRISPR4 arrays prevent uptake of active CRISPR-Cas I-F systems. *Nat Microbiol.* (2016) 1:81. doi: 10.1038/nmicrobiol.2016.81
110. Vale PF, Lafforgue G, Gatchitch F, Gardan R, Moineau S, Gandon S. Costs of CRISPR-Cas-mediated resistance in *Streptococcus thermophilus*. *P Roy Soc B-Biol Sci.* (2015) 282:41–49. doi: 10.1098/rspb.2015.1270
111. Agari Y, Sakamoto K, Tamakoshi M, Oshima T, Kuramitsu S, Shinkai A. Transcription profile of *Thermus thermophilus* CRISPR systems after phage infection. *J Mol Biol.* (2010) 395:270–81. doi: 10.1016/j.jmb.2009.10.057
112. Perez-Rodriguez R, Haitjema C, Huang QQ, Nam KH, Bernardis S, Ke AL, et al. Envelope stress is a trigger of CRISPR RNA-mediated DNA silencing in *Escherichia coli*. *Mol Microbiol.* (2011) 79:584–99. doi: 10.1111/j.1365-2958.2010.07482.x
113. Meaden S, Capria L, Alseth E, Gandon S, Biswas A, Lenzi L, et al. Phage gene expression and host responses lead to infection-dependent costs of CRISPR immunity. *Isme J.* (2021) 15:534–44. doi: 10.1038/s41396-020-00794-w
114. Bondy-Denomy J, Pawluk A, Maxwell KL, Davidson AR. Bacteriophage genes that inactivate the CRISPR/Cas bacterial immune system. *Nature.* (2013) 493:429–181. doi: 10.1038/nature11723
115. Pawluk A, Bondy-Denomy J, Cheung VHW, Maxwell KL, Davidson AR. A new group of phage anti-CRISPR genes inhibits the type I-E CRISPR-Cas system of *Pseudomonas aeruginosa*. *Mbio.* (2014) 5:869. doi: 10.1128/mBio.00896-14
116. Yi H, Huang L, Yang B, Gomez J, Zhang H, Yin Y. AcrFinder: genome mining anti-CRISPR operons in prokaryotes and their viruses. *Nucleic Acids Res.* (2020) 48:W358–65. doi: 10.1093/nar/gkaa351
117. Bobay LM, Touchon M, Rocha EPC. Pervasive domestication of defective prophages by bacteria. *Proc Natl Acad Sci USA.* (2014) 111:12127–32. doi: 10.1073/pnas.1405336111
118. Czajkowski R. The phage be with you? Prophage-like elements in the genomes of soft rot *Pectobacteriaceae*: *Pectobacterium spp*. and Dickeya spp. *Front Microbiol.* (2019) 10:138. doi: 10.3389/fmicb.2019.00138
119. Chen L, Xiong Z, Sun L, Yang J, Jin Q. VFDB 2012 update: toward the genetic diversity and molecular evolution of bacterial virulence factors. *Nucleic Acids Res.* (2012) 40:D641–5. doi: 10.1093/nar/gkr989
120. Bingle LEH, Bailey CM, Pallen MJ. Type VI secretion: a beginner's guide. *Curr Opin Microbiol.* (2008) 11:3–8. doi: 10.1016/j.mib.2008.01.006
121. Schwarz S, West TE, Boyer F, Chiang WC, Carl MA, Hood RD, et al. Burkholderia type VI secretion systems have distinct roles in eukaryotic and bacterial cell interactions. *PLoS Pathog.* (2010) 6:e1001068. doi: 10.1371/journal.ppat.1001068
122. Si MR, Zhao C, Burkinshaw B, Zhang B, Wei DW, Wang Y, et al. Manganese scavenging and oxidative stress response mediated by type VI secretion system in *Burkholderia thailandensis*. *Proc Natl Acad Sci USA.* (2017) 114:E2233–42. doi: 10.1073/pnas.1614902114
123. Huang Y, Du P, Zhao M, Liu W, Du Y, Diao B, et al. Functional characterization and conditional regulation of the type VI secretion system in *Vibrio fluvialis*. *Front Microbiol.* (2017) 8:528. doi: 10.3389/fmicb.2017.00528
124. Speare L, Cecere AG, Guckes KR, Smith S, Wollenberg MS, Mandel MJ, et al. Bacterial symbionts use a type VI secretion system to eliminate competitors in their natural host. *Proc Natl Acad Sci USA.* (2018) 115:E8528–37. doi: 10.1073/pnas.1808302115
125. Bjornsdottir B, Hjerde E, Bragason BT, Gudmundsdottir T, Willassen NP, Gudmundsdottir BK. Identification of type VI secretion systems in *Moritella viscosa*. *Vet Microbiol.* (2012) 158:436–42. doi: 10.1016/j.vetmic.2012.02.030
126. Rodrigues S, Paillard C, Van Dillen S, Tahrioui A, Berjeaud JM, et al. Relation between biofilm and virulence in *Vibrio tapetis*: a transcriptomic study. *Pathogens.* (2018) 7:92. doi: 10.3390/pathogens7040092
127. Peng Y, Wang XR, Shou J, Zong BB, Zhang YY, Tan J, et al. Roles of Hcp family proteins in the pathogenesis of the porcine extraintestinal pathogenic *Escherichia coli* type VI secretion system. *Sci Rep-Uk.* (2016) 6:26816. doi: 10.1038/srep26816
128. Zhou Y, Tao J, Yu H, Ni J, Zeng L, Teng Q, et al. Hcp family proteins secreted via the type VI secretion system coordinately regulate *Escherichia coli* K1 interaction with human brain microvascular endothelial cells. *Infect Immun.* (2012) 80:1243–51. doi: 10.1128/IAI.05994-11
129. Ma AT, Mekalanos JJ. *In vivo* actin cross-linking induced by *Vibrio cholerae* type VI secretion system is associated with intestinal inflammation. *Proc Natl Acad Sci USA.* (2010) 107:4365–70. doi: 10.1073/pnas.0915156107
130. Seibt H, Aung KM, Ishikawa T, Sjöström A, Gullberg M, Atkinson GC, et al. Elevated levels of VCA0117 (VasH) in response to external signals activate the type VI secretion system of *Vibrio cholerae* O1 El Tor A1552. *Environ Microbiol.* (2020) 22:4409–23. doi: 10.1111/1462-2920.15141
131. Metzger LC, Stutzmann S, Scrignari T, Van Der Henst C, Matthey N, Blokesch M. Independent regulation of type VI secretion in *Vibrio cholerae* by TfoX and TfoY. *Cell Rep.* (2016) 15:951–8. doi: 10.1016/j.celrep.2016.03.092
132. Ishikawa T, Sabharwal D, Broms J, Milton DL, Sjostedt A, Uhlin BE, et al. Pathoadaptive conditional regulation of the type VI secretion system in *Vibrio cholerae* O1 strains. *Infect Immun.* (2012) 80:575–84. doi: 10.1128/IAI.05510-11
133. Salomon D, Gonzalez H, Updegraff BL, Orth K. *Vibrio parahaemolyticus* type VI secretion system 1 is activated in marine conditions to target bacteria, and is differentially regulated from system 2. *PLoS ONE.* (2013) 8:e061086. doi: 10.1371/journal.pone.0061086
134. Yang Z, Zhou X, Ma Y, Zhou M, Waldor MK, Zhang Y, et al. Serine/threonine kinase PpkA coordinates the interplay between T6SS2 activation and quorum sensing in the marine pathogen *Vibrio alginolyticus*. *Environ Microbiol.* (2018) 20:903–19. doi: 10.1111/1462-2920.14039
135. Pieper R, Huang ST, Robinson JM, Clark DJ, Alami H, Parmar PP, et al. Temperature and growth phase influence the outer-membrane proteome and the expression of a type VI secretion system in *Yersinia pestis*. *Microbiol-Sgm.* (2009) 155:498–512. doi: 10.1099/mic.0.022160-0
136. Al-Khodor S, Price CT, Kalia A, Abu Kwaik Y. Functional diversity of ankyrin repeats in microbial proteins. *Trends Microbiol.* (2010) 18:132–9. doi: 10.1016/j.tim.2009.11.004

137. Koskiniemi S, Lamoureux JG, Nikolakakis KC, De Roodenbeke CT, Kaplan MD, Low DA, et al. Rhs proteins from diverse bacteria mediate intercellular competition. *P Natl Acad Sci USA*. (2013) 110:7032–7. doi: 10.1073/pnas.1300627110
138. Diniz JA, Coulthurst SJ. Intraspecies competition in serratia marcescens is mediated by type VI-Secreted Rhs effectors and a conserved effector-associated accessory protein. *J Bacteriol.* (2015) 197:2350–60. doi: 10.1128/JB.00199-15
139. Pei TT, Li H, Liang X, Wang ZH, Liu G, Wu LL, et al. Intramolecular chaperone-mediated secretion of an Rhs effector toxin by a type VI secretion system. *Nat Commun.* (2020) 11:1865. doi: 10.1038/s41467-020-15774-z
140. Gadda G, Mcallister-Wilkins EE. Cloning, expression, and purification of choline dehydrogenase from the moderate halophile *Halomonas elongata*. *Appl Environ Microbiol.* (2003) 69:2126–32. doi: 10.1128/AEM.69.4.2126-2132.2003
141. Tang D, Wang X, Wang J, Wang M, Wang Y, Wang W. Choline-betaine pathway contributes to hyperosmotic stress and subsequent lethal stress resistance in *Pseudomonas protegens* SN15-2. *J Biosci.* (2020) 45:60. doi: 10.1007/s12038-020-00060-3
142. Zhang DP, Iyer LM, Aravind L. A novel immunity system for bacterial nucleic acid degrading toxins and its recruitment in various eukaryotic and DNA viral systems. *Nucleic Acids Res.* (2011) 39:4532–52. doi: 10.1093/nar/gkr036

Conflict of Interest: The authors declare that the research was conducted in the absence of any commercial or financial relationships that could be construed as a potential conflict of interest.

Publisher's Note: All claims expressed in this article are solely those of the authors and do not necessarily represent those of their affiliated organizations, or those of the publisher, the editors and the reviewers. Any product that may be evaluated in this article, or claim that may be made by its manufacturer, is not guaranteed or endorsed by the publisher.

frontiers in Veterinary Science

ORIGINAL RESEARCH
published: 09 March 2022
doi: 10.3389/fvets.2022.847977

Co-infection of *Candidatus* Piscichlamydia Trichopodus (Order *Chlamydiales*) and *Henneguya* sp. (Myxosporea, Myxobolidae) in Snakeskin Gourami *Trichopodus pectoralis* (Regan 1910)

Nguyen Dinh-Hung[1,2], *Ha Thanh Dong*[3], *Chayanit Soontara*[4], *Channarong Rodkhum*[1,2], *Sukkrit Nimitkul*[4], *Prapansak Srisapoome*[4,5], *Pattanapon Kayansamruaj*[4,5*†] and *Satid Chatchaiphan*[4*]

[1] The International Graduate Program of Veterinary Science and Technology, Faculty of Veterinary Science, Chulalongkorn University, Bangkok, Thailand, [2] Center of Excellence in Fish Infectious Diseases, Department of Veterinary Microbiology, Faculty of Veterinary Science, Chulalongkorn University, Bangkok, Thailand, [3] Department of Food, Agriculture and Bioresources, Aquaculture and Aquatic Resources Management Program, Asian Institute of Technology, School of Environment, Klong Luang, Thailand, [4] Department of Aquaculture, Faculty of Fisheries, Kasetsart University, Bangkok, Thailand, [5] Center of Excellence in Aquatic Animal Health Management, Faculty of Fisheries, Kasetsart University, Bangkok, Thailand

The present study describes a simultaneous infection of a novel *Chlamydia*-like organism (CLO) with a Myxozoa parasite, *Henneguya* sp. in snakeskin gourami *Trichopodus pectoralis* in Thailand. A new CLO is proposed "*Candidatus* Piscichlamydia trichopodus" (CPT) based on 16S rRNA phylogenetic analysis. Systemic intracellular CPT infection was confirmed by histological examination, *in situ* hybridization, PCR assay, and sequencing of 16S rRNA. This novel pathogen belongs to the order *Chlamydiales* but differs in certain aspects from other species. The histopathological changes associated with CPT infection were different from the typical pathological lesions of epitheliocystis caused by previously known CLO. Unlike other CLO, CPT localized in the connective tissue rather than in the epithelial cells and formed smaller clumps of intracellular bacteria that stained dark blue with hematoxylin. On the other hand, typical myxospores of the genus *Henneguya* with tails were observed in the gill sections. Infection with *Henneguya* sp. resulted in extensive destruction of the gill filaments, most likely leading to respiratory distress. Due to the frequency of co-infections and the unavailability of culture methods for CLO and *Henneguya* sp., it was difficult to determine which pathogens were directly responsible for the associated mortality. However, co-infections may increase the negative impact on the host and the severity of the disease. Given the commercial importance of the snakeskin gourami and its significant aquaculture potential, the findings of this study are important for further studies on disease prevention.

Keywords: ***Chlamydiales***, ***Chlamydia*-like organism**, ***Henneguya* sp.**, **snakeskin gourami**, ***Candidatus* Piscichlamydia trichopodus**, **16S rRNA**

OPEN ACCESS

Edited by:
Valentina Virginia Ebani, University of Pisa, Italy

Reviewed by:
Dieter Steinhagen, University of Veterinary Medicine Hannover, Germany
Luis Garcia Prieto, Universidad Nacional Autónoma de México, Mexico

***Correspondence:**
Pattanapon Kayansamruaj
pattanapon.k@ku.th
Satid Chatchaiphan
satid.ch@ku.th

†*Deceased*

Specialty section:
This article was submitted to Veterinary Infectious Diseases, a section of the journal Frontiers in Veterinary Science

Received: *03 January 2022*
Accepted: *03 February 2022*
Published: *09 March 2022*

Citation:
Dinh-Hung N, Dong HT, Soontara C, Rodkhum C, Nimitkul S, Srisapoome P, Kayansamruaj P and Chatchaiphan S (2022) Co-infection of Candidatus Piscichlamydia Trichopodus (Order Chlamydiales) and Henneguya sp. (Myxosporea, Myxobolidae) in Snakeskin Gourami Trichopodus pectoralis (Regan 1910). Front. Vet. Sci. 9:847977. doi: 10.3389/fvets.2022.847977

INTRODUCTION

Snakeskin gourami, *Trichopodus pectoralis,* is native to Southeast Asia and commonly found in the Mekong and Chao Phraya basins of Cambodia, Thailand, Southern Vietnam, and Laos (1). In Thailand, the snakeskin gourami is a highly economic species and has become one of the five most important freshwater species in aquaculture (2, 3). Increased incidence of parasitic and bacterial diseases is one of the major obstacles to the farming of this species (4). However, studies on the occurrence of diseases in *T. pectoralis* are still very scarce (5). The pathogen fauna of this species is poorly understood and may contain pathogens that have not yet been described in the literature.

Myxosporeans are diverse and widespread parasites that cause severe economic damage to fish worldwide (6–8). The genus *Henneguya* includes more than 200 species and is one of the most diverse myxosporean genera in the family *Myxobolidae* (8). Morphologically, this genus is distinguished from the other genera of the family *Myxobolidae* by its elongated myxospores, which consist of two shell valves, each with a caudal projection, a usually binucleate sporoplasm, and two apical polar capsules (6, 9, 10). Some species of the genus *Henneguya* are responsible for diseases leading to high mortality rates, but most species are thought to have little or no negative impact on fish health (6, 11). Infection from *Henneguya* sp. usually occurs in the gills and is characterized by the presence of cyst-like structures on the gill filaments (6, 7, 12). Infection can devastate fish populations when the parasites multiply in high densities on the gills and leads to respiratory failure, especially in juvenile fish (13, 14). Other commonly known pathogens that cause gill cysts in fish are bacteria from the order *Chlamydiales*. These bacteria typically cause epithelial cysts in the skin and gills called epitheliocystis (15–17). However, it is noteworthy that different *Chlamydia*-like organisms (CLOs) have been found to have different pathology upon infection, possibly depending on the chlamydial species, the infected host, and the affected tissue (18). To date, unavailability of culture techniques for chlamydial pathogens has been a major obstacle for *in vitro* studies (15, 18).

In the present study, we described for the first time a systemic pathology caused by a novel *Chlamydia*-like organism, *Candidatus* Piscichlamydia trichopodus (order *Chlamydiales*) and a gill parasite *Henneguya* sp. (Myxosporea, Myxobolidae) infecting the same fish population. Pathogen characterization was performedbased on molecular analyses with detailed histopathological observations and confirmation by *in situ* hybridization (ISH).

MATERIALS AND METHODS

Fish and Case History

In March 2021, higher than average mortality was observed in snakeskin gourami fingerlings in two nursery ponds in Suphan Buri province, central Thailand. History entails that snakeskin gourami fingerlings ($0.3\ g \pm 0.05$) reared by traditional methods (19) were purchased from a hatchery. Male and female broodstock were naturally mated in an earthen pond. Eggs were spawned in natural bubble nests made by male gourami in the same pond. Offspring were harvested at the size of 3.0 cm (weight 0.2–0.3 g) and 150,000 fish were delivered to the two ponds mentioned above. The fish were kept in a 5 m^2 net in the pond and fed daily with a commercial pellet diet containing 28% protein (Betagro, Thailand), administered at a rate of 3% of body weight.

Gross Necropsy and Histopathology

Representative 10 fingerlings were collected on day 6 after disease onset for further examination approved by the Institutional Animal Care and Use Committee of Kasetsart University (Approval ID: ACKU63-FIS-009). After euthanasia with clove oil (150 ppm/l), fresh skin mucus and gill samples were collected for microscopic examination. Bacteriological examination of brain, liver and kidney tissue samples was performed by streaking on tryptic soy agar and brain-heart infusion agar (BHIA) (Himedia, India) and incubation at 28°C for 48 h. Samples from whole body fish ($n = 5$) and detached gills ($n = 10$) were fixed in 10% neutral buffered formalin and processed routinely for histology. Paraffin-embedded gills were sectioned at 5 μm, stained with haematoxylin and eosin and examined under a light microscope. The morphology of the spore and polar capsules were used to make a tentative genus classification of myxospores in this study, as previously described by Lom and Arthur (6, 9) and Fiala et al. (20).

DNA Extraction, 16S rRNA Amplification, and Sequencing

Genomic DNA was isolated from infected gills using the Tissue Genomic DNA Mini kit (Geneaid, Taiwan) according to the manufacturer's instructions. The presence of chlamydial DNA was first examined using primers 16SIGF (5′-CGGCGTGGATGAGGCAT-3′) and 16SIGR (5′-TCAGTCCCAGTGTTGGC-3′) described in the previous study (21). All positive samples were subjected to further PCR with *Chlamydiales*-specific primers 16SIGF (5′-CGGCGTGGATGAGGCAT-3′) and 806R (5′-GGAC TACCAGGGTATCTAAT-3′) according to Relman (22). PCR amplification reaction and cycling conditions for these assays were as previously described by Sood et al. (23) and Draghi et al. (24). The expected amplicons of the first and second PCR methods were 300 and 766 bp, respectively. Amplified PCR products (766 bp) from each fish were isolated using NucleoSpin™ Gel PCR Clean-up Kit (Fisher Scientific, Sweden) according to the manufacturer's protocol and then submitted for sequencing service (U2Bio, Thailand).

Phylogenetic Analyses

A BLASTn query against available nucleotide sequences was deposited in the GenBank database (www.ncbi.nlm.nih.gov) to determine taxonomic identity. The closest known relatives and several sequences from related species of *Chlamydia*-like organisms were obtained from the NCBI database and used for phylogenetic analysis. The phylogenetic tree was constructed using the neighbor-joining method with 1,000 bootstraps after multiple alignments against the closely related *Chlamydia* bacteria using ClustalW in MEGA X version 10.2.4 (25). To

root the tree, sequences from a Betaproteobacterium, *Candidatus* Branchiomonas cysticola (Accession number JQ723599.1), were used as outgroup.

In situ Hybridization

To confirm localization of CPT in the infected tissues, *in situ* hybridization (ISH) with a CLO-specific probe was performed on tissues from five representative diseased fish. A 766 bp probe was produced firstly by PCR using DNA extracted from infected fish as DNA template and the primers 16SIGF and 806R (22). The product was labeled with digoxigenin (DIG) using a commercial PCR DIG labeling mixture (Roche Molecular Biochemicals, Germany) according to the manufacturer's instructions. *In situ* hybridization was performed as previously described by Dinh-Hung et al. (26) with some modifications. Briefly, unstained 4-μm sections on HistoGrip-coated slides (Fisher Scientific, Sweden) were deparaffinized 2 times for 5 min in xylene and then rehydrated through a graded series of ethanol and distilled water. After rapid treatment with cold acetic acid for 20 s and washing in distilled water, each section was covered with prehybridization buffer [4× SSC contain 50% (v/v) deionized formamide] for at least 10 min at 37°C. The probe was diluted in hybridization buffer [50% deionized formamide, 50% dextran sulfate, 50× Denhardt's solution (Sigma-Aldrich, Germany), 20× SSC, 10 mg per ml salmon sperm DNA (Invitrogen, USA)], heated to 95°C for 10 min, and then cooled on ice. The specific probe was added to the slides, then covered with coverslips and incubated overnight at 42°C in a humidity chamber. For control slides, no probe was added to the hybridization solution. After hybridization, slides were washed in a series of graded sodium citrate solutions for 5 min in 2× SSC at room temperature (RT), 15 min in 2× SSC (37°C), 15 min in 1× SSC (37°C), 30 min in 0.5× SSC (37°C), and then equilibrated for 5 min in buffer I (1 M Tris-HCl, 1.5 M NaCl, pH 7.5). The tissue sections were then blocked with blocking solution buffer II (containing 0.1% Triton X-100 and 2% normal sheep serum) at room temperature for 30 min before being covered with anti-digoxigenin, Fab fragments (Roche Molecular Biochemicals, Germany, diluted 1:500 in buffer II) for 1 h at 45°C. After washing twice for 10 min each with buffer I, sections were treated for 10 min in buffer III (100 mM Tris-HCl, 1.5 M NaCl, 50 mM $MgCl_2$, pH 9.5). Signals were developed using the BCIP/NBT substrate, followed by counterstaining with nuclear fast red. The slides were then mounted, observed and photographed under a digital microscope.

RESULTS

Initial Diagnosis

Mortality was recorded on the second day after the fry were introduced. Daily mortality recorded from 1 to 5 days after onset of disease (dao) were 20, 50, 150, 200, and 400 fish, respectively. The infected fish exhibited lethargy, fish gasping at the water surface, and loss of appetite followed by mortality. Disease diagnosis carried out in the field on 6 dao showed no external lesions on the body surface of the fish (**Figure 1A**). Wet-mount examination of the skin mucus and gills showed no external parasites, although the formation of several characteristic cysts in the gill filaments was prevalent (**Figure 1B**). This observation initially led us to a preliminary misdiagnosis as an "epitheliocystis" case. At 3 dao, sea salt was added daily to the pond (total 200 kg), but no reduction in mortality was observed. Subsequently, oxytetracycline (OTC) (200 mg/g active ingredient, Pharmatech, Thailand) was continuously administered to the fish *via* feed admixture (5 g OTC per 1 kg of feed) for 7 days. After treatment with OTC, there was a significant decrease in daily mortality of 150, 50, and 16 fish at 7, 8, and 9 dao, respectively. No mortality (0 dead fish) was observed after treatment with OTC for 4 days (10 dao).

Histopathology and *in situ* Hybridization

Histological examination revealed colonization by intracellular bacteria in several organs, including the gill filaments (**Figure 2A.1**), submucosa of the intestine (**Figure 2B.1**), and caudal fin tissue (**Figure 2C.1**). Dense, roundish to oval intracellular bacteria with a great affinity for connective tissue rather than epithelial cells were observed (**Figures 2A.2–C.2**). Apparently, the bacteria infected the primary gill filaments rather than the secondary gill filaments. In particular, the cartilaginous junctions between primary and secondary gill filaments were apparently more susceptible to infection than others, resulting in the separation of the two components (**Figure 2A.2**). Similar changes were also observed at the cartilaginous junction of the caudal fin (data not shown). With respect to ISH, the DIG-labeled probe was specifically bound to intracellular bacterial foci (**Figures 2A.3–C.3**), whereas no binding signal was observed in tissue sections incubated with no probe (**Figures 2A.4–C.4**). Furthermore, no culturable bacteria were isolated from the internal organs on nutrient agar plates as well as on brain-heart infusion agar plates even after 48 h of incubation.

Interestingly, histological analysis showed that the "cysts" found in the infected fish were not epitheliocystis, as tentatively diagnosed and later identified as plasmodia of a myxosporean. The presence of numerous plasmodia was observed on the gill filaments (**Figure 3A**). Myxospores and plasmodia demonstrated asynchronous development with young round plasmodia encased in a wall of epithelial cells of the gill filaments (**Figure 3B**). As the plasmodium grew, the envelope ruptured and released myxospores into the adjacent tissue (**Figure 3C**). The myxospores exhibited typical features of the genus *Henneguya*: two equal polar capsules, sporoplasm at the posterior pole of the spore, and two long, superimposed caudal processes (**Figure 3D**). Histological analysis of the infected gills of *Henneguya* showed that the plasmodia caused severe distortion of the lamellar structure and obstruction of the gills by compression of the cysts (**Figures 4A–C**). The plasmodia occupied the part extent of the gill lamellae and produced marked dilatation and discrete epithelial hyperplasia (**Figures 4D,E**). The extensive dilatation of the infected lamellae caused displacement and deformation of the adjacent lamellae. As the plasmodia grew, they compressed the adjacent tissue and caused tissue necrosis in the infected area (**Figures 4E,F**).

FIGURE 1 | (A) Snakeskin gourami (*Trichopodus pectoralis*), no external lesions on the body surface of the fish. **(B)** Wet mount preparations of infected fish gill showing numerous morphological characteristics of "cysts" (arrowheads). Scale bars are shown in the pictures.

Molecular Analyses

All collected samples ($n = 4$) were positive after repeated PCR amplification of the 16S rRNA gene of *Chlamydiales* (**Supplementary Figure 1**). Multiple sequence alignment of the partial 16S rRNA gene sequence of the *T. pectoralis* chlamydial pathogen from 4 representative infected fish, showed that the sequences were identical, and the consensus sequence (766 bp) was deposited in GenBank under accession number MW832782. BLAST-n search of consensus sequence in the NCBI database revealed closest sequence similarity (93.5%) with the partial 16S rRNA gene of a non-cultured bacterium (Accession number LN612734.1) obtained from a case of gill disease in Mediterranean Sea bream, followed by *Candidatus* Piscichlamydia sp. (92.3%) (Accession Number KY380090.1), which is associated with epitheliocystis infections in cyprinids. These bacteria formed a clade as an unclassified family belonging to the genus *Candidatus* Piscichlamydia within the order *Chlamydiales*. The accession numbers and taxonomic identities, as well as the origin of the organisms included in this phylogenetic analysis, are shown in **Figure 5**. This phylogenetic analysis confirmed that the bacterial pathogen in the case of the snakeskin gourami separated in a unique branch, representing a novel species, proposed name "*Candidatus* Piscichlamydia trichopodus", a new member of the order *Chlamydiales*.

DISCUSSION

Members of the order *Chlamydiales* are a diverse group of Gram-negative, obligate intracellular bacteria that are distributed worldwide and cause a wide variety of diseases in humans, livestock, domestic animals, wildlife, and exotic species (18, 27, 28). *Chlamydia*-like organisms (CLOs), commonly found in aquatic environments, have been identified as causing disease in at least 90 fish species in both freshwater and marine environments (16–18). A common feature of these bacteria is the infection of epithelial cells of fish, causing typical lesions in the form of epitheliocystis (15–18, 29, 30). Epitheliocystis as a result of CLOs infection have been described in several farmed fishes, including common carp *Cyprinus carpio* (31), red seabream *Pagrus major* (15), African catfish *Clarias gariepinus* (32), yellowtail kingfish *Seriola lalandi* (33), striped trumpeter *Latris lineata* (34) barramundi *Lates calcarifer* (35), striped catfish *Pangasius hypophthalmus* (36), and rohu *Labeo rohita* (23). In contrast to previous studies, our result showed that the histopathological changes associated with CPT infection revealed massive intracellular colonization but not obvious as epitheliocystis. Interestingly, the microbial pathogen in this study likely shares similarities with the CLO pathogen that causes systemic microbial disease in the Dungeness crab, *Cancer*

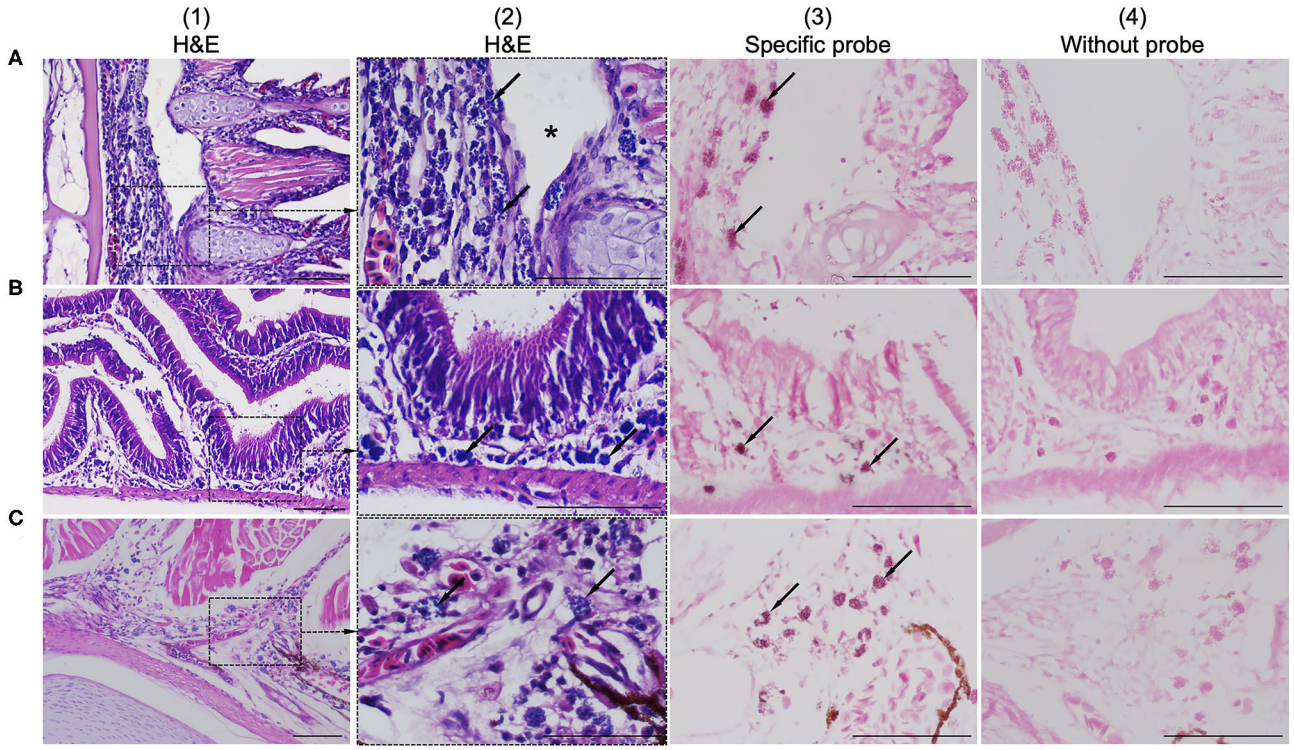

FIGURE 2 | Comparison of consecutive gill sections of infected fish stained with H&E **(A.1–C.1; A.2–C.2)**, ISH with a specific probe **(A.3–C.3)** and ISH without probe **(A.4–C.4)** as control. Infected fish showed the presence of a novel intracellular bacterium in the gill **(A.1)**, intestinal submucosa **(B.1)**, and caudal/tail fin **(C.1)**. Higher magnification showed that the connective tissue was more susceptible to infection than others due to colonization by dense, roundish to oval, blue-stained intracellular bacteria (arrows in **A.2–C.2**). The bacteria were observed near the cartilaginous junctions of the primary and secondary gill filaments, resulting in disruption of the tissue junction (asterisk in **A.2**). ISH positive reactivity of intracellular bacterial foci is indicated by distinct dark signals (arrows in **A.3–C.3**). Scale bar = 50 μm.

magister (37). Both pathogens show systemic infection with numerous colonies of the organism having strong affinity for connective tissue and connective tissue cells, while rarely infecting epithelial cells. Several previous studies reported that CLOs can infect other cell types, including mucous cells in common carp *Cyprinus carpio L.* (38), pillar cells in tiger puffer *Takifugu rubripes* (39), macrophages in brown bullhead *Ictalurus nebulosus* (40) and chloride cells in Atlantic salmon *Salmo salar* (41). These studies have also indicated that epitheliocystis due to CLO is typical but not always observed. Moreover, the localization of CPT near the damaged cartilaginous tissue suggests that these bacteria may require cartilage for their metabolism. This histopathological feature could be considered in the presumptive diagnosis of this new pathogen. It is increasingly recognized that these pathogens are actually diverse in their morphology, e.g., the morphology of CLO organisms in the epithelial cysts and their staining characteristics, as well as the morphology of their capsules and their location in fish tissue (42–44). This is the first detection of CLO in snakeskin gourami and may represent another *Chlamydia* that is not associated with epitheliocystis. Since CLO pathogens cannot be distinguished by morphology or conventional culture methods, molecular methods are widely used to detect and characterize the causative pathogen. Apart from histopathological lesion of the bacterial foci, CLO infection was confirmed by ISH and specific PCR assay. Although the short 16S rRNA signature sequence detected in infected tissue is not ideal for detailed phylogenetic analysis, it is unique. Our sequence showed only a distant similarity of 93.5 and 92.3%, respectively, with a query coverage of 98% to the uncultured bacterium from gilthead sea bream and *Candidatus* Piscichlamydia sp. associated with epitheliocystis infections in cyprinids (30). There bacteria formed a clade as an unclassified family belonging to the genus *Candidatus* Piscichlamydia within the order *Chlamydiales* and also shared >90% sequence similarity with other members of the family *Candidatus* Piscichlamydiaceae, suggesting that these pathogens belong to the same family (21) or are closely related. Since the causative agent shared < 95% similarity with other previously reported *Chlamydia*-like 16S rRNA sequences, the sequenced bacteria are new to the order *Chlamydiales* (21). These results highlight the wide genetic diversity within this bacterial group and are consistent with previous findings (29) that each new fish host indicates the existence of a phylogenetically distinct and novel *Chlamydia* infection.

In the present case, the diagnosis was challenging due to mixed infection of CPT along with a *Henneguya* sp. parasite in the affected gill tissues. The classification of *Henneguya* sp. was tentatively based on a unique morphological characteristic

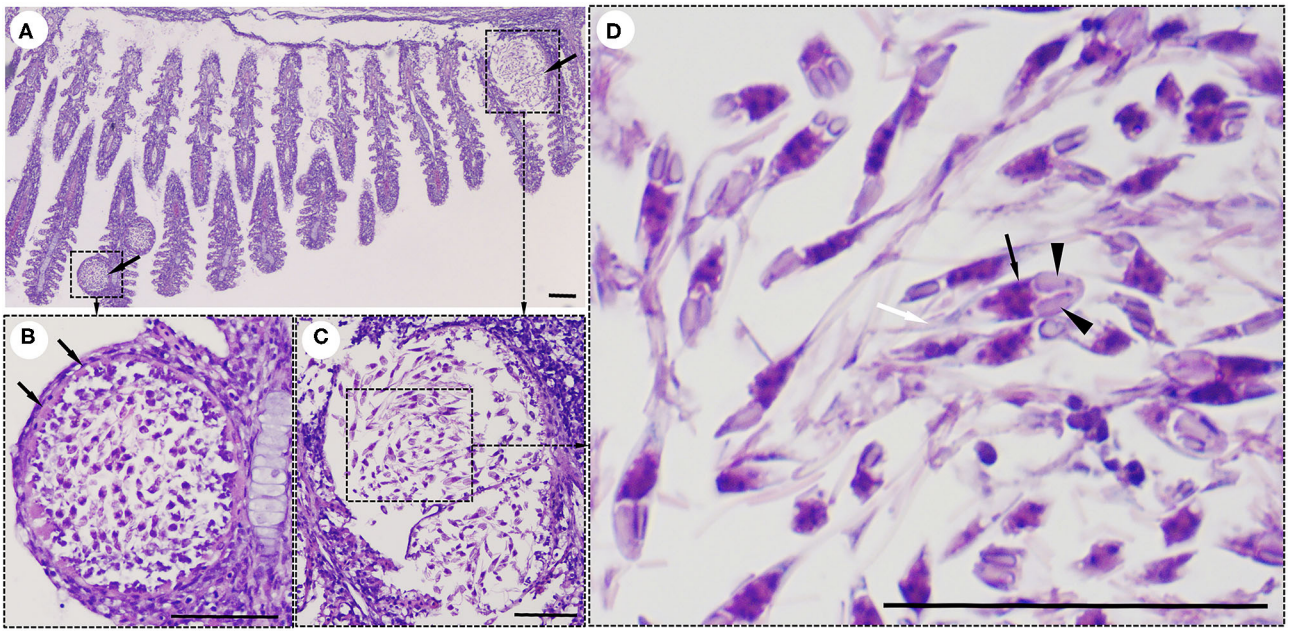

FIGURE 3 | Histological lesions in the gills of the snakeskin gourami (*Trichopodus pectoralis*) infected with *Henneguya* sp. **(A)** Plasmodia (arrows) showing different developmental stages. **(B)** Young plasmodium was roundish and encased in a wall of epithelial cells (arrows). Immature myxospores were located in the periphery of the plasmodia and mature myxospores in the center. **(C)** A grown plasmodium ruptured the envelope. **(D)** The myxospores have typical features of a *Henneguya* sp. including two equal polar caps (arrowheads), sporoplasm at the posterior pole of the spore (black arrow), and two long, superimposed caudal processes (white arrow). Slides were stained with hematoxylin and eosin (H&E), scale bar = 50 μm.

of its spore with caudal appendage (6, 9, 20, 45). Accurate identification of species therefore requires a combination of systematic morphological descriptions and sequencing of the small subunit ribosomal RNA gene (SSU) for phylogenetic analysis (10, 46). Previous studies have described that *Henneguya* sp. has the characteristic morphological feature of two equal polar capsules, sporoplasm on the posterior pole, and 2 independent caudal processes, which distinguishes it from the other genera of the family *Myxobolidae* (7, 9, 10, 47). The species of the genus *Henneguya* interact with the gill structures of fish in different manners, resulting in varying degrees of disease (11, 12, 48). The clinical signs noted by the farmer in the snakeskin gourami, particularly lethargy, gasping for oxygen at the water surface, and loss of appetite, are comparable with those previously documented in fish affected by *Henneguya* sp. (49–51). The most common histological lesions found in this case were distortion of the lamellar structure and obstructions of the gills due to compression of the cysts, which most likely caused respiratory distress and contributed to the observed mortality. Histopathological features similar to those described in this study have been observed in previous studies (52–54), in which parasitism by *Henneguya* sp. resulted in marked dilatation and discrete epithelial hyperplasia, and continued growth of the parasitic cyst resulted in tissue necrosis in the surrounding infected area. The observation of areas of cystic lesions associated with tissue necrosis caused by the compression of cysts in the epithelial cells of the gill lamellae in this study has also been reported in previous studies (55). The growth of *Henneguya* plasmodia results in a displacement and distortion of the lamellar structures, possibly adversely affecting gas exchange and associated with mortality in the fish population.

Unfortunately, due to the occurrence of co-infections and the unavailability of culture methods for fish CLOs, it was not possible to determine which pathogens were directly responsible for the associated mortality. Interestingly, the disease is sensitive to tetracyclines, since the antibiotic treatment with oxytetracycline in the field was effective, hence we assumed that the disease might have been caused primarily by the CLO. As previously reported by Goodwin et al. (56), OTC significantly reduced mortality due to chlamydial infection and supported this treatment regimen for future outbreaks. The cause and pathogenesis of this dual infection remain speculative and await the development of a culture technique and isolation of the *Chlamydia*-like organism before further *in vitro* studies. It is unclear whether *Henneguya* sp. and CPT has the potential of causing a significant impact on snakeskin gourami aquaculture. Given the commercial importance of the snakeskin gourami *Trichopodus pectoralis* and its great aquaculture potential, the results of this study highlight the need of follow up investigations on ultrastructural morphology, host range, prevalence, risk factors for disease, and mode of transmission. This could lead to a better understanding of the pathogen's biology and disease epidemiology for development of effective control measures.

In conclusion, the presence of pathogenic potential of mixed infection of a novel intracellular CLO (*Candidatus* Piscichlamydia trichopodus) and a gill parasite *Henneguya* sp. in snakeskin gourami in Thailand is reported for the first time. This study expands the knowledge of the pathology of snakeskin

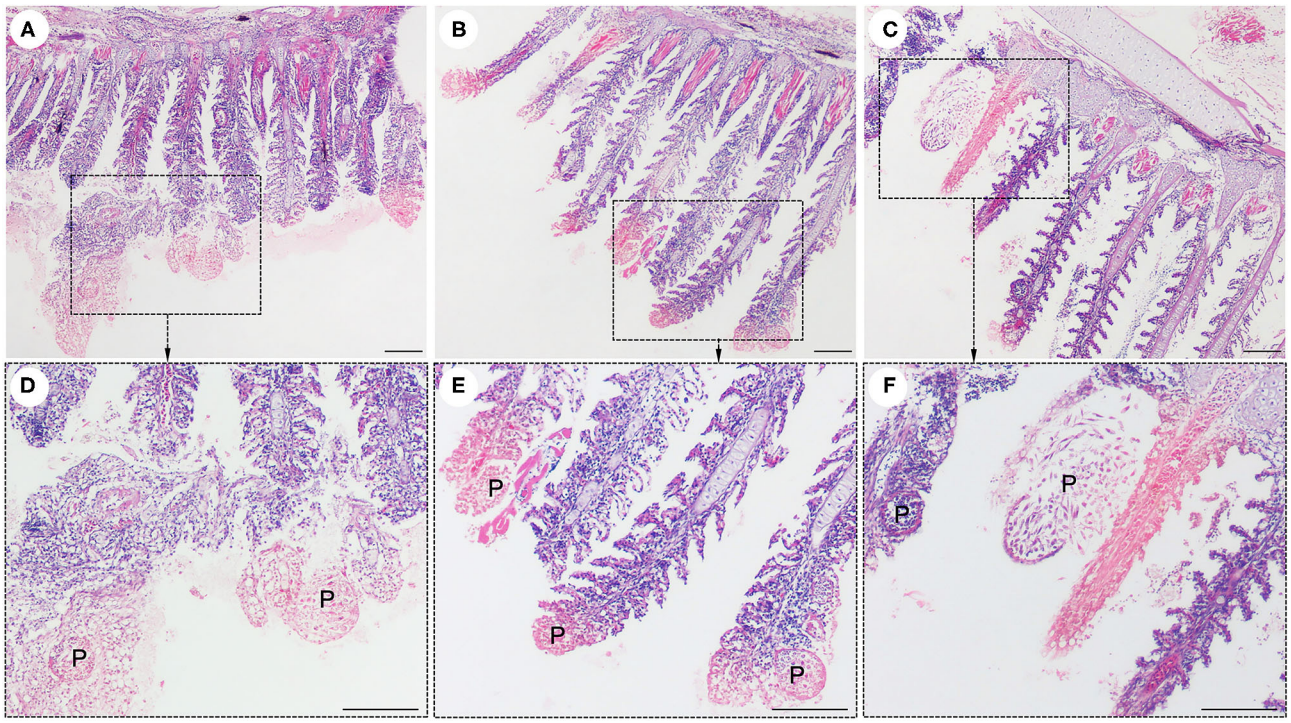

FIGURE 4 | Histological lesions in the gills of the snakeskin gourami (*Trichopodus pectoralis*) infected with *Henneguya* sp. The plasmodia (P) caused severe distortion of the lamellar structure and obstruction of the gills by compression of the cysts **(A–C)**. Higher magnification indicated plasmodia occupied part of the gill lamellae and caused marked dilation and discrete epithelial hyperplasia **(D,E)**. The plasmodia grew and compressed the adjacent tissue and caused tissue necrosis in the infected area **(E,F)**. Slides were stained with hematoxylin and eosin (H&E), scale bar = 100 μm.

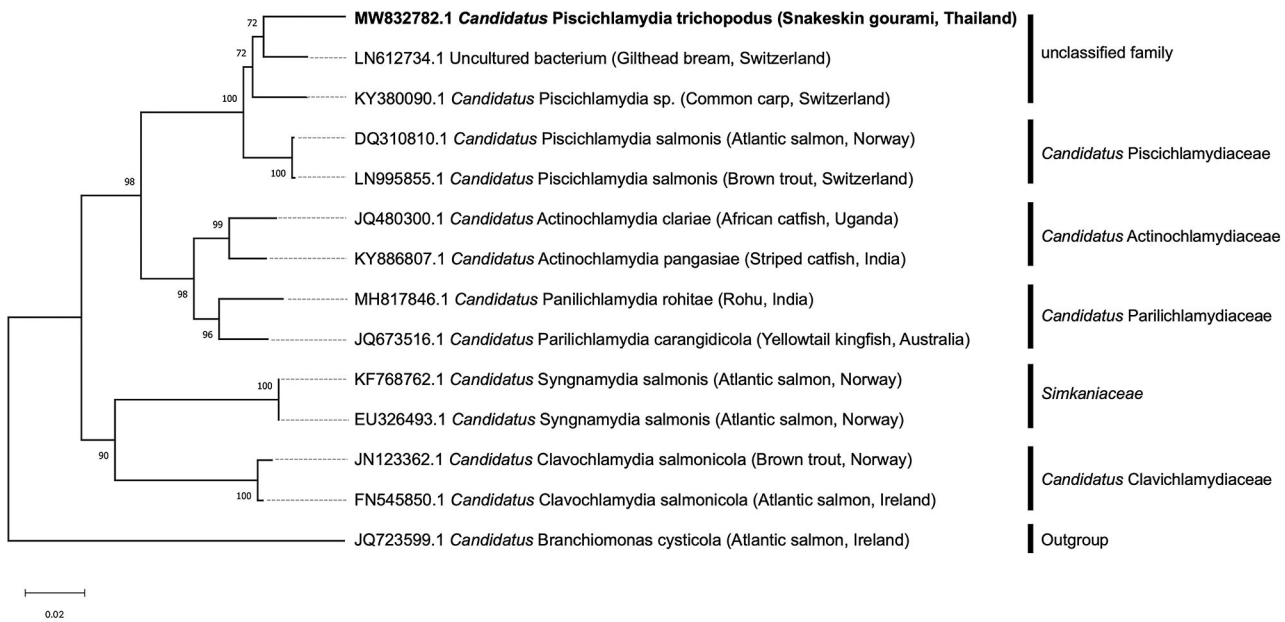

FIGURE 5 | Phylogenetic tree was constructed based on the partial 16S rRNA sequence (766 bp) of the snakeskin gourami (*Trichopodus pectoralis*) from this study (MW832782) and closely related species. The accession numbers and taxonomic identities, as well as the host origin of the organisms included in this phylogenetic analysis, are shown. *Candidatus* Branchiomonas cysticola was selected as the outgroup. The tree was constructed using the neighbor-joining method. The scale bar represents 0.02—nucleotide substitution per site, while the number at the node of the tree indicates the bootstrap value in percent.

gourami, an important fish species in Asian aquaculture, and contributes to initial understanding of diseases in this fish species.

DATA AVAILABILITY STATEMENT

The datasets presented in this study can be found in online repositories. The names of the repository/repositories and accession number(s) can be found in the article/**Supplementary Material**.

ETHICS STATEMENT

The animal study was reviewed and approved by the Institutional Animal Care and Use Committee of Kasetsart University (Approval ID: ACKU63-FIS-009).

AUTHOR CONTRIBUTIONS

PK and HD: involved in conceptualization. ND-H, CS, SN, and PK: underwent investigation. SN: resources. ND-H, HD, and PK: performed formal analysis and wrote the original draft. ND-H, HD, CS, CR, SN, PS, SC, and PK: reviewed and edited. PK: one of the lead authors and was deceased prior to the submission of this manuscript. All authors have read and agreed to the current version of the manuscript.

FUNDING

This work was carried out with support from the Center of Excellence in Aquatic Animal Health Management, Faculty of Fisheries, Kasetsart University.

SUPPLEMENTARY MATERIAL

The Supplementary Material for this article can be found online at: https://www.frontiersin.org/articles/10.3389/fvets.2022.847977/full#supplementary-material

Supplementary Figure 1 | Confirmation of PCR test results under agarose gel electrophoresis of samples from four representative fish. Lanes 1 and 6 were amplified without DNA template using primer set 1 and 2, respectively, as negative controls. Lanes 2, 3, 4, and 5 were amplified with the DNA template from primer set 1 (300 bp). Lanes 7, 8, 9, and 10 were amplified with the DNA template from primer set 2 (766 bp). Lane M was a DNA marker (Himedia, India).

REFERENCES

1. Paepke H. The nomenclature of *Trichopodus pectoralis* Regan, 1910*; Trichopus cantoris* Sauvage, 1884 *and Osphronemus saigonensis* Borodin, 1930 (Teleostei: Peciformes*: Osphronemidae). Vertebr Zool.* (2009) 59:49–56.
2. FAO. *Fishery and Aquaculture Statistics. Global Aquaculture Production 1950-2019 (FishstatJ)*. Rome: FAO Fisheries Division. Available online: http://www.fao.org/fishery/countrysector/naso_thailand/en (accessed June 19, 2021).
3. DOF. Statistics of Freshwater Aquaculture Production. *Fisheries Development Policy and Strategy Division No. 8/2018*. (2016). Bangkok: Department of Fisheries, Ministry of Agriculture and Cooperatives (2018).
4. Kanchan C, Imjai P, Kanchan N, Chaiyara A, Panchai K. Occurrence of parasitic and bacterial diseases in Thai freshwater fish. *J Agric Crop Resh.* (2020) 8:210–4. doi: 10.33495/jacr_v8i10.20.168
5. U.S Fish & Wildlife Service. *Snakeskin Gourami (Trichopodus pectoralis) Ecological Risk Screening Summary*. (2019). Available online: https://www.fws.gov/fisheries/ans/erss/uncertainrisk/ERSS-Trichopodus-pectoralis_Final.pdf (accessed June 19, 2021).
6. Lom J, Dyková I. Myxozoan genera: definition and notes on taxonomy, life-cycle terminology and pathogenic species. *Folia Parasitol.* (2006) 53:1–36. doi: 10.14411/fp.2006.001
7. Molnár K. Site preference of fish myxosporeans in the gill. *Dis Aquat Organ.* (2002) 48:197–207. doi: 10.3354/dao048197
8. Eiras JC, Adriano EA. A checklist of new species of *Henneguya* Thélohan, 1892 (Myxozoa: Myxosporea, Myxobolidae) described between 2002 and 2012. *Syst Parasitol.* (2012) 83:95–104. doi: 10.1007/s11230-012-9374-7
9. Lom J, Arthur JR, A. guideline for the preparation of species descriptions in Myxosporea. *J Fish Dis.* (1989) 12:151–6. doi: 10.1111/j.1365-2761.1989.tb00287.x
10. Fiala I, Bartošová-Sojková P, Whipps CM. Classification and Phylogenetics of Myxozoa. In: *Myxozoan Evolution, Ecology and Development*, eds. Okamura B, Gruhl A, Bartholomew JL. *Springer International Publishing*. (2015), p. 85–110.
11. Kent ML, Andree KB, Bartholomew JL, El-Matbouli M, Desser SS, Devlin RH, et al. Recent advances in our knowledge of the Myxozoa. *J Eukaryot Microbiol.* (2001) 48:395–413. doi: 10.1111/j.1550-7408.2001.tb00173.x
12. Dykova I, Lom J. Histopathological changes in fish gills infected with myxosporidian parasites of the genus *Henneguya*. *J Fish Biol.* (1978) 12:197–202. doi: 10.1111/j.1095-8649.1978.tb04165.x
13. Whitaker JW, Pote LMW, Hanson LA. Assay to detect the actinospore and myxospore stages of proliferative gill disease in oligochaetes and pond water. *N Am J Aquac.* (2005) 67:133–7. doi: 10.1577/A03-059.1
14. Haaparanta A, Valtonen ET, Hoffmann RW. Pathogenicity and seasonal occurrence of *Henneguya-creplini* (Protozoa, Myxosporea) on the gills of perch *Perca-Fluviatilis* in central Finland. *Dis Aquat Organ.* (1994) 20:15–22. doi: 10.3354/dao020015
15. Nowak BF, LaPatra SE. Epitheliocystis in fish. *J Fish Dis.* (2006) 29:573–88. doi: 10.1111/j.1365-2761.2006.00747.x
16. Blandford MI, Taylor-Brown A, Schlacher TA, Nowak B, Polkinghorne A. Epitheliocystis in fish: an emerging aquaculture disease with a global impact. *Transbound Emerg Dis.* (2018) 65:1436–46. doi: 10.1111/tbed.12908
17. Pawlikowska-Warych M, Deptula W. Characteristics of *Chlamydia*-like organisms pathogenic to fish. *J Appl Genet.* (2016) 57:135–41. doi: 10.1007/s13353-015-0303-8
18. Borel N, Polkinghorne A, Pospischil A. A review on chlamydial diseases in animals: still a challenge for pathologists? *Vet Pathol.* (2018) 55:374–90. doi: 10.1177/0300985817751218
19. Yoonpundh R, Little D. Trends in the farming of the snakeskin gourami (*Trichogaster pectoralis*) in Thailand. *Naga, The WorldFish Center.* (1997) 20:18–20.
20. Fiala I, Bartošová-Sojková P, Okamura B, Hartikaine H. Adaptive radiation and evolution within the myxozoa. In: *Myxozoan Evolution, Ecology and Development*, editors. Okamura B, Gruhl A, Bartholomew JL. *Springer International Publishing*. (2015). p. 69–84. doi: 10.1007/978-3-319-14753-6_4
21. Everett KDE, Bush RM, Andersen AA. Emended description of the order *Chlamydiales*, proposal of *Parachlamydiaceae* fam. nov and Simkaniaceae fam nov, each containing one monotypic genus, revised taxonomy of the family Chlamydiaceae, including a new genus and five new species, and standards for the identification of organisms. *Int J Syst Bacteriol.* (1999) 49:415–40. doi: 10.1099/00207713-49-2-415
22. Relman D, Universal bacterial 16S rRNA amplification and sequencing. In: Persing DH, Smith TF, Tenover FC, White TJ, editors. *Diagnostic Molecular Biology, Principles and Applications*. (1993). p. 489–95.
23. Sood N, Pradhan PK, Verma DK, Gupta S, Ravindra, Dev AK, et al. Epitheliocystis in rohu *Labeo rohita* (Hamilton, 1822) is caused by novel *Chlamydiales*. *Aquaculture*. (2019) 505:539–43. doi: 10.1016/j.aquaculture.2019.03.007
24. Draghi AII, Popov VL, Kahl MM, Stanton JB, Brown CC, Tsongalis GJ, et al. Characterization of "C*andidatus* piscichlamydia salmonis" (order

Chlamydiales), a chlamydia-like bacterium associated with epitheliocystis in farmed Atlantic salmon (*Salmo salar*). *J Clin Microbiol.* (2004) 42:5286–97. doi: 10.1128/JCM.42.11.5286-5297.2004
25. Kumar S, Stecher G, Li M, Knyaz C, Tamura K. MEGA X molecular evolutionary genetics analysis across computing platforms. *Mol Biol Evol.* (2018) 35:1547–9. doi: 10.1093/molbev/msy096
26. Dinh-Hung N, Sangpo P, Kruangkum T, Kayansamruaj P, Rung-Ruangkijkrai T, Senapin S. et al. Dissecting the localization of Tilapia tilapinevirus in the brain of the experimentally infected Nile tilapia, *Oreochromis niloticus* (L). *J Fish Dis.* (2021) 44:1053–64. doi: 10.1111/jfd.13367
27. Corsaro D, Valassina M, Venditti D. Increasing diversity within *Chlamydiae*. *Crit Rev Microbiol.* (2003) 29:37–78. doi: 10.1080/713610404
28. Horn M. *Chlamydiae* as symbionts in eukaryotes. *Annu Rev Microbiol.* (2008) 62:113–31. doi: 10.1146/annurev.micro.62.081307.162818
29. Stride MC, Polkinghorne A, Nowak BF. Chlamydial infections of fish: diverse pathogens and emerging causes of disease in aquaculture species. *Vet Microbiol.* (2014) 170:19–27. doi: 10.1016/j.vetmic.2014.01.022
30. Sellyei B, Molnár K, Székely C. Diverse Chlamydia-like agents associated with epitheliocystis infection in two cyprinid fish species, the common carp (*Cyprinus carpio* L.) and the gibel carp (*Carassius auratus gibelio* L.). *Acta Vet Hung.* (2017) 65:29–40. doi: 10.1556/004.2017.003
31. Kim DJ, Park JH, Seok SH, Cho SA, Baek MW, Lee HY, et al. Epitheliocystis in carp (*Cyprinus carpio*) in South Korea. *J Vet Med Sci.* (2005) 67:119–20. doi: 10.1292/jvms.67.119
32. Steigen A, Nylund A, Karlsbakk E, Akoll P, Fiksdal IU, Nylund S, et al. 'Cand. Actinochlamydia clariaeh gen nov, sp nov, a unique intracellular bacterium causing epitheliocystis in catfish (Clarias gariepinus) in Uganda. *PLoS ONE.* (2013) 8:e66840. doi: 10.1371/journal.pone.0066840
33. Stride MC, Polkinghorne A, Miller TL, Groff JM, Lapatra SE, Nowak BF. Molecular characterization of "*Candidatus* Parilichlamydia carangidicola," a novel *Chlamydia*-like epitheliocystis agent in yellowtail kingfish, *Seriola lalandi* (Valenciennes), and the proposal of a new family, "*Candidatus* Parilichlamydiaceae" fam. nov (order Chlamydiales). *Appl Environ Microbiol.* (2013) 79:1590–7. doi: 10.1128/AEM.02899-12
34. Stride MC, Polkinghorne A, Miller TL, Nowak BF. Molecular characterization of "*Candidatus* Similichlamydia latridicola" gen. nov, sp nov (Chlamydiales: "Chlamydial Parilichlamydiaceaeary a novel Chlamydia-like epitheliocystis agent in the striped trumpeter, Latris lineata (Forster). *Appl Environ Microbiol.* (2013) 79:4914–914 doi: 10.1128/AEM.00746-13
35. Stride MC, Polkinghorne A, Powell MD, Nowak BF. "*Candidatus* Similichlamydia laticola", a novel *Chlamydia*-like agent of epitheliocystis in seven consecutive cohorts of farmed Australian barramundi, *Lates calcarifer* (Bloch). *PLoS ONE.* (2013) 8:e82889. doi: 10.1371/journal.pone.0082889
36. Sood N, Pradhan PK, Verma DK, Yadav MK, Ravindra, Dev AK, et al. Candidatus Actinochlamydia pangasiae sp nov (Chlamydiales, Actinochlamydiaceae), a bacterium associated with epitheliocystis in Pangasianodon hypophthalmus. *J Fish Dis.* (2018) 41:281–90. doi: 10.1111/jfd.12711
37. Sparks AK, Morado JF, Hawkes JW. A systemic microbial disease in the Dungeness crab, *Cancer magister*, caused by a *Chlamydia*-like organism. *J Invertebr Pathol.* (1985) 45:204–17. doi: 10.1016/0022-2011(85)90010-2
38. Paperna I, Alves de Matos AP. The developmental cycle of epitheliocystis in carp, *Cyprinus carpio* L. *J Fish Dis.* (1984) 7:137–47. doi: 10.1111/j.1365-2761.1984.tb00916.x
39. Miyazaki T, Fujimaki Y, Hatai K. A light and electron microscopic study on epitheliocystis disease in cultured fishes. *Nippon Suisan Gakkaishi.* (1986) 52:199–202. doi: 10.2331/suisan.52.199
40. Desser S, Paterson W, Steinhagen D. Ultrastructural observations on the causative agent of epitheliocystis in the brown bullhead, *Ictalurus nebulosus Lesueur*, from Ontario and a comparison with the *Chlamydiae* of higher vertebrates. *J Fish Dis.* (1988) 11:453–60. doi: 10.1111/j.1365-2761.1988.tb00744.x
41. Nylund A, Kvenseth AM, Isdal E. A morphological study of the epitheliocystis agent in farmed Atlantic Salmon. *J Aquat Anim Health.* (1998) 10:43–55. doi: 10.1577/1548-8667(1998)010<0043:AMSOTE>2.0.CO;2
42. Work TM, Rameyer RA, Takata G, Kent ML. Protozoal and epitheliocystis-like infections in the introduced bluestripe snapper *Lutjanus kasmira* in Hawaii. *Dis Aquat Organ.* (2003) 57:59–66. doi: 10.3354/dao057059
43. Crespo S, Zarza C, Padrós F, Marín de Mateo M. Epitheliocystis agents in sea bream Sparus aurata: morphological evidence for two distinct Chlamydia-like developmental cycles. *Dis Aquat Organ.* (1999) 37:61–72. doi: 10.3354/dao037061
44. Guevara Soto M, Vaughan L, Segner H, Wahli T, Vidondo B, Schmidt-Posthaus H. Epitheliocystis distribution and dharacterization in brown trout *(Salmo trutta)* from the headwaters of two major European rivers, the Rhine and Rhone. *Front Physiol.* (2016) 7:131. doi: 10.3389/fphys.2016.00131
45. Atkinson S, Bartošová-Sojková P, Whipps C. Approaches for characterizing myxozoan species. In: Okamura B, Gruhl A, Bartholomew JL, editors. *Myxozoan Evolution, Ecology and Development*, editors. Switzerlan: Springer International Publishing (2015). p. 111–23.
46. Liu Y, Lövy A, Gu Z, Fiala I. Phylogeny of Myxobolidae (Myxozoa) and the evolution of myxospore appendages in the Myxobolus clade. *Int J Parasitol.* (2019) 48:523–30. doi: 10.1016/j.ijpara.2019.02.009
47. Eiras JC. Synopsis of the species of the genus *Henneguya* Thélohan, 1892 (Myxozoa: myxosporea: myxobolidae. *Syst Parasitol.* (2002) 52:43–54. doi: 10.1023/A:1015016312195
48. Molnár K, Eszterbauer E. Specificity of infection sites in vertebrate hosts. In: Okamura B, Gruhl A, Bartholomew JL, editors. *Myxozoan Evolution, Ecology and Development*. Springer International Publishing (2015). p. 295–313.
49. Sabri DM, Eissa IAM, Danasoury MA, Khouraiba HM. Prevalence of Henneguya branchialis in Catfish *(Clarias gariepinus)* in Ismailia, Egypt. *Int J Agric Biol.* (2010) 12:897–900.
50. Videira M, Velasco M, Malcher CS, Santos P, Matos P, Matos E. An outbreak of myxozoan parasites in farmed freshwater fish *Colossoma macropomum* (Cuvier, 1818) (Characidae, Serrasalminae) in the Amazon region, Brazil. *Aquac.* (2016) 3:31–4. doi: 10.1016/j.aqrep.2015.11.004
51. Stilwell JM, Camus AC, Leary JH, Khoo LH, Griffin MJ. Pathologic changes associated with respiratory compromise and morbidity due to massive interlamellar *Henneguya exilis* infection in Channel × Blue Hybrid Catfish. *J Parasitol.* (2019) 105:686–92. doi: 10.1645/19-28
52. Özer A, Özkan H, Gürkanli CT, Yurakhno V, Çiftçi Y. Morphology, histology and phylogeny of *Henneguya sinova* sp. nov (Myxobolidae: Myxozoa) infecting gills of Parablennius tentacularis in the Black Sea, Turkey. *Dis Aquat Organ.* (2016) 118:207–15. doi: 10.3354/dao02968
53. Úngari LP, Vieira DHMD, da Silva RJ, Santos ALQ, de Azevedo RK, O'Dwyer LH, et al. new myxozoan species *Henneguya unitaeniata* sp. nov (Cnidaria: Myxosporea) on gills of Hoplerythrinus unitaeniatus from Mato Grosso State, Brazil. *Parasitol Res.* (2019) 118:3327–36. doi: 10.1007/s00436-019-06533-1
54. Yokoyama H, Itoh N, Tanaka S. *Henneguya pagri* n. sp (Myxozoa: Myxosporea) causing cardiac henneguyosis in red sea bream, Pagrus major (Temminck & Schlegel). *J Fish Dis.* (2005) 28:479–87. doi: 10.1111/j.1365-2761.2005.00655.x
55. Figueredo RTA, de Oliveira JEF, Vilhena MPSP, Berredo J, dos Santos WJP, Matos E, et al. Henneguyosis in gills of *Metynnis hypsauchen*: an Amazon freshwater fish. *J Parasit Dis.* (2020) 44:213–20. doi: 10.1007/s12639-019-01183-7
56. Goodwin AE, Park E, Nowak BF. Successful treatment of largemouth bass, *Micropterus salmoides* (L), with epitheliocystis hyperinfection. *J Fish Dis.* (2005) 28:623–5. doi: 10.1111/j.1365-2761.2005.00662.x

Conflict of Interest: The authors declare that the research was conducted in the absence of any commercial or financial relationships that could be construed as a potential conflict of interest.

Publisher's Note: All claims expressed in this article are solely those of the authors and do not necessarily represent those of their affiliated organizations, or those of the publisher, the editors and the reviewers. Any product that may be evaluated in this article, or claim that may be made by its manufacturer, is not guaranteed or endorsed by the publisher.

frontiers | Frontiers in Veterinary Science

BRIEF RESEARCH REPORT
published: 10 June 2022
doi: 10.3389/fvets.2022.887174

Detection of Virulence-Associated Genes and *in vitro* Gene Transfer From *Aeromonas* sp. Isolated From Aquatic Environments of Sub-himalayan West Bengal

Preeti Mangar[1], *Partha Barman*[2], *Anoop Kumar*[2], *Aniruddha Saha*[1] *and Dipanwita Saha*[2]*

[1] *Department of Botany, University of North Bengal, Siliguri, India,* [2] *Department of Biotechnology, University of North Bengal, Siliguri, India*

OPEN ACCESS

Edited by:
Huanying Pang,
Guangdong Ocean University, China

Reviewed by:
Guilherme Campos Tavares,
Federal University of Minas Gerais, Brazil
Hiroshi Asakura,
National Institute of Health Sciences (NIHS), Japan

***Correspondence:**
Dipanwita Saha
dipanwitasaha@nbu.ac.in

Specialty section:
This article was submitted to Veterinary Infectious Diseases, a section of the journal Frontiers in Veterinary Science

Received: *01 March 2022*
Accepted: *03 May 2022*
Published: *10 June 2022*

Citation:
Mangar P, Barman P, Kumar A, Saha A and Saha D (2022) Detection of Virulence-Associated Genes and in vitro Gene Transfer From Aeromonas sp. Isolated From Aquatic Environments of Sub-himalayan West Bengal. Front. Vet. Sci. 9:887174. doi: 10.3389/fvets.2022.887174

Aeromonas is omnipresent in aquatic environments and cause disease within a wide host range. A total of thirty-four isolates from water samples of small fish farms were identified as *Aeromonas* based on biochemical characteristics and 16S rRNA gene sequence. A total of six virulent factors were analyzed which indicated 100% of isolates as beta-haemolytic and proteolytic, whereas 44.1, 38.2, and 70.6% of isolates produced DNAse, siderophore, and amylase, respectively. Studies on the occurrence of four genetic determinants of virulence factors revealed that *aer/haem* (haemolytic toxin) and *flaA* (polar flagella) genes were present in 44.1% of strains whereas *ascV* (type 3 secretion system) and *aspA* (serine protease) genes were detected in 21.5 and 8.82% of strains, respectively. Fish (*Anabas testudineus*) challenge studies showed that the isolate GP3 (*Aeromonas veronii*) bearing five virulent factors with the combination of $aer/haem^{+}/ascV^{+}/fla^{+}$ genes induced severe lesions leading to 100% of mortality. In contrast, RB7 possessing four virulence factors and three genes ($aer/haem^{+}/ascV^{+}/aspA^{+}$) could not produce severe lesions and any mortality indicating the absence of correlation between the virulence factors, its genes, and the pathogenicity in fishes. GP3 was cytotoxic to human liver cell line (WRL-68) in trypan blue dye exclusion assay. The 431 bp *aer/haem* gene of GP3 was transferable to *E. coli* Dh5α with a conjugational efficiency of 0.394×10^{-4} transconjugants per recipient cell. The transfer was confirmed by PCR and by the presence of 23-kb plasmids in both donor and transconjugants. Therefore, the occurrence of mobile genetic elements bearing virulence-associated genes in *Aeromonas* indicates the need for periodic monitoring of the aquatic habitat to prevent disease outbreaks.

Keywords: *Aeromonas*, 16S rRNA gene, virulence related genes, *Anabas testudineus*, cytotoxicity, conjugational efficiency, plasmid

INTRODUCTION

The genus *Aeromonas* is a pervasive group of microorganisms in the aquatic environment (1). It has the ability to induce diseases in fishes, mammals, reptiles, and amphibians (2). *Aeromonas* has been recognized as an etiological agent of several pathogenic conditions such as motile aeromonad syndrome (MAS), haemorrhagic septicaemia, fin rot, red sore disease, and scale protrusions in fish (3). Additionally, its role as an opportunistic pathogen in immunocompromised human and in infections such as septicaemia, bacterial endocarditis, gastroenteritis, wound sepsis, and traveller's diarrhea cannot be undermined (4). At present, *Aeromonas* is an important water-borne pathogen and has gained significance with its ability to induce multiple infections in a wide host range (5). A total of 75% of freshwater fish production in India is contributed by the state of West Bengal (6). About 251 species of freshwater fishes are found here in various freshwater resources such as tanks, ponds, creeks, beels, barrages, reservoirs, small river streams, major rivers, and an interlinked river drainage system (7). However, the yield is largely affected by mortality due to infections. Several species of highly pathogenic motile aeromonads including *Aeromonas hydrophila*, *Aeromonas caviae,* and *Aeromonas sobria* were found to be associated with diseases with mass mortalities in fishes (8). Pathogenicity in *Aeromonas* spp. has been reported to be due to multiple virulence factors that contribute to different mechanisms of the infection process. These factors include haemolysins, proteases, elastases, lipases, enterotoxins, phospholipases, chitinases, and deoxyribonucleases which can cause tissue damage and lethality (9). The genes encoding virulence factors determine the pathogenicity of a microorganism (10, 11). Pore-forming toxin genes *aerA* (encoding aerolysin), *act* (encoding cytotoxic toxins), and *alt* and *ast* (encoding cytotonic enterotoxins) are the primary elements of virulence within *Aeromonas* spp. (12). In addition, virulence genes encoding serine protease (*ser*, *aspA*), polar flagella (*flaA*), lateral flagella (*lafA*), DNase (*exu*), elastase (*ahyB*), glycerophospholipid: cholesterol acyltransferase (*gCAT*), and type III secretion system (*ascV*) have also been traced within *Aeromonas* (13). The invasiveness and adherence of *Aeromonas hydrophila* to HEpG2 cell monolayers, Vero cells, Chinese hamster ovarian cells, and erythrocytes have also been documented (14). Mobile genetic elements that carry virulence factors have been reported as widespread in the aquatic environment among different genera of bacteria such as *Vibrio* (15, 16), *Photobacterium damselae* (17), and *Staphylococcus aureus* (18). Some pieces of evidence show that *Aeromonas* can actively participate in processes of transfer of genetic material (*via* conjugation) with phylogenetically distant bacteria (19). In a study on the whole-genome sequence, Poole et al. (20) observed that *A. hydrophila* may be capable of transferring resistance and virulence genes to other related genera in the environment. This study aims at the isolation of *Aeromonas* spp. from fish farming environments of North Bengal, India for investigating the occurrence and distribution of molecular markers responsible for virulence. The current work provides experimental evidence of the conjugational spread of virulence genes to *E. coli* Dh5α.

MATERIALS AND METHODS

Sample Collection and Isolation of *Aeromonas* sp.

The *Aeromonas* populations from water samples of 9 different fish farming sites across Darjeeling and Jalpaiguri districts of Sub-Himalayan West Bengal were investigated. Samples were collected in sterilized vials, kept at 4°C, and analyzed within 24 h of procuring. For isolation of the bacteria, 0.1 ml of ten-fold diluted samples prepared in sterile distilled water was spread plated on *Aeromonas* isolation medium (HiMedia Laboratories Ltd., Mumbai, India). The plates were incubated for 24 h at 30°C in the bacterial incubator. Altogether, 83 single colonies were selected based on the expected morphology from the spread plates, and pure cultures were maintained by streaking them on tryptone soya agar slants (21). Glycerol stocks of cultures were maintained in 10% glycerol at −20°C. All of the isolates were initially screened presumptively using a slightly modified key test called Aerokey II, described by Carnahan et al. (22), to identify the genus *Aeromonas*. The isolates were tested for Gram-staining, oxidase, catalase, glucose fermentation, resistance to 0/129 discs, and esculin hydrolysis (23). The strains were labeled as presumptive *Aeromonas* spp. depending on the tests.

Detection of Phenotypic Attributes of Virulence

Haemolytic activity of *Aeromonas* positive bacterial isolates was assessed by cultivating on tryptone soya agar (TSA) medium supplemented with 5% sheep blood (vol/vol) for 24 h at 30°C. Expression of haemolysin was depicted by a zone of clearance around bacterial colonies (24). Protease production was determined by the growth of bacterial isolates in nutrient agar containing 1.5% of skimmed milk and incubated for 24 h at 30°C. Casein-degrading bacteria showed clear zone around the colonies (24). DNase production was tested by inoculating the isolates in DNAse agar medium (HiMedia Laboratories, Mumbai) for 24 h at 30°C. The appearance of pale pink to white halos around the colonies indicated a positive result (25). Lipolytic activity was tested by growing the isolates in Tween-80 medium for 24 h at 30°C. Opaque zones around streaked cultures indicating crystal formation were considered positive for lipase (26). Amylase production was determined in starch agar plates following the method given by Barrow and Feltham (25). Siderophore production was determined using the Universal Chromazurol S (CAS) assay (27).

Molecular Identification of the Isolates

Sequence Similarity and Phylogenetic Analysis

The bacterial isolates were identified by 16S rRNA gene sequencing using universal primers. The total genomic DNAs were isolated from all the strains by CTAB method (28). Amplification of the 16S rRNA gene was performed in 25 μl reaction using the universal primers 27F (5′-AGAGTTTGATCCTGGCTCAG-3′) and 1498R (5′-GGTTCACTTGTTACGACTT-3′) (29) following specific cycling conditions: initial denaturation at 95°C for 3 min, 30 cycles of denaturation at 95°C for 30 s, annealing at the temperature of

52.2°C for 30 s, extension at 72°C for 30 s, and a final extension at 72°C for 5 min on a thermal cycler (Applied Biosystems GeneAmp PCR 2400). The amplified product was purified using PCR purification kit (BR Biochem Life Sciences Pvt. Ltd) and sequenced at Eurofins sequencing services, Bangalore. All the obtained sequences were submitted to NCBI and GenBank accession numbers are given in the tree. The phylogenetic tree was constructed with the neighbor-joining method using MEGA 6.0 (30). Confidence in the tree topology was determined by bootstrap analysis using 1,000 resamplings of the sequences (31).

Pathogenicity Testing in Fishes

Healthy small-sized fishes (weight ∼25–30 g) of *Anabas testudineus* were collected from fish farms in nearby areas of Sonapur and Gangarampur of Darjeeling district and maintained for 15 days in glass aquaria measuring 90 cm × 35 cm × 35 cm (10–12 fishes in each aquarium) for acclimatization. Water temperature was maintained at 25–30°C. For the fish pathogenicity testing, six strains (GP3, RB7, BP3, RJB1, MG8, and PP21) bearing two or more virulence properties and isolated from different locations were selected. The selected isolates were cultured in tryptic soy broth (HiMedia Laboratories, Mumbai) for 18 h at 30°C with constant shaking at 90 rpm. The cells were harvested as pellets following the centrifugation at 10,000 g for 10 min at 4°C and resuspended in 0.85% saline solution. The suspension was then adjusted to cell density of 1×10^7 cfu/ml by measuring O.D. at 600 nm (O.D. = 0.8) in a spectrophotometer. Prior to infection, the fishes were anesthetized by keeping in benzocaine solution (25 mg L^{-1}) for 1–2 min. Intramuscular injection was given at 0.4 ml per 25 g of body weight with each of the prepared bacterial cell suspensions. The fishes injected with individual bacterium were maintained in separate aquaria (10 fishes in each aquarium). The control set of fishes kept in a separate aquarium was administered with 0.85% saline solution at similar dose. A negative control set was additionally maintained under similar conditions in which the fishes did not receive any injection. Development of ulcers and damage to the surface tissue were monitored every 24 h postadministration for 1 week (32). The Kaplan–Meier survival analysis was performed using the GraphPad Prism software (version 9.3.1).

Cytotoxicity Test

Cytotoxicity of the *Aeromonas* isolate GP3 was tested in WRL-68 cell lines. GP3 was grown in LB broth at 30°C for 16 h under shaking at 90 rpm. The resultant culture was centrifuged at 10,000 g for 30 min at 4°C and the cell-free supernatant was collected carefully and filtered through a 0.45-mm filter. Cell-free filtrates of a non-pathogenic strain *Lactobacillus* sp. were similarly prepared and included in the experiment as the positive control, whereas sterile LB medium was used for negative control. WRL-68 cell line (human, liver, embryonic) obtained from National Centre for Cell Science (NCCS) Pune, Maharashtra, India was grown in Dulbeco's modified Eagle's medium (DMEM) with 10% foetal calf serum in an atmosphere containing 5% CO_2. For morphological examination, cells were seeded in 60-mm polyvinyl-coated culture plates and incubated at 37°C for 24 h in CO_2 incubator. Next day, 1.5 ml of the two cell-free filtrates and sterile LB medium was added to the cells taken in three separate sets and incubated for 1 h at 25°C. Changes in the cell morphology were recorded by observing under phase-contrast inverted microscope (Olympus CK40-SLP) at 200X magnification. Trypan blue dye exclusion assay was used to confirm cell death. By this method, nonviable cells are stained whereas viable cells exclude the dye (33). Percent viability was determined as follows: [total number of viable cells per ml of aliquot/ total number of cells per ml of aliquot] × 100. The experiment was repeated three times and data were averaged. Standard error was calculated using the statistical software OriginPro® version 9.9 freely available from https://www.originlab.com

Detection of Virulence Factor Encoding Genes by Polymerase Chain Reaction (PCR)

A total of 34 isolated strains were tested for the occurrence of four genetic determinants of virulence factors, *aer/haem* (haemolytic toxin), *aspA* (serine protease), *ascV* (type 3 secretion system), and *flaA* (polar flagella) by PCR using gene-specific primers (34). The primers have been listed in **Supplementary Table 1**. PCR amplification was performed with a 25 μl reaction volume containing 5 μl of 5X Flexi-Taq DNA polymerase buffer, 0.5 μl of 10 mM dNTP mix, 0.25 μl of the gene primers (100 mM-both forward and reverse), 2 μl of 25 mM $MgCl_2$, 2 μl template DNA, and 0.25 μl of 5U Taq polymerase. PCRs were carried out in thermal cycler (Applied Biosystems GeneAmp PCR 2,400) with the following cycling conditions: initial denaturation at 95°C for 3 min, 30 cycles of denaturation at 95°C for 30 s, annealing at temperature of 50–55°C appropriate for each primer pair for 30 s, extension at 72°C for 30 s, and a final extension at 72°C for 5 min. The amplicons were separated electrophoretically in 2% agarose gel stained with ethidium bromide (0.5 μg/ml). Electrophoresis was performed in a tank containing 1X TAE buffer for 1 h at 55V and bands viewed under UV-transilluminator (Bio-Rad Laboratories). PCR products were extracted using Gel/PCR DNA Fragments Extraction Kit (BR Biochem Life Sciences Pvt. Ltd.) according to the supplier's protocol. The products were cloned using pGEM–T easy vector kit (PROMEGA Corporation, U.S.A.) following the manufacturer's instructions. The amplicons were sequenced at Eurofins sequencing services, Bangalore, India. The obtained sequences were subjected to the similarity search using the BLAST search program of the National Center for Biotechnology Information (NCBI) (35). The sequences obtained were annotated and thereafter deposited in the NCBI GenBank through the Bankit tool.

Conjugation and Plasmid Detection

The potential donor GP3 strain bearing the haemolytic gene and nalidixic acid-resistant *Escherichia coli*-DH5α recipient strain which tested negative in PCR with *aer/haem* primers was incubated overnight in LB broth at 37°C. Both were grown to equal optical densities of 0.5 as measured by spectrophotometer (10^7 cells/ml). Broth conjugation was performed by mixing equal volumes of donor and recipient strains and incubating at 25°C for 24 h without shaking. A ten-fold serial dilution of each mating mixture was spread on LB agar plates supplemented with 5%

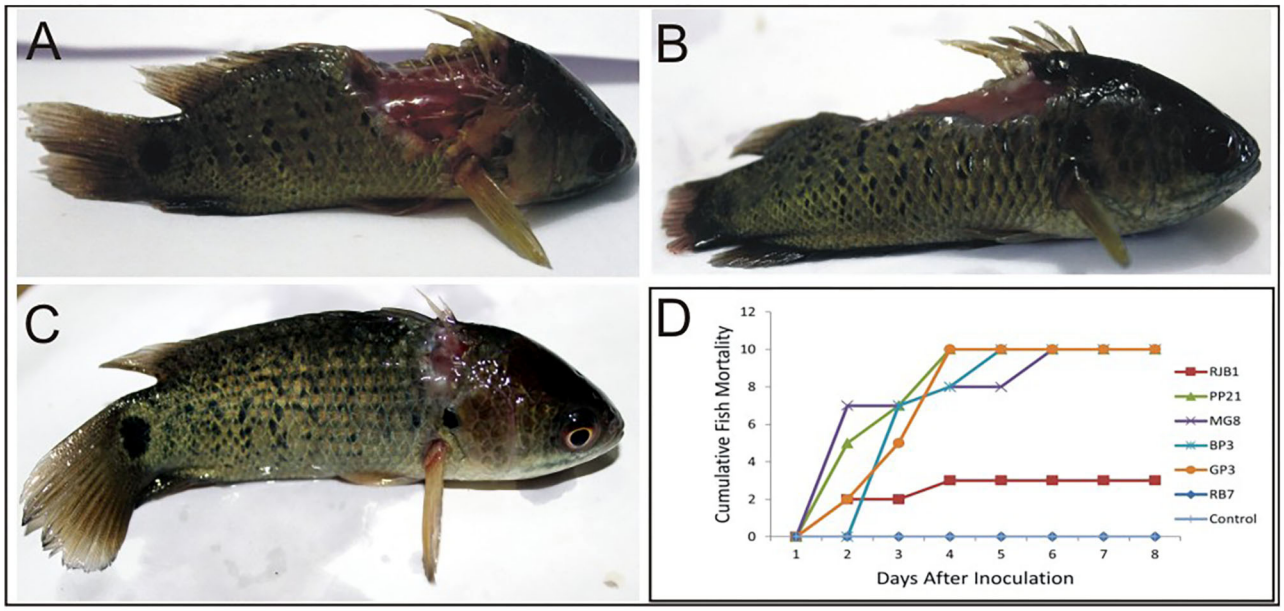

FIGURE 1 | Pathogenicity testing of isolated *Aeromonas* strains in *A. testudineus*. **(A)** Extremely severe lesion in fish injected intramuscularly with cell suspension of GP3. **(B)** Fish injected with PP21 showing severe lesion. **(C)** Fish injected with RJB1showing superficial lesion. **(D)** Graph depicting cumulative mortality of fishes injected with bacterial cell suspensions within a 7-day observation period.

sheep blood and 20 μg/ml nalidixic acid. Colonies growing on these double selective plates after 24–48 h of incubation at 37°C were treated as the putative transconjugants (32). The efficiency of conjugation was estimated as the number of transconjugants per initial number of recipients. Subsequently, boiling lysis of the selected transconjugants was carried out, and PCR was performed using *aer/heam* primers to detect the presence of the transferred gene. The donor and transconjugants as well as recipients prior to conjugation were also screened for the presence of plasmids as described by Birnboim and Doly (36).

RESULTS

Occurrence and Presumptive Identification of *Aeromonas*

Out of the total 83 strains, 34 strains were morphologically and biochemically identified as *Aeromonas* sp. (**Supplementary Table 2**), and the identity was further confirmed by 16S rRNA gene sequencing. The genetic relationship among the sequences was established by a phylogenetic tree constructed by MEGA software (version 7) (**Supplementary Figure 1**). The neighbor-joining tree method showed that all the 34 isolates clustered with the reference strains of *Aeromonas* species: *A. veronii* ($n = 19$), *A. hydrophila* ($n = 7$), *A. cavie* ($n = 3$), and *Aeromonas jandei* ($n = 5$).

Virulence Characteristics

The virulence characteristics of all isolates were studied, and the results are summarized in **Supplementary Table 3**. Haemolytic and proteolytic activity was a common trait exhibited by all the 34 (100%) isolates. On the other hand, 15 (44.1%), 13 (38.2%), and 24 (70.6%) isolated strains displayed DNase, siderophore, and amylase production, respectively. Only 2 (5.8%) isolates showed lipolytic activity.

Pathogenicity in Fish

Virulence of six potential pathogenic *Aeromonas* strains isolated from different locations (GP3, RB7, BP3, RJB1, MG8, and PP21) was tested in *A. testidineus* using intramuscular injection, and the results are presented in **Figure 1**. Superficial lesions were observed initially at the site of injection in most fishes, which progressively became severe with time. Ulcers induced by GP3 were found to be most severe and all the fishes died by the 3rd day (**Figure 1A**). PP21-injected fishes also showed 100% mortality on the 3rd day with severe to moderate ulcers at the site of injection (**Figure 1B**). Fishes injected with BP3 and MG8 exhibited mild to moderate ulcers2 with 100% of mortality on 4th and 5th day, respectively (**Figure 1D**). RJB1-injected fishes produced superficial lesions in 30% of the fishes and recorded low mortality (**Figure 1C**). However, fishes injected with strain RB7 did not record any mortality. The fishes in the control group were healthy with no signs of ulcers or disease. The median survival time of fishes injected with PP21, MG8, BP3, and GP3 was found to be 1.5, 1, 2, and 2.5. For RJB1, RB7, and the control group, it was undefined because some fishes survived at the end of the observation period (**Supplementary Figure 2**). The results obtained were statistically significant with $p < 0.0001$ in the log-rank test.

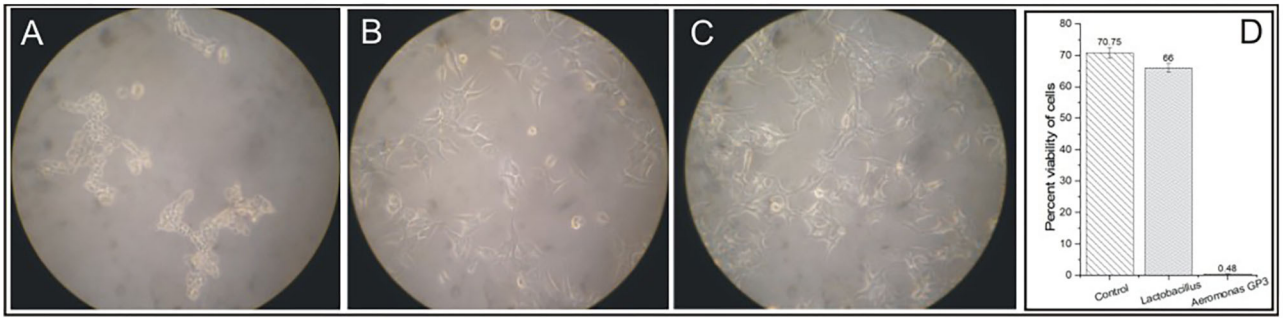

FIGURE 2 | Cytotoxicity of isolated *Aeromonas* strain GP3 in WRL-68 cell line. **(A)** Treated with culture filtrate of GP3 showing visible rounding off and detachment of monolayers. **(B)** Treated with cell-free filtrate of *Lactobacillus* sp. showing minor morphological changes. **(C)** Control (treated with sterile LB medium) showing no change in cell morphology. **(D)** Graph representing the cell viability assay.

Cytotoxicity

The cell-free culture filtrate of isolate GP3 induced cytotoxic activity on WRL-68 human liver cell lines. Degenerative changes such as visible rounding off and adherence loss from the plate surface in cell cultures were observed (**Figure 2A**). However, no visible changes in morphology were induced in cell lines exposed to *Lactobacillus* cell-free culture filtrates (**Figure 2B**) as well as in control (**Figure 2C**). In the cell viability assay, a significant reduction in percent viability was observed in the GP3-exposed cells when compared to the control. GP3-exposed cells recorded a percent viability of only 0.48% which was much lower than *Lactobacillus* treated cells (66%) (**Figure 2D**).

Virulence Genes

The virulence genes were detected in 23 of the 34 isolates which were identified as *Aeromonas*. The *aerA/haem* and *flaA* gene were amplified in 44.11% of the isolates (**Supplementary Figures 3A,B**). The *ascV* and *aspA* gene were detected in 23.5 and 8.82% of the isolates, respectively (**Supplementary Figures 3C,D**). The isolates could be classified into eight groups depending upon the occurrence of virulence genes (**Table 1**). A total of eleven isolates did not show the presence of any of the virulence genes. The GenBank accession numbers of the virulence genes are given as *aer/haem* (MT704303-MT704309, MT707932-MT707935, MH607886, MT591426, and MTT813045) *aspA* (MT909568-MT909570), *ascV* (MW001219-MW001222, MH607887-MH607890), and *flaA* (MT942623-MT942626, MT977537- MT977539).

Conjugation and Plasmid Isolation

Conjugation experiments revealed that determinants of haemolytic property of the isolated *Aeromonas* strain GP3 was transferable to recipient *E. coli*. GP3 contained a 23-kb plasmid which was also detectable in the transconjugants (**Figure 3A**). PCR analysis revealed the presence of the 431bp *aer/haem* gene in both donor and transconjugants (**Figure 3B**). The gene was not detected in recipient strains prior to conjugation. The frequency of conjugal transfer was recorded as 0.394×10^{-4} transconjugants per recipient cell in a mating mixture.

DISCUSSION

In this study, several environmental strains of *Aeromonas* sp. harboring multiple virulence encoding genes were isolated from water samples of 10 fish-farming sites distributed across three districts of the Sub-Himalayan West Bengal. Furthermore, few isolates proved to be pathogenic in fish and cytotoxic to mammalian liver cells. Conjugational studies on the transfer of haemolysin-encoding gene from a virulent strain to *E. coli* Dh5α were also successfully demonstrated.

During the process of isolation, a lot of background microflora with similar cultural characteristics and morphology was obtained on *Aeromonas* isolation medium (37). Furthermore, we accurately identified the strains belonging to this genus using the aero key scheme proposed by Carnahan et al. (22) followed by 16S rRNA gene sequencing (38). Phylogenetic tree showed that all 34 isolates rearranged between four reference species with a highest number of species clustering to *A. veronii* followed by *A. hydrophila*. Few isolates formed distinct clades with *A. jandaei* and three isolates clustered with *A. caviae*. Such prevalence of variable species from the area of our study has not yet been reported elsewhere.

The foothill of Sub-Himalayan region is a geographically diverse region and serves as a habitat for a lot of endemic species of fish (39). A huge impact of bacterial diseases on fish productivity (40) and the role of *Aeromonas* in fish infections due to multiple virulence factors has been previously reported (41). In this study, all the strains isolated from water samples of small fish farms were found to be beta-haemolytic and proteolytic. This supports the theory of close association between the two factors since proteases have a prominent role in cleavage and activation of haemolysin (42). Additionally, 70.6% of the strains produced amylase whereas lesser isolates produced siderophore and DNase. Lower detection of siderophore-producing bacteria in this study may be due to alternate iron acquisition mechanisms found in *Aeromonas* for utilization in the process of host colonization (43). Likewise, DNase and amylase production are less as it depends on the nutritional requirement of the pathogen (42, 44).

TABLE 1 | *Aeromonas* isolates summarized into groups based on occurrence of virulence genes.

Groups	Virulence related genes				Number of isolates (isolate names)
	aer/haem	***aspA***	***ascV***	***flaA***	
A	+	−	+	+	5 (PP7, PP12, FP2, GP3, MG8)
B	+	+	−	+	1 (RJB1)
C	+	+	+	−	1 (RB7)
D	+	−	−	+	3 (PP21, PP22, FP8)
E	+	+	−	−	1 (BP6)
F	+	−	−	−	4 (HP1, HP6, BP2, GD3)
G	−	−	−	+	6 (SFM1, SFM2, PP19, PP23, GD1, RB5)
H	−	−	+	−	2 (BP3, GP1)
I	−	−	−	−	11
Total % of isolates	44.1%	8.82%	21.5%	44.1%	

"+" indicates presence.
"–" indicates absence.

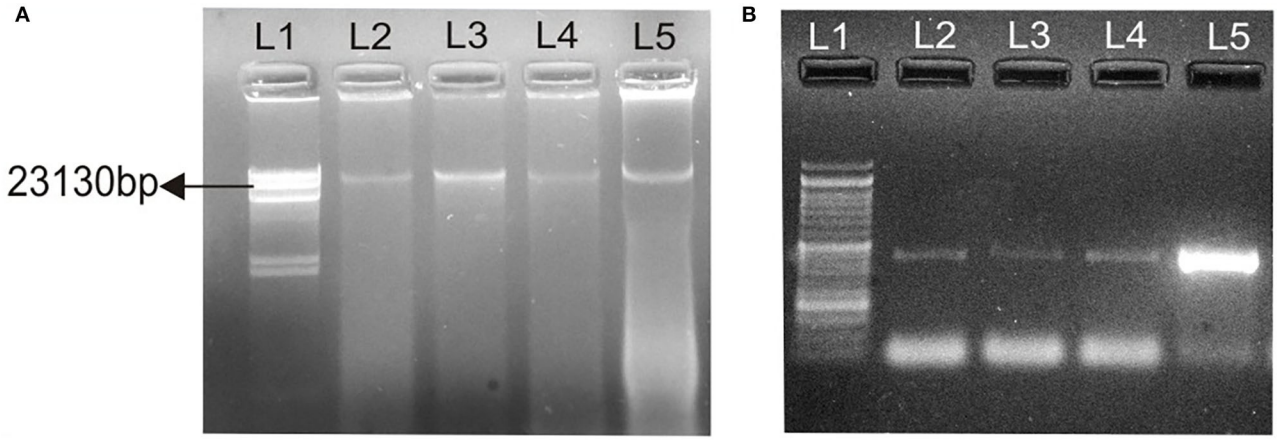

FIGURE 3 | Transfer of virulence gene from isolated *Aeromonas* strain GP3 to *E. coli* DH5α. **(A)** lane 1, Lambda DNA/*Hind* III digest: molecular weight marker; lane 2, 23-kb plasmid (23,130 bp) of GP3 (donor); L3, L4, L5, 23 kb plasmids detected in transconjugants, **(B)** 431-bp PCR amplicons of the aerolysin/haemolysin (*aer/haem*) encoding gene from donor and transconjugants; lane 1, molecular weight marker as 50-bp DNA ladder; lanes 2-4, transconjugants and lane 5, donor GP3.

In our study, four important virulence-related genes encoding haemolysin (*aerA/haem*), alkaline serine protease (*aspA)*, inner component of type III secretion system (*ascV),* and polar flagella (*flaA)* had a heterogenous distribution among the isolates. Among these four genes, a prevalence of at least one virulence-related gene was observed in 67.7% of the total isolates. A higher percent (44.1%) of strains was found to harbor the *aer/haem* and *flaA* genes, which was similar to the findings by other authors (45, 46). However, lesser proportion of strains showed the presence of *ascV* (21.5%) and *aspA* (8.82%), indicating the possible involvement in proteases other than serine protease and secretion systems other than type III (47). *Aeromonas* isolates harboring at least one virulence gene were summarized into groups based on the presence of the type of gene. A total of eight different combinations were revealed, of which, the presence of single *flaA* gene, found in six isolates, was the most common. A total of five isolates showed the virulence gene pattern aer/$haem^{+}$/$ascV^{+}$/$flaA^{+}$. The *aerA* (encoding aerolysin) and *hlyA* (encoding haemolysin) gene in *Aeromonas hydrophila* has been previously categorized as strong virulence determinant for pathogenicity (48, 49). Li et al. (12) indicated a strong link between bacterial virulence and the presence of *aerA* and *ahp* (encoding serine protease) gene. Hence, in *Aeromonas,* the presence of multiple virulence factors encoding genes either acting singly or in a synergistic pattern leads to disease development in the host (46).

In the fish challenge studies, all the six selected isolates of *Aeromonas* were found to be pathogenic to *A. testudineus*. Mortality was reported in 72.2% of fishes along with lesion

development at the site of administration of bacteria. An isolate GP3 exhibiting five virulence characteristics and harboring three of the four tested virulence-related genes showed a highest pathogenicity with severe lesions leading to 100% of mortality. PP21, with only two virulent phenotype (protease and haemolysin) and genes *aer/haem* and *flaA,* also showed 100% of mortality on the 3rd day following injection. On the other hand, RB7 which exhibited four virulent phenotypes (haemolysin, protease, DNase, and amylase) and three genes (*aer/haem*$^+$/*ascV*$^+$/*aspA*$^+$) did not record any mortality. Further, BP3 which showed four virulence traits and harbored only one of the four tested genes (*ascV*) was found to be strongly pathogenic to fishes. Therefore, no distinct correlation among the exhibition of virulence phenotypes, harboring of specific genes, and the mortality in fishes was evident. Similar results were obtained by Oliviera et al. (50) as they found no statistically significant relationship between the presence of virulence factors and mortality in Nile tilapia infected by *A. hydrophila.* Such absence of correlation between virulence factors and pathogenicity has also been reported by many other researchers (51, 52). However, several authors observed that the presence of specific virulence factors in aeromonads is closely related to mortality in injected fishes (9, 53).

The virulence of GP3 was further evaluated by assessing its ability to induce cytotoxic changes in liver cell lines in comparison with a non-virulent strain *Lactobacillus.* In our study, clear rounding off and detachment of monolayers were visible in liver cells exposed to cell-free GP3 filtrate. The cell viability reduced to only 0.48%, indicating extreme cytotoxicity. In similar studies, previous authors have reported rounding off, shriveling, and detachment of cell lines treated with bacterial filtrates of *Aeromonas* (54). The cytotoxicity in WRL-68 human liver cell lines indicated the possibility of disease-causing ability of *Aeromonas* in human, and similar reports suggesting its role in gastroenteritis and soft tissue infections of humans have been reported earlier (2).

Another significant finding of our study is the successful transfer of a component of haemolytic gene *via* conjugation from a virulent isolate GP3 to an *E. coli* recipient strain. A 23-kb plasmid was isolated from donor and transconjugants. Previous studies demonstrating the transfer of virulence genes from other genera such as *Vibrio* and *S. aureus* have been reported (15, 16, 18), but such reports involving aeromonads are rare. Most of the reports in *Aeromonas* sp. have their prime focus on the distribution of genetic determinants of several virulence factors, but there is very less evidence to suggest the transfer ability of these genes to non-pathogenic strains of bacteria belonging to a same or different genus. Majumdar et al. (55) observed that curing of a particular 21-kb plasmid detected in virulent *Aeromonas* isolate from environmental sources led to the loss in virulence. In this study, the 23-kb plasmid may be carrying the haemolysin gene as it was isolated from donor and transconjugants but not from the recipient strain prior to conjugation. Such mobile genetic elements contribute to the gene pool in aquatic reservoirs (56) and could be easily transferred to other microorganisms helping them thrive in nutrient-limiting conditions and increase their survivability within hosts (57).

In conclusion, this study revealed the occurrence of virulence factors and some of their genetic determinants in *Aeromonas* strains of aquatic origin. Further extensive studies on a greater number of virulence genes shall serve to accurately discriminate the various pathotypes of *Aeromonas* spp. We further studied the probability of horizontal spread of haemolytic property from the isolated *Aeromonas* to *E. coli* recipient strain. To our knowledge, this is the first report of the transfer of *aer/haem* gene encoding a haemolysin from a strain of virulent *Aeromonas* to any recipient strain. As the aquatic bodies provide a perfect environment for the interaction of microbes leading to gene transfer among cohabitant microflora, the occurrence of transferable virulence traits in bacteria especially in fish farming habitats is alarming. Being opportunistic pathogens, these bacteria may also infect humans as indicated by cytotoxicity studies. Future studies on the involvement of mobile genetic elements in virulence of *Aeromonas* spp. from aquaculture sources will allow to accurately assess the risk of spread of virulence traits to other non-pathogenic bacteria and the threat this poses to public health. Therefore, periodic monitoring of *Aeromonas* is required as these serve as the indicators of poor fish culture conditions and would possibly lead to zoonotic outbreaks.

DATA AVAILABILITY STATEMENT

The datasets presented in this study can be found in online repositories. The names of the repository/repositories and accession number(s) can be found in the article/**Supplementary Material**.

ETHICS STATEMENT

Ethical review and approval were not required as the study is in accordance with the institutional requirements and the institution has reviewed and approved the animal studies (Approval no. 161-(A)/R-2022). The fish used here is marketed in live condition commercially for purpose of human consumption. However, all fish handling and experimentation was done with maximum veterinary care.

AUTHOR CONTRIBUTIONS

DS designed the study, helped in interpreting the study results, and critically revised the manuscript. PM and PB carried out the methodology, collected, and analysed the data. PM and DS drafted the manuscript. AS has helped in fish studies. AK has contributed in cytotoxicity studies. All authors contributed to the article and approved the submitted version.

FUNDING

This work was supported by funds from University Grants Commission (UGC), India (www.ugc.ac.in/) Grant No. F. No. 42-187/2013(SR) dated 02.07.2014. PM received fellowship from University Grants Commission (UGC), India (www.ugc.ac.in/)

Grant No. F.25-1/2014-15(BSR)/7-132/2007(BSR) dated 07.10.2015. PB received fellowship from Department of Biotechnology, Govt. of India. The funders had no role in study design, data collection and analysis, decision to publish, or provide any funds for publishing.

SUPPLEMENTARY MATERIAL

The Supplementary Material for this article can be found online at: https://www.frontiersin.org/articles/10.3389/fvets.2022.887174/full#supplementary-material

REFERENCES

1. Araujo RM, Pares R, Lucena F. The effect of terrestrial effluents on the incidence of *Aeromonas* spp. in coastal waters. *J Appl Bacteriol.* (1990) 69:439–44. doi: 10.1111/j.1365-2672.1990.tb01535.x
2. Janda JM, Abbott SL. The genus *Aeromonas:* taxonomy, pathogenicity, and infection. *Clinic Microbiol Rev.* (2010) 23:35–73. doi: 10.1128/CMR.00039-09
3. Hoai TD, Trang TT, Van Tuyen N, Giang NT, Van Van K. *Aeromonas veronii* caused disease and mortality in channel catfish in Vietnam. *Aquaculture.* (2019) 513:734425. doi: 10.1016/j.aquaculture.2019.734425
4. Grim CJ, Kozlova EV, Sha J, Fitts EC, van Lier CJ, Kirtley ML, et al. Characterization of *Aeromonas hydrophila* wound pathotypes by comparative genomic and functional analyses of virulence genes. *MBio.* (2013) 4:e00064–13. doi: 10.1128/mBio.00064-13
5. Lamy B, Baron S, Barraud O. *Aeromonas*: the multifaceted middleman in the One Health world. *Curr Opin Microbiol.* (2022) 65:24–32. doi: 10.1016/j.mib.2021.09.012
6. Abraham TJ, Bharathkumar G. Distribution of motile aeromonads, pseudomonads and oxytetracycline resistant bacteria in freshwater catfish *Pangasius pangasius* Hatcheries of West Bengal, India. *J Bio-Sci.* (2009) 17:13–20. doi: 10.3329/jbs.v17i0.7094
7. Patra BC, Kar A, Bhattacharya M, Parua S, Shit PK. Freshwater fish resource mapping and conservation strategies of West Bengal, India. *Spatial Inform Res.* (2017) 25:635–45. doi: 10.1007/s41324-017-0129-z
8. Sahoo PK, Swaminathan TR, Abraham TJ, Kumar R, Pattanayak S, Mohapatra A, et al. Detection of goldfish haematopoietic necrosis herpes virus (Cyprinid herpesvirus-2) with multi-drug resistant *Aeromonas hydrophila* infection in goldfish: First evidence of any viral disease outbreak in ornamental freshwater aquaculture farms in India. *Acta tropica.* (2016) 161:8–17. doi: 10.1016/j.actatropica.2016.05.004
9. Mzula A, Wambura PN, Mdegela RH, Shirima GM. Virulence pattern of circulating aeromonads isolated from farmed Nile tilapia in Tanzania and novel antibiotic free attenuation of *Aeromonas hydrophila* strain TZR7-2018. *Aquaculture Rep.* (2020) 17:100300. doi: 10.1016/j.aqrep.2020.100300
10. Gao CX, Ren Y, Wang Q, Zeng WW, Li YY, Wang YY, et al. Isolation, identification antimicrobial susceptibility of pathogenic *Aeromonas veronii* isolated from grass carp. *J Anhui Agr Univ.* (2018) 45:409–415. doi: 10.13610/j.cnki.1672-352x.20180620.019
11. Kingombe CIB, Huys G, Tonolla M, Albert MJ, Swings J, Peduzzi, et al. PCR detection, characterization, and distribution of virulence genes in *Aeromonas* spp. *Appl Environ Microbiol.* (1999) 65:5293–5302. doi: 10.1128/AEM.65.12.5293-5302.1999
12. Li J, Ni XD, Liu YJ, Lu CP. Detection of three virulence genes alt, ahp and aerA in *Aeromonas hydrophila* and their relationship with actual virulence to zebra fish. *J Appl Microbiol.* (2011) 110:823–30. doi: 10.1111/j.1365-2672.2011.04944.x
13. Pattanayak S, Priyadarsini S, Paul A, Kumar PR, Sahoo PK. Diversity of virulence-associated genes in pathogenic *Aeromonas hydrophila* isolates and their *in vivo* modulation at varied water temperatures. *Microb Pathogene.* (2020) 147:104424. doi: 10.1016/j.micpath.2020.104424
14. Illanchezian S, Jayaraman S, Manoharan MS, Valsalam S. Virulence and cytotoxicity of seafood borne *Aeromonas hydrophila*. *Brazil J Microbiol.* (2010) 41:978–83. doi: 10.1590/S1517-83822010000400016
15. Castillo D, Kauffman K, Hussain F, Kalatzis P, Rørbo N, Polz MF, et al. Widespread distribution of prophage-encoded virulence factors in marine *Vibrio* communities. *Scientific Rep.* (2018) 8:1–9. doi: 10.1038/s41598-018-28326-9
16. Deng Y, Xu H, Su Y, Liu S, Xu L, Guo Z, et al. Horizontal gene transfer contributes to virulence and antibiotic resistance of *Vibrio harveyi* 345 based on complete genome sequence analysis. *BMC Genom.* (2019) 20:1–9. doi: 10.1186/s12864-019-6137-8
17. Osorio CR. *Photobacterium damselae*: how horizontal gene transfer shaped two different pathogenic lifestyles in a marine bacterium. *Horizontal Gene Trans.* (2019) 9:175–99. doi: 10.1007/978-3-030-21862-1_6
18. Alibayov B, Baba-Moussa L, Sina H, Zdenková K, Demnerová K. *Staphylococcus aureus* mobile genetic elements. *Mol Biol Rep.* (2014) 41:5005–18. doi: 10.1007/s11033-014-3367-3
19. Bello-López JM, Cabrero-Martínez OA, Ibáñez-Cervantes G, Hernández-Cortez C, Pelcastre-Rodríguez LI, Gonzalez-Avila LU, et al. Horizontal gene transfer and its association with antibiotic resistance in the genus *Aeromonas* spp. *Microorganisms.* (2019) 7:363. doi: 10.3390/microorganisms7090363
20. Poole TL, Schlosser WD, Anderson RC, Norman KN, Beier RC, Nisbet DJ. Whole-Genome sequence of *Aeromonas hydrophila* CVM861 isolated from diarrhetic neonatal swine. *Microorganisms.* (2020) 8:1648. doi: 10.3390/microorganisms8111648
21. Cipriano RC, Bullock GL. "Furunculosis and other diseases caused by *Aeromonas salmonicida*," in *National Fish Health Research Laboratory* (2001).
22. Carnahan AM, Behram S, Joseph SW. Aerokey II: a flexible key for identifying clinical *Aeromonas* species. *J Clinic Microbiol.* (1991) 29:2843–9. doi: 10.1128/jcm.29.12.2843-2849.1991
23. Gerhardt P, Murray R, Wood W, Krieg N. Methods for general and molecular bacteriology. *Am Soc Microbiol.* (1994) 4:21–42. doi: 10.1002/food.19960400226
24. Aneja KR. *Experiments in Microbiology Plant Pathology and Biotechnology*. New Delhi: New Age International (P) Limited, Publishers (2003).
25. Barrow GI, Feltham RKA. *Cowan and Steel's manual for identification of medical bacteria* Great Britain: Cambridge University Press, p. 331 (1993).
26. Smibert RM, Krieg NR. "Phenotypic characterization," In: editors Gerhardt P, et al. *Methods for General and Molecular Bacteriology*. Washington, DC: American Society for Microbiology, pp. 607–654 (1994).
27. Schwyn B, Neilands JB. Universal chemical assay for the detection and determination of siderophores. *Analytic biochemistr.* (1987) 160:47–56. doi: 10.1016/0003-2697(87)90612-9
28. Gomes LH, Duarte KM, Andrino FG, Tavares FC. A simple method for DNA isolation from *Xanthomonas* spp. *Scientia Agricola.* (2000) 57:553–5. doi: 10.1590/S0103-90162000000300028
29. Srinivasan R, Karaoz U, Volegova M, MacKichan J, Kato-Maeda M, Miller S, et al. Use of 16S rRNA gene for identification of a broad range of clinically relevant bacterial pathogens. *PloS one.* (2015) 10:e0117617. doi: 10.1371/journal.pone.0117617
30. Tamura K, Peterson D, Peterson N, Stecher G, Nei M, Kumar S. MEGA5: molecular evolutionary genetics analysis using maximum likelihood, evolutionary distance, and maximum parsimony methods. *Mol Biol Evol.* (2011) 28:2731–9. doi: 10.1093/molbev/msr121
31. Felsenstein J. Confidence limits on phylogenies with a molecular clock. *Systemat Zool.* (1985) 34:152–61. doi: 10.2307/sysbio/34.2.152
32. Das A, Saha D, Pal J. Antimicrobial resistance and *in vitro* gene transfer in bacteria isolated from the ulcers of EUS-affected fish in India. *Lett Appl Microbiol.* (2009) 49:497–502. doi: 10.1111/j.1472-765X.2009.02700.x
33. Strober W. Trypan blue exclusion test of cell viability. *Curr Protocols Immunol.* (2001) 1:21. doi: 10.1002/0471142735.ima03bs21
34. Aravena-Román M, Inglis TJ, Riley TV, Chang BJ. Distribution of 13 virulence genes among clinical and environmental *Aeromonas* spp. in Western Australia. *Euro J Clinic Microbiol Infect Dis.* (2014) 33:1889–95. doi: 10.1007/s10096-014-2157-0

35. Altschul SF, Gish W, Miller W, Myers EW, Lipman DJ. Basic local alignment search tool. *J Mol Biol.* (1990) 215:403–10. doi: 10.1016/S0022-2836(05)80360-2
36. Bimboim HC, Doly J. A rapid alkaline extraction procedure for screening recombinant plasmid DNA. *Nucleic Acids Res.* (1979) 7:1513–23. doi: 10.1093/nar/7.6.1513
37. Chaix G, Roger F, Berthe T, Lamy B, Jumas-Bilak E, Lafite R, et al. Distinct *Aeromonas* populations in water column and associated with copepods from estuarine environment (Seine, France). *Front Microbiol.* (2017) 8:1259. doi: 10.3389/fmicb.2017.01259
38. Pandove G, Sahota P, Vikal Y, Kaur B. Multiplex PCR water testing kit for rapid, economic and simultaneous detection of *Escherichia coli*, *Yersinia enterocolitica* and *Aeromonas hydrophila* from drinking water. *Curr Sci.* (2013) 10:352–8.
39. Panja S, Podder A, Chakrabarty M, Homechaudhuri S. Spatial pattern of freshwater habitats and their prioritization using additive partitions of beta diversity of inhabitant piscine assemblages in the Terai–Dooars ecoregion of Eastern Himalayas. *Limnology.* (2022) 23:57–72. doi: 10.1007/s10201-021-00666-y
40. Samayanpaulraj V, Velu V, Uthandakalaipandiyan R. Determination of lethal dose of *Aeromonas hydrophila* Ah17 strain in snake head fish *Channa striata*. *Microbial Pathogene.* (2019) 127:7–11. doi: 10.1016/j.micpath.2018.11.035
41. Shameena SS, Kumar K, Kumar S, Kumar S, Rathore G. Virulence characteristics of *Aeromonas veronii* biovars isolated from infected freshwater goldfish (*Carassius auratus*). *Aquaculture.* (2020) 518:734819. doi: 10.1016/j.aquaculture.2019.734819
42. Pemberton JM, Kidd SP, Schmidt R. Secreted enzymes of *Aeromonas*. *FEMS Microbiol Lett.* (1997) 152:1–0. doi: 10.1111/j.1574-6968.1997.tb10401.x
43. Maltz M, Levarge BL, Graf J. Identification of iron and heme utilization genes in *Aeromonas* and their role in the colonization of the leech digestive tract. *Front Microbiol.* (2015) 6:763. doi: 10.3389/fmicb.2015.00763
44. Campbell CM, Duncan D, Price NC, Stevens L. The secretion of amylase, phospholipase and protease from *Aeromonas salmonicida,* and the correlation with membrane-associated ribosomes. *J Fish Dis.* (1990) 13:463–74. doi: 10.1111/j.1365-2761.1990.tb00805.x
45. Hoel S, Vadstein O, Jakobsen AN. Species distribution and prevalence of putative virulence factors in mesophilic *Aeromonas* spp. isolated from fresh retail sushi. *Front Microbiol.* (2017) 8:931. doi: 10.3389/fmicb.2017.00931
46. Chen JS, Hsu GJ, Hsu BM, Yang PY, Kuo YJ, Wang JL, et al. Prevalence, virulence-gene profiles, antimicrobial resistance, and genetic diversity of human pathogenic *Aeromonas* spp. from shellfish and aquatic environments. *Environ Pollut.* (2021) 287:117361. doi: 10.1016/j.envpol.2021.117361
47. Hossain S, De Silva BC, Wickramanayake MV, Dahanayake PS, Wimalasena SH, Heo GJ. Incidence of antimicrobial resistance genes and class 1 integron gene cassettes in multidrug-resistant motile *Aeromonas* sp. isolated from ornamental guppy (Poecilia reticulata). *Lett Appl Microbiol.* (2019) 69:2–10. doi: 10.1111/lam.13162
48. Wang G, Clark CG, Liu C, Pucknell C, Munro CK, Kruk TM, et al. Detection and characterization of the hemolysin genes in *Aeromonas hydrophila* and *Aeromonas sobria* by multiplex PCR. *J Clinic Microbiol.* (2003) 41:1048–54. doi: 10.1128/JCM.41.3.1048-1054.2003
49. Heuzenroeder MW, Wong CY, Flower RL. Distribution of two hemolytic toxin genes in clinical and environmental isolates of *Aeromonas* spp.: correlation with virulence in a suckling mouse model. *FEMS Microbiol Lett.* (1999) 174:131–6. doi: 10.1111/j.1574-6968.1999.tb13559.x
50. Oliveira ST, Veneroni-Gouveia G, Costa MM. Molecular characterization of virulence factors in *Aeromonas hydrophila* obtained from fish. *PesquisaVeterináriaBrasileira.* (2012) 32:701–6. doi: 10.1590/S0100-736X2012000800004
51. Wu CJ, Ko WC, Lee NY, Su SL, Li CW, Li MC, et al. *Aeromonas* isolates from fish and patients in Tainan City, Taiwan: Genotypic and phenotypic characteristics. *Appl Environ Microbiol.* (2019) 85:e01360–19. doi: 10.1128/AEM.01360-19
52. Roges EM, Gonçalves VD, Cardoso MD, Festivo ML, Siciliano S, Berto LH, et al. Virulence-associated genes and antimicrobial resistance of *Aeromonashydrophila*isolates from animal, food, and human sources in Brazil. *BioMed Res Int.* (2020) 20:2607. doi: 10.1155/2020/1052607
53. Li T, Raza SH, Yang B, Sun Y, Wang G, Sun W, et al. *Aeromonasveronii*infection in commercial freshwater fish: a potential threat to public health. *Animals.* (2020) 10:608. doi: 10.3390/ani10040608
54. Kim KT, Lee SH, Lee KK, Han JE, Kwak D. Enhanced Virulence of *Aeromonas hydrophila* is induced by stress and serial passaging in mice. *Animals.* (2021) 11:508. doi: 10.3390/ani11020508
55. Majumdar T, Ghosh S, Pal J, Mazumder S. Possible role of a plasmid in the pathogenesis of a fish disease caused by *Aeromonas hydrophila*. *Aquaculture.* (2006) 256:95–104. doi: 10.1016/j.aquaculture.2006.02.042
56. Redondo-Salvo S, Fernández-López R, Ruiz R, Vielva L, de Toro M, Rocha EP, et al. Pathways for horizontal gene transfer in bacteria revealed by a global map of their plasmids. *Nature Commun.* (2020) 11:1–3. doi: 10.1038/s41467-020-17278-2
57. Di Lorenzo M, Stork M, Tolmasky ME, Actis LA, Farrell D, Welch TJ, et al. Complete sequence of virulence plasmid pJM1 from the marine fish pathogen *Vibrio anguillarum* strain 775. *J Bacteriol.* (2003) 185:5822–30. doi: 10.1128/JB.185.19.5822-5830.2003

Conflict of Interest: The authors declare that the research was conducted in the absence of any commercial or financial relationships that could be construed as a potential conflict of interest.

Publisher's Note: All claims expressed in this article are solely those of the authors and do not necessarily represent those of their affiliated organizations, or those of the publisher, the editors and the reviewers. Any product that may be evaluated in this article, or claim that may be made by its manufacturer, is not guaranteed or endorsed by the publisher.

Frontiers in Veterinary Science

Transforms how we investigate and improve animal health

The third most-cited veterinary science journal, bridging animal and human health with a comparative approach to medical challenges. It explores innovative biotechnology and therapy for improved health outcomes.

Discover the latest Research Topics

See more →

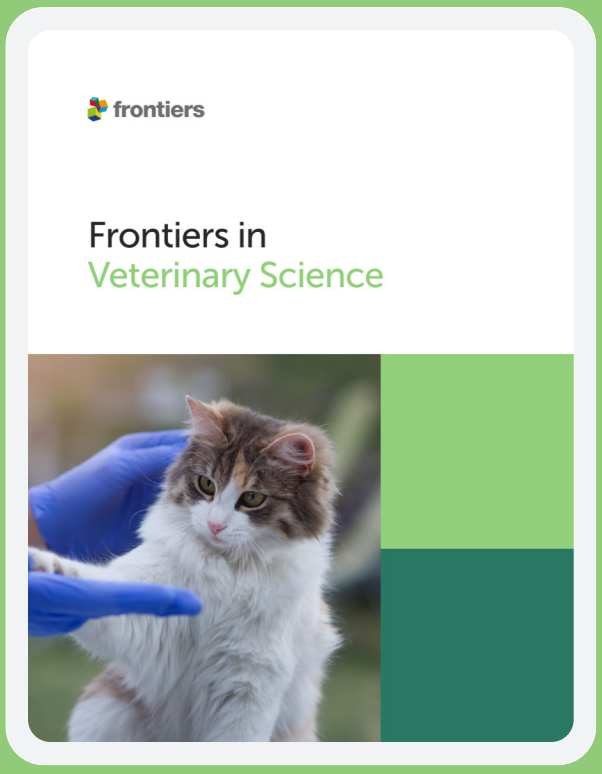

Frontiers

Avenue du Tribunal-Fédéral 34
1005 Lausanne, Swizerland
frontiersin.org

Contact us

+41 (0)21 510 17 00
frontiersin.org/about/contact